Isolating valuable ingredients of saffron using extraction and preparative chromatography

Dissertation

zur Erlangung des akademischen Grades

Doktoringenieur
(Dr.-Ing.)

von M.Sc. Mohsen Fotovati

geb. am 09. May 1991 in Qom, Iran

genehmigt durch die Fakultät für Verfahrens- und Systemtechnik

der Otto-von-Guericke-Universität Magdeburg

Promotionskommission:	Prof. Dr.-Ing. Andreas Seidel-Morgenstern (Vorsitz)
	Prof. Dr.-Ing. Stephan Scholl (Gutacher)
	Prof. Dr. Alireza Ghassempour (Gutacher)
	Prof. Dr. -Ing. habil. Christof Hamel (Mitglied)
eingereicht am:	29. August 2023
Promotionskolloquium am:	24. November 2023

Abstract

The stigmas of *Crocus sativus Linnaeus* are the basis for the most expensive spices in the world (saffron). Picrocrocin (PC), crocine I (CI), and crocin II (CII) are the main valuable constituents of saffron extract, responsible for the bitter taste, the red color of saffron, and for its usage as the fragrance. Crocin and picrocrocine have significant potential for the treatment of human diseases and disorders, such as depressive disorders, multiple sclerosis, eye diseases, inflammatory diseases and cancer. Since the production of pure crocines and picrocrocin is not well developed, two main separation methods, namely solid-liquid extraction and solid-liquid chromatography are used to efficiently extract and purify these valuable components from high quality Iranian saffron.

With respect to extraction, a systematic experimental study was performed to identify a suitable solvent and to determine key thermodynamic and kinetic properties of the three mentioned valuable saffron ingredients. These parameters were used in a theoretical study predicting both batch-wise and continuous counter-current extraction operation. A simplified model for the counter-current operation using the determined parameters was used to predict process productivities.

Regarding chromatographic purification, a three-step gradient elution method was developed to perform the separation of the three target molecules. The innovative aspect is the application of the equilibrium theory. It applies validate Henry constants to design a simple step-gradient elution. The developed three-step gradient elution was first validated on the analytical column. Then, preparative chromatography was used. It achieved good performance productivities. A prove of the applicability is the provision of three fractions of very pure picrocrocin, crocin I, and crocin II.

Kurzzusammenfassung

Die Narben von *Crocus sativus Linnaeus* sind die Grundlage für das teuerste Gewürz der Welt (Safran). Picrocrocin (PC), Crocin I (CI) und Crocin II (CII) sind die wichtigsten wertvollen Bestandteile von Safranextrakten, die für den bitteren Geschmack, die rote Farbe des Safrans und für seine Verwendung als Duftstoff verantwortlich sind. Crocin und Picrocrocin haben ein erhebliches Potenzial für die Behandlung menschlicher Krankheiten und Störungen wie depressive Störungen, multiple Sklerose, Augenkrankheiten, entzündliche Erkrankungen und Krebs. Da die Produktion von reinem Crocin und Picrocrocin sowohl hinsichtlich der Extraktion als auch der Reinigung noch nicht weit entwickelt ist, wurden zwei Haupttrennmethoden, nämlich Fest-Flüssig-Extraktion und Fest-Flüssig-Chromatographie, eingesetzt, um diese wertvollen Bestandteile aus hochwertigem iranischem Safran effizient zu extrahieren und zu reinigen .

Im Hinblick auf die Extraktion wurde eine systematische experimentelle Studie durchgeführt, um ein geeignetes Lösungsmittel zu identifizieren und die wichtigsten thermodynamischen und kinetischen Eigenschaften der drei genannten wertvollen Safraninhaltsstoffe zu bestimmen. Diese Parameter wurden in einer theoretischen Studie zur Vorhersage sowohl des diskontinuierlichen als auch des kontinuierlichen Gegenstromextraktionsvorgangs verwendet. Ein vereinfachtes Gegenstrommodell wurde unter Verwendung der ermittelten Parameter zur Vorhersage der Prozessproduktivitäten verwendet.

Bezüglich der chromatographischen Reinigung wurde eine dreistufige Gradientenelutionsmethode zur Durchführung der Trennung der drei Zielmoleküle entwickelt. Der innovative Aspekt ist die Anwendung der Gleichgewichtstheorie. Mit validierten Henry-Konstanten wurden einfache Stufengradientenelution entworfen. Die entwickelte dreistufige Gradientenelution wurde auf einer Analysesäule validiert. Später wurde die präparative Chromatographie unter Verwendung der Stufengradientenelution eingesetzt. Dabei wurden gute Leistungsproduktivitäten erzielt. Nachweis der Anwendbarkeit des Konzeptes ist die Bereitstellung von drei hochreinen Fraktionen an Picrocrocin, Crocin I und Crocin II.

Dedication

To my lover.

Acknowledgments

Contents

List of Figures

List of Tables

List of Symbols

Symbol	Unit	Designation
Å	$10^{-10}m$	Angstrom
$\bar{A}$	m^2	Interface area between two phases
A^{Peak}	$mAU.s$	Peak area
c	g_i/ml	Liquid phase concentration
$\tilde{c}$	$-$	Dimensionless concentration of extract phase
D_{app}	cm^2/min	Apparent axial dispersion
D_S	g_S/l	Dosage of the solid phase
F	$-$	Phase ratio
$\bar{F}$	$-$	Calibration factor
k^{eff}	$1/min$	Effective kinetic rate constant
$\tilde{k}^{eff}$	$1/min$	Modified effective kinetic rate constant
k	m/min	Initial kinetic phrase
K	$-$	Linear equilibrium constant of solid-liquid
$\tilde{K}$	$-$	Modified equilibrium function
K_H	$-$	Henry constant, linear adsorption equilibrium function
L	cm	Column length
m	g	Mass
$\dot{m}$	g_i/min	Mass transfer rate
N	$-$	Number of experiments and/or components
$\bar{N}$	$-$	Number of theoretical plates
Pr	$g_i/min/l$	Productivity
Pu	$\%$	Purity
q	g_i/g_S	Solid phase concentration
$\tilde{q}$	g_i/g_S	Modified concentration of solid phase
$Scale$	l	Volume of container
T	$°C$	Temperature
t	min	Time
t_0	min	Dead time
t^*	min	Time Intersection point in x and y

Symbol	Unit	Designation
u	cm/min	Linear migration velocity
V	l	Volume
$\dot{V}$	ml/min	Volumetric flow rate
w	min	Peak width
x	g/g	Mass fraction
Y	$\%$	Recovery yield
z	$- or cm$	Column length ($z = [0, L_c]$)
z^*	cm	Space Intersection point in x and y
Greek symbols		
Δt	min	Time difference
ρ	g/l	Density
σ	$-$ or min	Standard deviation and/or central moment
μ	g	Average mass
τ	min	Dimensionless total residence time
ε	$ml\ (liquid)/ml\ (total)$	Volume fraction
λ	nm	Wavelength
Superscript		
An	-	Analytical
eq	-	Equilibrium time
$exp.$	-	Experimental
in	-	Inlet
max	-	Maximum
$norm.$	-	Normalized
out	-	Outlet
$Pred.$	-	Predicted
$Prep.$	-	Preparative
$the.$	-	Theoretical
0	-	Zero time (initial state)
Subscript		
$Ads.$	-	Adsorbent
$base$	-	Base of peak
c	-	Column
$coll$	-	Collected
cyc	-	Cycle
E	-	Extraction
eff	-	Effective
$est.$	-	Estimated
i	-	Component
$Imp.$	-	Impurity
inj	-	Injection

Symbol	Unit	Designation
$Iso.$	-	Isocratic
j	-	Number of stage, step, and/or extractor
L	-	Liquid phase
mod	-	Modifier
n	-	Class of weight term $(n = I, IV)$
R	-	Residence
sw	-	switch
S	-	Solid phase
tot	-	Total
0.5	-	Half height of peak

Abbreviation	Subscription
Ba	Single Batch extraction process
CC	Counter-Current extraction process
CI	Crocin I, saffron ingredient
CII	Crocin II, saffron ingredient
CRE	Chemical Reaction Engineering
$CSTR$	Continuous Stirrer Tank Reactor
DAC	Dynamic Axial Compression
DCM	Dichloromethane
$EtOH$	Ethanol
$HETP$	Height of the Theoretical Plates
$HPLC$	High Performance Liquid Chromatography
IC	Initial Condition
ID	Inner Diameter
LC	Liquid Chromatography
$LC-MS$	Liquid Chromatography – Mass Spectrometry
LDF	Linear Driving Force
MPC	Modern Preparative Chromatography
ODE	Ordinal Differential Equation
OF	Objective Function
PC	Picrocrocin, saffron ingredient
PDE	Partial Differential Equation
$Q-TOF$	Quadrupole-Time Of Flight
rpm	Rotate Per Minute
RT	Room Temperature
SBa	Sequential Batch extraction process
SLE	Solid-Liquid Extraction
SMB	Simulated Moving Bed
WLS	Weighted Least Squares

Chapter 1

Introduction

1.1 Motivation and Goal of Thesis

Plants have been considered and used throughout history for their nutritional properties and medicinal effects. The medicinal and nutritional properties of plants are due to the presence of secondary metabolites such as phenolic compounds (about 8,000), alkaloids (about 12,000), terpenes and terpenoids (about 25,000). These bioactive compounds have attracted the attention of many researchers who have focused on extracting and purifying them from natural sources for pharmaceutical, food, and cosmetic applications. Unfortunately, many studies have not fully utilised these valuable and natural compounds. One of these valuable plants is *Crocus Sativus L* . and/or saffron. Saffron is one of the most expensive spices in the world that contains compounds with medicinal properties, such as anti-cancer, anti-depression, multiple sclerosis, etc. Other applications of saffron extract and its pure components can be found in the food and cosmetic industries [1–10]. Due to the high price of saffron and the even higher price of its purified valuable constituents, this has motivated us to work on the extraction and purification of the valuable constituents of saffron in developed and highly productive processes that have never been studied before.

Therefore, the aim of this study is to contribute to the efficient extraction and purification of the valuable constituents of saffron, namely picrocroin (PC), crocin I (CI) and crocin II (CII). On the other word, we will test separation techniques such as solid-liquid extraction and solid-liquid chromatography to see if they work, and we want to quantify them, which will allow us to estimate productivities and make assessments for scale-up. Hence, we try to present technical and developed procedures to obtain reproducible and pure valuable constituents of saffron with acceptable productivity and high yield by extraction and chromatography techniques.

1.2 *Crocus Sativus L.*: Agricultural Aspects

Crocus Sativus Linnaeus is one of 85 species of Crocus, descended from the wild form *C. Cartwrightianus*. It is an autumn-flowering taxon and a triploid ((2n)×(3X)=24) infertile plant that therefore cannot form seeds [11, 12]. *C. Sativus* is known to be hysterantic, i.e. its multiplication is done via corms [13]. The more common and familiar name of *C. Sativus* is saffron and comes from the Persian word (Zarparan), which literally means "golden leaves". The stigmas of saffron flowers contain high levels of carotenoids. It is believed that this plant originated in Iran. However, Mesopotamia and Greece are also mentioned as possible regions of origin of saffron. In recent years, it has also been reported in the Kashmir region of India, in China (especially in Tibet) and in Morocco [14, 15]. The annual world production of saffron is estimated at 400 tons (in 2023), with Iran recognized as the main producer in the world (about 88% of the total). Although Iran is the main producer of saffron in the world, Spain is the largest exporter of saffron spice [16]. Each saffron flower has three crimson stigmas, which are known as saffron spice after drying. Therefore, saffron spice is not obtained from the whole plant [14, 17]. Saffron is the most expensive spice (it can cost more than 2000 dollars per kilogram) due to the number of factors, including the cost of cultivation operations, the short flowering period of only 15 days (mid or late October), the low mass of the stigmas, and the narrow cultivation areas (ISO /TS 3632 2003) [18]. Due to the high price of saffron in the world market, it is highly affected by adulteration, which is usually done by artificial colorants and the addition of external plant material to increase the orange color or mass [19]. To avoid fraud, the International Standards Organization ISO / TS 3632 2003 proposed to determine the quality by standard tests. At ISO, saffron is classified into three main classes in terms of physical and chemical characteristics such as microscopic features, contamination with plant/flower debris, moisture content (should be ≤12%) [20], and the characteristics of the three main bioactive ingredients, namely crocine (responsible for the red color), picrocrocin (bitter taste), and safranal (fragrance) [21, 22]. Several methods are used to characterise saffron, but UV-visible spectrophotometry at wavelengths $E_{1cm}^{1\%}$ 440 nm, $E_{1cm}^{1\%}$ 257 nm, $E_{1cm}^{1\%}$ 330 nm (maximum absorb wavelengths of crocines, picrocrocin, and safranal, respectively) are widely used [23–25]. Due to the adsorbance interference between crocines and picrocroicn of saffron, this method is not accurate enough [24–26]. To solve this problem, Michelli and Corradi suggested the addition of a ΔE_{PC} factor for the calculation of the amount of picrocrocin, and other authors advocated the use of complementary quantitative analyses to better determine the quality of saffron [27].

As mentioned earlier, the dried red stigma of *Crocus Sativus* is used as the saffron spice, and only the *C. Sativus* corms produce this saffron spice. Saffron is an autumn flower. The narrow leaves of saffron are 6-10 cm long and 2-3 cm wide. The flowers are almost 8 cm long and have light purple to lilac leaves. Sometimes there are red or

white stripes on the leaves. Each saffron flower contains three bright crimson stigmas that are 25-33 mm long. *C. Sativus*, as a triploid sterile monocot, is unable to produce viable seeds by crossing. Therefore, the plant is grown by vegetative propagation (see Table 1.1) [21, 28].

Table 1.1: Effective production of cormlets

Production of daughter corms
A) Shallow planting and pre-sprouting of the apical bud
B) Regular control of planted corms to prevent the spread of disease
C) Replanting corms found on the ground
D) Frequentative removal of weeds

During the spring growing season, the mother corm of *C. Sativus* produces smaller daughter corms in the surrounding area. At the end of the growing season, the daughter corms of *C. Sativus* consume the mother corm. Usually, corms are planted during their dormant period at the end of summer or beginning of fall. In the following fall season the daughter corms produce new flowers. The annual cycle growth of saffron essentially includes five main cycles that occur at different intervals depending on the area and climate. These growth stages include budding, flowering, leaf growth, development of daughter corms and corm latency [13, 21, 29]. The life cycle of *C. Sativus* begins in mid-autumn with flowering and vegetative growth, which requires water from rainfall or irrigation, and ends in spring after the formation of replacement corms. The entire life cycle lasts about 220 days (see table 1.2).

Table 1.2: Growth stages of C.sativus and corm cultivation

Corm planting	Flowering	Vegetative growth	Withering of leaves	Cormlets uprooting
September or October	November or December	December to April	May	July or August

1.2.1   Climate and Soil Conditions

Saffron is grown in very different climates. However, it is adapted to mild and sub-tropical climates and semi-arid regions. It is mainly grown in Asia, where Iran in particular accounts for about 90% of the world's saffron production [30, 31]. *C. Sativus L.* is also adaptable to a wide range of soil types, ranging from well-drained to sandy loam soils (see table 1.3) [21]. Observations show that *C. Sativus* grows better compared to cultivation at higher altitudes or in plastic tunnels on the coast with high productivity and reasonable yield. It is better to grow saffron in barren soils than in semi-barren soils. Saffron can also endure the cold winter up to -10 °C. Optimal conditions for growing saffron are sunlight and not shade, where it withers [32] (see table 1.3).

Table 1.3: Climate and soil characteristics of *C. Sativus* cultivation in different regions [21, 28, 30, 33]

Region	Rainfall	Temperature	Soil	Altitude (above sea level)
India (Kashmir)	100 mm	Sub-temperate	pH 7.2-8.4 available K_2O	32-36 °N 1600 m
Iran (Khorasan)	443 mm	Not specified	pH 8-8.1, Potassium 270 mg/Kg Clay 22.6% Sand 46%	2064 m
Italy (Navelli Highlands)	Frequent rainfall	Moderate	Not specified	Not specified
Greece (Kozani)	>500 mm	Moderate	pH 7.4 K_2O 70 mg/Kg,	710 m

1.2.2   Harvest and Post-Harvest

In saffron production, harvesting is a crucial step. Researchs show that delaying harvest by as little as two days after full flowering can significantly affect some saffron quality parameters [34]. Harvesting of saffron flowers is done early in the morning after the dew has evaporated and before the flowers fade. It is done manually and the stigmas are sorted by hand [21, 22, 34]. After harvesting of saffron flowers, the drying process takes place, which gives the stigmas of Crocus Sativus the definitive name of saffron spice and its particular organoleptic properties [20]. The ingredient responsible for the saffron fragrance is safranal, which is produced during dehydration and drying by the breakdown of picrocrocin. During the dehydration and drying process, the stigma loses almost 80% of its weight. The process is finished when the saffron stigmas have some elasticity and do not fall into pieces. In the world market, saffron stigmas are called saffron spice while they contain 12% of moisture (ISO 3632). Drying methods vary widely from country to country [21, 22, 34, 35]. Overall, they can be divided into two methods. The first method, where moderate heat is used for a long time (under sunlight and/or in rooms with air conditioning), which is a classical method, and the second method, where moderate to high temperatures are applied for a shorter time (by drying equipment), which are known as modern methods. Several studies and procedures have been carried out to optimise drying processes, including sun, shade, microwave, freeze-drying and vacuum oven (see table 1.4) [20, 24–26, 35–37].

Table 1.4: Various drying processes of saffron. RT: Room Temperature

Drying process	Final moisture content	Countries
RT and sunlight (3-10 $days$)	8-10%	Iran-India-Morocco
Air ventilated	Not specified	Not specified
Medium to high temperature	5-20%	Spain-Greece-Italy

Scientific research has shown that drying saffron at low temperatures is not suitable and affects the quality of the product [24, 25, 35]. Recent research and studies have

shown that the light color of saffron stigmas is due to a rapid drying process at high temperature [38]. The evaluation of the valuable ingredients of saffron has shown that the content of trans-crocin and safranal increases due to rapid drying at high temperatures [20, 24, 25].

1.3   Active Compounds and Properties

Saffron stigmas contain about 63% carbohydrates, 12% proteins, 5% minerals, 5% fat, and 5% crude fiber (in wt%) [39]. In addition, a large number of secondary metabolites were detected at trace levels, such as zeaxanthin, lycopene, flavonoids, and some carotenoids such as α- and β-carotene [11, 40]. The organoleptic properties of saffron are due to the presence of three types of carotenoids, namely picrocrocin, crocins and safranal [20]. These constituents are produced through the biological pathway of zeaxantins (oxidative cleavage, oxidative modifications and glycosylation) (Figure 1.2) [41, 42]. It is believed that these carotenoids are produced in the flowering phase in the cytoplasm of the cell matrix or in the chromoplasts (non-mevalonic acid pathway) [20, 43–45].

1.3.1   Crocins

Crocins are mainly responsible for the red color of saffron. Chemically, these pigments are diesters of the mono- or diglycosyl of polyendicarboxylic acid crocetin ($C_{20}H_{24}O_4$) (Figure 1.1). Among the group of crocins, crocin I or the digentiobiosester of crocetin has the highest amount, which in a high quality saffron it can be as high as 30% [46]. This compound is the most biologically active ingredient in saffron [47]. There are five crocins in saffron, which are either cis- or trans-glycosides of crocetin (Figure 1.1) [15].
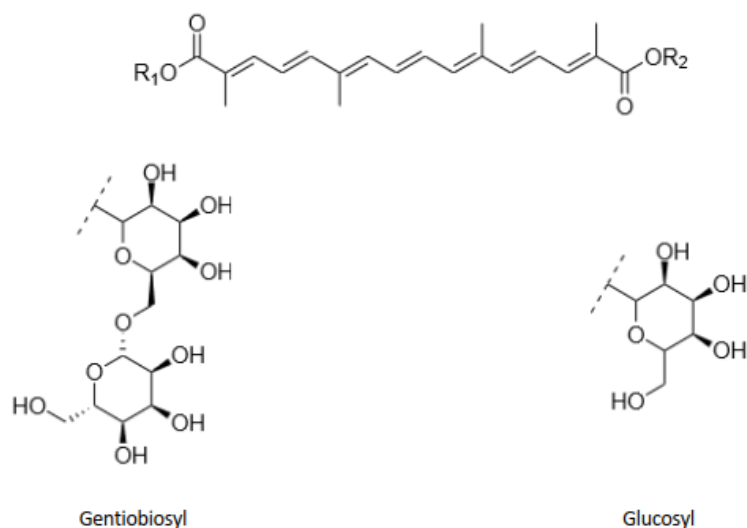
Figure 1.1: Structural features of the crocins of saffron. Crocin I (CI) ($R_1=R_2=$ gentiobiosyl-), Crocin II (CII) ($R_1=$ gentiobiosyl-, $R_2=$ glucosyl-), Crocin III (CIII) ($R_1=R_2=$ glucosyl-), Crocin IV (CIV) ($R_1 =$ gentiobiosyl-, $R_2=$ H), Crocin V (CV) ($R_1=$ glucosyl-, $R_2=$ H); Crocetin ($R_1=R_2=$ H)

Crocin I ($C_{44}H_{64}O_{24}$) is the main and major compound in saffron and has received more attention as a compound with effective medicinal properties [48, 49]. Nagatoshi proposed the biosynthetic pathway of crocin I, which starts with the cleavage of zeaxanthin and the formation of crocetin dialdehyde as the first step. In the second step, oxidation of crocetin dialdehyde leads to the crocetin compound, and at the end, glycosylation of crocetin by various glucosyltransferases leads to crocin I as the final product (crocetin-di-(β-gentiobiosyl)-ester) (see Figure 1.2) [46].
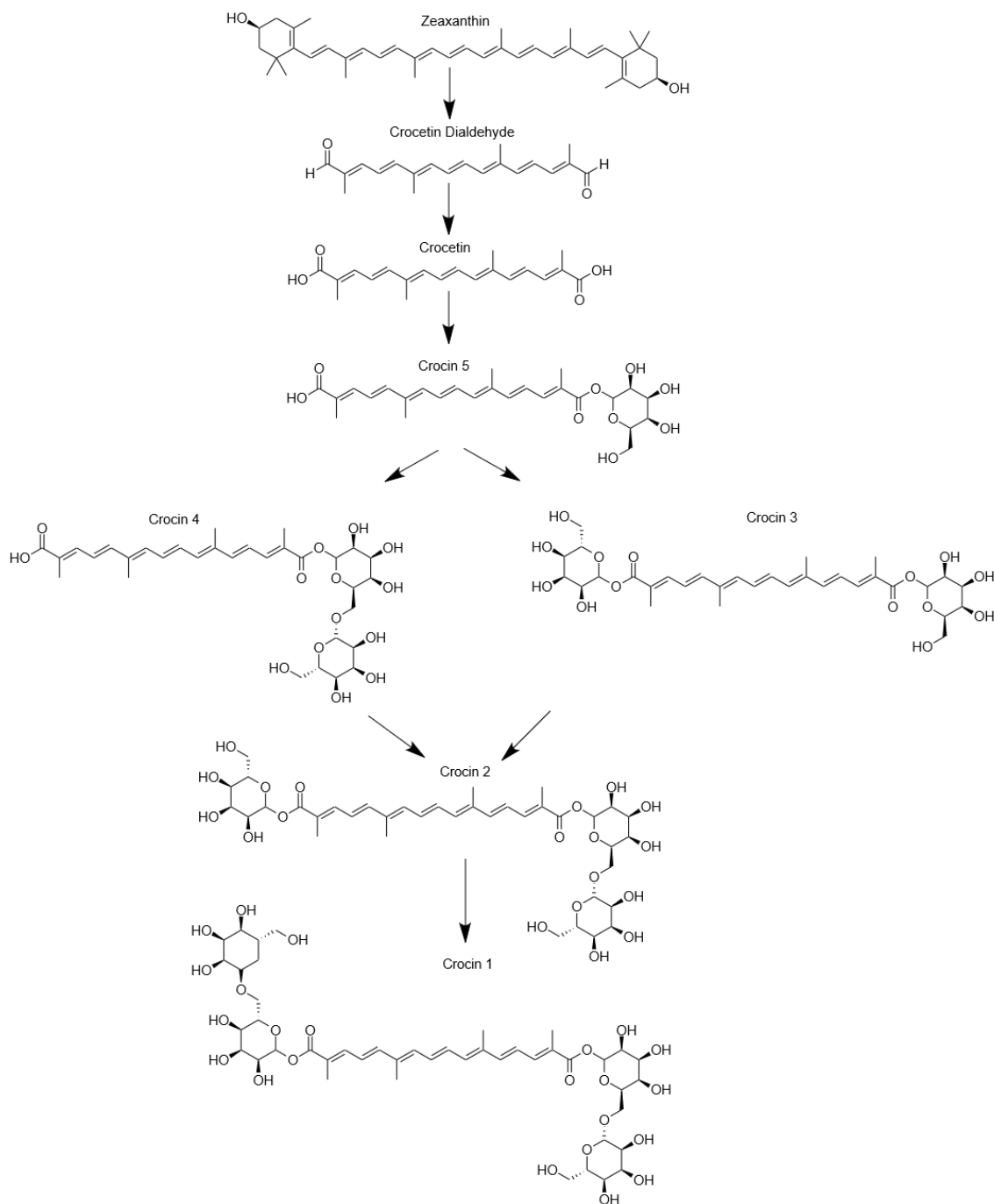
Figure 1.2: Biosynthesis pathway of crocins

It should be mentioned that trans di-gentiobiosyl ester of crocetin can be converted to the cis di-gentiobiosyl ester of crocetin under light or high temperature. Cis/trans isomers could be determined only with UV-spectra [50].

1.3.2   Picrocrocin

Picrocrocin ($C_{16}H_{26}O_7$) is the compound responsible for the typical spicy flavour of saffron and is a monoterpene glycoside that is one of the carotenoid products of the enzymatic cleavage of zeaxanthin in saffron [22]. Picrocrocin (PC) is an intermediate compound between crocin and safranal (see Figure 1.3). Picrocrocin releases the agly-

cone 4-hydroxy-2,6,6-trimethyl-1-cyclohexene-1-carboxaldehyde, HTCC, ($C_{10}H_{16}O_2$) under enzymatic action of β-glucosidase (Figure 1.3) [19, 39]. Depending on the quality of saffron, the content of picrocrocin in the dried stigmas has been reported in the range of 0.8 to 27% [51–53].

1.3.3   Saffranal

Saffranal (2,6,6-trimethyl-1,3-cyclohexadiene-1-carboxaldehyde) is a terpene aldehyde responsible for the fragrance and aromatic odor of saffron. It is a volatile component and has very low solubility in water [15, 51]. Safranal is released from picrocrocin by enzymatic action during drying process. Therefore, the drying process is a critical step in the production of saffron spice from *C. Sativus*. During the drying process, picrocrocin is hydrolyzed by β-glucosidase to the aglycone HTCC. At the end, safranal is released by dehydration of HTCC (Figure 1.3) [54].
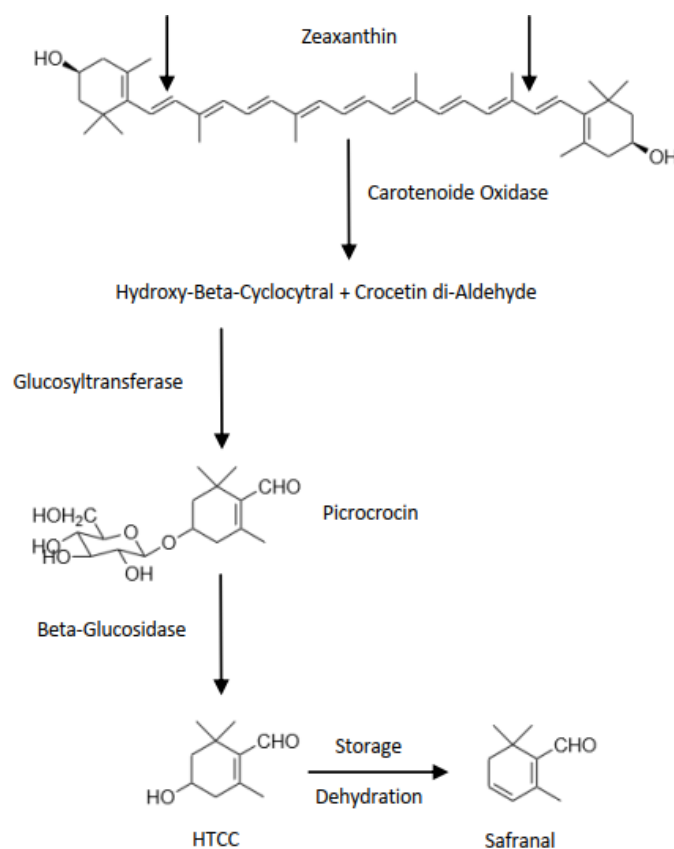
Figure 1.3: Biosynthetic pathway of picrocrocin and safranal in saffron

1.3.4   Solubility

The compatibility of a solvent to dissolve a target molecule (solute) depends on the polarity of the solute, the polarity of the solvent, and the solubility of the solute. The main constituents of saffron (picrocrocin and crocins) belong to the carotenoid family. Carotenoids are lipophilic compounds that are insoluble in water, but soluble in some solvents such as chloroform, acetone and alcohol. However, due to the sugar

moieties such as glucosyl and gentiobiosyl in the chemical structures of picrocrocin and crocins, they are polar carotenoids in nature [12, 15, 18, 51, 55]. Therefore, due to the sugary functional groups in these compounds and according to the "like dissolves like" rule, picrocrocin and crocins have the highest solubility in polar solvents. Polar solvents, such as water and ethanol-water mixture, showed higher solubilities power and capacity for the dissolution and extraction of picrocrocin and crocins from the saffron stigmas [47, 51].

1.4 Applications of saffron and its ingredients

The first use of saffron dates back to the seventh century BC in the Assyrian botanical treatise compiled under Ashurbanipal. It was used for its culinary properties and as a medicinal plant (herbal cure). Overall, saffron was used by many civilizations primarily as a nutritional spice. The uses of dried saffron stigmas in the food industry can be divided into three main aspects: (a) natural food colorant, (b) food flavoring, and (c) antioxidant. Antioxidants are not only used in the pharmaceutical industry, but are also increasingly used in the food industry. Many foods contain unsaturated fatty acids, which are easily spoiled by oxidation. Using antioxidants to prevent food spoilage is a good solution. The protective effect of these compounds has extended the shelf life of foods and facilitated their storage. There are various synthetic antioxidants and colorants that prevent oxidation and are used as food additives. However, with the emphasis on using natural ingredients in food to protect people's health, the food industry is looking for natural additives that are more likely to be accepted by consumers. Another popular application of saffron is its use in the cosmetics industry as a natural colorant [1, 56, 57].

The most important application part of saffron goes back to its medicinal motives. Hippocrates in 5-4th century BC, Diokles in 3rd century BC and Discorides in 1st century AD used saffron to treat eye diseases, such as corneal diseases and eye infections, and other diseases such as ulcers, earaches and toothaches. It was commonly known as a sedative and hemostatic ingredient [58]. In recent years, the literature dealing with the use of saffron as a medicine to treat various diseases such as anti-tumour, anti-oxidant, antidepressant and sometimes used for phototherapy , proving the increasing interest of scientists in the therapeutic effects of saffron ingredients [15, 59–69]. Studies show that the main ingredients of saffron have various pharmaceutical effects. Treatment of cancer with conventional methods such as radio-, chemo-, photolysis- and catalytic therapy is expensive, difficult and has many side effects [70]. Therefore, due to the low toxicity, strong effects and low side effects of natural products, the demand for them is increasing [71, 72]. It has been proven that fruits high in carotenoids and a plant-based diet have a protective effect via repairing activity, reducing DNA damage and increasing LDL oxidation effect [73]. Saffron contains many

carotenoids with anti-cancer properties, mainly influenced by the following effects:

a) Influencing the proteins responsible for cell division (cytoskeletal proteins)

b) Inhibition of key DNA enzymes

c) Inhibition of the chain reaction of free radicals [74]

Another pharmaceutical property of saffron is its antidepressant effect. The disease and mortality due to depression are increasing considerably in the world and is the fourth disease causing incapacity worldwide [75]. Among the cited literatures, crocin I and crocetin have shown dominant antidepressant effect. Therefore, the use of saffron stigmats for the treatment of depression is steadily increasing [15, 67–69, 76]. Observations show that higher concentrations of crocin (and lower doses of crocetin) have an antidepressant effect in mice, implying that crocetin is more effective [76]. Studies by a Japanese group show that after crocin use (oral administration), these ingredients are hydrolyzed to crocetin before and during enteric absorption [77].

1.5 Analytical Techniques

An analytical technique is a procedure for determining the physical and chemical properties of a chemical molecule, substance, or mixture. There are a variety of analytical techniques, from gravimetric analysis (weighing), titrimetric analysis to the use of highly specialized equipment [78]. The qualitative and quantitative characteristics of a saffron sample are very important to the relevant industries. The most common analytical techniques are UV-vis spectrometry, thin layer chromatography (TLC), high performance liquid chromatography (HPLC) and gas chromatography (GC). NMR and IR analysis techniques are less common [30, 51, 79–81]. Many researchers use TLC, HPLC and GC analysis techniques to specify a saffron sample.

1.5.1 Thin Layer Chromatography

One of the most common and well-known chromatography techniques is thin layer chromatography (TLC), which is used to separate non-volatile mixtures. TLC is performed on a plate made of an inert substrate such as aluminum foil, plastic, or glass, usually coated with silica gel, cellulose, or alumina as an adsorbent. This thin layer of adsorbent is called the stationary phase. After the sample is applied onto the plate, the solvent(s) is drawn up the plate as the mobile phase by capillary movement. Due to the different affinity of components to the adsorbent, they move in different speeds, which leads to the separation of the components. One of the analytical methods used to characterize saffron is the TLC technique. The International Organization for Standardization (ISO) uses TLC and spectrophotometry to analyze the color strength, volatile content and moisture content of a saffron sample (ISO 3632/ TS or ISO /DIS

3532.2) [37].

Crocins and picrocrocin of a saffron crude extract can be separated on TLC by the solvent composition water-acetic acid-n-butanol (1:1:4). Safranal is extracted with diethyl ether and separated on TLC with hexane-ethyl acetate (9:1). After the determination of the main constituents of the saffron extract by TLC, they are analyzed spectrophotometrically at their extinction coefficient and maximum absorption wavelength (10100, 250 nm for picrocroicn and 89000, 443 nm for crocins) [37, 82–85]. One of the developed TLC methods is high performance thin layer chromatography (HPTLC), which is used for better separation of saffron components by TLC technique [37, 86–88].

1.5.2   Gas Chromatography

One of the most common types of chromatography is gas chromatography (GC) and gas chromatography-mass spectrometry (GC-MS), which are used to separate and analyze components that can be evaporated without decomposition, such as saffranal [80, 89–91]. Saffron diethyl ether extract or supercritical carbon dioxide extract containing saffranal and probably some other impurities are usually separated and purity tested by HRGC-MS. Cossignani used a Perkin-Elmer Auto System Gas Chromatography equipped with split/splitless injector and FID. Separation was performed on an HP1-ms capillary column (30 m × 0.25 mm i.d., 0.25 μm f.t., Agilent technologies Inc., USA). The temperature of the injector and detector was set at 250 and 300 °C, respectively. The oven temperature was held at 50 °C for 3 minutes and then increased to 180 °C in 43.33 minutes (at a flow rate of 3 °C/min), then increased to 250 °C in 4.66 minutes (at a flow rate of 15 °C/min), and then held for 5 minutes. In this procedure, the flow rate of the carrier gas (He) was 1 ml/min; the injection volume was 1 μl with a split ratio of 1:70 [37].

1.5.3   High Performance Liquid Chromatography

Among the aforementioned techniques, high-performance liquid chromatography is the more powerful, accurate, and sensitive technique for the analysis and determination of adulterants. HPLC, also known as high-pressure liquid chromatography, is a powerful technique for separating, identifying, and quantifying each compound in a composite sample. The HPLC instrument consists of eluent, degasser, pumps, injector, column, column oven and detector. The pumps pass the mobile phase containing the sample mixture under high pressure through a column filled with a solid adsorbent. The different migration velocities of the components in a so-called separation column lead to the separation of the components. The driving force of separation is usually due to the different distribution equilibria of the components between stationary and mobile phases. This technique is particularly suitable for the separation

of active pharmaceutical ingredients (API) and biomolecules [82]. There are a variety of chromatographic techniques that differ in stationary and mobile phases. The most common chromatography method is adsorption chromatography (about 80%). In adsorption chromatography, there are two types of stationary phases:

a) The normal (polar) phase, which consists of silica gel. Silica gel is amorphous silicon dioxide (SiO_2) with a very porous structure and contains siloxane groups (-Si-O-Si-O -) and silanol groups (-Si-OH), which are very polar and reactive

b) Reversed phase (RP, non-polar), i.e. coated silica with C_n (C_4, C_8, C_{18} etc.)

The selection of the stationary phase depends on the polarity of the compound to be separated. In almost all saffron projects, a reverse phase C18 (RP-C18) HPLC column is used to separate, identify, and quantify the components of a saffron extract. These components (picrocrocin and crocins) can be separated on the HPLC-C18 column (L_c=150 mm, d_c=4.6 mm, 5 µm, 120 Å) by a gradient elution method of water (A) and acetonitrile (B)(20% of B to 80% B) at the wavelengths of 254, 440, 330 nm (wavelengths with highest absorbance value of picrocrocin, crocines and safranal, respectively) [16, 54, 82, 92–94]. The usual detector is a diode array detector (DAD) which can be combined with various mass spectrometry techniques such as electrospray ionization (ESI), quadrupole time-of-flight (Q-TOF) and various tandem mass spectrometry techniques. Mass analysis can be performed in both positive and negative modes with a scan range and scan rate of 100-1200 m/z and 1.3 scans/s, respectively. In the on-line HPLC-MS analysis technique, the output of the HPLC detector is the input of the MS instrument. The mass of the target molecules usually adduct to hydrogen $[M+H]^+$, sodium $[M+Na]^+$, potassium $[M+K]^+$ or ammonium $[M+NH4]^+$ [11, 22, 52, 81, 94, 95].

Ultra Pressure Liquid Chromatography (UPLC) is another method of adsorption chromatography. In this method, the back pressure of the column is high due to the very small particle size of the stationary phase. The use of a UPLC system with an RP-C18 column (2.1×100 mm, 1.7 µm) for the separation and analysis of the components of the saffron extract shows that the separation of all crocines is achieved in less than two minutes, which is very suitable for rapid analytical studies [15].

1.6   Isolation and Purification Techniques

1.6.1   Extraction

The definition of extraction in chemistry is a separation process involving the separation of a substance from a starting material (matrix); for example, liquid-liquid extraction (LLE), solid-phase extraction (SPE), and solid-liquid extraction (SLE) and/or leaching. Leaching is a process of dissolving and extracting a substance (by

the liquid phase) from the solid material in a solid-liquid mixture. This process is known as an extraction process, especially in the chemical industry. The leaching process involves three basic steps: contact, separation, and extraction. On the other hand, the term "extract" refers to the substance(s) obtained by extracting a portion of a raw material, often using polar and/or non-polar solvents. The equilibrium condition described by partition theory is the distribution of an analyte between two phases. This is based on the theory of how solutes move from the starting material (solid or liquid) into the extracting solvent. It should be noted that the term "washing" is also sometimes used to refer to an extraction process in which some impurities are extracted from the solvent containing the target molecules (extracting solvent) [96, 97].

The solid-liquid extraction method is usually used to extract the valuable ingredients of saffron. Saffron contains mainly picrocrocin and apocarotenoids (crocins), the quantity of which determines the value and quality of a saffron sample. The quality of a saffron sample is influenced by various factors such as cultivation, drying conditions and extraction methods used [37]. Extraction plays the most important role in saffron utilization. Therefore, many different techniques have been used to increase the quantity and quality of saffron extraction. Several common techniques, namely stirring, supercritical carbon dioxide (SC-CO2) and ultrasound-assisted extraction (UAE), are used to extract the main constituents of saffron. However, for the extraction of saffron aroma compounds such as safranal, polyphenols, anthocyanins, kaempfrol and its derivatives (flavones), techniques and equipment such as steam distillation (SD), Vacuum headspace method (VHS), ultrasound-assisted extraction (UAE), solvent-assisted aroma evaporation (SAFE), supercritical carbon dioxide extraction (SC-CO2) and microwave-assisted extraction (MAE) are used [12, 15, 37, 47, 54, 80, 89, 98–109].

In saffron extraction, the leaching technique with continuous stirring on a magnetic stirrer is more popular and effective to achieve acceptable extract amount. For this reason, the stirring method with suitable solvents has been studied in more details in the literatures. Jose Luis Iborra used a number of different solvents such as acetone, acetonitrile, diethyl ether, isopropanol, methanol, ethanol, ethanol-water (50%), methanol-water (80:20) and water for the extraction of saffron ingredients. In this study, 10 mg of saffron powder was mixed with 1 ml of the above mentioned solvents and shaken for 1 hour at room temperature and in a dark place. The remaining wet powder was separated and extracted two more times. At the end, the extracts were combined, filtered, freeze-dried and stored at -20 °C. The polar solvents such as water and ethanol-water (50%) showed more power and capacity for the extraction of saffron components [47, 51]. In another study, 100 mg of ground saffron was added to ethanol-water (80:20) and centrifuged at 5000 rpm for 10 minutes. The procedure was repeated three times; then the supernatants were separated and analyzed. The

total weight percentage of saffron components was 20.07% [82].

Like the other plants, saffron has some nonpolar compounds. In an interesting study, 50 mg of saffron powder was defatted and pre-extracted with dichloromethane (DCM) in Soxhlet apparatus for 12 hours. The remaining powder was added in 400 ml ethanol-water and mixed with a high-speed mixer (9500 rpm) for 4 minutes. The procedure was repeated three times. The saffron extract was concentrated in a rotary evaporator (at 40 °C) and dried in a freeze dryer [15]. In another study, Sánchez used cyclohexane to reduce the co-extraction of non-polar components [23, 53]. Due to the presence of sugary structures (gentiobiosyl and glucosyl) in picrocrocin and crocines, they are highly soluble in polar solvents, especially in water and ethanol, which was observed in all literatures.

Due to the use of large amounts of solvents and the lengthy extraction time, the reported extraction methods are not yet economical enough for the recovery and purification of picrocrocin and crocins. Thus, saffron has a great potential in terms of extraction and purification that has not yet been fully exploited. Therefore, this raises an open question: are there developed batch and continuous extraction procedures to achieve the reproducible and acceptable productivity of saffron's valuable constituents?

1.6.2 Chromatography

The crude extract of a plant or the chemical synthesis of a desired product usually contains impurities or by-products. Therefore, separation and purification problems must also be solved in addition to optimizing the extraction and/or reaction conditions. A number of methods known from thermal process engineering are available, one possible separation method, usually expensive, is chromatography. Chromatography is a separation technique for separating a mixture into its components. The origin of chromatography and the first experimental work can be traced back to Tswett (1906). The name is borrowed from the Greek word chromos (color). Chromatography is a separation process in which the components of a mixture are divided into two phases, the mobile phase and the stationary phase. Unequal distribution equilibria are the driving force for separation. There are a variety of chromatographic methods depending on the nature of the stationary and mobile phases. Adsorption chromatography is the most widely used chromatographic method (about 80%), using relatively small and nonionic solid particles as the stationary phase. Isolation and purification of saffron components is usually performed by analytical or preparative adsorption chromatography. Chromatography aimed at obtaining "pure substances" is referred to as industrial or preparative chromatography [110, 111].

S.Z. Bathaie and et.al were able to separate and purify the components of Iranian saffron by adsorption column chromatography. All the constituents were isolated and

analyzed using a reversed phase HPLC column (C18). Crocin and picrocrocin were purified using a classical glass column (2×80cm) packed with alumina 90-active as stationary phase. Jose Luis separated and purified metabolites of saffron by analytical and preparative TLC on alumina in the same study. Quantitative analysis was performed on a C18 HPLC column. The purified picrocrocin and crocin had yields of 88% and 70% with purities of 98% and 70%, respectively [14, 51]. Other studies show that crocin I can also be obtained by the fast centrifugal partition chromatography (FCPC) technique. In the FCPC technique, the upper phase of hexane:ethyl acetate:ethanol:water (1:8:4:7) served as the mobile phase and the lower phase as the stationary phase. The yield of crocin I obtained was 48% (Eq. 2.103) (based on saffron extract) [15].

In summary, the isolation and characterization of the saffron components by high performance liquid chromatography is well known and common. Nevertheless, the number of studies on the purification of the valuable components of saffron is not very much. On the other hand, the purified picrocrocin and crocin(s) are extremely expensive and very important for related industries, which means that there is still a great potential for the purification of the valuable ingredients of saffron that has not been very well exploited until now. In this study, analytical and large-scale, low-cost preparative chromatographic techniques are used to separate and purify the components of saffron extract, namely crocin I, crocin II and picrocrocin.

1.6.3   Crystallization

Crystallization is a process of solid formation in which molecules and atoms are arranged in a regular structure called a crystal. Crystallization is also a separation and purification technique in which a mass transfer of a dissolved target molecule occurs from the liquid phase to the almost pure crystalline phase. Some of the methods of crystal formation are freezing, precipitation from a solution, and very rarely precipitation directly from a gas. The properties of a crystal depend on some factors such as temperature, atmospheric pressure and time of liquid evaporation. Crystallization occurs in two main steps, nucleation and crystal growth. Nucleation refers to the formation of a crystalline phase from a supersaturated solvent or supercooled liquid; crystal growth refers to the increase in size of the small crystals formed, leading to a crystal state. Montalvo-Hernández B. applied the crystallization technique to separate and purify crocines from an ethanolic (80%) saffron extract. It is clear that temperature plays a very important role in the crystallization process and has an effective influence on the purity and yield of a crystal obtained. After testing different temperatures, the results show that at temperatures lower than -5 °C, the two steps of nucleation and crystal growth are faster, resulting in lower purity and quality of the product. On the other hand, higher temperatures lead to slower crystallization with lower yield. The reason of this kind of behavior back to the high solubility of

these polar carotenoids. The analysis shows that pure crystals are formed at -5 °C; therefore, this temperature was considered to be the optimum temperature for the crystallization of crocins. Crystallization of crocins at this temperature was performed twice. In the first crystallization, the purity was 85% and the amount of crocin obtained was 17% of the stigma powder. To increase the purity of the obtained crystals, they were washed with acetone and dissolved again in 80% ethanol solution for the second crystallization (recrystallization). After recrystallization, the purity and yield of the obtained crystals of the total crocins were 97% and 10%, respectively [12].

The crystallization method is not able to purify each crocin individually with high yield. Hence, this method was not an option for us and is not further discussed.

1.7 Structure of Thesis

The following structure was chosen for the thesis in order to achieve the goal stated in section 1.1.

Chapter 1: This chapter is about all the details of *Crocus Sativus L.* (saffron). Saffron is the most expensive spice in the world and its name comes from Persian word *Zarparan*, which literally means "golden leaves". The production of high quality saffron begins with the agricultural aspects such as climate, soil conditions, harvest and post-harvest (drying and storage). Each saffron flower has three red stigmas. After the stigmas are harvested and dried, they become saffron spice. Saffron stigmas contain three main categories of constituents, namely picrocrocin, apocarotenoids (crocins) and safranal, which are responsible for the flavor, color and fragrance of saffron, respectively. Saffron and its valuable ingredients are used in the food, cosmetic and pharmaceutical industries. In recent years, researchers have become increasingly interested in the effects of the ingredients of saffron namely picrocrocin and crocins as the antidepressant, antioxidant and anti-cancer agents. Therefore, efforts to separate and purify these compounds by techniques such as extraction and chromatography have increased. However, the reported separation techniques are not yet economical enough to provide picrocrocin, crocin I and II on a large scale.

Chapter 2: In this chapter, the theoretical background of separation techniques such as extraction and chromatography is explained. These techniques follow a general structure, (a) principle and fundamentals, (b) process variations, and (c) modeling. In the Principle and Fundamentals sections, the key thermodynamic and kinetic parameters for each separation technique are well-defined. In the Process variants and Modeling sections, the theoretical background of the key experiments, methods and procedures, mass balance equations, and subsequently formulated mathematical solutions for each separation process are clarified. Finally, the performance criteria such as productivity, recovery yield and purity for each separation process are defined and

formulated.

Chapter 3: This chapter contains the experimental program and is divided into three main sections, namely preliminary experiments, solid-liquid extraction, and solid-liquid chromatography. At the beginning, some general preliminary experiments are performed. The preliminary experiments concern the stability of the components picrocrocin, crocin I and crocin II in different compositions of aqueous ethanol solutions, LC/MS analyzes of the mentioned components and the preparation of calibration curves for the quantitative analysis of the unknown concentrations are explained. The solid-liquid extraction section also includes preliminary experiments as a prerequisite for the main extraction experiments. These include pre-extraction of saffron powder by Soxhlet to remove some unwanted compounds from the saffron, exhaustive extraction to determine the initial concentration of picrocrocin, crocin I and crocin II in the treated saffron powder, determination of kinetic and equilibrium states to find the right time for the main extraction experiments. Then, the planned closed single batch extraction (single batch), the extraction in several successive batches (Multiple sequential batches) and the continuous counter-current extraction operation are explained.

The last part of this chapter deals with the solid-liquid chromatography, which also starts with some preliminary experiments, including sample preparation as the chromatography feed, packing of the preparative column by dynamic axial compression (DAC) technique, and investigation of retention times and efficiency of the packed preparative column. In the next section, the main experiments are investigated. At first, the effects of different volume fractions of the modifier (ethanol), under isocratic elutions, on the retention times of picrocrocin, crocin I and crocin II, on an analytical C18 column, and the column efficiency are investigated. In other words, the analytical-scale isocratic elution experiments are used to study the effects of different volume fractions of the modifier on the Henry constant (isothermal linear equilibrium parameter) of picrocrocin, crocin I and crocin II. The Henry constants of the components are used to develope a three-step gradient elution that increases throughput, reduces cycle time, and maximizes productivity while maintaining acceptable product purity and recovery yield of the target components. In the end, the developed three-step gradient elution method is scaled-up to the peparative chromatography-based purification.

Chapter 4: This chapter contains the experimental results, interpretation and discussion. In the first section, the results of the general preliminary experiments including the highest stability of the components in 80% (vol%) ethanol aqueous solution , the retention times and the mass analysis of picrocrocin, crocin I and crocin II by LC /MS analysis, and calibration curves are presented. The second section deals with the solid-liquid extraction results. The results of the preliminary experiments showed that almost 50% of the treated saffron contains picrocrocin, crocin I and crocin II, and

that the equilibrium state of all components in a solid-liquid batch extraction process is reached in 15 minutes. Knowledge of the initial concentration of the components and their equilibrium time in a batch extraction process formed a favorable condition for conducting experiments on extraction in a closed single batch process and in several successive batches (multiple sequential batches) to estimate the thermodynamic and kinetic parameters of each component. These parameters were used in modeling the continuous counter-current extraction process. In the continuous counter-current extraction model, the influence of parameters such as thermodynamic and kinetic parameters, number of stages, phase ratio, and the residence time on the outlet concentration of components from a continuous countercurrent column is studied and a wide range for each of these parameters is investigated. It is worth mentioning that the continuous counter-current model can be reduced to a batch model. Therefore, the results of the parameter study can also be applied to the batch scale. At the end, the productivity and recovery yield of the counter-current process were higher thean the batch extraction process.

The fourth section is located to solid-liquid chromatography. This section begins with the thermodynamic parameters and/or Henry's constant of each constituent obtained by isocratic elution of the constituents in various volume fractions of modifier (ethanol) between 0.05 and 0.5 (volume/total volume). Then, the kinetic parameter and/or the number of theoretical plates and subsequently HETP of each associated peak are estimated. The parameters of Henry's constant and the number of theoretical plates are used in the process modeling of the three-step gradient elution. The developed three-step gradient elution was performed several times on an analytical C18 column. The retention times of the separated components agreed well with the predicted times, and the separation profile was repeatable. Before transferring the three-step gradient elution to a preparative column, the column efficiency of the preparative packed column with uracil and a real sample of a saffron crude extract was investigated. The peak shapes, retention times and separation profiles were quite acceptable and repeatable. Finally, the preparative three-step gradient elution based purification was implemented for the purification of picrocrocin, crocin I and crocin II. The separation profiles in both analytical and preparative columns were repeatable. The productivity, recovery yield, and purity were quite acceptable.

Chapter 2

Relevant Theoretical Background of Separation Techniques Used

In this chapter, the theoretical background of the two main separation methods, namely extraction and chromatography is reviewed. There are several techniques for each of these methods.

In extraction, one of the known procedures is solid-liquid extraction and/or leaching. In this process, the components are extracted from the raw material, called the solid phase, by a suitable extraction solvent, called the liquid phase. The selection of solvent depends on the polarity of the component(s) to be extracted. The distribution of a solute between two phases is called the equilibrium condition, which is based on the theory of how solutes move from the starting material to the extract solution (partition theory) [1, 97, 112, 113].

The crude extract of a plant usually contains some impurities. Therefore, not only extraction conditions must be optimized, but also separation and purification problems must be solved.

One of the most reliable separation and purification techniques is adsorption chromatography. Adsorption chromatography is a separation technique in which the compounds of a mixture distribute between stationary and mobile phases. An unbalanced distribution equilibrium and different migration rates are the driving forces for the separation of the components. In the end, the analytical separation method is scaled up to preparative chromatography for the purification target [97, 111, 114–118].

2.1 Solid-Liquid Extraction

2.1.1 Principle

The extraction method used in this study is known as the solvent extraction method. The principles of this method are very simple. In this method, the target molecule(s) is dissolved in a suitable solvent and then extracted from the plant. The process is carried out in a specific time and at a specific temperature. This process is also known as solid-liquid extraction (SLE). The main objectives of the extraction process can be (a) high yield: the target molecules are almost completely extracted, (b) high purity/selectivity: the final extract has a low content of unwanted co-extracted components, (c) high sensitivity: the obtained extract can be used for various quantification analysis methods that produce accurate calibration curves, (d) low limit of detection: the compounds of a crude extract are detected and quantified in low amounts [1, 97, 112]. Depending on the process scale, each of these goals is emphasized. For example, in the analytical scale, limit of detection, sensitivity, and selectivity are the most important goals. However, in semi-preparative, preparative and industrial separation, the purity and yield are the most important properties [1, 97, 112].

Extraction is a mass transfer process of a target molecule(s) from one phase to another. The extraction mechanism of a target molecule(s) from a solid matrix (plant) involves five steps (Figure 2.1) [1, 97, 112, 113]:

(a) Transfer of the solvent from the liquid phase to the solid surface and its enclosure

(b) Diffusion of the solvent into the solid phase by molecular diffusion

(c) Desorption of the target molecule(s) from the solid matrix and dissolution into the extraction solvent

(d) Penetration of the solution containing the target molecule(s) by molecular diffusion through the solid phase to the solid surface

(e) Transfer of the solution from the solid surface to the main liquid phase by forced or natural convection
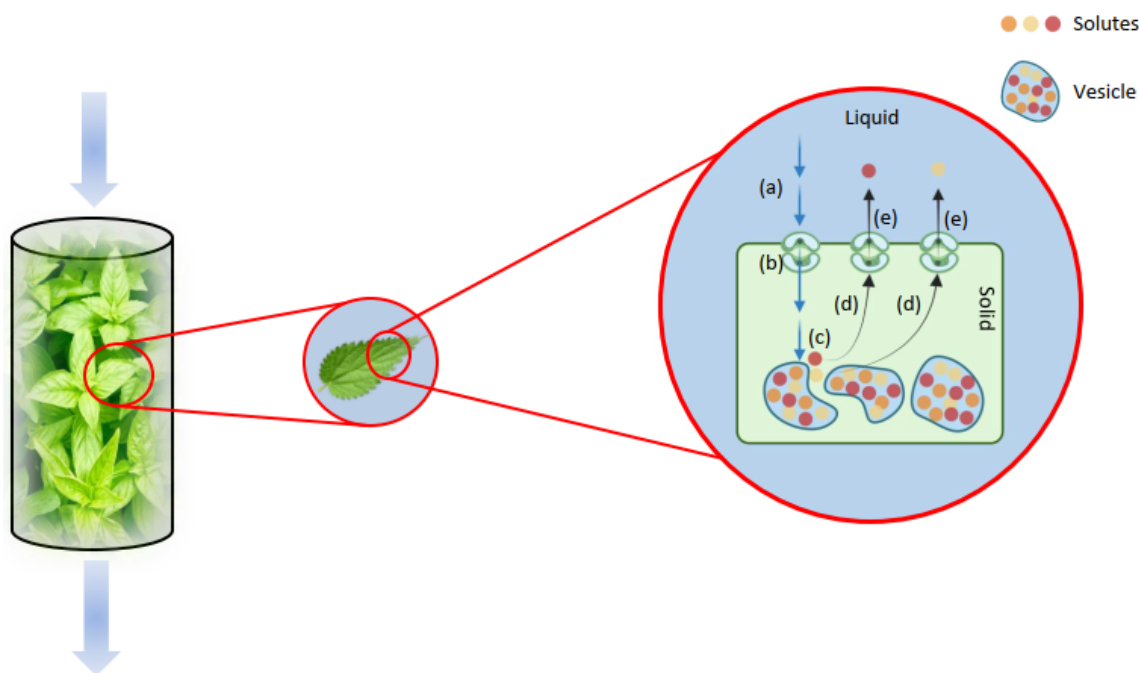
Figure 2.1: Schematic representation of the mechanism of the solid-liquid extraction process [112]

In the SLE process, there are five major factors of action, namely the thermodynamics and/or the duration of the process, the polarity of the solute and the solvent, the temperature, the preparation of the solid, and the dosage (ratio of starting material to solvent). These factors affect the solubility of the target molecules and the yield of the extraction process. Understanding them can help control and improve the efficiency of the process [1, 97, 112, 113].

Between these factors, the thermodynamic and subsequently the kinetic parameters, as well as the polarity of the solute and the solvent, are inherent and cannot be changed in the given condition. In an extraction process, **thermodynamics** is known as process duration. It is a valuable piece of information to know how long to stir the solvent and the solute (solid). To find the right extraction time, we need to find the partition coefficient, known as the thermodynamic parameter, and then the equilibrium time of each molecule between two phases. This valuable information is obtained through concentration analysis experiments [1, 97, 112, 113].

The **polarity** of solute and solvent, which means the effectiveness/compatibility of a solvent to dissolve a target molecule (solute), depends on the polarity of the solute, the polarity of the solvent, and the solubility of the solute. Polarity is a chemical property in which the opposite directions of a molecule or its chemical groups have a positively charged end and a negatively charged end. A molecule can be polar, slightly polar, or nonpolar. Polar solvents can dissolve polar compounds and nonpolar solvents can dissolve nonpolar compounds. This process is commonly known as the "like dissolves like" principle. A common example of this principle is the dissolution

of sugar as a polar compound in water as a polar solvent. In the structure of the main components of saffron (picrocrocin and crocins), there are sugar units, namely gentiobiosyl and glucosyl. The presence of sugar structures has led to the polarization of these compounds. Therefore, the polarity of the solvent plays a very important role here, which means that non-polar solvents are not suitable for the extraction of the main constituents of saffron. To extract picrocrocin and crocins with high yield and reasonable productivity, polar solvents such as water, ethanol or a composition thereof should be used [1, 97, 112, 113].

Other factors are not inherent and can be changed. For instance, temperature affects the solubility of a target molecule(s). An increase in temperature results in a significant increase in the solubility of a solute. We can again use the example of sugar. At room temperature, sugar is soluble in water until the solution is completely saturated; however, in warm and/or hot water, the solubility of sugar increases significantly and more sugar dissolves in it. However, the use of high temperatures is not always beneficial. Some compounds are degradable at high temperatures. The extraction of the main compounds of saffron is performed very well at room temperature. On the other hand, picrocrocin is degradable to safranal at high temperatures. Therefore, extraction at room temperature is a reasonable choice [1, 97, 112, 113].

Preparation of the solid is another important factor that can affect the yield of the extraction process. The solid phase of an SLE procedure may consist of dried or fresh, whole or powdered samples. The smaller particle size creates a larger contact area between the solid and liquid phases, which creates favorable conditions for mass transfer of target molecules. Therefore, dried powder samples are usually preferred over fresh whole samples [1, 97, 112, 113].

The next modifiable important factor is dosage (phase ratio), i.e., the mass and/or volume ratio between the solid phase (S) and the liquid phase (L). The performance of an extraction process increases the higher the feed to solvent ratio. A low dosage means a large amount of solvent, which consumes more energy to remove the solvent. Therefore, the dosage should be as high as possible without compromising the desired yield of the process. In a batch extraction, a low dosage is usually used, while in a continuous extraction, a high dosage is usually used [1, 97, 112, 113].

It should be noted that other factors such as solid phase particle size, process type (batch or continuous), and flow rate ("rotation rate" for batch extraction and "flow rate" for continuous counter-current extraction) are other important parameters. All mentioned factors play an important role and should be considered in the extraction process [1, 97, 112, 113].

2.1.2   Phase Equilibrium

In a **closed single batch extraction** process, the distribution of a constituent be-tween two immiscible phases occurs when the constituent can pass from one phase to another. After a certain time, the extraction state changes to the equilibrium state $(t \rightarrow \infty(eq))$, which means the mass amount of component i in solid phase is in equilibrium with the mass amount of component i in liquid phase [1, 97, 111, 112]:

$$Mass \; amount \; of \; i \; in \; solid \; phase \leftrightarrow Mass \; amount \; of \; i \; in \; liquid \; phase \tag{2.1}$$

Or

$$m_{i,S} \leftrightarrow m_{i,L} \tag{2.2}$$

Absolute mass definitions lead to the mass fraction of component i in both phases:

$$x_{i,L} = \frac{m_{i,L}}{m_L} \tag{2.3}$$

$$x_{i,S} = \frac{m_{i,S}}{m_S} \tag{2.4}$$

and the relative mass definitions (per volume) lead to the concentration of component i in both phases (c and q):

$$c_i = c_i(x_{i,L}, x_{i,S}, \rho_L) \tag{2.5}$$

$$q_i = q_i(x_{i,L}, x_{i,S}, \rho_S) \tag{2.6}$$

Therefore, according to the density of liquid and solid phases (ρ_L and ρ_S) the concen-tration (per volume) of component i in both phases are:

$$c_i = \frac{m_{i,L}}{V_L} \tag{2.7}$$

$$q_i = \frac{m_{i,S}}{V_S} \tag{2.8}$$

Here $m_{i,L}$, m_L, V_L, $m_{i,S}$, m_S and V_S are the mass of component i in the liquid phase, mass of liquid phase, the volume of liquid phase, the mass of component i in the solid phase, mass of solid phase, and the volume of solid phase, respectively. Hereby the two volume fractions of the total volume V_{tot} can be defined as the volume fraction of

the liquid phase:

$$\varepsilon_L = \varepsilon = \frac{V_L}{V_L + V_S} = \frac{V_L}{V_{tot}} \tag{2.9}$$

It should be mentioned that V_L refers to the volume of the external liquid phase, and V_S comes from balk density of the saffron powder. Consequently the volume fraction of the solid phase:

$$\varepsilon_S = 1 - \varepsilon_L = 1 - \varepsilon \tag{2.10}$$

Volume fractions of the solid and liquid phases can be used in the phase ratio definition:

$$F = \frac{1 - \varepsilon}{\varepsilon} \tag{2.11}$$

This phase ratio is a volume base dosage of solid phase to the liquid phase. Other definition of dosage (D_S) in the extraction process is the ratio of the mass of the solid phase $(m_S(\varepsilon, \rho_S))$ to the volume of the liquid phase. In addition to ε, we will use below also a dosage of the solid phase defined as:

$$D_S = \frac{m_S}{V_L} \tag{2.12}$$

For the other equations, we follow the volume-based concentrations (equations 2.7 and 2.8). Before presenting the mass balance equations, we define the equilibrium situation, i.e. the compositions of the two phases which establish in a closed system after infinite time $(t = \infty(eq))$. The equilibrium state is usually represented by the extraction partition coefficient and/or the extraction distribution coefficient of component i $(K_{i,E})$ as the thermodynamic parameter. The partition coefficient and the duration of the process are important factors. The time of an extraction process is over when the concentration equilibrium state between two phases is established. On the other word, the mass transfer process starts after the solid and liquid phases are mixed and continues until the equilibrium state is reached (see figure 2.2). In the equilibrium state, the extraction content is not increased and the time of the process is over [1, 97, 111–113]. Under isothermal conditions, low concentration and subsequent linear behavior, a linear equilibrium relation for component i, which is not influenced by the possible presence of other components, holds:

$$K_{i,E} = \frac{c_i^{eq}}{q_i^{eq}} \quad ; \quad i = 1, N_C \tag{2.13}$$

The term of N_C is the number of components.
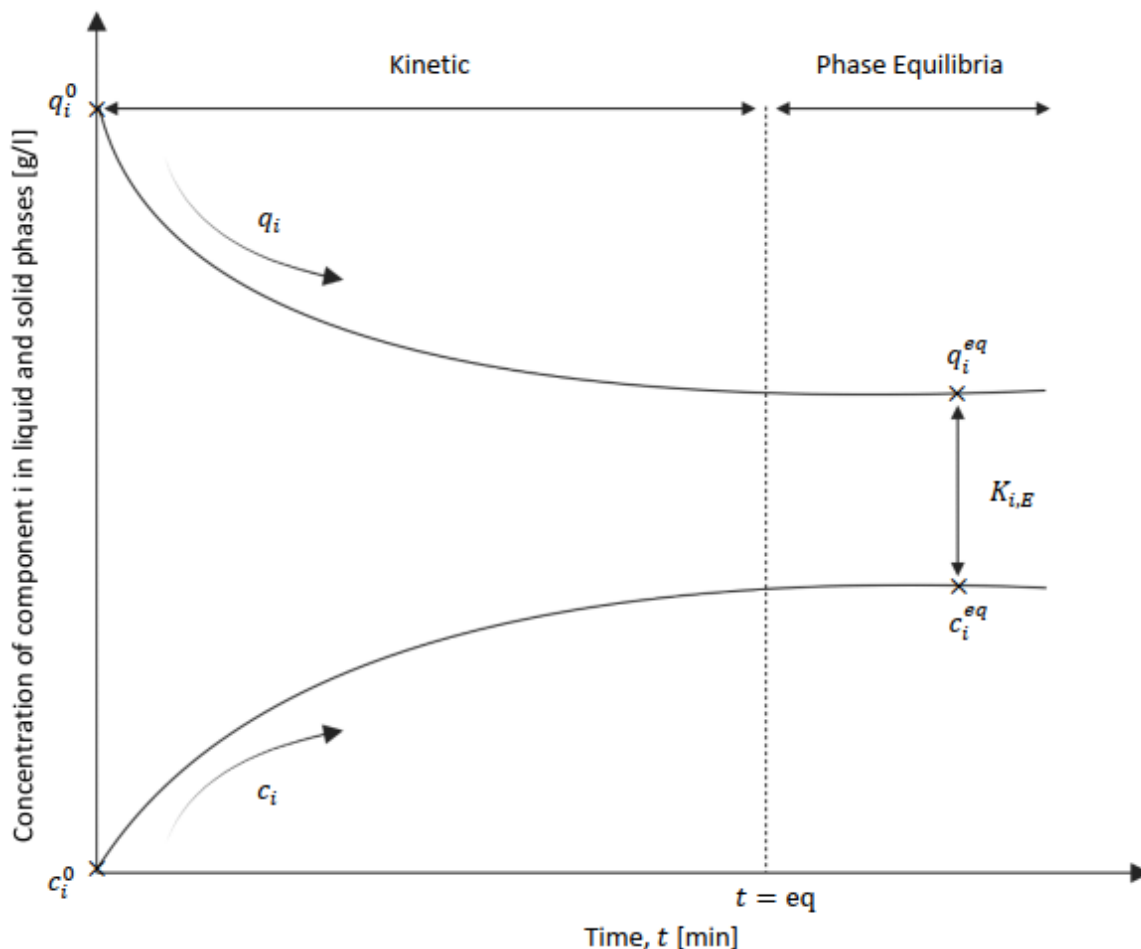
Figure 2.2: Schematic representation of the partition coefficient between solid and liquid phases. Inspired by the adsorption equilibrium experiments [114]

Usually, an equilibrium curve must be drawn to measure the extraction partition coefficient ($K_{i,E}$). The concepts for drawing equilibrium curves are based on the concepts for measuring adsorption isotherms. Various dynamic and classical static methods are used to measure adsorption isotherms. For example, in the static methods, no analysis of the concentration-time curve is performed, but only information and data from the equilibrium state are used [97, 114, 119].

The extraction process is a kind of adsorption process. Therefore, the concepts of adsorption isotherms can be generalized to the extraction process. Based on the concepts of adsorption isotherms, the extraction partition coefficient of a target molecule can also be determined by analyzing the equilibrium concentration of that target molecule at a fixed temperature (static method). Analysis of the equilibrium concentration of a component at different dosages (m_S/V_L or V_S/V_L) at an ambient temperature yields an equilibrium curve and/or equilibrium line whose slope indicates the partition coefficient (see Figure 4.5) [114]. However, due to some sources of error in extraction experiments, the slope of an equilibrium curve alone is not sufficient. To obtain a

reliable $K_{i,E}$ value, these errors are taken into account in the Weighted Least Squares equation WLS (Eq. 4.1) [97, 114].

2.1.3   Kinetics

In a **closed single-batch extraction** process, the dissolution rate of a target - molecule(s) in the liquid phase is controlled by the resistance of the mass transfer rate (kinetics) of the solute moving from the solid phase into the solvent. The mass transfer rate is typically finite. Kinetic parameters affect the speed of an extraction process; therefore, proper understanding of these parameters helps us optimize the overall time and speed of an extraction process. For each extraction process, there is a kinetic curve indicating that the mass transfer rate is not constant. The extraction kinetic curves generally contain three regions: a constant extraction rate (CER) , falling extraction rate (FER), and a diffusion controlled (DC) regions [97, 112]:
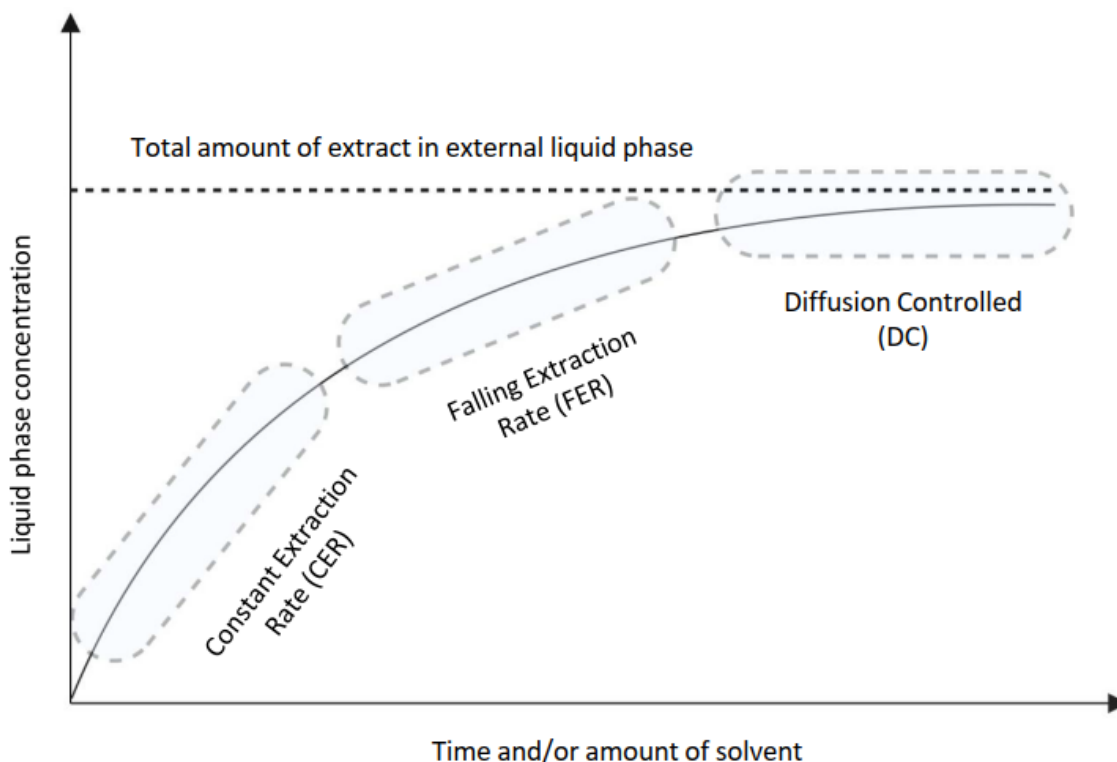
Figure 2.3: Schematic illustration of a kinetic curve during the extraction of a natural product. Inspired by [97, 112]

In the CER part, the readily available solutes surrounding the solid particles (see components 1 and 2 in Figure 2.4) are extracted at a nearly constant rate. The primary mechanism for mass transfer is convection. During CER part, a stagnant film surrounds the solid particles, which is the primary cause of mass transfer resistance. Therefore, the performance of the process is improved by creating turbulence (agitation or stirring). In the FER part, some fractures become visible in the surface layer of the solute covering the solid particles; thus, mass transfer resistance begins at the

solid-liquid interface. In this part, due to the reduction of the effective mass transfer area, the extraction rate decreases rapidly, and the diffusion mechanism becomes important. In this transition state, mass transfer resistance is present in both the liquid and solid phases, and both diffusion and convection mechanisms are important. In the DC part, the target molecules are depleted from the easily accessible solute layer. Therefore, the extraction rate depends on the diffusion rate of the liquid into the solid phase and the diffusion rate of the liquid and target molecule(s) from the solid phase into the liquid mass. This mechanism leads to a slow phase of the extraction process.
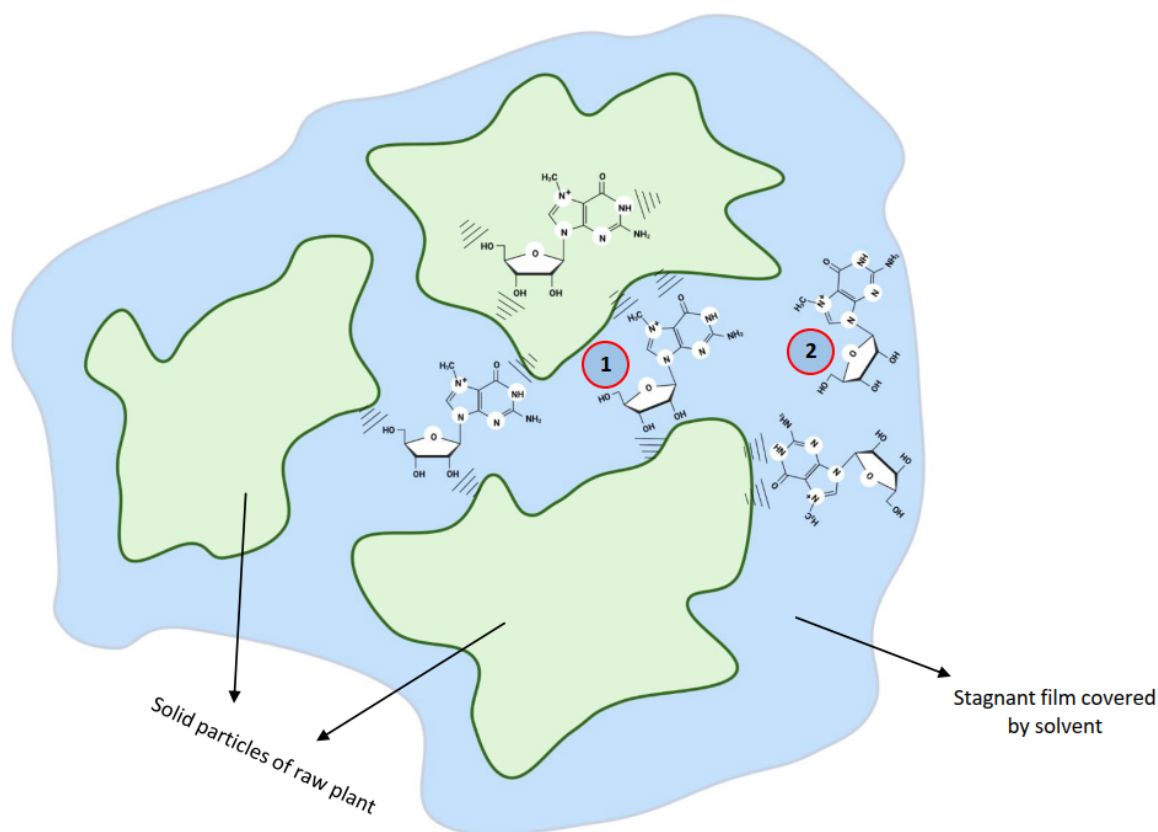
Figure 2.4: Schematic representation of a natural matrix and the possible locations where the target molecule(s) can be found. Inspired by [112]

It is worth noting that in some cases the target molecule(s) is not easily accessible and interacts with other compounds such as carbohydrates, lipids and proteins in the solid particle. In this case, prior to the establishment of new intermolecular interactions between target molecule(s) and solvent, the intermolecular interactions between solutes must be broken. This bond between the compounds and the raw matrix can be broken by supplying sufficient energy. Therefore, the amount of energy consumed affects the efficiency of the extraction process [97, 112]. These cases show that the properties of the raw material can play an important role in the extraction of certain categories of compounds.

The kinetic part of an extraction process is divided into the dynamic part, the CER- and the FER-part. The equation for estimating the effective kinetic parameter, k_i^{eff},

can be obtained by solving the mass balance of a target molecule(s) in the dynamic region ($0 < t < \infty(eq)$) of a batch extraction process [97, 112]. The differential mass balance of a component i present in a mixture of N_C other components, for the liquid and solid phases present in the volume with their fractions ε and $(1 - \varepsilon)$ are:

$$V_L \frac{dc_i}{dt} = \varepsilon V_{tot} \frac{dc_i}{dt} = d\dot{m}_{i,E} \tag{2.14}$$

$$V_S \frac{dq_i}{dt} = (1 - \varepsilon) V_{tot} \frac{dq_i}{dt} = -d\dot{m}_{i,E} \tag{2.15}$$

In these equations $\dot{m}_{i,E}$ is the extraction mass transfer rate of component i, which stands for the exchange term (Eq. 2.13). To solve the above two ODE we need to provide a rate law quantifying the extraction kinetics. We use below the following simplified first order linear driving force (LDF) model [97, 120]:

$$d\dot{m}_{i,E} = k_{i,E} \bar{A} \left(q_i - q_i^{eq} \left(c_i^{eq} \right) \right) \tag{2.16}$$

The phrases $k_{i,E}$ and $\bar{A}$ are kinetic phrase of component i in liquid and solid phases, and identical interface area between two phases, respectively. Introduction of Eq. 2.13 into the Eq. 2.16:

$$d\dot{m}_{i,E} = k_{i,E} \bar{A} \left(q_i - \frac{c_i}{K_{i,E}} \right) \tag{2.17}$$

Since the liquid phase is the source of the adsorbing components, we consider the driving force of the liquid phase to solve the equation 2.14. Substituting Eq 2.17 into the equation 2.14 and dividing by the volume of the liquid phase, we get:

$$\frac{dc_i}{dt} = \frac{1}{\varepsilon} \frac{k_{i,E} \bar{A}}{V_{tot}} \left(q_i - \frac{c_i}{K_{i,E}} \right) \tag{2.18}$$

The expression $\bar{A}/V_{tot}$ is a constant volume-specific interface area, which is not easy to determine. For this reason, lumping $\bar{A}/V_{tot}$ and $k_{i,E}$ into the effective kinetic rate constant of component i ($k_i^{eff}[1/time]$) provides:

$$\frac{dc_i}{dt} = \frac{1}{\varepsilon} k_i^{eff} \left(q_i - \frac{c_i}{K_{i,E}} \right) \tag{2.19}$$

To solve this equation, we need to replace q_i with the mass balance for the solid phase. Instead of solving the second mass balance for the solid phase, we can also use the total mass balance, which reads:

$$V_L \left(c_i(t) - c_i^0 \right) + V_S \left(q_i(t) - q_i^0 \right) = 0 \tag{2.20}$$

Here c_i^0 and q_i^0 are the concentration (g/l) of component i in the liquid phase at time zero, which is zero in a **single-batch extraction** process, and starting concentration (g/l) of component i in solid phase, which is never zero:

$$c_i^0 = 0 \tag{2.21}$$

$$q_i^0 \neq 0 \tag{2.22}$$

The equation 2.20 can be rearranged as follows:

$$q_i(t) = q_i^0 - \frac{\varepsilon}{1-\varepsilon}\left(c_i(t) - c_i^0\right) \tag{2.23}$$

Inserting Eq. 2.23 into the Eq. 2.19 provides the following simple first order linear ODE for $c_i(t)$:

$$\frac{dc_i}{dt} = \frac{k_i^{eff}}{\varepsilon}\left(q_i^0 - \frac{\varepsilon}{1-\varepsilon}\left(c_i - c_i^0\right) - \frac{c_i}{K_{i,E}}\right) \tag{2.24}$$

Further rearrangement provides:

$$\frac{dc_i}{dt} = \frac{k_i^{eff}}{\varepsilon}\left(q_i^0 + \frac{\varepsilon}{1-\varepsilon}c_i^0\right) - \frac{k_i^{eff}}{\varepsilon}\left(\frac{\varepsilon}{1-\varepsilon} + \frac{1}{K_{i,E}}\right)c_i \tag{2.25}$$

This equation can be simplified by using a general and linear expression, i.e.:

$$\frac{dy}{dx} = \alpha + \beta y \tag{2.26}$$

Solving the above equation with the following well-known solution for $y(x=0) = y_0$ leads to:

$$y(x) = \frac{\alpha}{\beta}\left(e^{\beta x} - 1\right) + y_0 e^{\beta x} = -\frac{\alpha}{\beta} + \left(y_0 + \frac{\alpha}{\beta}\right)e^{\beta x} \tag{2.27}$$

The phrases α and β for component i applies:

$$\alpha_i = \frac{k_i^{eff}}{\varepsilon}\left(q_i^0 + \frac{\varepsilon}{1-\varepsilon}c_i^0\right) \tag{2.28}$$

$$\beta_i = -\frac{k_i^{eff}}{\varepsilon}\left(\frac{\varepsilon}{1-\varepsilon} + \frac{1}{K_{i,E}}\right) \tag{2.29}$$

The back substitution of α_i, β_i, $y = c_i(t)$, $y_0 = c_i^0$, and $x = t$ into the Eq. 2.27 leads to:

$$c_i(t) = \frac{q_i^0 + \frac{\varepsilon}{1-\varepsilon}c_i^0}{\frac{\varepsilon}{1-\varepsilon} + \frac{1}{K_{i,E}}} + \left(c_i^0 - \frac{q_i^0 + \frac{\varepsilon}{1-\varepsilon}c_i^0}{\frac{\varepsilon}{1-\varepsilon} + \frac{1}{K_{i,E}}}\right) e^{-\frac{k_i^{eff}}{\varepsilon}\left(\frac{\varepsilon}{1-\varepsilon} + \frac{1}{K_{i,E}}\right)t} \tag{2.30}$$

Therefore, the concentration of component i in the solid phase at time t will obtain by Eq. 2.23:

$$q_i(t) = q_i^0 - \frac{\varepsilon}{1-\varepsilon}\left(\frac{q_i^0 + \frac{\varepsilon}{1-\varepsilon}c_i^0}{\frac{\varepsilon}{1-\varepsilon} + \frac{1}{K_{i,E}}} + \left(c_i^0 - \frac{q_i^0 + \frac{\varepsilon}{1-\varepsilon}c_i^0}{\frac{\varepsilon}{1-\varepsilon} + \frac{1}{K_{i,E}}}\right) e^{-\frac{k_i^{eff}}{\varepsilon}\left(\frac{\varepsilon}{1-\varepsilon} + \frac{1}{K_{i,E}}\right)t} - c_i^0\right) \tag{2.31}$$

This general equation (Eq. 2.30) is used to calculate the concentration of compound i in the liquid phase at different times and different effective kinetic coefficients. By fitting the experimentally determined concentration-time curve (Figure 4.4) to the calculated concentration-time curves (see figure 4.9), the effective kinetic coefficient k_i^{eff} is estimated (Table 4.7). For infinite time ($t \to \infty$) this solution provides:

$$c_i^{eq} = -\frac{\alpha}{\beta} = \frac{q_i^0 + \frac{\varepsilon}{1-\varepsilon}c_i^0}{\frac{\varepsilon}{1-\varepsilon} + \frac{1}{K_{i,E}}} \tag{2.32}$$

Using the general mass balance equation (Eq. 2.23) and Eq. 2.32, the concentration of component i in the solid phase at the equilibrium time q_i^{eq} is obtained as follows:

$$q_i^{eq} = q_i^0 - \frac{\varepsilon}{1-\varepsilon}\left(\frac{q_i^0 + \frac{\varepsilon}{1-\varepsilon}c_i^0}{\frac{\varepsilon}{1-\varepsilon} + \frac{1}{K_{i,E}}} - c_i^0\right) \tag{2.33}$$

This result is in agreement with the linear equilibrium function, Eq. 2.13. Last but not least, the important parameters in Eq. 2.30 are partition coefficient ($K_{i,E}$), effective kinetic rate constant (k_i^{eff}), and epsilon (ε) as an operating parameter. These parameters play a key role in the modeling of continuous steady-state countercurrent operation in section 2.1.4.1.

2.1.4   Process Variants

There are many options to contact a solid and a liquid phase in order to perform an extraction process. Two important variants are (a) batch operation (as already discussed in the above section and quantitatively described with a simple rate model), and (b) continuous operation. There are numerous further options for continuous operation. Classifications include [1, 97, 111, 112, 114, 121]:

a) Mixed systems vs. not mixed systems. It is well known and has been studied in particular in chemical reaction engineering (CRE) that in case of reactions characterized by positive reaction orders stirring is less favorable than a flow arrangement.

b) A cascade of well-mixed units (designated in CRE as a cascade of CSTR) is better than a single well-mixed CSTR.

c) When we evaluate a cascade of more than one CSTR, a counter-current procedure is always better than a co-current procedure. The reason is that the equilibrium limits can be exceeded by transporting the phases in different directions. The more stages that can be used (see figure 2.6), the higher the efficiency of the extraction process, i.e., the higher the final extract concentration and the lower the loss at the solid phase outlet.

These transports in option (c) can be derived in a rigorous manner by deriving and analyzing the mass balance equations for the specific mode mentioned (counter-current mode). This is done in more detail in the companion dissertation by M.Sc. Giang Truong Vu (Experimental investigation and modeling of extracting natural products from plants: from batch to continuous processes, 2023).

In the following section, we will present and evaluate the most flexible model based on the assumption of rate-limited extraction processes in a cascade of N-CSTR operated under steady-state conditions. In the next section, we will summarize the key equations of this model and illustrate its potential using the results of selected parametric calculations.

2.1.5　Model to Describe Counter-Current Steady State Operation in a Cascade of N Stages

The design of a continuous counter-current extraction process requires some essential steps, such as the selection of the extraction system and the most suitable process concepts for the scale-up from batch to continuous processes. Predictions based on numerical simulations and approximations can significantly reduce the time and material required for the analysis and optimization of the process. Validated process models are typically used to determine appropriate operating parameters and optimal process design. In an important categorization of models, two types are distinguished. In one type, the entire column is considered as a series connection of a certain number of discretized parts of the column (stages or cells) (Craig model, 1940s). In the other type, continuous formulations are used to characterize the time-dependent local concentration profiles (Martin and Synge, 1941). **Equilibrium stage models** are often considered in the discrete stage models of chromatography. Therefore, the solution requires knowledge of the equilibrium functions. **Martin and Synge** (1941) presented a very successful equilibrium stage model that represents a column as a series connection of cells (stages) through which a continuous flow of liquid at a fixed flow rate and in which the solid and liquid phases are constantly in equilibrium [97, 111]. The principles of Martin and Synge's model can also be applied to continuous multistage counter-current extraction (CC) of solids and liquids. In this process, the

liquid and solid phases move in opposite directions in a counter-current column at a given flow rate [112]. The main goal of the CC process is to achieve high productivity and recovery yield of the extracted target molecules. Factors such as flow velocity and temperature can affect the yield and kinetics of this process [1, 97]. In this process, there are several theoretical stages $,j = 1, N$, within the counter-current column, like a discretized lattice (see figure 2.5).
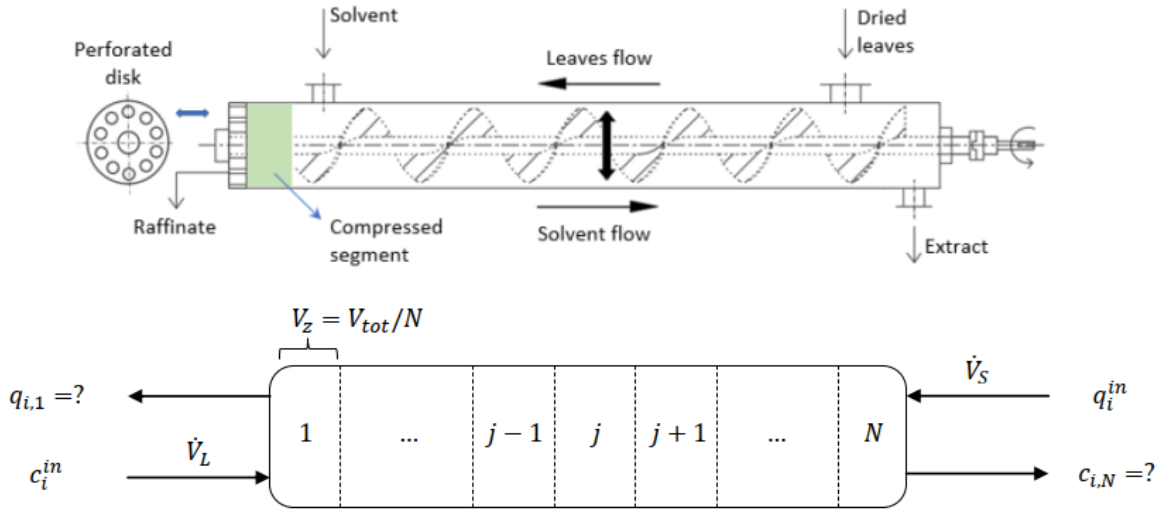
Figure 2.5: Upper figure: Conceptual design of continuous counter-current extractor using a screw type of apparatus (from Giang Truong Vu's thesis, 2023). Bottom figure: Schematic representation of the discretized counter-current extraction process structured into N well mixed stages

Each stage has a volume equal to $V_{j,tot} = V_{tot}/N$ occupied by the volume fraction of the liquid phase (ε) and the volume fraction of the solid phase $(1 - \varepsilon)$. The volume of air is assumed to be zero. This leads to a mass balance of component i and stage j, with the total accumulation balanced by the inequality between the input current of stage $j - 1$ and the output current. Following the thesis of our collaborator M.Sc. Giang Truong Vu, 2023, who has worked on the batch and continuous extraction of Artemisisnin, it is convenient to introduce the following definitions, which allow to use the corresponding solutions:

$$\tilde{c}_i = c_i \varepsilon \tag{2.34}$$

$$\tilde{q}_i = q_i (1 - \varepsilon) \tag{2.35}$$

The above tilde parameters are pseudo-homogeneous phase concentration definition. It is a new concentration after mixing and using the total volume (as a base). The concentrations $\tilde{c}_i$ and $\tilde{q}_i$ will always be smaller than those of the separated phases are. After splitting, all the material should return to this smaller volume, which means that the concentrations will increase again. However, to mix them, we can calculate

$\tilde{c}_i$ and $\tilde{q}_i$ for simplicity. Therefore, the use of epsilon to tilde equilibrium and rate parameters leads to the following equations:

$$\tilde{K}_{i,E} = \frac{\varepsilon}{1-\varepsilon} K_{i,E} \tag{2.36}$$

$$\tilde{k}_i^{eff} = \frac{k_i^{eff}}{1-\varepsilon} \tag{2.37}$$

This allows for example for a batch system to substitute Eq. 2.19 by:

$$\frac{d\tilde{c}_i}{dt} = \tilde{k}_{eff,i}\left(\tilde{q}_i - \frac{\tilde{c}_i}{\tilde{K}_{E,i}}\right) \tag{2.38}$$

Furthermore, the total balance can be changed into:

$$\tilde{q}_i(t) = \tilde{q}_i^0 + \tilde{c}_i^0 - \tilde{c}_i(t) \tag{2.39}$$

Hence, the solution for the time dependency of the liquid phase concentration is:

$$\tilde{c}_i(t) = \frac{\tilde{K}_{i,E}}{1+\tilde{K}_{i,E}}\left(\tilde{q}_i^0 + \tilde{c}_i^0\right) - \left(\frac{\tilde{K}_{i,E}}{1+\tilde{K}_{i,E}}\tilde{q}_i^0 - \frac{1}{1+\tilde{K}_{i,E}}\tilde{c}_i^0\right) e^{-\left(1+\frac{1}{\tilde{K}_{i,E}}\right)\tilde{k}_i^{eff}t} \tag{2.40}$$

This agrees with equation 2.30 after division by ε. This approach pays off especially in the formulation of the set of equations describing the **steady-state** counter-current operation in a cascade of N equally sized CSTRs with total volume V_{tot}. The flow rates of the liquid and solid phases through this cascade are $\dot{V}_L$ and $\dot{V}_S$, respectively. This allows to define an important operating parameter, namely the total residence time in the cascade:

$$\tau = \frac{V_{tot}}{\dot{V}_{tot}} = \frac{V_{tot}}{\dot{V}_L + \dot{V}_S} \tag{2.41}$$

The total residence time of the process τ is a degree of freedom. The modeling approach is illustrated in figure 2.6, where there is a constant change between a pseudo-homogeneous situation, in which extraction occurs, and a 2-phase situation, in which counter-current transport occurs between stages.
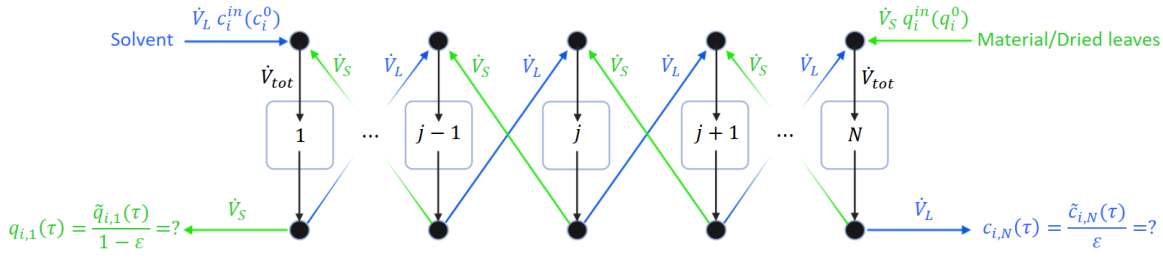
Figure 2.6: Description of N-stage counter-current operation. The unknowns are the concentration of component i in every stage. The most important unknowns are the outlet concentrations of component i in the liquid phase at stage N, $c_{i,N}$, and in the solid phase at stage 1, $q_{i,1}$ (Adapted from M.Sc. Giang Truong Vu's thesis, 2023)

The discretized continuous counter-current column is constructed like a cascade of N continuously stirred-tank reactors (**N-CSTR**), which is a matrix system of N **Ordinary Differential Equations** (**ODEs**) with a linear partition coefficient. **Numerical solution** of these differential equations yield predictions for this **dimensionless dynamic linear rate-limited extraction model** [1, 97, 111, 120]. Classically, these models are developed for homogeneous phase systems. The arrangement consisting out of N connected stages ($j = 1, N$) is represented by the following mass balance equations for the two phases (in total $2N$ linear equations):

$$
\begin{aligned}
0 &= -A_1\tilde{c}_i^{in} + \tilde{c}_{i,1}(\tau) - A_2\tilde{q}_{i,2}(\tau) \;\; ; \;\; j = 1 \\
0 &= -(1 - A_1)\tilde{c}_i^{in} + \tilde{q}_{i,1}(\tau) - (1 - A_2)\tilde{q}_{i,2}(\tau) \;\; ; \;\; j = 1 \\
0 &= -A_1\tilde{c}_{i,j-1}(\tau) + \tilde{c}_{i,j}(\tau) - A_2\tilde{q}_{i,j+1}(\tau) \;\; ; \;\; j = 2, N-1 \\
0 &= -(1 - A_1)\tilde{c}_{i,j-1}(\tau) + \tilde{q}_{i,j}(\tau) - (1 - A_2)\tilde{q}_{i,j+1}(\tau) \;\; ; \;\; j = 2, N-1 \\
0 &= -A_1\tilde{c}_{i,N-1}(\tau) + \tilde{c}_{i,N}(\tau) - A_2\tilde{q}_i^{in} \;\; ; \;\; j = N \\
0 &= -(1 - A_1)\tilde{c}_{i,N-1}(\tau) + \tilde{q}_{i,N}(\tau) - (1 - A_2)\tilde{q}_i^{in} \;\; ; \;\; j = N
\end{aligned}
\tag{2.42}
$$

This system of linear equations is used to distinguish between co-current and/or batch operation (see Eq. 2.40) and counter-current operation for N-CSTRs (see Eq. 2.42) and to prove mathematically that counter-current operation is better than co-current operation. The comparison refers only to A_1 and A_2. The structure of this system of equations (Eq. 2.42) is illustrated in matrix form (Figure 2.7):
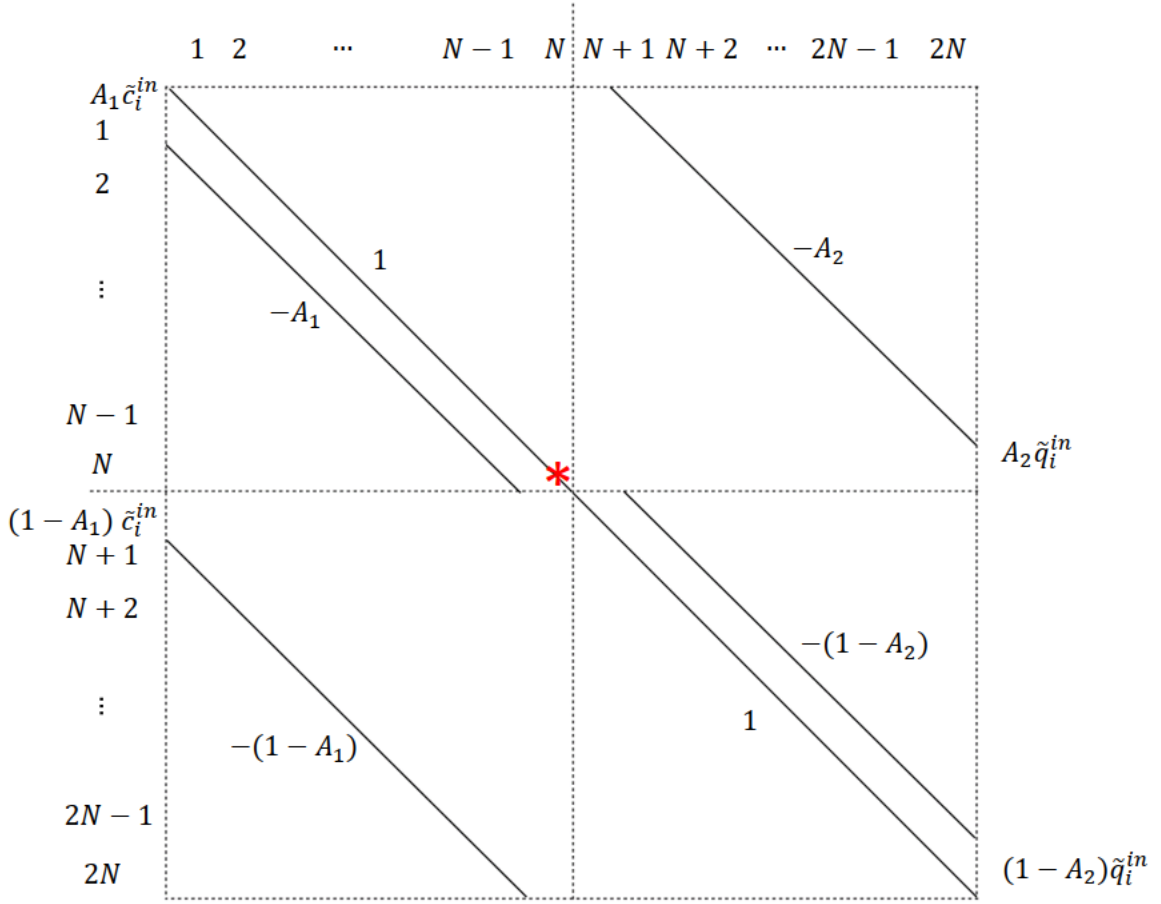
Figure 2.7: The matrix of system of equations (Eq. 2.42) describes the kinetically controlled operation for N-CSTR counter-current extraction process (Adapted from Giang Truong Vu's thesis, 2023), $*$: Outlet liquid phase concentration of component i $(c_{i,N})$

The two key parameters in these equations are A_1 and A_2 (equations 2.43 and 2.44), which capture other essential parameters, such as the thermodynamics and kinetics of the extraction process (via $(\tilde{K}_{i,E})$ and $(\tilde{k}_i^{eff})$), the number of stages as a measure of back-mixing (or deviations from plug flow behavior), and the design parameter τ. Tau is an operator parameter because we can design the operation so that the flow rates are high or low, or perhaps even one is fixed and the other is shifted.

$$A_1 = \frac{\left(1 + \frac{N}{\tilde{k}_i^{eff}\tau}\right)}{1 + \frac{1}{\tilde{K}_{i,E}} + \frac{N}{\tilde{k}_i^{eff}\tau}} \tag{2.43}$$

$$A_2 = \frac{1}{1 + \frac{1}{\tilde{K}_{i,E}} + \frac{N}{\tilde{k}_i^{eff}\tau}} \tag{2.44}$$

The dimensionless timescale parameter called Damköhler number $(Da_i = \tilde{k}_i^{eff} \times \tau)$ can also be replace in Eq. 2.43 and Eq. 2.44:

$$A_1 = \frac{\left(1 + \frac{N}{\tilde{k}_i^{eff}\tau}\right)}{1 + \frac{1}{\tilde{K}_{i,E}} + \frac{N}{Da_i}} \tag{2.45}$$

$$A_2 = \frac{1}{1 + \frac{1}{\tilde{K}_{i,E}} + \frac{N}{Da_i}} \tag{2.46}$$

These equations contain essential parameters that can be used for counter-current adsorption, counter-current chromatography, and counter-current extraction. Everything is expressed as a function of $K_{i,E}$, k_i^{eff}, N, ε, and τ. These equations can be solved numerically with any standard program for solving linear equations. Solving these equations using the analytical linear solver, linsolve, provided by MATLAB, gives the concentration of component i in the liquid and solid phases at stage j $(j = 1, N)$, $\tilde{c}_{i,j}$ and $\tilde{q}_{i,j}$, over the residence time τ of the continuous counter-current operation. It should be mentioned that these tilde terms, Loss and Gain, must be transformed into absolute values by equations 2.34 and 2.35, if we want to use them for the calculations of productivities and yields.

Special case: Equilibrium controlled counter-current operation for N-CSTR

Infinite effective extraction rate, k_i^{eff}, means that there is a permanent equilibrium in each stage (implying that this is the model reduction), and it also means that τ is infinite. This means that either the flow is so slow or the system is so large. Then we have:

$$A_1 = A_2 = \frac{1}{1 + \frac{1}{\tilde{K}_{i,E}}} = \frac{\tilde{K}_{i,E}}{\tilde{K}_{i,E} + 1} \tag{2.47}$$

This simplifies the structure of the problem. Now that one phase is expressed by the other phase, we should not have two sets of equations (2N), but only one (N). The new structure is illustrated in figure 2.8:
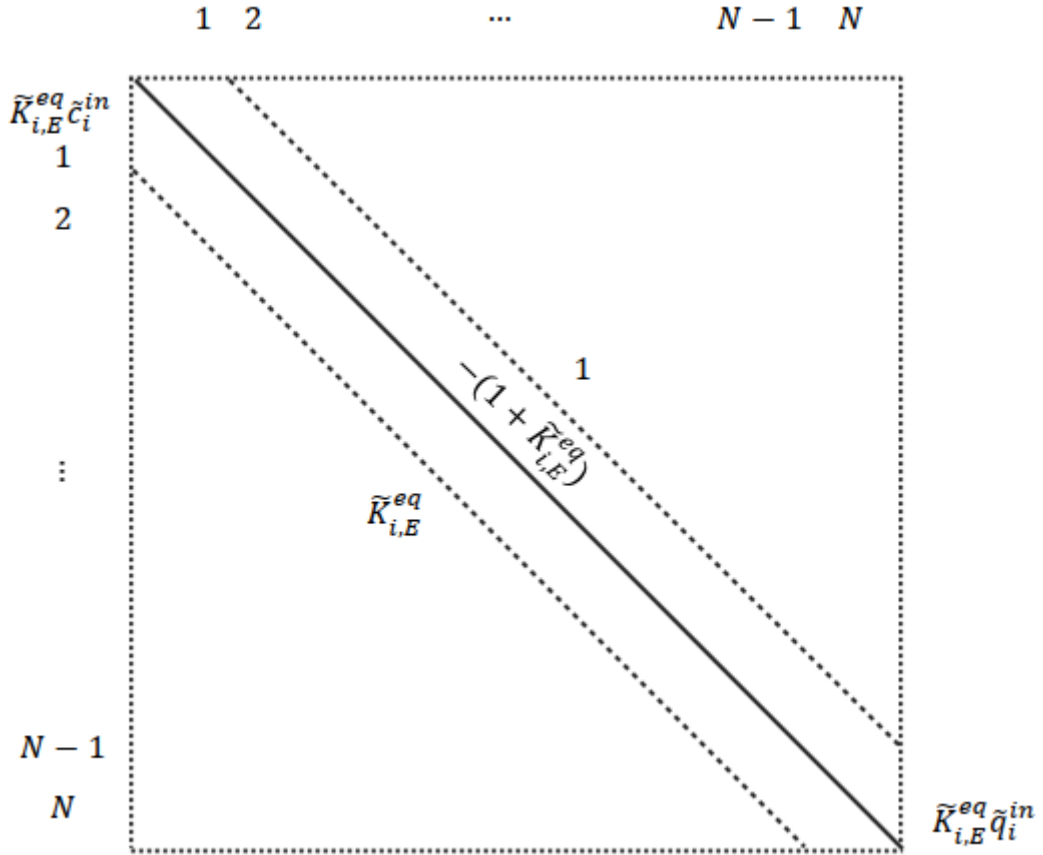
Figure 2.8: The matrix of system of equations equilibrium controlled counter-current operation for N-CSTR (special case) (Adapted from Giang Truong Vu's thesis, 2023)

The corresponding equations are expressed via the equilibrium constant ($\tilde{K}_{i,E}^{eq}$):

$$-\left(\tilde{K}_{i,E}^{eq} + 1\right)\tilde{c}_{i,1}(\tau) + \tilde{c}_{i,2}(\tau) = -\tilde{K}_{i,E}^{eq}\tilde{c}_i^{in} \quad ; \quad j = 1$$

$$\tilde{K}_{i,E}^{eq}\tilde{c}_{i,j-1}(\tau) - \left(\tilde{K}_{i,E}^{eq} + 1\right)\tilde{c}_{i,j}(\tau) + \tilde{c}_{i,j+1}(\tau) = 0 \quad ; \quad j = 2, N-1 \qquad (2.48)$$

$$\tilde{K}_{i,E}^{eq}\tilde{c}_{i,N-1}(\tau) - \left(\tilde{K}_{i,E}^{eq} + 1\right)\tilde{c}_{i,N}(\tau) = -\tilde{K}_{i,E}^{eq}\tilde{q}_i^{in} \quad ; \quad j = N$$

This tri-diagonal system of linear equations can be solved analytically using the Kremser approach [122, 123]. Based on Giang's thesis, the main results depend on N stages, the equilibrium constant $\tilde{K}_{i,E}^{eq}$ and the quantity $\tilde{q}_i^{in}$:

$$\tilde{q}_{i,1} = \left(\frac{\tilde{K}_{i,E}^{eq^N} - 1}{\tilde{K}_{i,E}^{eq^{N+1}} - 1}\right)\tilde{c}_i^{in} + \left(\frac{\tilde{K}_{i,E}^{eq} - 1}{\tilde{K}_{i,E}^{eq^{N+1}} - 1}\right)\tilde{q}_i^{in} \qquad (2.49)$$

$$\tilde{c}_{i,N} = \left(\frac{\tilde{K}_{i,E}^{eq^{-1}} - 1}{\tilde{K}_{i,E}^{eq^{-(N+1)}} - 1}\right)\tilde{c}_i^{in} + \left(\frac{\tilde{K}_{i,E}^{eq^{-N}} - 1}{\tilde{K}_{i,E}^{eq^{-(N+1)}} - 1}\right)\tilde{q}_i^{in} \qquad (2.50)$$

For $\tilde{c}_i^{in} = 0$ and divided by $\tilde{q}_i^{in}$, the following measure of **Loss** and **Gain** (yield) is

obtained:

$$Loss = \frac{\tilde{q}_{i,1}}{\tilde{q}_i^{in}} = \left(\frac{\tilde{K}_{i,E}^{eq} - 1}{\tilde{K}_{i,E}^{eq^{N+1}} - 1} \right) \tag{2.51}$$

$$Gain(yield) = \frac{\tilde{c}_{i,N}}{\tilde{q}_i^{in}} = \left(\frac{\tilde{K}_{i,E}^{eq^{-N}} - 1}{\tilde{K}_{i,E}^{eq^{-(N+1)}} - 1} \right) \tag{2.52}$$

Last but not least, this result can be evaluated for the case when N goes to infinity $(N \to \infty)$ and $\tilde{c}_i^{in} = 0$. Then the hypothetical "**ideal**" extraction process results from Eq. 2.50:

$$\tilde{c}_{i,N}^{max} = \tilde{q}_i^{in} \tag{2.53}$$

This is the Plug Flow Tank Reactor (PFTR) situation that never exists in reality. It is merely a borderline case. Therefore, the maximum outgoing dimensioned concentration of component i in the liquid phase will be as follow:

$$c_{i,N}^{max} = \frac{q_i^{in} \times (1 - \varepsilon)}{\varepsilon} \tag{2.54}$$

Hence, the normalization of the liquid phase concentration in the counter-current process, $c_{i,N}$, can be done based on the maximum outgoing concentration:

$$c_{i,N}^{norm.} = \frac{c_{i,N}}{c_{i,N}^{max}} \quad ; \quad [0, 1] \tag{2.55}$$

Normalization of concentration leads to the same normalized productivity and normalized recovery yield values:

$$c_{i,N}^{norm.} \simeq Pr_i^{norm.} \simeq Y_i^{norm.} \tag{2.56}$$

At the end, following figure shows the effect of thermodynamic parameter $\tilde{K}_{i,E}$, kinetic parameter $\tilde{k}_i^{eff}$, and number of stages N on the outlet concentration of component i by the model describes the kinetically controlled operation for N-CSTR counter-current extraction process (by Eq. 2.42):
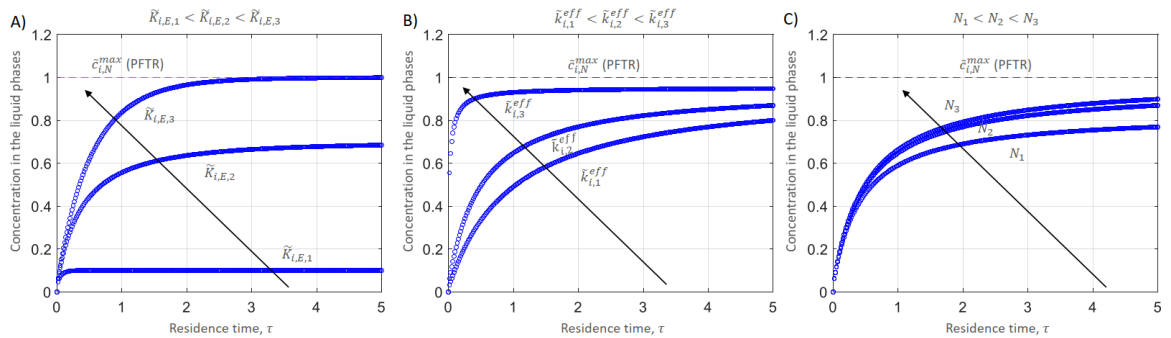
Figure 2.9: The effect of thermodynamic parameter $\tilde{K}_{i,E}$, kinetic parameter $\tilde{k}_i^{eff}$, and number of stages N on the outlet concentration of component i in the counter-current process (Eq. 2.42)

It is clear that higher $\tilde{K}_{i,E}$, $\tilde{k}_i^{eff}$, N leads to the higher outlet concentration of component i in the liquid phase. The effect of kinetic parameter $\tilde{k}_i^{eff}$ shows that the higher kinetic parameter has steeper starting slop (see figure 2.9), which is reasonable.

2.1.6 Final Processing of the Extractor Effluent

The crude extract contains a mixture of extracted components and therefore must be separated. There are several ways to separate the target constituent(s) from the mixture of ingredients in a crude extract. One would be liquid-liquid extraction with a different solvent that may not be miscible with the extraction solvent, and then taking the specific constituent(s) based on the octanol-water partition coefficient [97]. The other could be solid phase extraction, where the crude extract solution comes into contact with the solid phase (for example silica gel) and the solid then brings selectivity [97, 114]. Another way is evaporation crystallization to evaporate carefully to reach supersaturation, and then based on the different solubility of the ingredients the separation is done step by step; and/or cooling crystallization by plotting the solubility curve at different temperatures and find a meta-stable zone for the crystallization of the target component [97, 124–126]. As explained in the introductory chapter, the most common method for purifying the valuable ingredients of saffron is solid-liquid chromatography. To perform and compare these processes in a meaningful way, we need kinetic and thermodynamic parameters for each of them. In this study, the separation technique of the solid-liquid chromatography for the processing of crude extract is investigated.

Since the other separation methods mentioned are cheap and have very low yield, we particularly focus on solid-liquid chromatography for the separation and purification of picrocrocin, crocin I and crocin II from the crude extract solution. The chromatography technique is more powerful than other separation techniques because it has a larger surface area on porous materials (stationary phase), resulting in clear separation and purification with high yield and acceptable productivity [97, 111, 114, 119].

2.2   Solid-Liquid Chromatography

Chromatography is a separation process used to isolate a mixture and separate it into its components. Separations, including isolation, enrichment, purification, and refining, are important to chemical engineers and chemists. Chemists use analytical separation techniques, such as small-scale chromatographic separation, to recover and purify chemicals. Chemical and process engineers are more interested in producing chemicals or target molecules using cost-effective, large-scale separation processes that can differ significantly from laboratory processes [97, 111, 114, 115, 121]. In this study, analytical and large-scale preparative HPLC techniques are performed for the separation and purification of the target constituents in saffron crude extract, namely picrocrocin, crocin I, and crocin II.

2.2.1   Principle

As described in the section on analytical techniques, reversed-phase high-performance liquid chromatography, $RP - HPLC$, is the most common separation technique for isolating and purifying the components of saffron extract. Reversed-phase chromatography, RPC, also referred to as hydrophobic chromatography, includes all chromatographic techniques that use a hydrophobic stationary phase [116, 119, 121].

In the 1970s, the most common liquid chromatography was performed with a stationary phase of unmodified silica or alumina resins. This chromatography technique is now known as normal phase chromatography, NPC. Since the stationary phase in this technique is hydrophilic, the hydrophilic molecules in the mobile phase have a stronger affinity for it. However, the hydrophobic molecules have a lower adsorption affinity for the hydrophilic column packing (stationary phase) and are therefore eluted and detected first. The hydrophilic molecules adsorbed on the column packing are desorbed toward the mobile phase by using a larger amount of polar or hydrophilic solvent in the mobile phase.

In the RPC technique, the stationary phase particles (unmodified silica) are covalently bonded to the alkyl chains to form a hydrophobic stationary phase. The RPC is obviously the opposite of the NPC, since the polarity of the stationary and mobile phases is reversed, which is why it is also called reverse phase chromatography. Thus, the mobile phase of the RPC technique is a polar solvent. In the RPC technique, the stationary phase has a high affinity for hydrophobic or less polar molecules [117, 121]. Therefore, the hydrophobic molecules adsorb to the hydrophobic stationary phase, while the hydrophilic molecules elute first. Elution of the adsorbed hydrophobic molecules from the column is accomplished using an organic modifier that reduces the hydrophobic interactions. The more hydrophobic compounds bind more strongly to the stationary phase, which means that a higher percentage of organic modifier (organic solvent) is required to elute them. It should be noted that the organic solvent

and water must be miscible. The commonly used organic modifiers are methanol $\leq$ acetonitrile $<$ ethanol $\sim$ acetone $\sim$ dioxin $<$ iso-propanol $\leq$ tetrahydrofuran [118].

In RPC technique, there are a variety of silica-based stationary phases, such as C18 (octadecyl-carbon)-bonded silica, C8-bonded silica, phenyl-bonded silica, and cyano-bonded silica. Depending on the polarity and nature of the interaction of the molecules, one of the above stationary phases is selected. The most commonly used RP column is the $C18$ column (Figure 2.10):
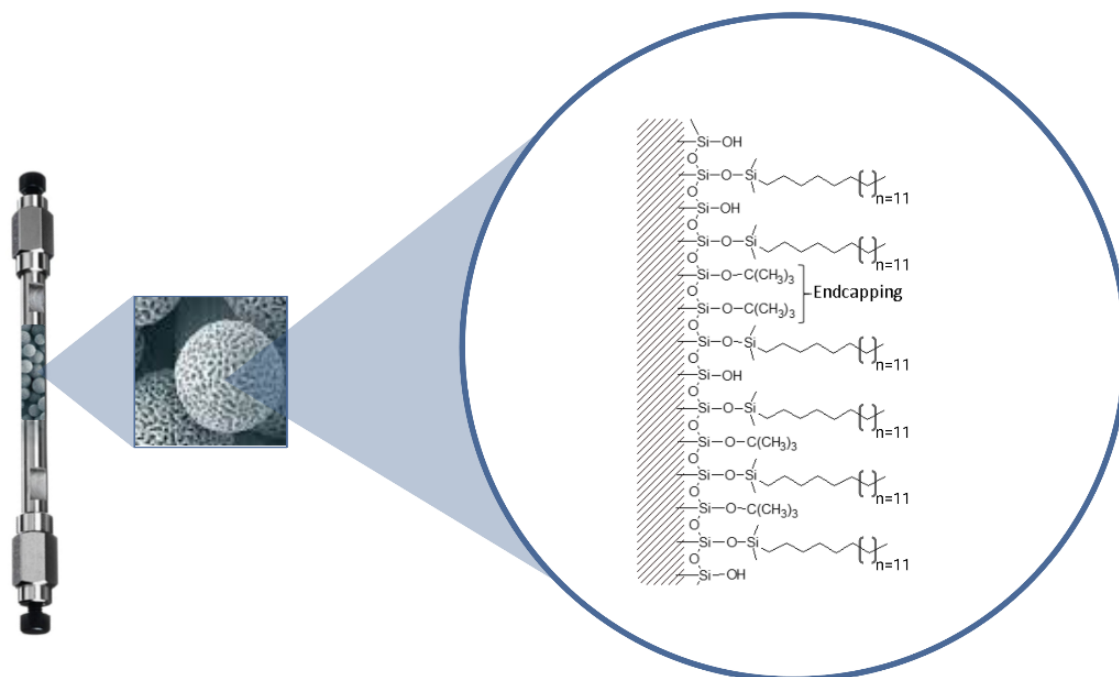
Figure 2.10: Schematic representation of a C18 column and chemical structure of the C18 packing [117, 121]

As can be seen, the $C18$ packing is the octadecyl carbon chain bonded to silica . Silica gel is amorphous silica, SiO_2, with a very porous structure and contains siloxane groups (- Si-O-Si-O -) and silanol groups (-Si- OH) (see figure 2.10). It should be mentioned that not all C18 column packings have the same retention properties. On the other hand, surface functionalization of the silica gel with short hydrocarbon chains (monomeric or polymeric reaction) can occur after the primary binding step to replace the remaining silanol groups (end-capping), resulting in the different retention properties of $C18$ columns [117, 121].

2.2.2   General Mass Balance of a Chromatographic Column and Equilibrium Theory

In similarity to the two-phase counter-current extraction model used above, we formulate a model where just the liquid phase is moving. Furthermore, we take into account that chromatographic processes are typically much more efficient than conventional extraction processes by formulating instead of a cascade model now a continuous PDE model as follows [97, 110, 111, 114, 115, 119, 121, 127–129]:

$$\frac{\partial c_i}{\partial t} + \frac{1 - \varepsilon_{tot}}{\varepsilon_{tot}}\frac{\partial q_i}{\partial t} + u_L\frac{\partial c_i}{\partial z} = D_{i,app}\frac{\partial^2 c_i}{\partial z^2} \quad ; \quad i = 1, N_C \tag{2.57}$$

Here c_i is the mobile phase concentration of component i in equilibrium with the stationary phase concentration of that component q_i. The parameters ε_{tot}, u_L, and $D_{i,app}$ are the total prosity (intraparticle and interparticle void volume) of the packing material, the linear velocity of the mobile phase, and the apparent axial dispersion of component i (kinetic), respectively [121, 127, 130]. It is expedient to use instead of ε_{tot} the phase ratio definition as F:

$$F = \frac{1 - \varepsilon_{tot}}{\varepsilon_{tot}} \tag{2.58}$$

Hence, the Eq. 2.57 can be rewrite as the following equation:

$$\frac{\partial c_i}{\partial t} + F\frac{\partial q_i}{\partial t} + u_L\frac{\partial c_i}{\partial z} = D_{i,app}\frac{\partial^2 c_i}{\partial z^2} \tag{2.59}$$

This equation can be simplified assuming a permanently established equilibrium. This means that q_i is an explicit function of c_i and $q_i(c_i)$ [121, 127]:

$$\frac{\partial c_i}{\partial t}\left(1 + F\frac{dq_i(c_i)}{dc_i}\right) + u_L\frac{\partial c_i}{\partial z} = D_{i,app}\frac{\partial^2 c_i}{\partial z^2} \tag{2.60}$$

Often $D_{i,app}$ is very small (an infinite efficiency is a good assumption for rough preliminary) and the last term can be neglected. This leads to the fundamental equation of equilibrium theory [97, 111, 115, 121, 127–129]:

$$\frac{\partial c_i}{\partial t}\left(1 + F\frac{dq_i(c_i)}{dc_i}\right) + u_L\frac{\partial c_i}{\partial z} = 0 \tag{2.61}$$

This equation allows for a constant concentration to estimate the corresponding migration velocity (Eq. 2.62):

$$u_i = \frac{u_L}{1 + F\frac{dq_i(c_i)}{dc_i}} \tag{2.62}$$

Here u_i is the migration velocity of a retained concentration front. The key is the ratio between the differential concentration of the stationary phase and the differential concentration of the mobile phase, $dq_i(c_i)/dc_i$. It is well known for isocratic conditions, i.e. the volume fraction of modifier $\varepsilon_{L,mod}$ is constant, and one only needs to know the one-component linear-isotherm valid for these solvent compositions to predict chromatograms. In other words, for a given column length L_c, the corresponding retention time is:

$$t_{R,i} = t_0 \left(1 + F\frac{dq_i(c_i)}{dc_i} \right) \tag{2.63}$$

With

$$t_0 = \frac{L_c}{u_L} \tag{2.64}$$

The velocity u_L can be also expressed via the volume flow rate of the liquid phase ($\dot{V}_L$) and the free volume of the column ($\frac{\pi}{4}d_c^2$) [111, 114, 119, 121, 127]:

$$u_L = \frac{\dot{V}_L}{\frac{\pi}{4}d_c^2\varepsilon_{tot}} \tag{2.65}$$

Under linear conditions, the migration velocity of component i (u_i) is constant and independent of the injection concentration. The migration rate of a component depends only on the concentration of the mobile phase. In other words, the velocity associated with a given mobile phase concentration is constant, and each concentration runs at a stable velocity along the entire length of the column. The point indicating this concentration moves in time and space (t, z) along a straight line (linear domain). The slope of this straight line corresponds to the migration rate of component i (see Figure 2.11). For example, for a sample with components 1, 2, and 3, the migration velocity of each component (u_i) is different for a constant mobile phase composition. This means that the linear domain (linear-isotherm) for each component has a different slope angle, resulting in a different retention time for each component $(t_{R,1}, t_{R,2}, t_{R,3})$ (see Figure 2.11). These linear trajectories are called characteristic lines [97, 111, 115, 127–129]:
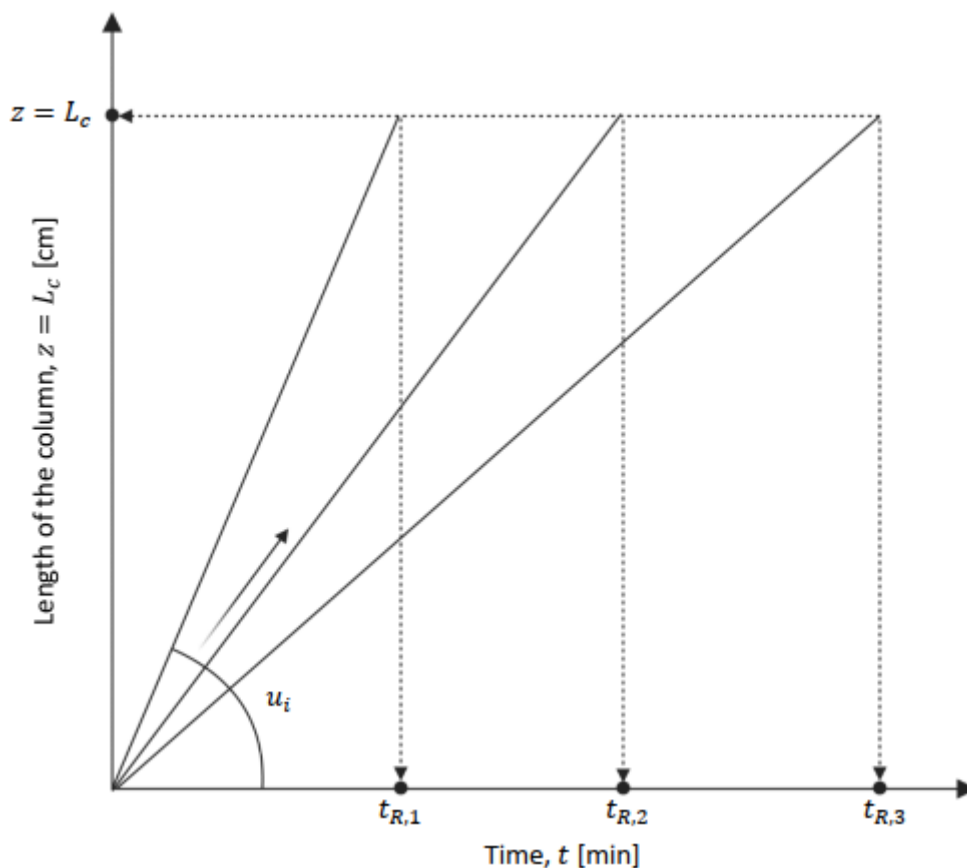
Figure 2.11: Linear trajectories of component i ($i = 1, 2, 3$) over time and space (column length) for a considered volume fraction of modifier ($\varepsilon_{L,mod}$) [121, 127]

These linear trajectories of component i will be used in the next section 2.2.5 to model the step-gradient elution method, predict the retention time of component i, and reduce the total cycle time.

2.2.3   Essential Parameters

2.2.3.1   Column Porosity

To determine the total porosity ε_{tot} (intraparticle and interparticle void volume) of the packing material, the column dead time t_0, the volume of the empty column V_c, and the volume flow rate of the mobile phase $\dot{V}_L$ are required [114, 119, 121, 127, 130, 131].

$$\varepsilon_{tot} = \frac{t_0^{exp.} \cdot \dot{V}_L}{V_c} \tag{2.66}$$

It is worth noting that the column dead time is usually determined by a non-retained compound such as uracil.

2.2.3.2   Phase Equilibria

At dilute feed concentrations, adsorption isotherms are usually **linear**:

$$q_i(c_i) = K_{i,H}c_i \tag{2.67}$$

Where $q_i(c_i)$ and c_i are the concentration of component i in the stationary and mobile phases, respectively. The validation of this equation, which is equivalent to Henry's equation, can be explained by the fact that the loading concentration is dilute and the adsorbed components are isolated on the surface of the adsorbent (stationary phase), with no interactions between them (**linear behavior**). However, for high loading concentrations and non-linear behavior, non-linear isothermal models must be used [114, 119, 127, 130]. In analytical HPLC or even GC, the equilibrium can be explained by the linear isotherms due to the very low concentrations. To determine Henry's constant ($K_{H,i}$) the experimental column dead time, $t_0^{exp.}$, the total porosity, ε_{tot}, and the experimental retention time of the solute, $t_{R,i}^{exp.}$, are required [97, 111, 132, 133]:

$$\frac{dq_i(c_i)}{dc_i} = K_{i,H} = \left(\frac{t_{R,i}^{exp}}{t_0^{exp}} - 1\right)\left(\frac{\varepsilon_{tot}}{1 - \varepsilon_{tot}}\right) \tag{2.68}$$

These Henry constants are known to be a function of temperature (T) and can be affected by the composition of the solvent. The latter can be expressed by the volume fraction of a modifier ($\varepsilon_{L,mod}$) added to the main solvent. This means:

$$K_{i,H} = K_{i,H}\left(\varepsilon_{L,mod}, T\right) \tag{2.69}$$

The temperature dependence can be expressed by an exponential function for which the enthalpy of adsorption is required. This can be estimated from a series of pulse experiments performed isothermally but at different temperatures. The composition of solvents is more complex and requires more mechanistic insight. Typically, the linear solvent strength model (LSS) [114, 128–130] is used, which provides the following:

$$K_{i,H}\left(\varepsilon_{L,mod}\right) = A_i e^{B_i \varepsilon_{L,mod}} \tag{2.70}$$

The study of the separation of the component i under isocratic elutions leads to the above analytical expression that depends on the volume fraction of the modifier to calculate Henry constants as a linear equilibrium parameter. In the above exponential function, A_i and B_i are experimental coefficients.

2.2.3.3　Column Efficiency, Plate Number and Axial Dispersion

The shape and position of chromatograms are influenced by many factors, particularly fluid dynamics in the packing bed, the rate of mass transfer around and within particles, and the frequency of adsorption and desorption steps, all of which cause the undesirable effect of band broadening. A general key parameter for chromatographic separation performance is the number of theoretical plates (equilibrium steps), $\bar{N}$, which is representative of column efficiency and thus the degree of deviation (axial dispersion($D_{i,app}$)) from ideal behavior. The number of plates of a solid-liquid chromatography process corresponds to the kinetic parameter [97, 111, 121, 127]. The larger the number of plates, the higher the efficiency and the narrower the peaks. However, due to non-ideal fluid dynamics and limited mass transfer rate, real columns have limited efficiency.

The apparent axial dispersion of component i ($D_{i,app}$) can be estimated from the corresponding number of stages used in the equivalent plate model. In analytical chromatography it is well known that this number can be estimated from a separation profile by analyzing the retention time $t_{R,i}$ for each component and its standard deviation σ_i as a criterion for peak width [97, 111, 114, 115, 119, 128, 129]:

$$\bar{N}_i = \left(\frac{t_{R,i}}{\sigma_i} \right)^2 \tag{2.71}$$

The detected peaks of high-efficiency columns are relatively symmetrical (see figure 2.12). In this case, the average retention time of a peak can be easily estimated from the peak maximum. Furthermore, for peaks with Gaussian distribution, there are several ways to estimate the standard deviation and/or variance. Figure 2.12 shows the options for determining peak width at different peak heights. One of the most commonly used options is to evaluate the peak width at half height, $w_{1/2}$, which is nearly 2.354σ.

$$\bar{N}_i \approx 5.54 \left(\frac{t_{R,i}}{w_{1/2,i}} \right)^2 \tag{2.72}$$

Similarly, the standard deviation is determined by analyzing the two inflection points (see figure 2.12 (ip_1, ip_2)) [97, 111, 119, 121]:

$$\bar{N}_i = 16 \left(\frac{t_{R,i}}{w_{base,i}} \right)^2 \tag{2.73}$$
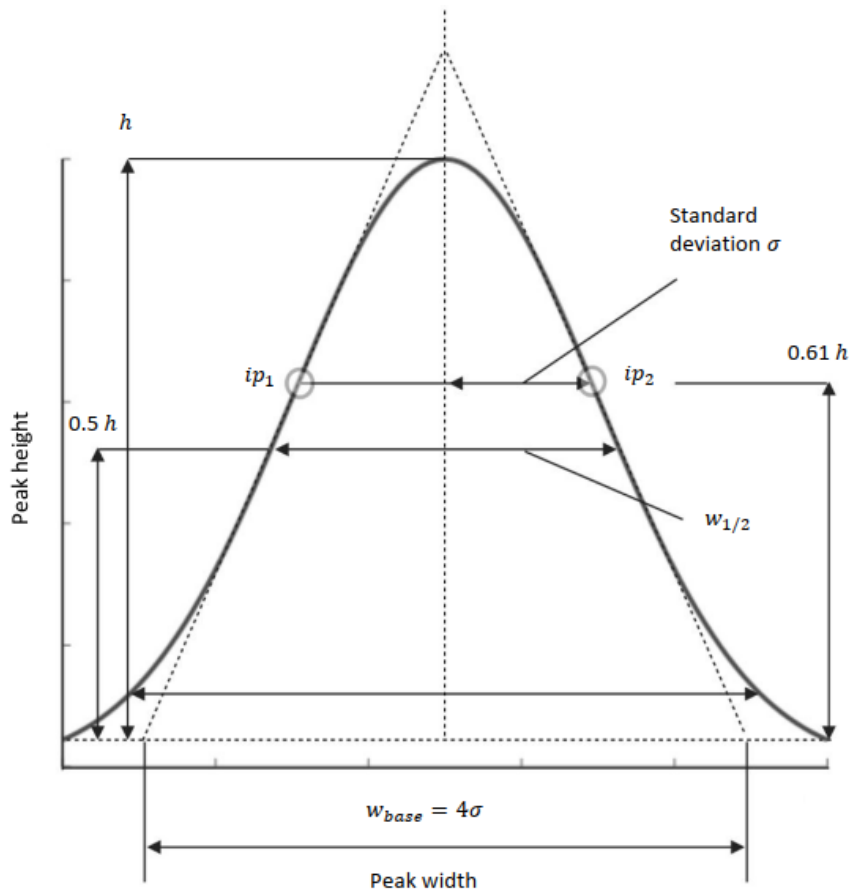
Figure 2.12: Evaluation of the variance for a Gaussian peak. Inspired by [111]

The number of theoretical plates and the corresponding height between them, $HETP$, are inversely related:

$$HETP_i = \frac{L_c}{\bar{N}_i} \tag{2.74}$$

By L_c is meant the length of the column. The correlation between $\bar{N}_i$ and $D_{i,app}$ assuming the same second moments is [97, 111, 114, 115, 119, 128, 129]:

$$D_{i,app} = \frac{u_L L_c}{2\bar{N}_i} \tag{2.75}$$

Already if $\bar{N}_i$ exceeds 100, the assumption of the equilibrium model (Eq. 2.61) will be relatively well fulfilled.

Therefore, to account for band broadening and to ensure that the peaks of a real separation profile do not overlap, the column efficiency for each peak should be examined.

Note that at the outset we should consider **three assumptions**: (**I**) the column efficiency for isocratic and gradient elution is constant, (**II**) there is no nonlinearity for the overloaded injections (assuming linear isotherms), (**III**) the band broadening is not enhanced when a larger volume of feed is injected during preparative runs.

2.2.4   Process Variants

2.2.4.1   Analytical vs. Preparative Chromatography (Scale Up)

The purpose of a chromatographic approach can be analytical or preparative. In analytical chromatography, the goal is to separate the components of the sample. Here, the goal is to analyze a substance in detail and collect information about it. This, in turn, can yield a qualitative profile or fingerprint of the sample. In the analytical scale, the mass injected of component i is very small with following mass balance:

$$m_{i,tot} = m_{i,inj} = c_{i,inj}V_{inj} = c_{i,inj}t_{inj}\dot{V}_L \tag{2.76}$$

Where $m_{i,inj}$, $c_{i,inj}$, V_{inj}, and t_{inj} are mass injection of component i, concentration injection of component i, volume injection, and injection time, respectively.

On the other hand, preparative chromatography (large $m_{i,inj}$) is about isolating and purifying sufficient amounts of a particular substance from the sample. The separation methods and parameters used in analytical chromatography can be scaled for preparative chromatography. The two techniques are complementary, one providing a fingerprint and the other a purification method. Furthermore, the two techniques are not mutually exclusive [111, 115, 119, 121].

The traditional technique of preparative liquid chromatography originated at the beginning of the last century, in 1903, when M. Twsett performed the first separation of carotene pigments [119]. As explained earlier, preparative chromatography requires high concentrations and large volumes of feed, which leads to a non-linearity effect. In nonlinear chromatography, the equilibrium concentrations of a component are not proportional between the stationary and mobile phases, resulting in nonlinear phase equilibrium isotherms. The equilibrium isotherm of each component depends on the concentrations of all other components present in the injected solution. Therefore, the band profile, retention time, and peak height of a component would be different for overcharged runs (nonlinear isotherms) than for low concentration injections (linear isotherms). According to the assumption **II**, we assumed that there is no non linearity in the overcharged injections. To scale-up the same conditions of the analytical scale, such as:

$$L_c^{small} = L_c^{large} \tag{2.77}$$

$$u_i^{small} = u_i^{large} \tag{2.78}$$

$$t_{R,i}^{small} = t_{R,i}^{large} \tag{2.79}$$

the following simple scale-up rule is applied based on keeping column length constant

and increasing inner diameter of the column (without considering non linearity) [111, 119, 121]:

$$\left(\frac{L_c d_c^{large}}{L_c d_c^{small}}\right)^2 = \frac{\dot{V}_L^{large}}{\dot{V}_L^{small}} = \frac{V_{inj}^{large}}{V_{inj}^{small}} \qquad (2.80)$$

The terms d_c^{large} and d_c^{small} refer to the inner diameters of the preparative and analytical columns, respectively.

One of the critical problems in the large-scale application of preparative chromatography has been achieving large-diameter columns with separation performance comparable to analytical columns. Long-term bed stability, low hydrodynamic resistance, and high column efficiency are important properties required of industrial columns. To achieve these properties and their often costly consequences, several options for bed compression have been proposed. Compression can be static or dynamic, with the latter offering the great advantage of automatically eliminating voids as they form, before their size can affect column efficiency [97, 111, 119, 121]. An important event in the history of preparative chromatography took place in 1974, when Roussel Uclaf (a former French pharmaceutical company, now part of Aventis) patented the concept of dynamically compressed columns (columns equipped with a piston capable of compressing the chromatographic bed), paving the way for modern preparative chromatography, MPC, which represents a real revolution in the history of chromatography and probably in the history of the pharmaceutical industry. MPC uses Dynamic Axial Compression (DAC) columns typically filled with 10 µm particles of robust silica-based material and operated at medium to near-high pressure (30-70 bar). Dynamic axial compression technology provides a user-friendly and simple method for packing chromatographic columns on a preparative scale. The DAC system enables rapid packing of columns from virtually any packing material. The DAC system enables optimal column efficiency and linear scalability from laboratory to industrial scale due to excellent packing and controlled liquid distribution [97, 111, 119, 121].

The column contains a movable piston attached to a hydraulic cylinder (jack). The piston is used to pack the column and maintains the stationary phase under adjustable and dynamic compression to ensure maximum efficiency and bed stability at any scale. The piston prevents mechanical degradation, and bed compression is kept constant regardless of bed swelling or shrinkage. For example, when solvent conditions cause particles to swell, the piston automatically allows the bed to expand to maintain constant compression.

The High Performance Concept is the concept behind MPC's outstanding story. This is essentially the use of columns that deliver a large number of theoretical plates in a relatively short time. This is indeed very similar to the situation with analytical

columns. Finally, it should be noted that MPC is probably one of the few physical-chemical methods that can be directly scaled up without any special adaptations: a method developed using a column with an internal diameter of a few mm can be scaled up more than 100,000 times! This is certainly a very important description for the success of MPC in the industry [97, 111, 119, 121].

2.2.4.2   Isocratic vs. Solvent Gradient Elutions

The major components of saffron crude extract, namely picrocrocin, crocin I, and crocin II, are able to be separated on a $C18$ column by both isocratic and gradient elutions. In isocratic elution, the concentration of the mobile phase composition (weaker solvent A, stronger solvent B (modifier)) and the temperature remain constant ($\varepsilon_{L,mod} = Const., T = Const.$), which means that the Henry constant of component i is also constant in isocratic elution ($K_{i,H} = Const.$). However, in linear gradient elution, the volume fraction of modifier ($\varepsilon_{L,mod}$) is gradually increased during the gradient time (e.g., from 10% B ($\varepsilon_{L,mod} = 0.1$) to 80% B ($\varepsilon_{L,mod} = 0.8$) (Figure 2.13A)), apart from PH, temperature, flow rate, and other conditions, whereas in segmented gradient elution (Figure 2.13B) and step-gradient elution (Figure 2.13C) the volume fraction of the modifier changes periodically and step-wise, respectively [114, 119, 121, 131, 134]. For instance, the segmented gradient elution in Figure 2.13B has three segments ($\varepsilon_{L,mod,1}, \varepsilon_{L,mod,2}, \varepsilon_{L,mod,3}$) with two switching times ($t_{sw,1}, t_{sw,2}$) in 20 minutes. The concentration of the modifier in each segment is changed gradually depending on the separation purpose, and at the end of each segment, it is switched to the new segment with new concentration of the modifier. However, the step-gradient elution in Figure 2.13C has three steps with constant volume fraction of modifier in each step. The duration of each step and corresponding switching times are considered based on the shortest cycle time of each run and the highest productivity of component i.
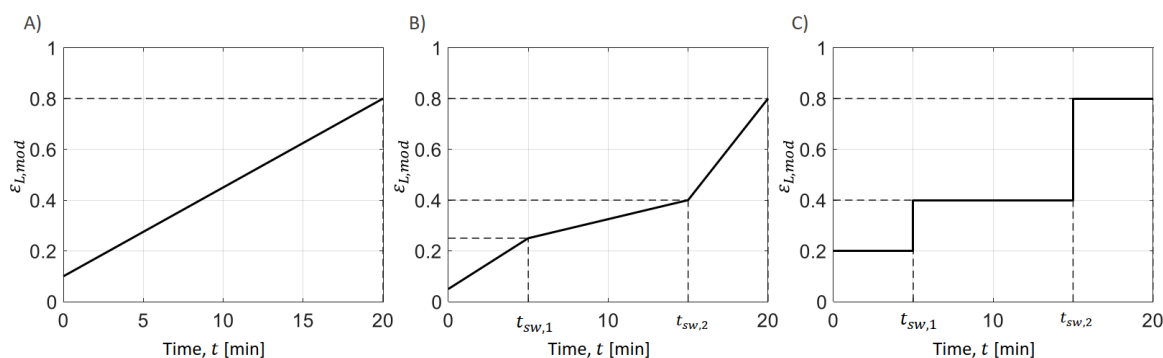
Figure 2.13: Examples of gradient elutions: (A) linear gradient program from 10% B ($\varepsilon_{L,mod} = 0.1$) to 80% B ($\varepsilon_{L,mod} = 0.8$) in 20 minutes (10/80% B at 0/20min); (B) segmented gradient program, 5/25/40/80% B at 0/5/15/20min. (C) step-gradient program, $\varepsilon_{L,mod,1} = 0.2$ for $0 < t < (t_{sw,1} = 5min)$, $\varepsilon_{L,mod,2} = 0.4$ for $t_{sw,1} < t < (t_{sw,2} = 15min)$, and $\varepsilon_{L,mod,3} = 0.8$ for $t_{sw,2} < t < (t_{sw,M-1} = 20min)$. Inspired by [121]

The onset of gradient elution with larger values of the modifier (%B) degrades the separation and resolution of early peaks, while smaller values of the modifier further increase the values of retention factor (k) and run time, leading to a decrease in peak height and detection sensitivity. Usually, changes in the %B value are made to shorten the gradient time but otherwise maintain the same separation with the same retention factor. Such changes in the initial and final %B values are equivalent to removing the (wasted) parts of the chromatogram where no peaks are present. Further details, figures, and equations are given in Ref. [121, 131, 135, 136]. Hence, in gradient elution, the Henry's constant of component i is function of $\varepsilon_{L,mod}$ and T in different time and space (t,z):

$$K_{i,H}(t, z) = K_{i,H}(\varepsilon_{L,mod}(t, z), T(t, z)) \tag{2.81}$$

Isocratic and gradient elution methods complement each other. The isocratic method is generally preferred for its simplicity, convenience, and reproducibility, but is unsuitable for complex samples containing solutes with different polarities in a short time frame (0≤retention factor (k)≤50) [114, 119, 121, 131, 137]. Gradient elution is routinely used in the analysis of complex mixtures. This method was first introduced in the 1950s [114, 121, 130, 131]. Because the inhibitory behavior of compounds at the stationary phase is affected by the composition of the solvent mixtures, the gradient elution method provides more robust results than the isocratic elution method [111, 119, 121, 131, 132]. Therefore, gradient methods allow the separation of solutes that have a wider range of polarity than isocratic elution. Separations where gradient elution is commonly used in $HPLC$ include the separation of amino acids, phenols, polyaromatic hydrocarbons (PAH's), tetracyclines, and proteins. In general, gradient elution is needed when a large number of solutes with different polarities have to be separated in a short time. In this elution program, the solvents are relatively inexpensive, and the time for re-equilibration between gradient runs is short. Gradient methods are most commonly used in reversed-phase chromatography; however, the general concepts and principles are applicable to other HPLC separation modes, e.g., normal phase, ion exchange, etc. [114, 119, 121, 131, 135].

Successful $HPLC$ gradient chromatography requires a careful experimental procedure. In gradient separations, impurities from the weak solvent may stack on the column at the beginning of the run and elute later as the solvent strength increases. This can lead to additional peaks in the final chromatogram and affect the quality of the separation. Therefore, the best quality solvent possible should be used. Sufficient time must always be considered between runs for re-equilibration of the column. Insufficient re-equilibration time will result in non-reproducible chromatography and significant variations in retention times. On the other hand, re-equilibration of the column longer than necessary leads to time losses [114, 119, 121, 131, 135].

The solvents used in the gradient elution must be fully compatible, i.e., they must be fully miscible, and their compatibility and/or strength should not be too different, otherwise solvent segregation may occur. In addition, baseline shifts may occur during the gradient development run if one solvent has a significantly different background adsorbance than the other. Therefore, a blank gradient should always be run to check the extent of baseline shift and also to look for eluting impurity peaks. Finally, the effect of solvent mixtures on column backpressure must also be considered. For example, the viscosity of a 50/50 water-ethanol mixture is much higher than that of a single solvent. In practice, this means that the column backpressure approximately doubles in the middle of a gradient elution of 100% water to 100% ethanol, which may mean that lower flow rates must be used during the gradient run to avoid overpressurizing the column [114, 121, 131, 138].

This study first examined the effect of different volume fractions of modifier B, in isocratic elutions, on peak retention and peak broadening of picrocrocin, crocin I and crocin II. It provided the basis for the development of a step-gradient elution method (step-wise) with reduced cycle time, acceptable productivity, and high yield and purity of the components. The corresponding modelling for the development of the step-gradient elution method will be done in the (next) section 2.2.5 utilising the equilibrium theory based on Eq. 2.62 and Eq. 2.63.

2.2.5 Simplified Modeling of Step-Gradient Elution Using Equilibrium Theory

Gradient elution has been widely used in liquid chromatography since its introduction in the early 1950s [111, 119, 121, 130, 131]. Gradient elution can significantly reduce the batch time of analyses, improve the resolution of complex mixtures and providing more robust results compared to isocratic elution [111, 119, 121, 131, 133]. One mode that is easy to design and implement is step gradient chromatography. In this mode, M steps ($j = 1, M$) are interspersed with $M - 1$ different ideal switching times $t_{sw,j}^{ideal}$. Ideal switching time means ideal column efficiency and no band broadening. The solvent composition at the inlet is manipulated over time and space (t, z) as follows:

$$\varepsilon_{L,mod}(t, z) = \begin{cases} \varepsilon_{L,mod,1} \text{ for } \left[0 < t \leq \left(t_{sw,1}^{ideal} + \frac{z}{u_L}\right)\right] \\ \vdots \\ \varepsilon_{L,mod,j} \text{ for } \left[t_{sw,j-1}^{ideal} < t \leq \left(t_{sw,j}^{ideal} + \frac{z}{u_L}\right)\right] \\ \vdots \\ \varepsilon_{L,mod,M} \text{ for } \left[t_{sw,M-1}^{ideal} < t \leq \left(t_{end}^{ideal} + \frac{z}{u_L}\right)\right] \end{cases} ; z = 0, L_c \qquad (2.82)$$

It is worth noting that the duration of the first interval is between zero and the

summation of the ideal first switching time $t_{sw,1}^{ideal}$ and the dead time z/u_L (the time required for the solvent composition to move unretained throughout the column). In fact, when we switch to the new solvent composition, the entire column is still full of the previous solvent composition, which must be depleted (depletion of $\varepsilon_{L,mod,1}$). The interval j begins when the new solvent composition $\varepsilon_{L,mod,j}$ meets the old solvent composition $\varepsilon_{L,mod,j-1}$ at $t_{sw,j-1}^{ideal}$ (at the inlet of the column), and it ends at $(t_{sw,j}^{ideal} + z/u_L)$ (fully depletion of $\varepsilon_{L,mod,j}$). The last interval $\varepsilon_{L,mod,M}$ refers to the re-equilibrium of the column. Last but not least, t_{end}^{ideal} is the end of the ideal run-time, which means that a new run can be started afterwards.

It is assumed that the solvent composition perturbations move unretained through the column with velocity u_L. This gives complete knowledge of the solvent composition at any point in the column at any time, i.e., $\varepsilon_{L,mod}(t,z)$. With this knowledge, the change in migration velocity of component i (u_i) after each switching operation is predictable by the equilibrium theory (Eq. 2.61 and Eq. 2.62) [114, 121, 127, 130, 131]:

$$u_i \left(\varepsilon_{L,mod} \left(t, z \right) \right) = \frac{u_L}{1 + F K_{i,H} \left(\varepsilon_{L,mod} \left(t, z \right) \right)} \tag{2.83}$$

Under equilibrium conditions, the **changes in solvent composition** gradually - **change the specific Henry constants** of the components and hence the **specific migration rates**. In the characteristic diagrams, these changes in u_i are represented as changes in the slopes of the trajectories (see Figures 2.11 and 2.14), which is used to estimate the retention time of component i (by Eq. 2.63) at the exit of the column ($z = L_c$). For example, a sample contains components 1 and 2. Component 1 has a smaller Henry constant than component 2 ($K_{1,H} < K_{2,H}$), which means less retention of component 1 at the stationary phase and faster elution than component 2 (see Figure 2.14). To achieve faster elution of component 2, and thus shorten the separation time without compromising the achievable separation factor, a larger volume fraction of the modifier must be used. Thus, for example, if component 1 is eluted by $\varepsilon_{L,mod,1}$ in 3 minutes, component 2 is still somewhere in the column (see Figure 2.14). To switch to a larger volume fraction of modifier, $\varepsilon_{L,mod,2}$, to elute component 2, we need to calculate and optimize the ideal first switching time $t_{sw,1}^{ideal}$:

$$t_{sw,1}^{ideal} = \Delta t_{inj} + t_{R,1} - t_0 = \Delta t_{inj} + t_0 \left(1 + F K_{1,H} \left(\varepsilon_{L,mod,1}(t,z) \right) \right) - t_0 \tag{2.84}$$

When we switch to the new solvent composition, $\varepsilon_{L,mod,2}$, the corresponding component 2 is somewhere in the column (z^*) (see Figure 2.14). This means that based on the linear velocity of the mobile phase, u_L, (Eq. 2.64), the new solvent composition, $\varepsilon_{L,mod,2}$, requires a special time, z^*/u_L, to reach and hit the corresponding component 2 at z^* (see Figure 2.14). This means that for a precise determination of the ideal

second switching time, $t_{sw,2}^{ideal}$, the intersection in space and time (spatial and temporal) (z^* and t^* in Figure 2.14) must first be determined. In Figure 2.14, line 1 and line 3 meet at this intersection, which they can be illustrated mathematically as follows:

$$z_{Line1}(t) = z_{0,Line1} + u_{Line1}t \tag{2.85}$$

$$z_{Line3}(t) = z_{0,Line3} + u_{Line3}t \tag{2.86}$$

Therefore, for intersections at $t = t^*$ and $z = z^*$ (see Figure 2.14) there is:

$$z_{0,Line1} + u_{Line1}t^* = z_{0,Line3} + u_{Line3}t^* \tag{2.87}$$

and/or

$$t^* = \frac{z_{0,Line1} - z_{0,Line3}}{u_{Line3} - u_{Line1}} \tag{2.88}$$

To find the intersection in space (z^*) and time (t^*) we can start from the intersection in space for Line1 and Line3 (z^*) (see Figure 2.14):

$$z^* = z_{Line1}^*(t^*) = z_{Line3}^*(t^*) \tag{2.89}$$

Therefore, there is:

$$u_2\left(\varepsilon_{L,mod,1}(t,z)\right)\left(t^* - \Delta t_{inj}\right) = \frac{L_c}{t_0}\left(t^* - t_{sw,1}^{ideal}\right) \tag{2.90}$$

The intersection (of x and y) in time, t^*, would be:

$$t^* = \frac{u_2\left(\varepsilon_{L,mod,1}(t,z)\right)\Delta t_{inj} - \frac{L_c}{t_0}t_{sw,1}^{ideal}}{u_2\left(\varepsilon_{L,mod,1}(t,z)\right) - \frac{L_c}{t_0}} = \frac{\frac{\frac{L_c}{t_0}}{1+FK_{2,H}\left(\varepsilon_{L,mod,1}(t,z)\right)}\Delta t_{inj} - \frac{L_c}{t_0}t_{sw,1}^{ideal}}{\frac{\frac{L_c}{t_0}}{1+FK_{2,H}\left(\varepsilon_{L,mod,1}(t,z)\right)} - \frac{L_c}{t_0}} \tag{2.91}$$

Therefore, t^* is:

$$t^* = \frac{\Delta t_{inj} - t_{sw,1}^{ideal}\left(1 + FK_{2,H}\left(\varepsilon_{L,mod,1}(t,z)\right)\right)}{-FK_{2,H}\left(\varepsilon_{L,mod,1}(t,z)\right)} \tag{2.92}$$

Substituting Eq. 2.92 into Eq. 2.90 yields the intersection in space, z^*:

$$z^* = \frac{L_c}{t_0}\left(t^* - t_{sw,1}^{ideal}\right) = \frac{L_c}{t_0}\left(\frac{\Delta t_{inj} - t_{sw,1}^{ideal}\left(1 + FK_{2,H}\left(\varepsilon_{L,mod,1}(t,z)\right)\right)}{-FK_{2,H}\left(\varepsilon_{L,mod,1}(t,z)\right)} - t_{sw,1}^{ideal}\right)$$

$$(2.93)$$

Hence, the ideal second switching time can be determined based on these intersections:

$$t_{sw,2}^{ideal} = t_{R,2} - t_0 = t^* + \frac{L_c - z^*}{u_2\left(\varepsilon_{L,mod,2}(t,z)\right)} - t_0 \qquad (2.94)$$

Following equation is obtained by substituting t^*, z^*, and the migration velocity $u_2(\varepsilon_{L,mod,2}(t,z))$ into Eq. 2.94:

$$t_{sw,2}^{ideal} = \frac{\Delta t_{inj} - t_{sw,1}^{ideal}\left(1 + FK_{2,H}\left(\varepsilon_{L,mod,1}(t,z)\right)\right)}{-FK_{2,H}\left(\varepsilon_{L,mod,1}(t,z)\right)}\left(-FK_{2,H}\left(\varepsilon_{L,mod,2}(t,z)\right)\right)$$
$$+ \left(1 + FK_{2,H}\left(\varepsilon_{L,mod,2}(t,z)\right)\right)\left(t_0 + t_{sw,1}^{ideal}\right) - t_0$$

$$(2.95)$$

In the end, the sum of the ideal second switching time and the ideal equilibrium time t_{eq}^{ideal} gives the ideal total cycle time:

$$\Delta t_{cyc}^{ideal} = t_{sw,2}^{ideal} + t_{eq}^{ideal} \qquad (2.96)$$

In the ideal columns, equilibrium time is equal to the dead time ($t_{eq}^{ideal} = t_0$). Therefore, under ideal separation conditions the Eq. 2.96 reads:

$$\Delta t_{cyc}^{ideal} = \frac{\Delta t_{inj} - t_{sw,1}^{ideal}\left(1 + FK_{2,H}\left(\varepsilon_{L,mod,1}(t,z)\right)\right)}{-FK_{2,H}\left(\varepsilon_{L,mod,1}(t,z)\right)}\left(-FK_{2,H}\left(\varepsilon_{L,mod,2}(t,z)\right)\right)$$
$$+ \left(1 + FK_{2,H}\left(\varepsilon_{L,mod,2}(t,z)\right)\right)\left(t_0 + t_{sw,1}^{ideal}\right)$$

$$(2.97)$$
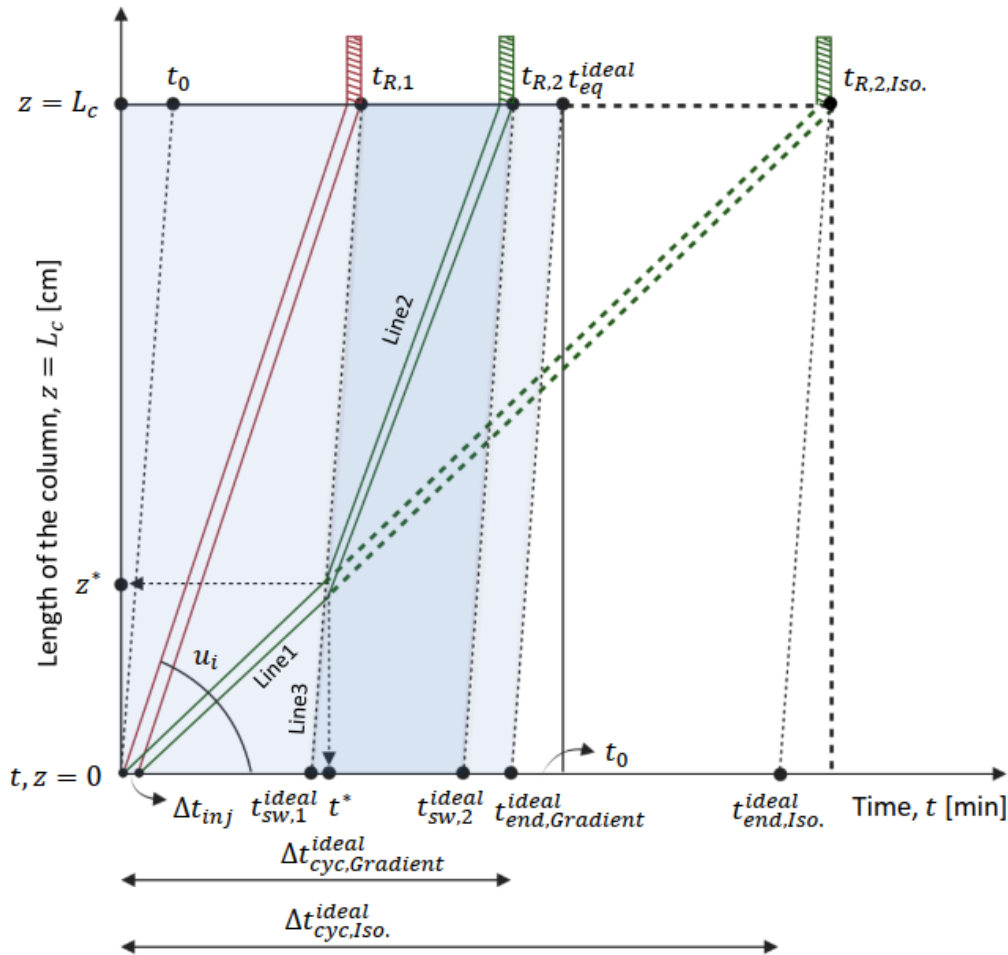
Figure 2.14: Step-Gradient and isocratic trajectories of component 1 and 2. The first light blue section: volume fraction of the modifier at first step ($\varepsilon_{L,mod,1}$). Dark blue section: volume fraction of the modifier at second step ($\varepsilon_{L,mod,2}$), ($\varepsilon_{L,mod,2} > \varepsilon_{L,mod,1}$). Second light blue section: return to the volume fraction of the modifier at first step to re-equilibrium of column. Red lines: Elution trajectory of component 1 at first step. Green lines: Elution trajectory of component 2 at first and second steps. Green dashed lines: Isocratic elution trajectory of component 2. Iso.: Isocratic. $\Delta t^{ideal}_{cyc,Iso.} > \Delta t^{ideal}_{cyc,Gradient}$ [47, 121, 127, 130]

The cycle time is the time interval between two injections (Figure 2.14, Δt_{cyc}). Note that these switching times are for an ideal chromatographic separation profile without considering band broadening (column efficiency). As explained in subsection 2.2.3.3, the standard deviation is determined by analyzing the two inflection points (see Figure 2.12. (ip_1, ip_2)), which is a criterion for peak width and/or column efficiency. To account for column efficiency and band broadening, and to ensure that peaks do not overlap in the real separation profile, half of the peak width of component i at the base of the peak $2\sigma_i$ should be added to the corresponding ideal switching times. In the end, the actual cycle time Δt^{real}_{cyc} is used for the productivity calculations.

2.3   Performance Criteria of Separation Processes

The performance of each process can be evaluated using three critical parameters, namely Purity, Productivity, and Yield. The aim of the performance-determining parameters is to evaluate and compare process variants in the both extraction and chromatographic processes. It should be mentioned that each process is balanced alone.

2.3.1   Purity

In crude extract processing (solid-liquid chromatography), purity is defined as the ratio of the mass of the purified target component i (m_i) to the total mass of the collected fraction, $\sum_{i=1}^{N} m_i$:

$$Pu_i = \frac{m_i}{\sum_{i=1}^{N} m_i} \times 100 \qquad (2.98)$$

2.3.2   Productivity

Generally, productivity is the rate production of a target molecule i at a given scale defined by the following equation:

$$Pr_i = \frac{m_i}{\Delta t_{cyc} Scale} \quad ; \quad [g/min/l] \qquad (2.99)$$

Where m_i is the mass of the collected target component i, $Scale$ is the scale of the process, i.e., the volume of the vessel in the extraction process and the mass of the adsorbent $(m_{Ads.}\ (g_{Ads.}))$ in the chromatography process, and Δt_{cyc} is the cycle time, i.e., the time interval between two batch runs in both extraction and chromatography processes:

$$\Delta t_{cyc} = \sum_{j=1}^{N} t_{start\ of\ batch\ j+1} - t_{start\ of\ batch\ j} \qquad (2.100)$$

It is worth noting that the cycle time of a **continuous extraction process** is the total residence time of the process. In the continuous countercurrent process (CC), there is a mass flow rate of the component i through the column, $\dot{m}_i$, which is the output **dimensioned** concentration of the component i in the liquid phase, $c_{i,N}$, multiplied by the volumetric flow rate of the liquid phase, $\dot{V}_L$. On the other hand, the volume of the countercurrent column is usually divided into three segments, namely the volume of solid phase, V_S, the volume of liquid phase, V_L, and the volume of air, V_{air}. However, the volume of air is assumed to be zero, $V_{air} = 0$. Therefore,

productivity in the continuous counter-current extraction process is the flow of a target molecule over the total volume V_{tot}:

$$Pr_i^{CC} = \frac{c_{i,N} \times \dot{V}_L}{V_{tot}} = \frac{\dot{m}_i}{V_{tot}} \quad ; \quad [g/min/l] \tag{2.101}$$

or in the simplified explicit form of neglecting a *Scale* factor as:

$$Pr_i^{CC} = \dot{n}_L = c_{i,N} \times \dot{V}_L \quad ; \quad [g/min] \tag{2.102}$$

The study and quantification of outgoing concentration, $c_{i,N}$, and fluid flow, $\dot{V}_L$, was discussed above in the section 2.1.5. The geometric characteristics of the extractor in different extraction modes and additional equipment (e.g., stirrer, screw occupancy) may affect the final results. Therefore, the *Scale* factor can be considered as the free volume. In addition to productivity, recovery yield is also of interest.

2.3.3   Recovery Yield

The recovery yield is the mass ratio of the collected product, $m_{i,coll.}$, to the total mass of the initial product, $m_{i,tot.}$:

$$Y_i = \frac{m_{i,coll}}{m_{i,tot}} \times 100 \tag{2.103}$$

In the purification (chromatography) process, the definition of yield is the ratio between the mass of the collected target component and the injected total initial mass of that component obtained by the exhaustive extraction, $x_{i,S}^0$ (see table 4.3). However, in both batch and steady state continuous counter-current extraction process, the recovery yield is calculated using the estimated outgoing concentration of the component i in the outgoing liquid phase by Eq. 2.31 (for batch) and Eq. 2.42 (for counter-current) :

$$Y_i = \frac{\varepsilon \times c_i^{out}}{(1 - \varepsilon) \times q_i^{in}} \times 100 \tag{2.104}$$

Concentration of component i in the starting solid phase $q_i^{in}(x_{i,S}^0)$ is taken from the table 4.3. The quantification of productivity and recovery yield for the batch and continuous extraction of picrocrocin, crocin I and crocin II from the *Crocus sativus L.* (saffron), and also for the analytical and preparative purification of them by HPLC will be done in chapter 4.

Chapter 3

Experimental

Two main separation techniques are used in this study, namely extraction and chromatography. The first step of any separation technique is the characterization of the target components by preliminary experiments.

3.1 Preliminary Experiments

3.1.1 Stability of Components

As explained earlier, the compatibility of a solvent to dissolve a target molecule (solute) depends on the polarity of the solute, the polarity of the solvent, and the solubility of the solute. Due to the sugar structure in the chemical structure of the main constituents of saffron, namely picrocrocin, crocin I and II, and according to the rule "like dissolves like", these compounds are more soluble in polar solvents. The polar solvents such as water, and ethanol-water mixtures showed higher performance and capacity in extracting of the saffron components [47, 51]. Another factor for the selection of one or more solvents is the stability time (life time) of the dissolved compound(s) in that solvent(s). To verify this, the stability of picrocrocin, crocin I and crocin II in low and high volumetric fractions of ethanol (0.22 and 0.8) in composition with water was studied during 24 hours. For this purpose, 1 g of saffron crude extract was dissolved in one liter of 0.22 and 0.8 volume fraction of ethanol in composition with water, and then the concentration of the above mentioned compounds was checked hourly for 24 hours. The changes in the concentration of the compounds indicate the duration of their stability (see Figure 4.1).

3.1.2 LC/MS Analysis

Liquid chromatography is a suitable technique for the separation and analysis of the components of saffron extract. In this study, analytical chromatography analysis of saffron crude extract, both LC and LC/MS, is performed on a C18 analytical col-

umn using a linear gradient elution method. This analysis provides a fingerprint of picrocrocin, crocin I and crocin II. The analysis of the constituents of the saffron extract and the study of their retention behavior are performed using a high performance liquid chromatography, HPLC, system (Agilent 1260 series, Germany) equipped with a degasser (1260 Degasser), a four-channel gradient pump (1260 Binary Pumps), an auto-sampler (1260 ALS), a reversed phase column (YMC-Triart Prep C18-S, 150×4.6 mm, 15 μm, 12 nm), a column oven (1260 TCC), and a UV-Vis photo-diode array detector (1260 MWD VL). Figure 3.1 shows schematic illustration of an HPLC system.
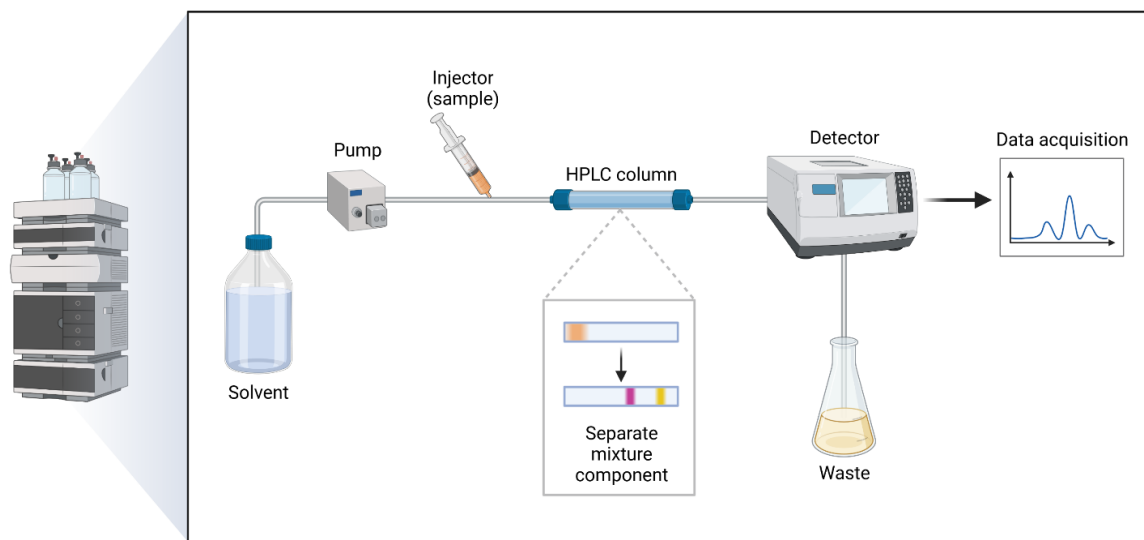
Figure 3.1: Schematic illustration of the High Performance Liquid Chromatography, $HPLC$, process

The target molecules of the saffron extract (picrocrocin, crocin I, and crocin II) were identified by LC-MS using a quadrupole time of flight mass detector (Q-TOF-LC-MS 6530, Agilent Technology, CA, US).

3.1.3   Dynamic Procedure to Calibrate Detector

One of the best and most well-known methods for quantifying chemicals is the calibration curve. Establishing a calibration curve for a component requires a pure sample (100%) of that component. Commercially available samples of picrocrocin and crocins contain some impurities and are not suitable for establishing a calibration curve. Therefore, picrocrocin, crocin I and crocin II were purified to 99.9% purity on an analytical scale (V_{inj}=100 μl, D_S=10 g/l) in our laboratory at the Max-Planck-Institute for Dynamics of Complex Technical Systems, Magdeburg. The separation method and column conditions are the same as in the $LC-MS$ analysis section in Chapter 4 (see Figure 4.2). The collected fractions of picrocrocin, crocin I and crocin II were concentrated using the rotary evaporator (BUCHI, Switzerland) and then dried by the freeze dryer (ZiRBUS technology GmbH, VaCo2, max temp -50

°C, Germany). The obtained fine powders of picrocrocin, crocin I and ccrocin II were used to prepare their calibration curves. The following figure shows a schematic representation of a peak from $HPLC$:
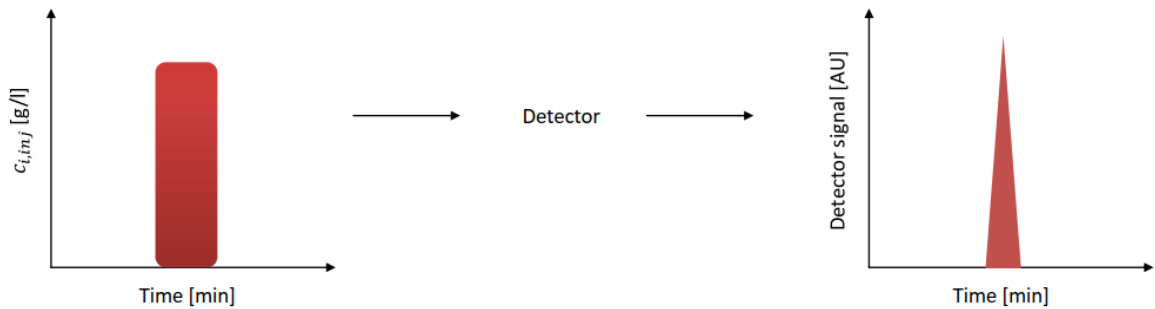
Figure 3.2: Schematic representation of a $HPLC$ peak for component i

At the inlet, the mass of component i in the injection sample is known:

$$m_{i,inj} = V_{inj}c_{i,inj} = \dot{V}_L t_{inj} c_{i,inj} \tag{3.1}$$

The outlet mass of component i can be introduced by the following equation:

$$m_{i,out} = \dot{V}_L \int_0^\infty c_{i,inj}(t)dt \tag{3.2}$$

Therefore, the mass balance of component i at the in- and outlets is:

$$m_{i,inj} = m_{i,out} \tag{3.3}$$

Thus, there is:

$$V_{inj}c_{i,inj} = \dot{V}_L \int_0^\infty c_{i,inj}(t)dt \tag{3.4}$$

On the other hand, the relationship between the injection concentration of the component i and its signal is generally linear:

$$c_{i,inj}(t) = \bar{F}signal(t) \tag{3.5}$$

In the above equation, $\bar{F}$ is the calibration factor. Combining the equations 3.4 and 3.5 gives the following mass balance relation:

$$V_{inj}c_{i,inj} = \dot{V}_L \int_0^\infty \bar{F}signal(t)dt = \dot{V}_L\bar{F} \int_0^\infty signal(t)dt \tag{3.6}$$

After the changeover there is:

$$\bar{F} = \frac{V_{inj}c_{i,inj}}{\dot{V}_L \int_0^\infty signal(t)dt} = \frac{m_{i,inj}}{\dot{V}_L A^{Peak}} \tag{3.7}$$

Here A^{Peak} is the peak area of the detected signal. Therefore, the slope of $m_{i,inj}$ versus $\dot{V}_L A^{Peak}$ introduces the calibration factor (see Figure 3.3A). In terms of knowing the injection time t_{inj}, Eq. 3.7 can be rearranged to:

$$\bar{F} = \frac{V_{inj}c_{i,inj}}{\dot{V}_L \int_0^\infty signal(t)dt} = \frac{t_{inj}c_{i,inj}}{\int_0^\infty signal(t)dt} = \frac{t_{inj}c_{i,inj}}{A^{Peak}} \tag{3.8}$$

Equation 3.8 shows the relationship between the known injection concentration of component i ($c_{i,inj}$) and the corresponding peak area based on the provisionally determined parameters $\bar{F}$ and t_{inj}. Based on this relationship, the unknown concentration of a sample can be calculated by the area of the peak (see Figure 3.3B):

A)   B)
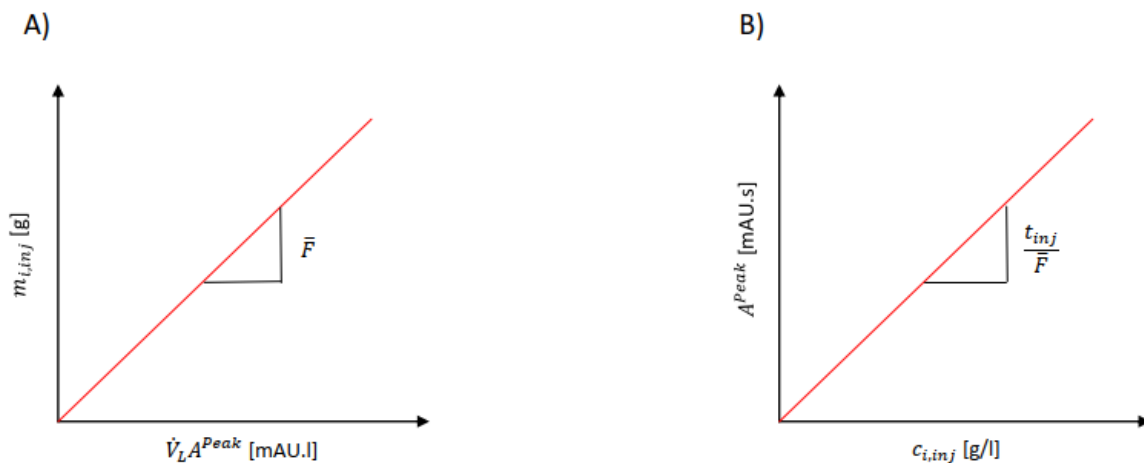
Figure 3.3: Calculation of the calibration factor (Figure A) and determination of the concentration using the peak area (Figure B)

The calibration curve depends on the injection volume, the flow rate of the elution method, and the wavelength. To use the calibration curve, these three parameters must be kept constant for both the standards and the unknown samples. However, if we want to use other conditions for the analysis, we should make the appropriate changes when calculating the calibration curve.

3.2   Solid-Liquid Extraction

3.2.1   Preliminary Experiments

3.2.1.1   Pre-Extraction

In this study, the exported saffron strain from Iran (Medicinal plants and drug research institute, Shahid Beheshti University, Tehran, Iran) was pulverized using a mortar and pestle. In a pre-extraction step with Soxhlet, the saffron powder was extracted with dichloromethane at 40 °C for 7 hours [14]. In this pre-extraction step, unwanted compounds in the saffron powder are eliminated, leading to a more efficient extraction of the target molecules in the following main extraction step with less crowded impurity profiles.

3.2.1.2   Efficient Provision of Crude Extract by Exhaustive Extraction

One of the important and necessary data for the continuous model calculations is the knowledge of the total amount of each component in the initial powder of saffron, $q_i^{in}(x_{i,S}^0)$. To increase the yield and productivity of the extraction and purification steps, all the target molecules of saffron should be extracted efficiently. One of the common methods to efficiently provide a crude extract is the exhaustive extraction method [112]. In exhaustive extraction, almost the entire amount of a component i is transferred from the solid to the liquid phase, either by increasing the mass transfer coefficient (by using a different solvent or temperature) or by reaching the partition equilibrium several times [97, 112]. In this study, the second method was used. In the exhaustive extraction experiments (main extraction), 0.1 g of the treated saffron powder from the pre-extraction step was added to 0.01 liters of 80% ethanol in composition with water and then stirred (350 rpm) for 15 minutes (equilibrium time) at room temperature. After settling the wet saffron powder, the liquid supernatant was separated. The separated wet saffron powder was extracted twice more with fresh 80% ethanol/water solution. By the third extraction, the wet saffron powder was completely yellow and the extraction solution contained only a very small amount of the components, indicating that the highest possible extraction amount is achieved in the first two extraction steps. Finally, the extract phases were concentrated using a rotary evaporator (55 $mbar$, 35 °C, 160 rpm) and dried in a freeze dryer. Concentration analysis was performed using the calibration curve of each component. It should be noted that the $HPLC$ separation method and column conditions are the same as the method used in the $LC-MS$ analysis section in Chapter 4 (see Figure 4.2). The exhaustive extraction process was repeated three times, and the results were included in the calculation of the population standard deviation:

$$\sigma = \sqrt{\frac{1}{N^{exp.}} \sum_{j=1}^{N^{exp.}} \left(m_{i,j} - \mu\right)^2} \qquad (3.9)$$

$$\mu = \frac{1}{N^{exp.}} \sum_{j=1}^{N^{exp.}} m_{i,j} \qquad (3.10)$$

Where σ, $N^{exp.}$, $m_{i,j}$, and μ are population standard deviation, the number of extractors, the mass of component i in extractor j, and the average mass of component i, respectively.

3.2.1.3   Kinetic and Equilibrium

Knowledge of the time required for each process such as extraction, synthesis, etc. is very valuable. Concentration analysis can be used to determine the equilibrium time required to complete an extraction process. For this purpose, concentration analysis must be performed at different time intervals to plot the concentration-time curves (see Figure 4.4). To do this, 0.1 g of saffron powder and 0.01 l of an 80% ethanol/water solution were mixed and stirred at room temperature in batch mode (350 rpm). The small sample volumes (10 μl) for concentration analysis were taken correctly every two minutes, and then the diluted samples filtered with a 0.45 μm PTFE filter were injected onto the HPLC column. The HPLC separation method and column conditions are the same as in the section on $LC - MS$ analysis in Chapter 4 (see Figure 4.2). The concentration analysis of picrocrocin, crocin I and crocin II was performed using the peak area and calibration curve. It is worth mentioning that this batch run experiment was performed several times and with different dosages (see Figures A.5, A.6, A.7). This is also a preliminary experiment to study the kinetics of an extraction process.

3.2.2   Closed Single Batch and Multiple Sequential Batches

Two of the required parameters in the continuous counter-current model calculations are kinetic and partition coefficient as the thermodynamic parameter (k_i^{eff}, $K_{i,E}$), which were estimated by the results of the closed single batch and multiple sequential batches extraction experiments. First, single batch extraction (Ba) was performed (see Figure 3.4). In the single batch extraction experiments, there are eight individual extractors with different dosages (D_S). There is no connection between the extractors. In this series of experiments, N^{Ba}, each extractor j contains a certain amount of saffron powder $m_{S,j}$ and 0.01 l of 80% ethanol in composition with water solution (see Table 3.1). The solid and liquid phases were stirred at room temperature for 15 min (350 rpm). After 15 min, the process was stopped and the extractors were allowed to stand for a few minutes until settling the solid phase. Then the two phases were

separated. The concentration of component i in the liquid phase at equilibrium time, c_i^{eq}, was measured using the HLPC technique (see Figure 4.2), and in the solid phase, q_i^{eq}, was calculated using the equation 2.23. The whole procedure was repeated three times.
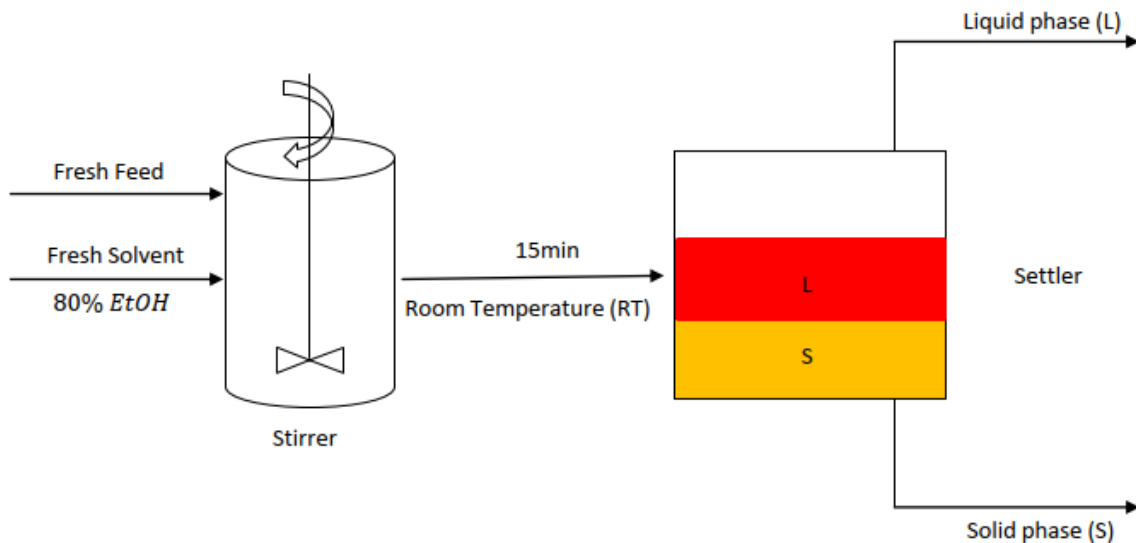
Figure 3.4: Schematic representation of a closed single-batch extraction process (Ba)

Table 3.1: Initial condition of the first series of experiments in the single-batch extraction procedure, N^{Ba}=8. i= picrocrocin, crocin I, and crocin II. $V_{L,j}$=0.01 l, c_i^0=0, $q_i^0(x_{i,S}^0)$=Table 4.3, Time of process=15 min, est.: estimated

No. (j)	$m_{S,j}$ [g]	$D_{S,j}$ [g/l] (Eq. 2.12)	$\varepsilon_{est.}$ (Eq. 2.9)
1	0.005	0.5	0.9994
2	0.025	2.5	0.9970
3	0.05	5	0.9940
4	0.1	10	0.9882
5	0.2	20	0.9766
6	0.3	30	0.9654
7	0.4	40	0.9544
N^{Ba}=8	0.5	50	0.9436

It is worth mentioning that the concentration analysis of picrocrocin was performed in dosages from 10 to 50 g/l; because the concentration analysis of picrocrocin in low dosages is not easy and has some errors.

In the second study, the sequential batches extraction (SBa) experiments were performed. In the SBa process, the extractors were interconnected (cascade). The extraction process in each extractor was stopped after 15 min and the separated phases were then used as starting material for the next extractors (see Figure 3.5). Therefore, the initial conditions (IC) were different for each extractor. It should be noted that the dosage in all extractors must be 50 g/l. For example, the first extractor starts with 0.5 g treated saffron powder and 0.01 l of 80% ethanol/water as solvent.

After stirring the solid and liquid phases for 15 minutes (equilibrium condition), the two phases are separated and used as the solid feed phase (wet feed) and liquid feed phase (loaded solvent) in the second and third extractors, respectively. The wet solid feed contains a certain volume of entrapped solvent, and the loaded solvent is less than $0.01\ l$. To maintain the dosage of $50\ g/l$ for all extractors, the volume of liquid phase in each extractor should be manipulated and adjusted. In this procedure, there are 10 batches, which were considered as the second series of experiments (N^{SBa}). The concentration of component i in the external liquid phase, c_i^{eq}, was measured by HPLC (see Figure 4.2), and in the solid phase, q_i^{eq}, was calculated by Eq. 2.23.
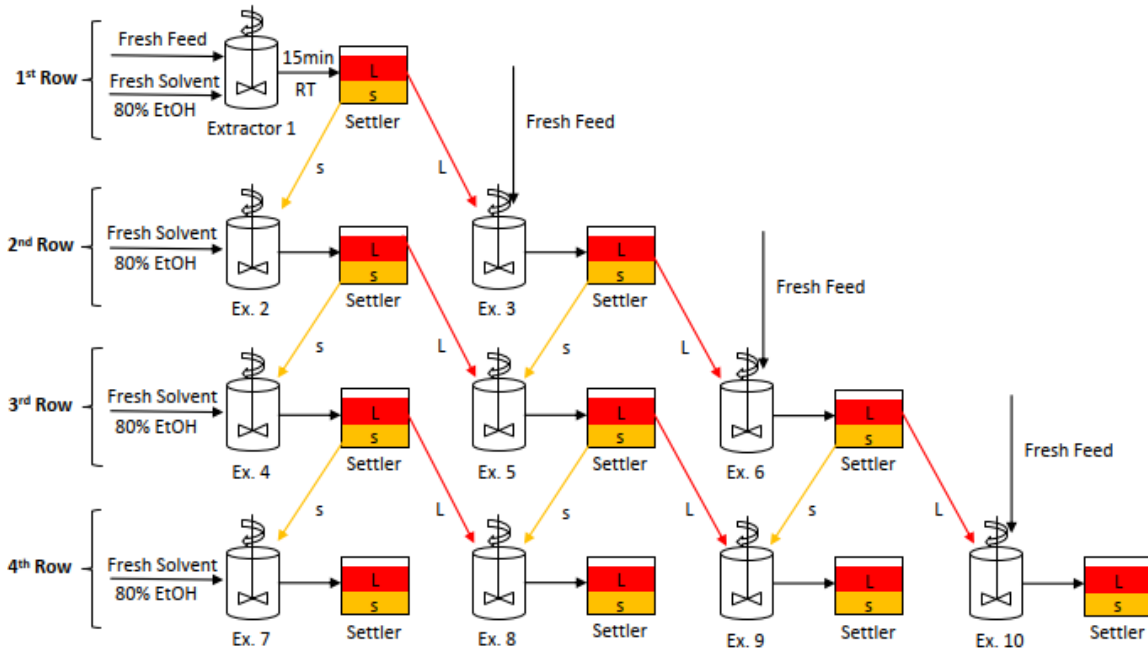
Figure 3.5: Schematic representation of the extraction procedure with multiple sequential batches (SBa). L=Liquid phase, S=Solid phase

These two set of experiments were used to estimate the kinetic and thermodynamic parameters of picrocrocin, crocin I, and crocin II.

3.2.3 Counter-Current Continuous Operation

Predictions based on numerical simulations and approximations can significantly reduce the time and materials required to analyze and optimize the process. Validated process models are typically used to determine appropriate operating parameters and optimal process design [97, 111].

The most flexible equation presented in section 2.1.5 that can quantify attractive counter-current operation (Eq. 2.42) includes the thermodynamic parameter, $\tilde{K}_{i,E}$, the effective kinetic rate constant, $\tilde{k}_i^{eff}$, operating parameters, (τ and ε), which can be used to determine volume flow rate of liquid and solid phases, and the number of stages, N, (hydrodynamic parameter), which is indicating deviation from the plug

flow status. The effect of each parameter on the outlet concentration of component i in the liquid phase ($c_{i,N}$) will be checked under reference values of other parameters (see Table 4.8 and the cited related figures in this table), and then the volumetric flow rate of the liquid phase for each condition, which is obtained by Eq. 2.41, will be used for productivity calculations (by Eq. 2.101).

In this thesis, due to high amount of saffron needed and high risk of the continuous process, the test of the counter-current extraction operation was not done. It is recommended to start with the cheaper material such as gardenia to test the counter-current operation (outlook). Instead of, selected simulation results will be presented in chapter 4 (section 4.2.5) using $K_{i,E}$ (experimental data), k_i^{eff} (experimental data), ε, τ, and N. Hence, the outlet liquid phase concentration of the components (picrocrocin, crocins I and crocin II) and the corresponding volume flow rate of the liquid and solid phases were determined based on the real thermodynamic and kinetic values for each component (chapter 4, subsection 4.2.5). The results showed higher productivity of the continuous counter-current extraction process vs. batch extraction process.

3.3   Solid-Liquid Chromatography

As we know, solid-liquid chromatography is one of the most powerful techniques to separate a mixture into its components and then purify them [111, 114, 115, 119]. In this study, isocratic and gradient elutions are used for the separation and purification of the target components of saffron extract, namely picrocrocin, crocin I and crocin II. The HPLC system and type of column are described in the section LC/MS analysis in Chapter 4.

3.3.1   Preliminary Experiments

3.3.1.1   Sample Preparation

To prepare the sample (feed) for the analytical and preparative chromatography separations, 13 g of the treated saffron powder was added to 1.3 l of an 80% (vol%) ethanol/water solution (80% EtOH,20% Water), and stirred for 15 min at room temperature. The stirrer was stopped at the time of equilibrium. After settling the wet saffron powder, the extract phase (liquid supernatant) was separated. The separated wet saffron powder, the nearly exhausted saffron, was again extracted with 1.3 l of fresh 80% ethanol/water solution. To isolate the residue solid particles (wet saffron powder) from the extract phase, the separated liquid supernatant was filtered by a Whatmann paper filter on an Erlenmeyer suction bottle. Finally, the filtered extract phase was concentrated using a rotary evaporator (BUCHI, Switzerland) and processed into fine dried saffron extract powder using a freeze dryer (ZiRBUS technology GmbH, VaCo2, max. temp. -50 °C, Germany). The following figure shows a schematic

representation of the sample preparation process:
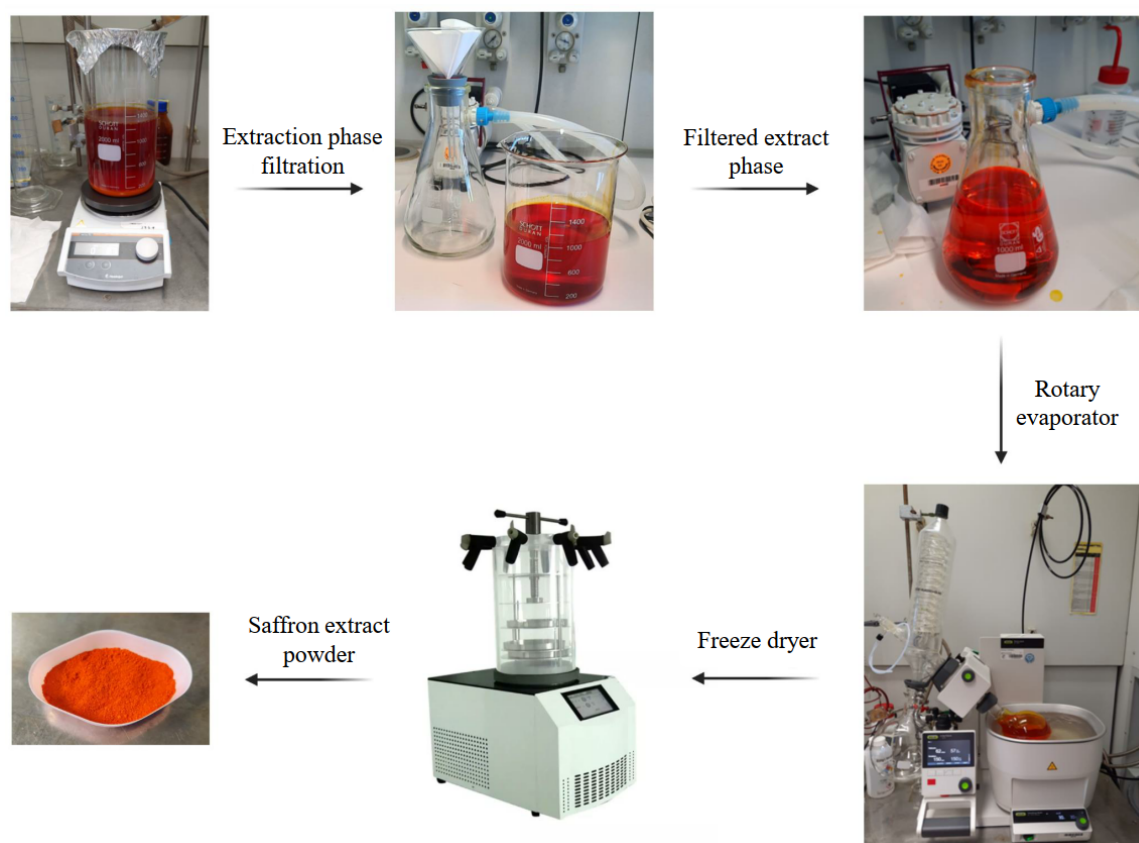
Figure 3.6: Preparation of the fine dried saffron extract powder

The fine dried saffron extract powder is used as the starting material (feed) for the elution procedures and separation studies, as well as for the preparative chromatography based purification experiments .

3.3.1.2 Packing the Preparative Column

The most important part of the preparative system is the preparative column, which was packed by ourselves in the Max Planck Institute for Dynamics of Complex Technical Systems, Magdeburg. The Dynamic Axial Compression, DAC, technique was used to pack the column with 25 mm inner diameter (the packing material is from the YMC company). To pack and obtain a DAC column, the following procedure should be followed (see Figure 3.7):

1. Assemble the bottom part of the DAC column and place on the hydraulic packing stand

2. Measurement of the length of the empty column, which was 16.51 cm

3. 42.7 g dry packing material was slowly poured into the empty column

4. Uncompressed piston length was 11.82 cm

5. Assemble the upper end cap and compress the column up to 100 bar

6. Connect the HPLC pump. 0.5 mm tubing was connected to the outlet of the pump, 1/8 $inch$ tubing was connected to the inlet of the column, and 0.5 mm tubing was connected to the outlet of the column

7. Flow isopropanol (HPLC grade) at 50 ml/min and waste effluent about 5 min

8. Recirculate effluent during 15 min

9. Stop the flow and compress the column to 100 bar, and then circulate again the effluent at 50 ml/min (about 41-42 bar) for 5 min

10. Repeat Step 9 until the column was not compressed any more

11. Compressed piston length was 10.12 cm

12. Compressed column length was approx. 14.81 cm $(16.51 - (11.82 - 10.12)\ cm)$
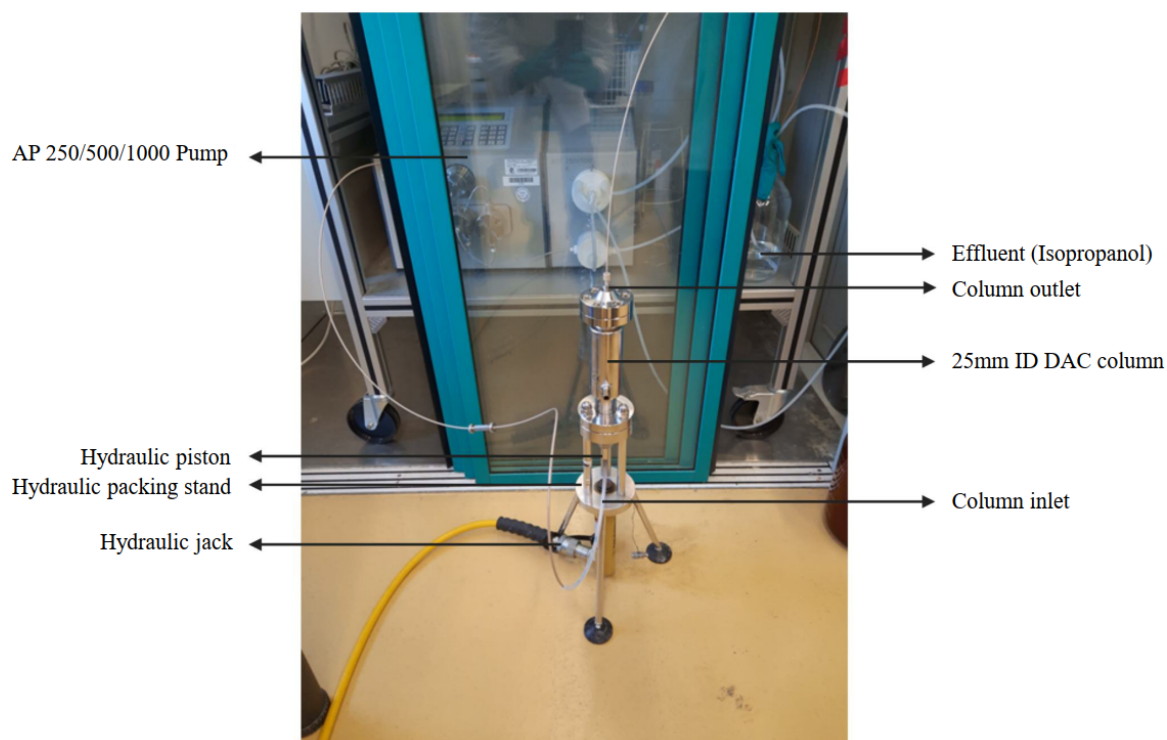
Figure 3.7: DAC column (YMC-Triart C18-S, $L_c = 148.1\ mm$, $d_c = 25\ mm$, 15 μm, 12 nm)

3.3.1.3   Preparative Column Efficiency

The performance of the packed column is evaluated using some test chromatograms. As a first test, two milliliters of 5 g/l uracil (10 mg uracil in 2 milliliters of 22% ethanol in composition with water) was injected as t_0 substance (Figure 4.25). Isocratic elution was run with 22% ethanol/water (22% EtOH+78% water) at a flow rate corresponding to the column diameter.

In the second experiment, 2 ml of 50 g/l saffron extract solution (100 mg saffron extract powder in 2 milliliters of 22% ethanol in composition with water) was injected onto the preparative column (Figure 4.26). The developed three-step gradient elution method (see Table 4.15) was run at the corresponding flow rate.

3.3.2 Analytical Scale

3.3.2.1 Isocratic Elution

In isocratic elutions, the composition of the mobile phase is kept constant. The retention time of component i and column efficiency can vary with different mobile phase compositions. For systematic method development, the retention behavior of the components and their peak widths in different volume fractions of the modifier (ethanol) ($0.05 \leq \varepsilon_{L,mod} \leq 0.5$) were studied by isocratic elutions. The mean retention times of picrocrocin, crocin I, and crocin II were observed in different volumetric fractions of ethanol ($\varepsilon_{L,mod}$) in composition with water (see Table 4.12). The dead time of the column, t_0^{exp}, was measured experimentally as 1.12 min with total porosity $\varepsilon_{tot} = 0.5376$ (section 4.3.1). It should be mentioned that the volumetric flow rate of 1.2 ml/min is the reference flow rate since the height of the equivalent theoretical plate, $HETP$, is minimized at this flow rate (see Figure A.1 in the Appendix).

This study provides a new analytical expression depending on the volumetric fraction of the modifier for the calculation of Henry constants, as the thermodynamic parameter, and band width, as the kinetic parameter (see Figures 4.19, 4.21 and Eqs. 4.9, 4.10). These analytical expressions provide the basis for developing the step-gradient elution conditions that can be used to shorten cycle time, increase productivity and yield in the delivery of the three target molecules.

3.3.2.2 Step-Gradient Elution

To develop the step-gradient elution, the gradient range was restricted to the range of the organic modifier (ethanol) studied in isocratic elutions ($0.05 \leq \varepsilon_{L,mod} \leq 0.5$). At $\varepsilon_{L,mod}$=0.5, picrocrocin and crocins elute within two minutes, and the difference between the retention times of the most and least retained components is less than 0.5 min, making the separation of three target components unlikely, while the target components are well separated at a volume fraction of 0.22 of the modifier (see Figure 4.20). At a volume fraction of modifier less than 0.22, the crocins are practically not eluted and/or are undetectable (massive band broadening) because the nonpolar part of the crocins structure, the polyene chain, tends strongly to the stationary phase and consequently low affinity to the mobile phase. On the other hand, at the volume fraction of 0.22 of modifier, picrocrocin is eluted in five minutes and sufficiently separated from the weakly retained undefined impurities. This is due to the polar structure of picrocrocin, which has a low affinity for the stationary phase.

This behavioral pattern of the components means that gradient elution, in which the volume fraction of the modifier is modulated from 0.22 to 0.5, can lead to shorter running time and higher productivity compared to isocratic elution. To accomplish this purpose, a gradient elution with three steps was considered, which is relatively simple and easy to implement (Figure 4.22, Table 4.15). The first two steps were designed for the isolation of picrocrocin and crocins (types I and II), respectively. Since the selectivity of the crocin I and crocin II is good enough to separate them in the same mobile phase composition, a one-step gradient was sufficient to isolate them. The third step was used to wash the strongly retained components as last impurities (Crocin III-V and Safranal) and rinse the column. At the end, a third change is required to re-equilibrate the column (see Figure 4.22).

3.3.3   Scale-Up and Preparative Chromatography

The developed three-step gradient elution was scaled up and implemented on a preparative scale. For this purpose, a preparative HPLC system with mobile phases (deionized water and HPLC-grade ethanol, Sigma Aldrich, Germany), a preparative HPLC pump (AP 250/500/1000, ARMEN INSTRUMENT, France), a manual injection system, a preparative column (25 mm ID DAC column, Merck NW25, Germany), a thermostat (LAUDA Ecoline Staredition RE304, Germany), a UV detector (L-2501, Knauer, Germany), and a computer data station (Labview software, SMB interface), were used (see Figure 3.8).

The pump unit (Max Flowrate: 250 ml/min, Max Pressure: 60 bar, 3 heads) is connected to an additional module (ACC) containing a binary gradient former, a through-pump-injection unit and a fraction collector (Figure 3.8A). All these devices can be controlled by a keyboard associated with LED, an automate integrated in the pump which execute memorized programs previously written by the user with the keyboard, and a remote computer with appropriate software. It should be mentioned that the injection unit with through pump is used only to pass the mobile phase, while the fraction collector is inactive and fractionation is performed manually. The following figure illustrates the hydraulic scheme (Figure 3.8A) and the real preparative HPLC system (Figure 3.8B):
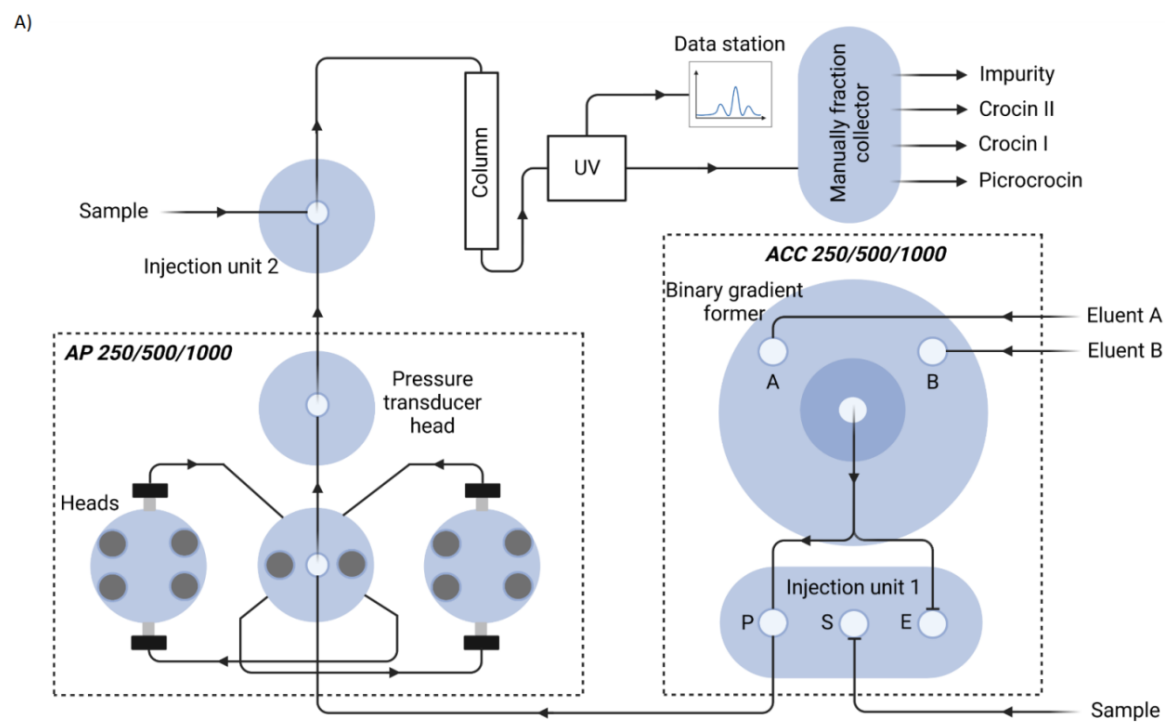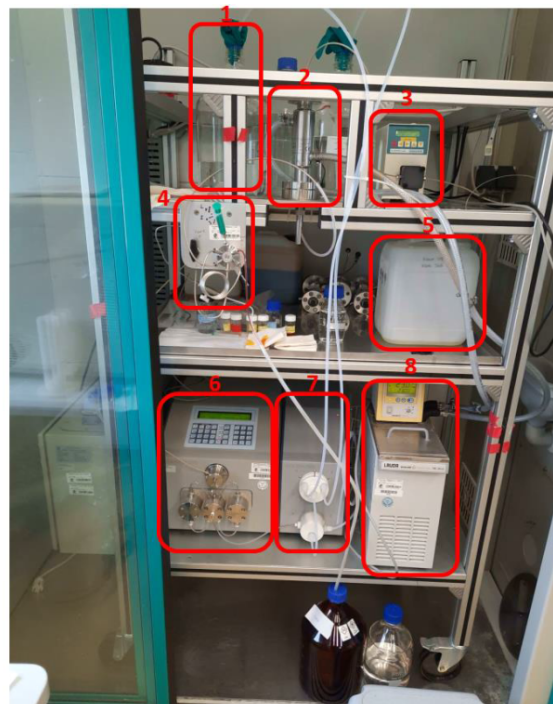
Figure 3.8: Hydraulic schematic (see Figure A) and real preparative HPLC system (see Figure B). Modules in Figure B include (1) mobile phases, (2) DAC-C18 column, (3) UV detector, (4) manual injection system (injection unit 2), (5) detector outlet, (6) AP 250/500/1000 pump, (7) ACC 250/500/1000, (8) thermostat (23 ℃)

Chapter 4

Results and Discussion

4.1 Preliminary Experiments

4.1.1 Stability of Components

The duration of stability of picrocrocin, crocin I and crocin II in different aqueous solutions of ethanol is different. The stability study of these components in aqueous ethanol solutions with low and high volume fraction of ethanol during 24 hours showed the following results:
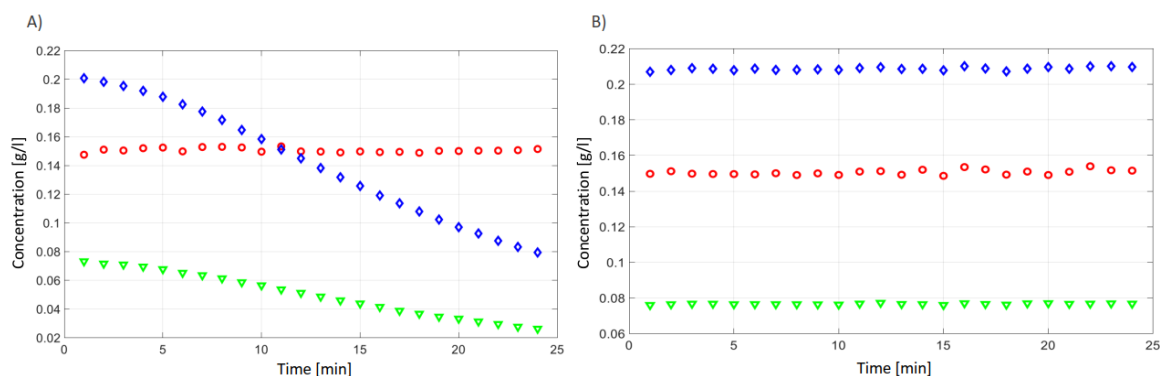
Figure 4.1: Stability study of picrocrocin (red circles), crocin I (blue diamonds), and crocin II (green triangles) in a volume fractions of 0.22 (figure A) and 0.8 (figure B) of ethanol in aqueous solution during 24 hours. $D_S = 1 \ g/l$ (Eq. 2.12)

Comparison of the concentration stability of picrocroicn, crocin I and crocin II in 0.22 and 0.8 volume fraction of ethanol shows that the stability of these compounds is sufficiently long at higher ethanol percentages solutions. Therefore, in agreement with the higher solubility and stability of picrocrocin and crocins, an aqueous solution containing 80% ethanol was chosen.

4.1.2 LC/MS Analysis

Preliminary separation of the components of the saffron crude extract was performed on an analytical reversed-phase C18 column (YMC-Triart C18-S, 150×4.6 mm, 15 μm, 12 nm) using segmented linear gradient elution with A→EtOH and B→water (see Figure 4.2 and its caption). The mobile phase flow rate and injection volume were 1 ml/min and 5 μl, respectively. The highest absorbance wavelengths of picrocrocin and crocins are 254 and 440 nm, respectively.
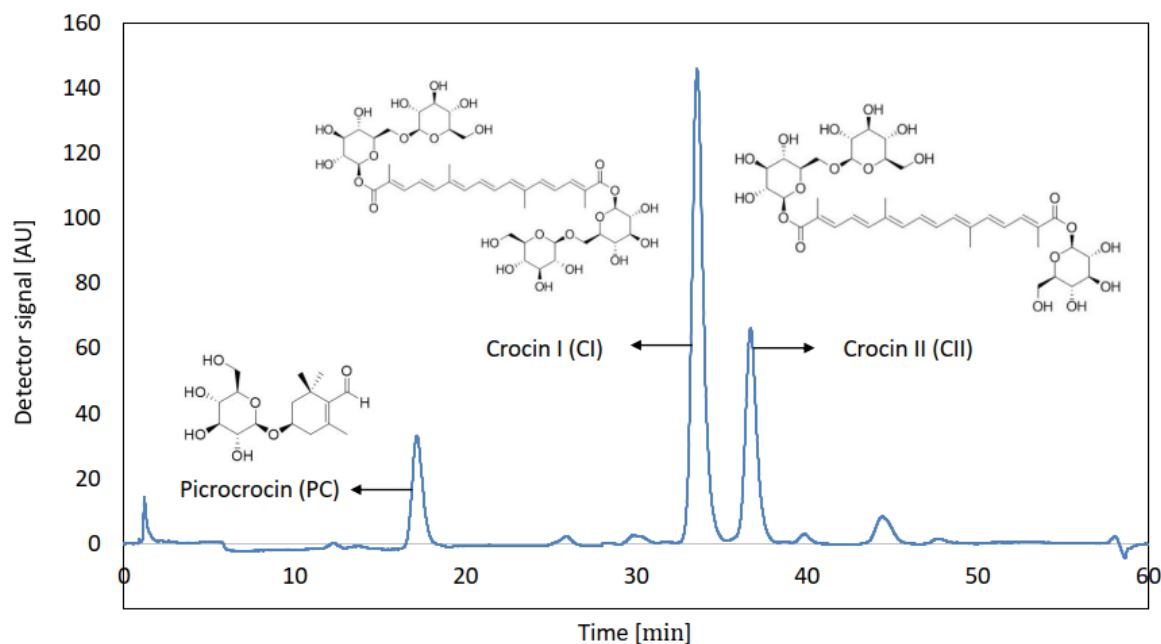
Figure 4.2: The chromatogram of the separated three major components of the saffron crude extract. Reverse phase mode (C18) with segmented linear gradient elution. The separation method is: 90% of B (0-5 min), 90% to 49% of B (5-50 min), 49% to 50% of B (50-51 min) and 50% of B (51-55 min), 50% to 90% of B (55-56 min) and 90% of B (56-60 min), $\lambda_{PC} = 254\ nm$, $\lambda_{CI,CII} = 440\ nm$

Mass analysis of picrocrocin, crocin I and crocin II in the separation profile described above was performed using the online LC-MS-QTOF technique (Q-TOF-LC-MS 6530, Agilent Technology, CA, US). In this analytical procedure, the flow rate was 0.4 ml/min. The detected Ammonium adduct mass $[M + NH_4]^+$ of picrocrocin and sodium adduct masses $[M + Na]^+$ of crocin II and crocin I were 348.2, 837.32 and 999.37 m/z, respectively (see Figures A.2, A.3, and A.4).

4.1.3 Calibration Curves

Pure picrocrocin, crocin I and crocin II were prepared at 6 different concentrations and then injected onto the C18 column to measure the peak area and construct their calibration curves. Detailed information is provided in the following table:

Table 4.1: Concentrations of standard picrocrocin (PC), crocin I (CI), and crocin II (CII) (g/l) used to construct their calibration curves. $V_{inj}=5e^{-3}\ ml$, $\lambda_{PC} = 254\ nm$, $\lambda_{CI,CII} = 440\ nm$

Component (i)	Sample 1	Sample 2	Sample 3	Sample 4	Sample 5	Sample 6
PC	1.96	0.98	0.49	0.24	0.13	0.061
CI	2	1	0.55	0.24	0.1	0.05
CII	1.93	0.96	0.48	0.24	0.12	0.06
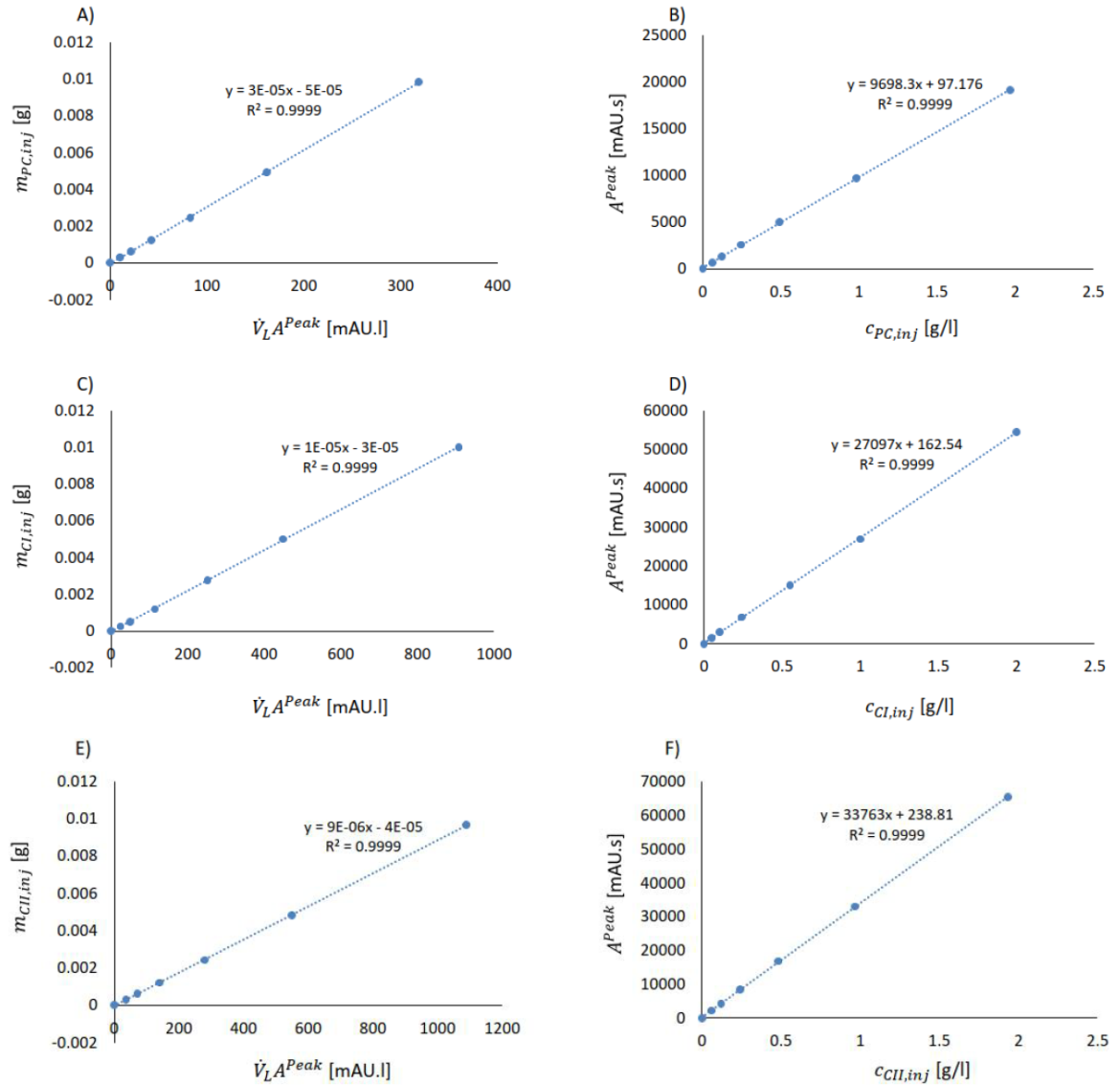
Figure 4.3: Calibration plots of picrocrocin (plots A and B), crocin I (plots C and D), and crocin II (plots E and F), $\lambda_{PC} = 254\ nm$, $\lambda_{CI,CII} = 440\ nm$

Thus, the calibration factor $\bar{F}$ of each component was obtained from the slopes of figures 4.3A,C, and E, which were $3e^{-5}$, $1e^{-5}$, and $9e^{-6}$ for picrocrocin, crocin I, and crocin II, respectively. As explained, Eq. 3.8 shows the relationship between the known input concentration, $c_{i,inj}$, and the corresponding peak area based on the provisionally determined parameters $\bar{F}$ and t_{inj}. Based on this relationship, the unknown concentration of a sample can be calculated by the area of the peak (see

Figure 4.3B,D,F). Therefore, these calibration plots were used for the concentration analysis of the components in the extraction, separation, and purification experiments. It should be noted that the analysis of the unknown concentrations must be performed in the linear concentration range considered for each calibration curve.

4.2 Solid-Liquid Extraction

4.2.1 Preliminary Experiments

4.2.1.1 Pre-Extraction

Iranian saffron stigmas were processed into powder with a mortar and pestle. The mass fractions of picrocroicn, crocin I, and crocin II in this unprocessed saffron powder were 0.135, 0.225, and 0.0847 $g_{S,i}^0/g_S^0$, respectively. After a pre-extraction step with Soxhlet, the final treated wet powder and extraction solution were dried and weighed. The mass balance was confirmed.

Table 4.2: Pre-extraction by Soxhlet

Solvent	Time [h]	Temperature [$°C$]	Starting powder [g]	Final powder [g]
DCM	7	40	10	9.02

Pre-extraction removes some non-polar and undesirable compounds from the saffron powder, which contributes to a better extraction of the main components and does not overcrowd the extract profile. Therefore, this treated saffron powder was used for the next extraction experiments.

4.2.1.2 Exhaustive Extraction

The total mass fractions of the picrocrocin, crocin I and crocin II in the treated saffron powder were obtained by exhaustive extraction:

Table 4.3: Measured total mass fraction and concentration of the main ingredients of the Iranian saffron by exhaustive extraction technique. Mass of treated saffron at zero time: m_S^0=0.1 g_S^0, ρ_S = 389.3 g/l

Component (i)	Total mass fraction, $x_{i,S}^0$ [$g_{i,S}^0/g_S^0$] (Eq. 2.4)	q_i^{in} [$g_{i,S}^{in}/l$] (Eqs. 2.6, 2.8)
PC	0.15 ± 0.020	58.40
CI	0.25 ± 0.025	97.33
CII	0.094 ± 0.023	36.60

The results illustrate that almost 50 percent of the treated saffron powder contains picrocrocin, crocin I and crcoin II.

4.2.1.3 Kinetic and Equilibrium

In a single batch extraction process, the concentration analysis of the picrocroin, crocin I and crocin II at regular time intervals led to the concentration-time curve. From this curve, the kinetic and equilibrium parts of the extraction process can be read (see Figure 4.4).
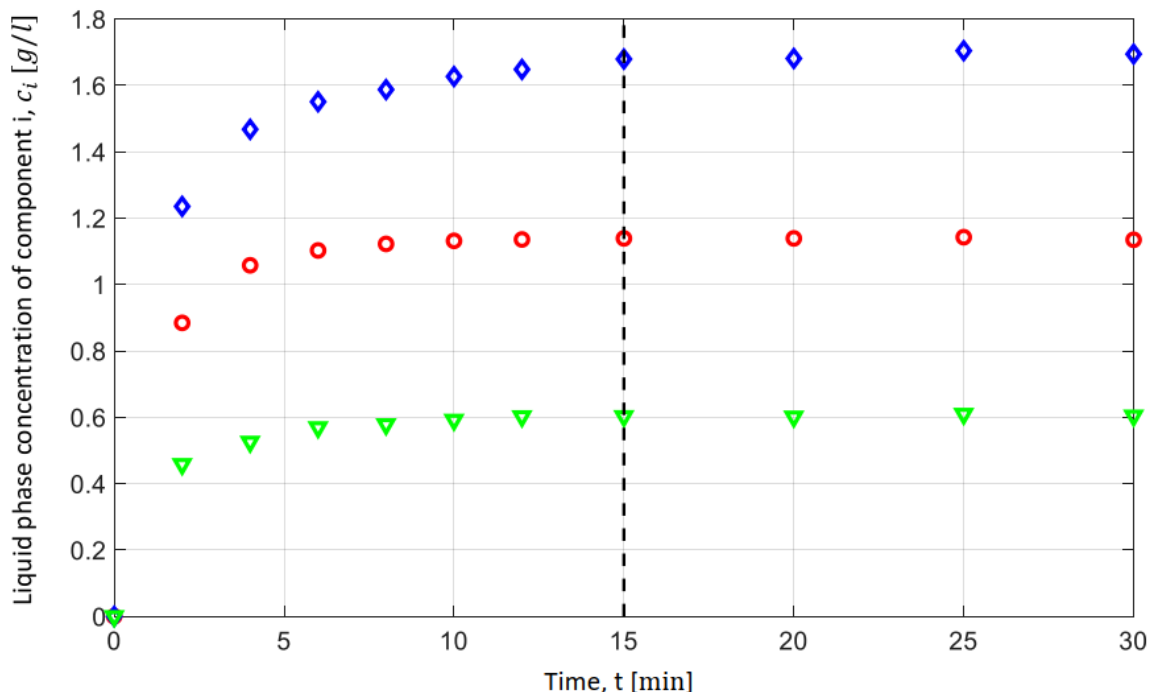
Figure 4.4: Concentration-time curves of crocin II (green triangles), picrocrocin (red circles), and crocin I (blue diamonds). Dosage = 10 g/l, $\varepsilon = 0.9882$ (Table 3.1)

The above curves show that the different final values of the components reach similar rates in a given time. For the given condition, the equilibrium states are reached in 10 min for picrocrocin, and almost in 15 min for both crocin I and crocin II. This means that after 15 minutes the distribution of all components between liquid and solid phases reaches the equilibrium state and the extraction process is practically completed (for a closed batch extraction process). Thus, the kinetic part is between 0 and 15 minutes, the equilibrium time is 15 minutes, and the phase equilibria is after 15 minutes (see Figure 4.4). The concentration-time curves of these three components in different dosages ($[10 : 50]$ g/l) are in the appendix (see figures A.5, A.6, A.7). It should be mentioned that the equilibrium concentration of each component in the given dosage and epsilon is in agreement with the Eq. 2.30 and Eq. 2.40.

These data are very valuable and allow us to draw the equilibrium curve, estimate the phase equilibrium and/or thermodynamic parameter, $K_{i,E}$, and determine the extraction rate constant for each target molecule, k_i^{eff}, in the closed single batch extraction process.

4.2.2   Estimation of Phase Equilibrium

As explained, the N^{Ba} series of experiments was performed with different dosages (see Table 3.1). Concentration analysis at the equilibrium time point for each dosage led to the following equilibrium diagrams of the picrocrocin, crocin I, and crocin II (see Figure 4.5):
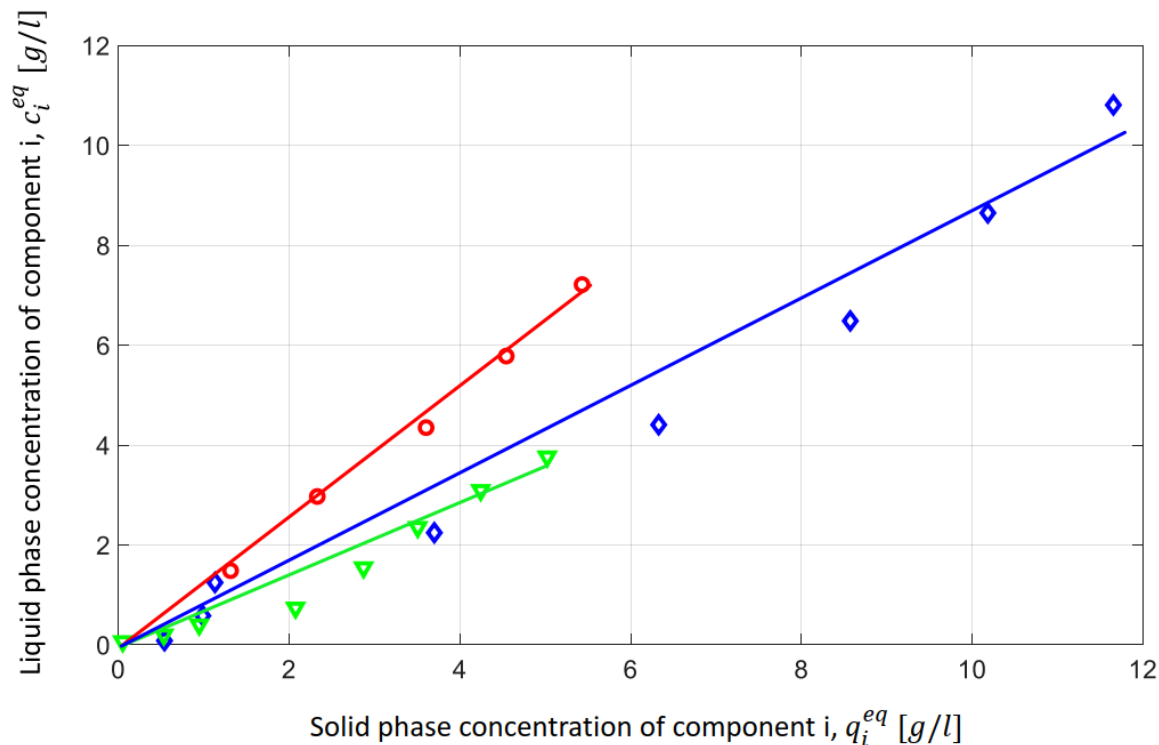
Figure 4.5: Measured equilibrium concentration points of picrocrocin (red circles), crocin I (blue diamonds), and crocin II (green triangles) from the closed single-batch extraction procedure. $x^0_{PC,CI,CII,S}$= Table 4.3. The points illustrate experimental data and the fitted lines are the assumed linear phase equilibrium

It is worth mentioning that it is a strong assumption just to consider linear equilibria between two phases. According to the linear equilibrium model, Eq. 2.13, the slopes of the lines show that the partition coefficient of crocin II is smaller than that of crocin I and picrocrocin, and the partition coefficient of crocin I is smaller than that of picrocroicn, $K_{CII,E}<K_{CI,E}<K_{PC,E}$. However, due to the different initial concentrations of these three components, $x^0_{CI,S}>x^0_{PC,S}>x^0_{CII,S}$, the concentration of the equilibrated liquid phase of them at low dosages (linear isotherm) is $c^{eq}_{CI}>c^{eq}_{PC}>c^{eq}_{CII}$.

As it is shown in Figure 4.5 there is non-linearity in the blue diamond points (equilibrium concentrations of crocin I) and green triangle points (equilibrium concentrations of crocin II). To check how much reliable is the linearity assumption of the equilibrium constant ($K_{i,E}$), we designed and performed the second set of experiments (the sequential batches extration experiments N^{SBa}). The sequential batches extration experiment (Figure 3.5) is similar to a discrete counter-current extraction procedure.

In the following figure there are the theoretically (Eq. 2.30 and/or Eq. 2.40) and experimentally liquid phase concentration of **crocin I** in each extractor of the sequential batches extraction process (Figure 3.5):

1st Row
$c_{CI,1}^{The.} = 11.65 \ [g/l]$
$c_{CI,1}^{exp.} = 10.91 \ [g/l]$
(Extractor 1)

2nd Row
$c_{CI,2}^{The.} = 3.78 \ [g/l]$ $c_{CI,3}^{The.} = 18.23 \ [g/l]$
$c_{CI,2}^{exp.} = 3.67 \ [g/l]$ $c_{CI,3}^{exp.} = 18.06 \ [g/l]$
(Extractor 2)   (Extractor 3)

3rd Row
$c_{CI,4}^{The.} = 1.32 \ [g/l]$ $c_{CI,5}^{The.} = 8.97 \ [g/l]$ $c_{CI,6}^{The.} = 19.71 \ [g/l]$
$c_{CI,4}^{exp.} = 1.09 \ [g/l]$ $c_{CI,5}^{exp.} = 8.43 \ [g/l]$ $c_{CI,6}^{exp.} = 20.94 \ [g/l]$
(Extractor 4)   (Extractor 5)   (Extractor 6)

4th Row
$c_{CI,7}^{The.} = 0.19 \ [g/l]$ $c_{CI,8}^{The.} = 2.42 \ [g/l]$ $c_{CI,9}^{The.} = 9.37 \ [g/l]$ $c_{CI,10}^{The.} = 18.96 \ [g/l]$
$c_{CI,7}^{exp.} = 0.37 \ [g/l]$ $c_{CI,8}^{exp.} = 3.37 \ [g/l]$ $c_{CI,9}^{exp.} = 10.72 \ [g/l]$ $c_{CI,10}^{exp.} = 18.06 \ [g/l]$
(Extractor 7)   (Extractor 8)   (Extractor 9)   (Extractor 10)

Figure 4.6: Theoretically and experimentally liquid phase concentration of **crocin I** (CI) in each extractor of the sequential batches extraction process (Figure 3.5). $x_{i,S}^{0} = 0.25 \ g_i/g_S$ (Eq. 2.4, Table 4.3), $\varepsilon_{est.} = 0.9436$ (Eq. 2.9), $D_S = 50 \ g/l$ (Eq. 2.12), $K_{i,E} = 0.66$ (Table 4.6)

In the low dosages and low liquid phase concentrations there is a good fit between the theoretical and experimental liquid phase concentrations. However, in high concentrations the differences of theoretical and experimental liquid phase concentrations is increased. Therefore, these results illustrates how much reliable is the linearity assumption of the equilibrium constant, which we believe it is relatively OK. The comparison for the picrocrocin and crocin II are in the appendix figures A.8 and A.9.

Figure 4.7 shows theoretically (dashed lines) and experimentally (solid lines) concentrations lines of picrocrocin, crocin I and crocin II over extractors number 1, 3, 6, and 10 in the sequential batches extraction process (SBa) (Figure 3.5).
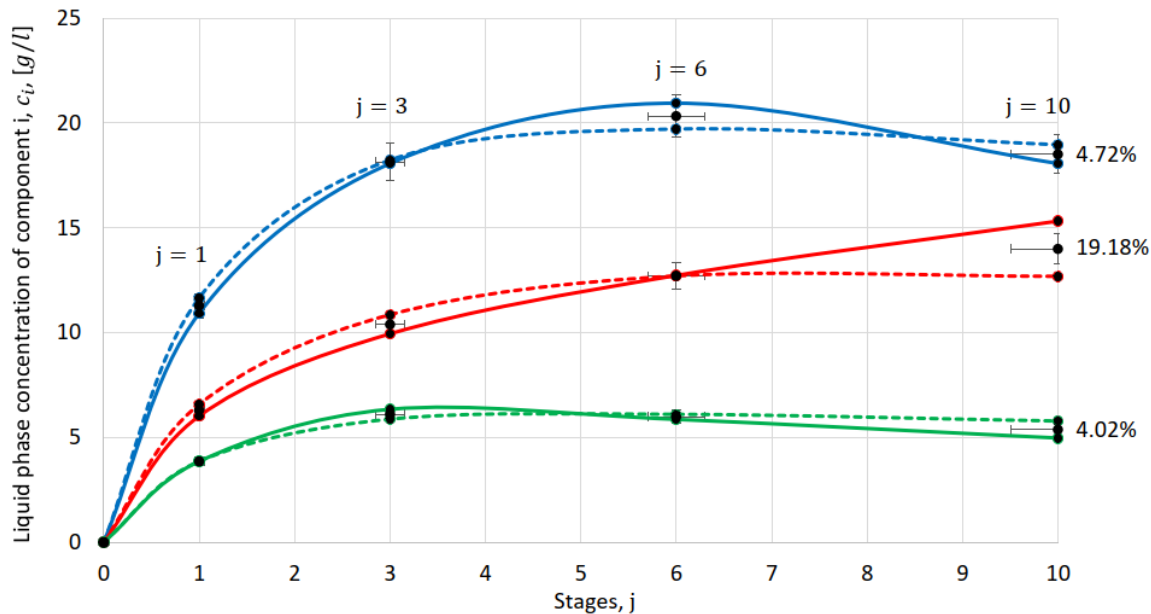
Figure 4.7: Liquid phase concentrations of picrocrocin (red line), crocin I (blue line), and crocin II (green line) over extractors number 1, 3, 6, and 10 in the sequential batches extraction process (SBa) (Figure 3.5). The points illustrate experimental data and the fitted lines are only a guide for the eyes

The results show that the concentration profile of the components turns to the constant amount at higher dosages and/or in the extractors with highly concentrated liquid phase (as the extractors 3, 6, and 10 (see Figures 3.5, 4.7)). Due to the error propagation and also higher dosage in extractor number 10, the difference between the theoretically concentration (dashed line) and experimentally ones is larger in higher stages (see error bar percent at j=10 in the Figure 4.7). The sources of errors can be related to the separation of solid and liquid phases, the initial dosage, and the concentration analysis.

The magnitude of the errors is passed from row to row. To obtain an accurate and realistic $K_{i,E}$ for both batch and continuous processes, these errors must be taken into account. They are included as the weight term W_n in the weighted least squares calculation (Eq. 4.1). The weighted least squares method, also called weighted linear regression, is a special case of generalized (ordinary) least squares in which knowledge of the random errors and variance of the experiments is included in the regression [97]. When the standard deviation (errors) in the observations is not constant across all categories of experiments and/or better to say there is a spread of errors, the weighted least squares method with different weights proportional to the magnitude of the errors leads to more accurate estimations. To estimate a reliable value for a particular parameter, the objective function equation (OF, Eq. 4.1) must be solved and plotted against that parameter. Where the derivative of the objective function in function of a desired parameter is ZERO, the value of that parameter obtains [97]. In this study, the phase equilibrium of component i ($K_{i,E}$) in the solid-liquid batch extractions of

saffron is estimated by the weighted least squares method:

$$OF(K_{i,E}) = \sum_{j=1}^{N} \sum_{n=I}^{IV} W_n \left(c_{i,j}^{exp.} - c_{i,j}^{the.}(K_{i,E}) \right)^2 \tag{4.1}$$

In this equation, the subscript j represents the number of extractors or stages, i.e., $j = 1, N$. The expression W_n refers to the weighting expression, which is different for each category of extractors n, where the value of the weighting expression depends on the size of errors. The expression $c_{i,j}^{exp.}$ is the experimental concentration of component i in the external liquid phase in extractor j at the equilibrium time. The solution of the objective function equation requires the calculation of the concentration of component i in the external liquid phase in function of phase equilibrium, $c_{i,j}^{the.}(K_{i,E})$, at the equilibrium time, which is obtained by the Eq. 2.32.

Therefore,the thermodynamic parameter $(K_{i,E})$ is estimated by substituting Eq. 2.32 into the Eq. 4.1 and solving the objective function equation in function of $K_{i,E}$. The unknown parameter in the objective function equation is only $K_{i,E}$. Specifying different thermodynamic parameter values will result in different values for the objective function. If the derivative of the objective function as a function of $K_{i,E}$ is ZERO, the value of the thermodynamic parameter is obtained. Solving the objective function equation requires special attention to the values of the weighting factor W_n. The weighting term plays a key role in finding a realistic $K_{i,E}$ value, and it should be considered according to the magnitude of the errors. In this study, due to the smallest error in the closed single batch extractions, we considered these experimental data as standard data with a constant weighting value equal to one, $W_n = 1$. However, if we want to consider this constant value of the weighting term for all experiments, the obtained $K_{i,E}$ will not be realistic. This is due to the error propagation from row to row in the sequential batches extraction experiments, which means we must consider a different weighting value for each experiment. These weighting values are different depending on the magnitude of errors in each row. On the other word, the weighting value is decreased from the first to the fourth row (see Figure 3.5). We considered 8 variants of weighting values to cover all error possibilities. In the following table, you can find detailed information about objective function calculations for crocin I:

Table 4.4: Expressions of the objective function equation for crocin I. A,B,...,H = Different variants of weight term. n: Class of weight term specific to each category of experiments. Ba : Extraction procedure with one batch, SBa : Extraction procedure with several sequential batches

Process	No. (j)	$c_{i,j}^{exp.}$	A	B	C	D	E	F	G	H	Class (n)
	-	-									-
Ba	1	0.1228	1	1	0	1	1	1	1	1	I
	2	0.6085									
	3	1.2076									
	4	2.2442									
	5	4.3958									
	6	6.4981									
	7	8.6556									
	N^{Ba}=8	10.7849	↓	↓							
SBa	$N^{Ba}+1$=9	10.9185	0	1	↓	↓	↓	↓	↓	↓	
	10	3.6726				0.9	0.9	0.9	0.9	0.8	II
	11	18.0652				↓	↓	↓	↓	↓	↓
	12	1.0919				0.7	0.6	0.5	0.4	0.4	III
	13	8.4371									
	14	20.9438				↓	↓	↓	↓	↓	↓
	15	0.3772				0.4	0.3	0.2	0.1	0.1	IV
	16	3.3748									
	17	10.7200									
	$N = N^{Ba} + N^{SBa}$=18	18.0652	↓	↓	↓	↓	↓	↓	↓	↓	↓

The information on picrocrocin and crocin II is in the Appendix (see Tables A.1, A.2). Thus, the thermodynamic parameters for the picrocrocin, crocin I and crocin II in the different variants of the weight term were:

Table 4.5: Thermodynamic parameters and/or phase equilibrium, $K_{i,E}$, in different variants of weight term (A,...,H)

-	Variants	$K_{picrocrocin,E}$	$K_{crocin\ I,E}$	$K_{crocin\ II,E}$
	A	1.19	0.66	0.5
Non-realistic	B	0.97	0.59	0.5
	C	1.21	0.66	0.5
	D	1.11	0.66	0.52
	E	1.09	0.66	0.53
Realistic	F	1.05	0.66	0.54
	G	1	0.66	0.55
	H	1.01	0.66	0.54

It should be noted that the obtained $K_{i,E}$ of variants A to C are not realistic. Because the weighting value cannot be one for all experiments or zero for some experiments. Figure 4.8 shows the objective function vs. thermodynamic paramter, $K_{i,E}$, for picrocrocin, crocin I and crocin II in variant D:
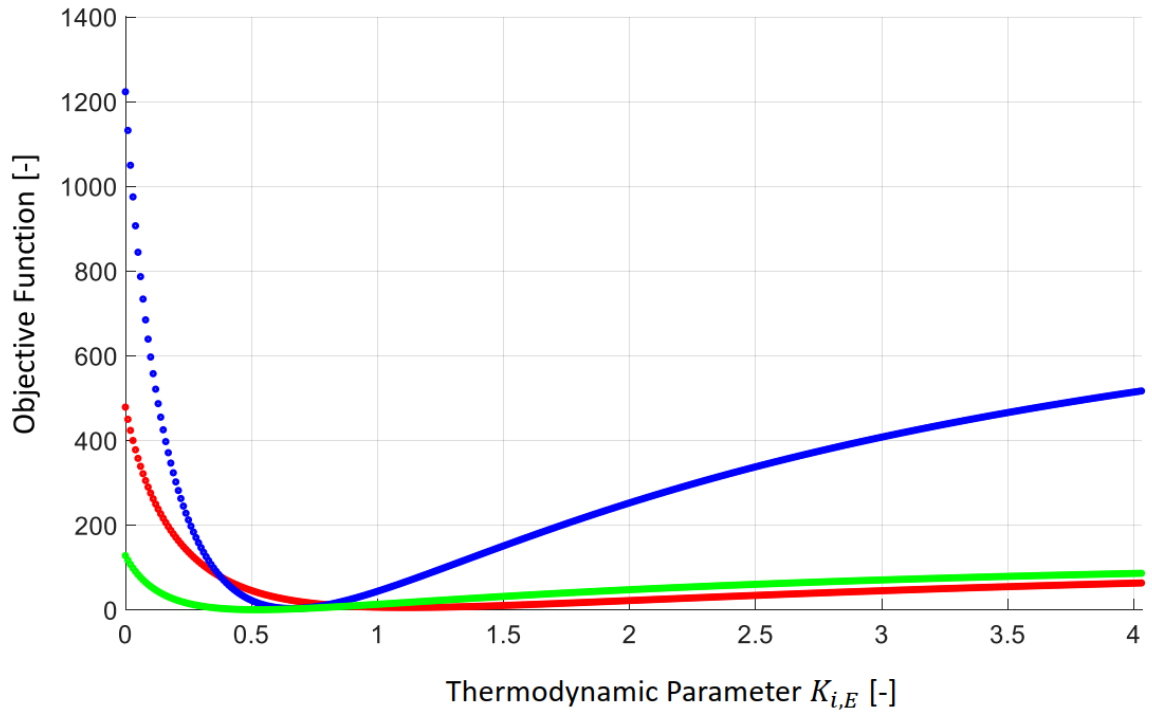
Figure 4.8: Objective Function vs. Thermodynamic Parameter for picrocrocin (red points), crocin I (blue points) and crocin II (green points). Variant D

Therefore, to estimate a realistic $K_{i,E}$, variants D through H must be considered:

Table 4.6: Range of the thermodynamic parameter and its estimated average for each component

Component (i)	$\bar{K}_{i,E}$	$\Delta K_{i,E}$
PC	1.052	1:1.11
CI	0.66	0.66:0.66
CII	0.536	0.52:0.55

These estimated average $K_{i,E}$ values were used to estimate the effective kinetic rate constant of each component, k_i^{eff}, in the single-batch extraction process (see next section (4.2.3)), and for the parametric studies of the dimensionless dynamic linear rate-limited extraction model for the continuous counter-current extraction process in the section 4.2.4.

4.2.3   Estimation of Kinetic Parameter

Estimation of the effective kinetic parameter of the picrocrocin, crocin I and crocin II (k_i^{eff}) in a closed single batch extraction process was obtained by solving the equation 2.30. That is, the variant effective kinetic rate constant, k_i^{eff}, and time, t, yields the calculated concentration-time curves. Finally, the kinetic parameters were estimated by fitting the measured concentration-time curves from figure 4.4 to the calculated curves (see Figure 4.9).
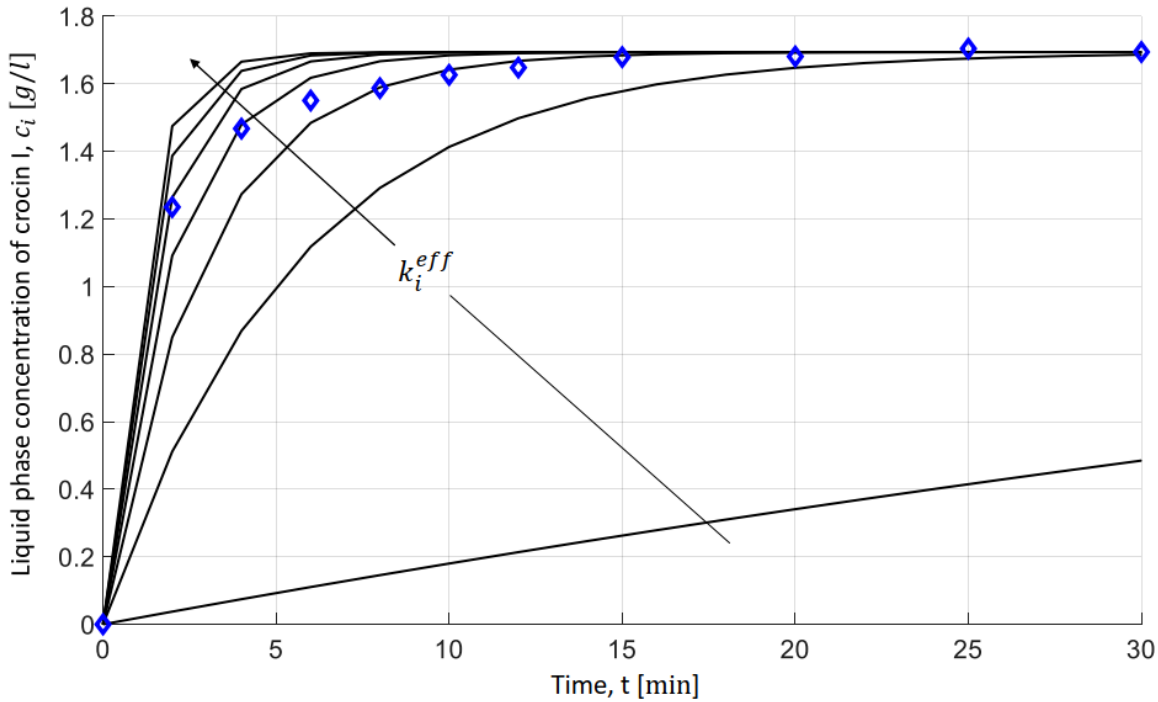
Figure 4.9: Overlapping of the experimental concentration-time curve of crocin I (blue diamonds from Figure 4.4) with the theoretical concentration-time curves (black curves) (calculated by Eq. 2.30). Enrichment of the liquid phase. The arrow shows the changes of the kinetic parameter from small to large values. $K_{i,E}=0.66$, $x_{i,S}^0=$ 0.25 $g_{i,S}^0/g_S^0$, $D_S=10$ g/l

The overlapping curves of picrocrocin and crocin II are in the appendix (Figures A.10 and A.11). Comparison of the theoretical and experimental curves yielded kinetic values of 0.49, 0.50, and 0.68 for crocin II, crocin I, and picrocrocin, respectively (see Table 4.7).

Table 4.7: Estimated effective kinetic parameter k_i^{eff}, for picrocrocin, crocin I, and crocin II

Component (i)	Effective kinetic parameter,k_i^{eff} $[1/min]$
PC	0.68 [0.52:0.85]
CI	0.50 [0.33:0.67]
CII	0.49 [0.33:0.67]

Overall, the average effective kinetic parameter value of 0.5 was considered for crocin I and crocin II, and 0.68 for picrocrocin. Based on this time-constant parameter, it can be seen whether the process is fast or slow. After estimating the thermodynamic and kinetic parameters, the continuous counter-current model was completed and used in parametric studies for optimization in the next section. It is worth noting that in the next section 4.2.4 the tilde terms of the thermodynamic and kinetic parameters $(\tilde{K}_{i,E}, \tilde{k}_i^{eff})$ are used, which are the modified parameters as treated in Eq. 2.36 and Eq. 2.37 by epsilon ε. From now so on we can use the Eq. 2.42 in the next sections.

4.2.4 Parametric Study of the Continuous Counter-Current Model

As it was mentioned in section 2.1.5, the dynamically controlled counter-current operation for N-CSTR (Eqs. 2.42) includes five important parameters $\tilde{K}_{i,E}$, $\tilde{k}_i^{eff}$, N, τ, and ε. By controlling these parameters, the productivity of the continuous counter-current extraction process is predictable. Therefore, it is not trivial to perform the parametric study for each parameter under reference values of other parameters to evaluate the effectiveness of the model and the sensitivity of the physical process. It also provides information about the range in which they affect the solution, i.e., the limiting cases.

The solutions of Eq. 2.42 were obtained by a MATLAB code and plotted below. The steady-state counter-current cascade model is used in this section for selected reference parameters to illustrate characteristic effects and parametric sensitivities. Before observing the influence of the parameters and comparing the different cases with the reference operation, an example of graphs is given and explained as follows (more details are in the Giang Truong Vu's thesis, 2023).
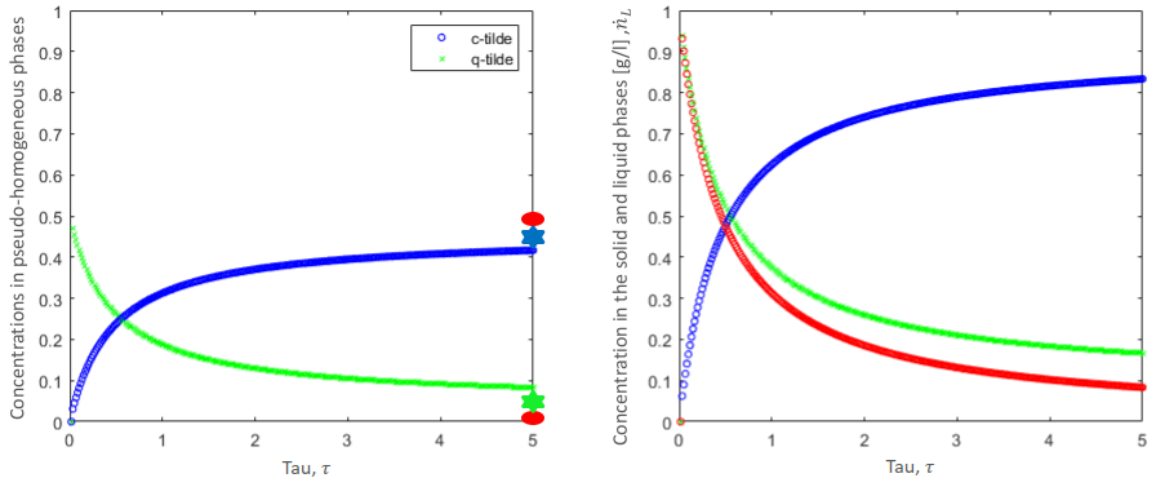
Figure 4.10: The concentration development of component i in the liquid and solid phases of counter-current operation. Green and blue points: solid and liquid phases concentrations. Red points: productivity (Eq. 2.102) . Left: The pseudo-homogeneous modified concentration as treated in Eq. 2.42; Right: The real concentration arising ε dependent after splitting into two individual phases. Given parameters: $\tilde{q}_i^{in} = 0.5$, $q_i^{in} = 1$(Eq. 2.35), $\tilde{c}_i^{in} = c_i^{in} = 0$, $\varepsilon = 0.5$, $\tilde{k}_i^{eff} = 1$, $\tilde{K}_{i,E} = 1$, $N = 20$, $\tau = 5$. The star points are derived from Kremser solutions (equilibrium controlled counter-current operation) (Eqs. 2.49, 2.50), Elliptical red points: PFTR (Eq. 2.53)

The concentration evolution of two phases is plotted over the entire length of the cascade characterized by the residence time τ (Eq. 2.41). The star-shaped points represent a finite number of equilibrated stages N in the liquid and solid phases and are calculated using equations 2.49, 2.50. The elliptical red points show the infinite number of stages N (PFTR) in two phases, calculated according to equation 2.53.

The next plots will illustrate the real concentrations c_i and q_i obtained by converting the modified concentrations $\tilde{c}_i$ and $\tilde{q}_i$ according to Eqs. 2.34 and 2.35. The productivity, one of the most interesting parameter, is introduced in section 2.3.2 (Eq. 2.102) and is also plotted as a red curve. Now the above mentioned important parameters are brought into consideration. These parameters can be separately adjusted as in Table 4.8.

Table 4.8: The relevant important parameters, reference values, and parameters range. $q_i^{in} = 1\ g_i/l$, $c_i^{in} = 0\ g_i/l$

Parameters	Units	Ref. values	Varied range	Figure
$\tilde{K}_{i,E}$	-	1	$[0.1 \div 10]$	4.11
$\tilde{k}_i^{eff}$	1/min	1	$[0.5 \div 10]$	4.12
N	-	20	$[5 \div 80]$	4.13
τ	min	5	$[0.5 \div 50]$	4.14
ε	-	0.5	$[0.1 \div 0.9]$	4.15

The following subsections present the influences of the important parameters on the counter-current performance.

4.2.4.1   Influence the Phase Equilibrium, $\tilde{K}_{i,E}$

The phase equilibrium $(\tilde{K}_{i,E})$ is the thermodynamic parameter of the problem in the counter-current extraction calculations. The following Figure 4.11 shows the influence of the three values of the $\tilde{K}_{i,E}$ (in the middle is the reference value), under reference values of other parameters (Table 4.8), on the liquid and solid phase concentration of component i $(c_{i,N}, q_{i,1})$, and subsequently on the productivity of extraction of component i.
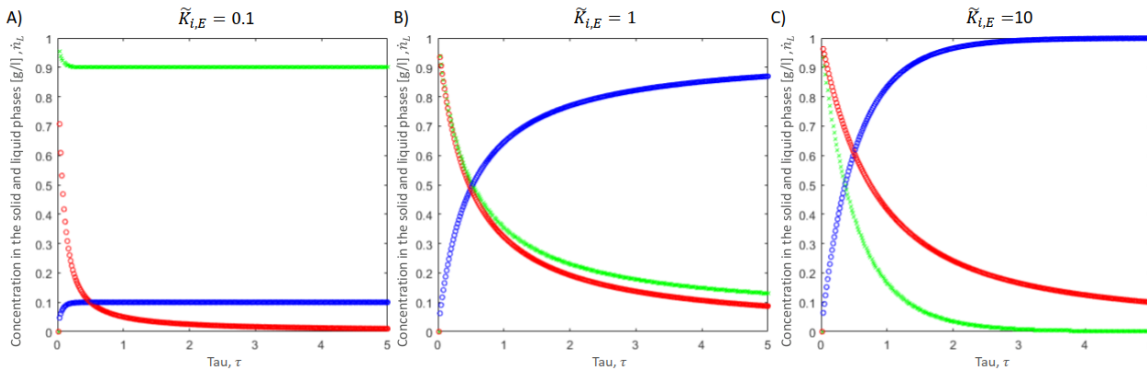
Figure 4.11: Sensitivity in case of phase equilibrium $\tilde{K}_{i,E}$ adjustment. Each plot corresponds to a specific value of $\tilde{K}_{i,E}$ and other parameters are kept at reference values (Table 4.8). The blue and green curves represent the concentrations in the liquid and solid phases, respectively. The red curve is for obtained amount of component i, which is direct related to productivity. Reference parameters: $q_i^{in} = 1$, $c_i^{in} = 0$, $\varepsilon = 0.5$, $\tilde{k}_i^{eff} = 1$, $N = 20$, $\tau = 5$

It is clear that the outlet liquid phase concentration of component i $(c_{i,N})$ and the cor-

responding productivity increase with the higher equilibrium distribution coefficient $\tilde{K}_{i,E}$ and that the solid phase concentration $q_{i,1}$ at the outlet subsequently decreases more.

4.2.4.2 Influence the Effective Kinetic Parameter, $\tilde{k}_i^{eff}$

Figure 4.12 illustrates the influence of the three values of the effective rate constant on the liquid and solid phase concentrations and the corresponding productivity.
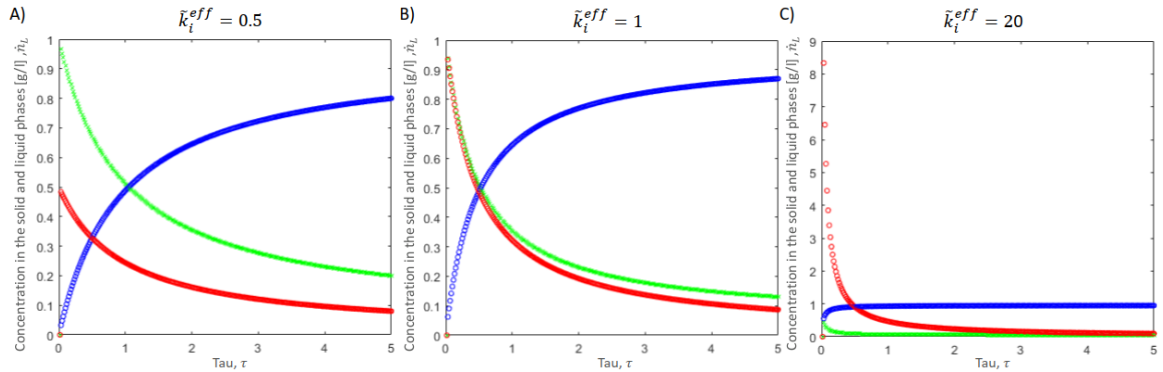
Figure 4.12: Sensitivity in case of effective kinetic paramtere $\tilde{k}_i^{eff}$ adjustment. Reference values of other parameters: Table 4.8

When the $\tilde{k}_i^{eff}$ is increased, the slops of compositions in the liquid phase (blue curves) and the obtained amount for productivity (red curves) are steeper at the beginning and are slightly increased at the outlet.

4.2.4.3 Influence the Number of Stages, N

Now, the influence of the three values of the number of stages N on the concentrations and productivity is investigated (Figure 4.13).
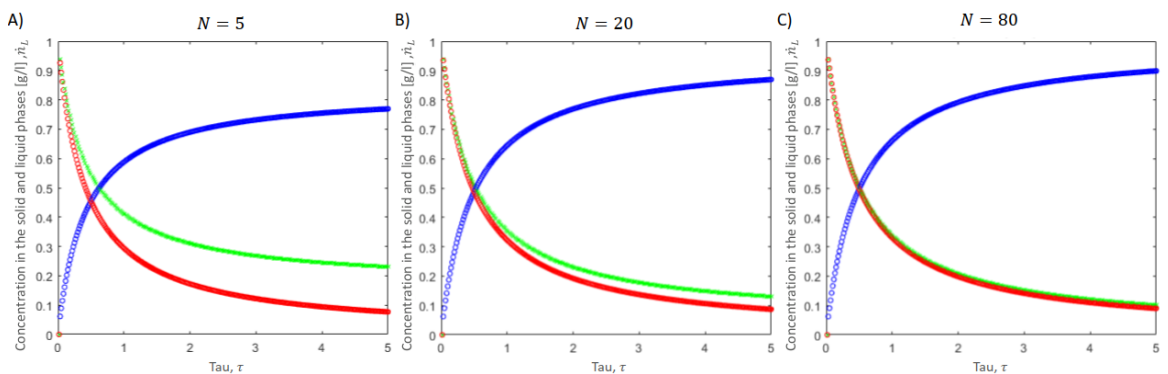
Figure 4.13: Influence of number of stages N on the liquid and solid phase concentrations. Reference values of other parameters: Table 4.8

It is clear that a higher number of stages leads to a higher value of the concentration of component i in the liquid phase at the output and to a corresponding productivity. After 10 stages, the influence of N is no longer very impressive.

4.2.4.4   Influence the Residence Time, τ

Furthermore, the influence of the three values of the residence time τ on the concentration evolution is of interest. It shows whether the solid phase stays long enough or the amount of component i in the waste. This behavior is shown in the following figure 4.14.
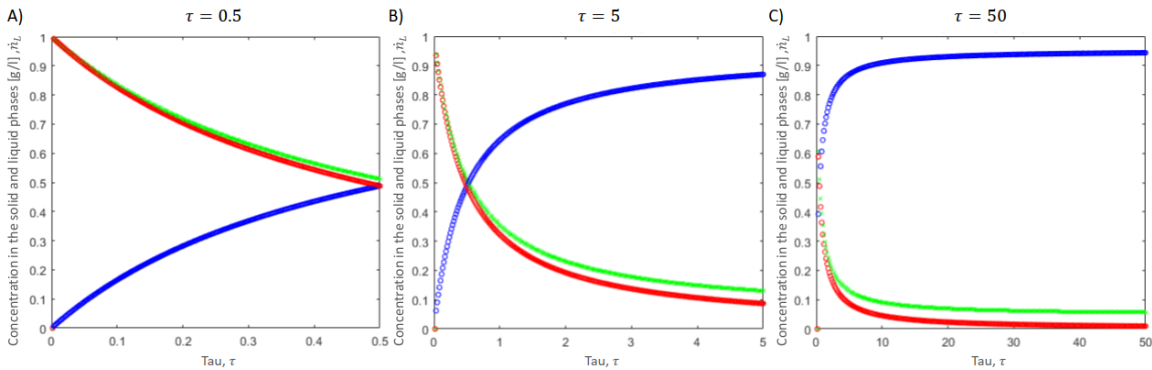
Figure 4.14: Influence of the residence time τ on the outgoing concentrations and productivity. Reference values of other parameters: Table 4.8

Increasing of residence time until reference value ($\tau = 5$) leads to the higher outgoing concentrations (see Figure 4.14B), however longer residence times have less influence on the outgoing concentration than shorter residence time, which leads to the smaller productivity (see Figure 4.14C).

4.2.4.5   Influence the Phase Ratio, ε

The phase ratio ε is a very important parameter for process performance. Following figure 4.15 illustrates the influence of the three values of ε on the concentrations of component i in both solid and liquid phases, and its productivity over the residence time, τ.
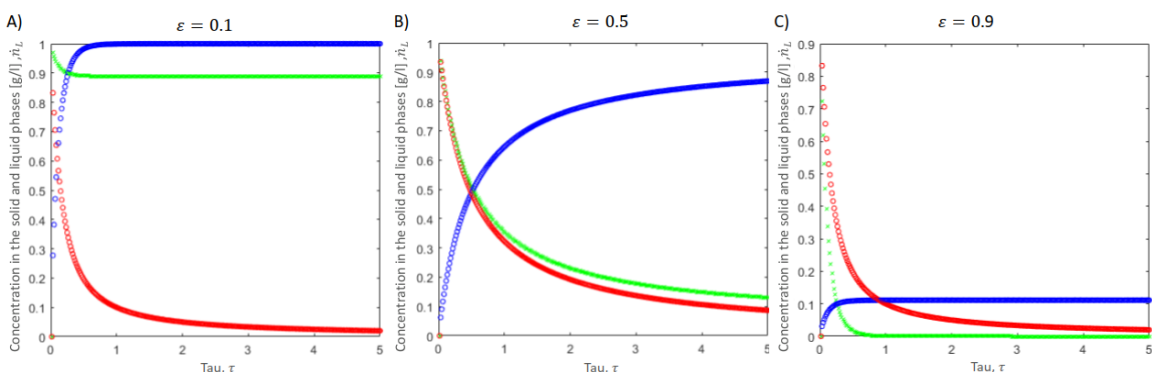
Figure 4.15: Influence of the phase ratio ε on the outgoing concentrations and productivity. Reference values of other parameters: Table 4.8

Low phase ratio means high amount of solid and low amount of solvent, which leads to the concentrated liquid phase and small productivity (see Figure 4.15A), while the

solid phase is still full of un-extracted components. When the phase ratio is half (see Figure 4.15B), there is higher amount of extraction and corresponding higher productivity. When the phase ratio is quite high (see Figure 4.15C), it means high amount of solvent and low amount of solid. In this case, the solid will be completely depleted, however liquid phase is diluted due to the high amount of solvent, which decreases the productivity. Hence, to have reasonable phase ratio with highest extraction productivity, we need to move between 0.2 to 0.8 values for epsilon.

It should be mentioned that this is the effect of each parameter in the fixed other parameters; and it is not the general effect of them. On the other hand, τ and ε are not individual and they are connected to each other by the volume flow rate of liquid and solid phases ($\dot{V}_L$ and $\dot{V}_S$) in the countinious counter-current operation. It means, when one of them changes, the other one also changes (see Eq. 2.9 and Eq. 2.41). Therefore to have more realistic and reliable effect of residence time, τ, and phase ratio, ε, on the outgoing concentration and productivity, we need to check their effect at the same time by a two-loop study (see next section 4.2.5).

4.2.5   Batch and Continuous Counter-Current Operations for the Parameters of the Case Study

Among the studied parameters in the above sections, phase ratio, ε, residence time, τ, and operation parameter, N, are free paramters. However, the equilibium rate constant, $K_{i,E}$, and extraction rate constant, k_i^{eff}, are coming from nature and are nor changeable at the given temperature and specific solvent.

Before examining the effects of ε, τ, and N on the outgoing concentration, productivity, and recovery yield in both batch (Eq. 2.30) and counter-current (Eq. 2.42) processes using the concrete numbers of the equilibrium rate constant $K_{i,E}$, the extraction rate constant k_i^{eff} and the initial solid phase concentration q_i^{in} (see Table 4.9), it is better to check them first in a normalized concentration (see Eq. 2.55, Eq. 2.56) to have a general attitude. Following table shows the concrete numbers of $K_{i,E}$, k_i^{eff}, and q_i^{in} for the picrocrocin, crocin I and crocin II:

Table 4.9: Concrete numbers for equilibrium rate constant ($K_{i,E}$, from Table 4.6), extraction rate constant (k_i^{eff}, from Table 4.7), and starting solid phase concentration (q_i^{in}, from Table 4.3) for picrocrocin (PC), crocin I (CI), and crocin II (CII)

Component i	k_i^{eff} [$1/min$]	$K_{i,E}$	q_i^{in} [g_i/l]
PC	0.68	1.052	58.4
CI	0.50	0.66	97.33
CII	0.49	0.536	36.6

Now the effect of ε and τ at high enough operating parameter ($N = 20$) on the **normalized** outgoing concentration, productivity and yield of component i (see Eq. 2.55,

Eq. 2.56) in batch (Eq. 2.30) vs. counter-current (Eq. 2.42) processes can be checked in one universal plot:
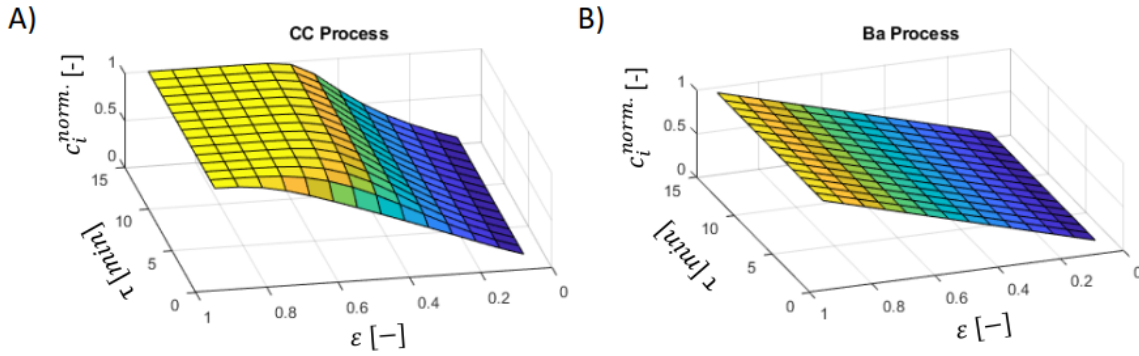
Figure 4.16: The effect of ε and τ on the **normalized** outgoing concentration, productivity and recovery yield of picrocrocin in both batch (Ba) (Eq. 2.30) and counter-current (CC) (Eq. 2.42) processes. $k_{PC}^{eff} = 0.68 \ [1/min]$, $K_{PC,E} = 1.052$, $q_{PC}^{in} = 58.4 \ [g_{PC}/l]$, $N = 20$, ε in $[0:1]$, τ in $[0.001:15]$

The operating parameter, N, and Damköhler number as a timescale parameter, ($Da = k_i^{eff} \times \tau_{end}$) (see Eq. 2.45, Eq. 2.46), were considered large enough (Eq. 4.2) to reach the highest concentration quantity:

$$Da_{PC} = k_{PC}^{eff} \times \tau_{end} = 0.68 \times 15 = 10.2 >> 1 \qquad (4.2)$$

The Damköhler number is very instructive number, which includes the time needed to carry out the extraction process (k_{PC}^{eff}), and the residence time of the process (τ_{end}). It is a very strong design parameter for the residence time (key parameter). Equation 4.2 shows that the Damköhler number should be more than 10 minutes, which is very important design information. It means, based on the requested production rate of the picrocrocin, crocin I, and crocin II, Damköhler number and corresponding residence time tell how big should be the Machin.

Description of Figure 4.16:

1) Low phase ratios at the short residence times show small outgoing normalized concentration, $c_i^{norm.}$, productivity, $Pr_i^{norm.}$, and recovery yield, $Y_i^{norm.}$, of component i in both batch and counter-current processes.

2) High phase ratios at long residence times show high outgoing normalized concentration, $c_i^{norm.}$, productivity, $Pr_i^{norm.}$, and recovery yield, $Y_i^{norm.}$, of component i in both batch and counter-current processes.

3) Because of 1) and 2) it is reasonable to evaluate the concentrations for epsilons in the range between 0.2 and 0.8 ($[0.2:0.8]$).

4) Higher concentration values are reached in counter-current operation compared to batch processes for the same ε and τ.

Now we can check the effect of the free parameters namely phase ratio (in $[0:1]$) and residence time (in $[0:15]$ min) at high enough operating parameter ($N = 20$) and concrete numbers of equilibrium rate constant ($K_{i,E}$), extraction rate constant (k_i^{eff}), and starting solid phase concentration (q_i^{in}) (see Table 4.9) on the **real (dimensioned)** outgoing concentration, productivity and recovery yield for picrocrocin, crocin I and crocin II.

Following figure illustrates the effect of different phase ratio and different residence time at the same time (two-loop) on the real outgoing concentration (c_i), productivity (Pr_i) and recovery yield (Y_i) of picrocrocin in batch (Ba) vs. counter-current (CC) processes:
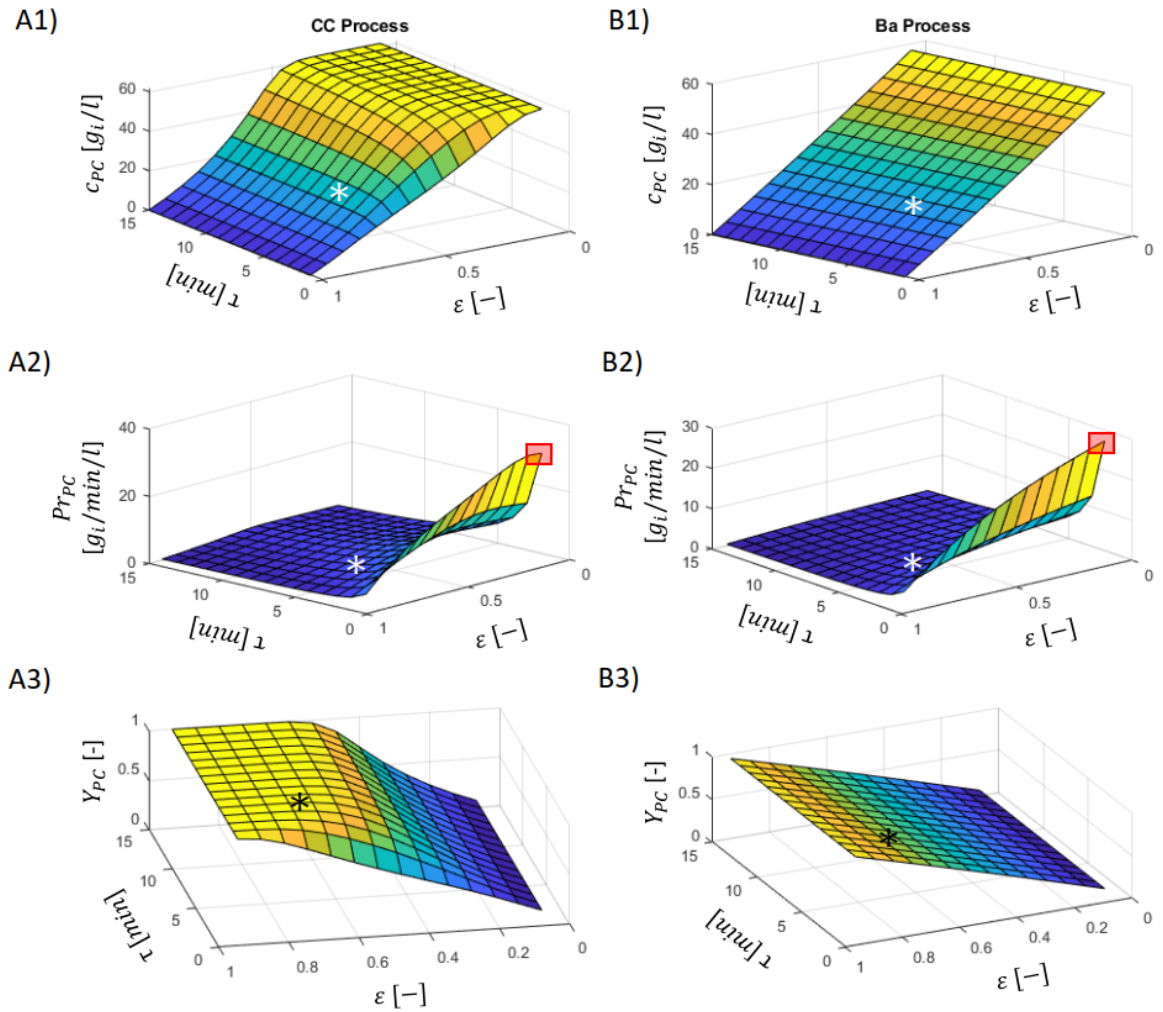
Figure 4.17: The effect of ε and τ (Eq. 2.43, Eq. 2.44) on the **real (dimensioned)** concentration, productivity and recovery yield of **picrocrocin** in both batch (Ba) (Eq. 2.30) and counter-current (CC) (Eq. 2.42) processes. $k_{PC}^{eff} = 0.68$ $[1/min]$, $K_{PC,E} = 1.052$, $q_{PC}^{in} = 58.4$ $[g_{PC}/l]$, $N = 20$, ε in $[0:1]$, τ in $[0.001:15]$. Star points: Concentration, productivity and recovery yield in $\varepsilon = 0.7$ and $\tau = 5$ $[min]$ for the special analysis based on independent experimental study. Red rectangles: Highest productivity predicted in CC and Ba

Small value of the phase ratio means high amount of solid phase and low amount

of liquid phase (High dosage) (Eq. 2.9), which leads to the high extract concentration (dimensioned) of picrocrocin, at any residence time, and high productivity (dimensioned), at short residence time, in both batch and continuous counter-current extraction processes (Figures 4.17A1,B1,A2,B2). It should also be noted that long extraction time means higher outgoing concentration (Figure 4.17A1), but lower productivity (Figures 4.17A2,B2) and vice versa.

It is worth mentioning, according to the investigations of the influence of the residence time and phase ratio in the subsections 4.2.4.4 and 4.2.4.5, the short residence time leads to the high productivity (see Figure 4.14A), and the low phase ratio leads to the low productivity (see Figure 4.15A). Due to the opposite effects of the low ε and short τ on the productivity, it prevents to have Gaussian shape and creates a plateau for the productivity in low ε at short residence time, τ, (red rectangles in Figures 4.17A2 and B2).

There is the highest productivity predicted for low epsilon at short residence time in both counter-current and batch processes (see red rectangles in Figures 4.17A2 and B2). It corresponds to quick extraction with a very small amount of solvent, which is not possible to implement in reality. Hence, it is better check the concentrations, productivity and recovery yield in realistic values of epsilon in the range between 0.2 and 0.8 ([0.2:0.8]).

On the other hand, high value of phase ratio means high amount of solvent and low amount of solid (low dosage), which leads to the low outgoing concentration and productivity (see Figure 4.17A1,B1,A2,B2), but high recovery yield in both CC and Ba (see Figures 4.17A3 and 4.17B3). Hence, high phase ratio and high residence time lead to high recovery yield (see Figures 4.17A3 and 4.17B3), but low productivity (see Figures 4.17A2 and 4.17B2), and vice versa. More figures for crocin I and crocin II are in the appendix (Figures A.12 and A.13).

Therefore, we need to select special phase ratio and residence time with acceptable productivity and high yield of target molecules.

More specific analysis based on independent experimental study

To check out the outgoing concentration of picrocrocin, crocin I and crocin II, and the productivity and recovery yield of batch vs. counter-current operations with concrete numbers, we picked up $\varepsilon = 0.7$ and $\tau = 5$ [min] (the white and black star points in Figure 4.17) from the independent work of empirical counter-current extraction of Artimisinin (from Giang Truong Vu's thesis, 2023) with repeatable and reliable results. Table 4.10 shows the estimated outgoing concentration (c_i) of the mentioned components in batch vs. counter-current processes:

Table 4.10: Esitimated outgoing concentration of picrocrocin, crocin I, and crocin II in batch (Ba) vs. counter-current (CC) processes using real numbers. $k^{eff}_{PC,CI,CII}$ = Table 4.9, $K_{PC,CI,CII,E}$ = Table 4.9, $N = 20$, $\varepsilon = 0.7$, $\tau = 5$ $[min]$

Component i	q^{in}_i $[g_i/l]$	c^{Ba}_i $[g_i/l]$ (Eq. 2.30)	c^{CC}_i $[g_i/l]$ (Eq. 2.42)
PC	58.4	17.8	25
CI	97.3	25.3	40
CII	36.6	8.7	14.5

Hence, Figure 4.18 shows the liquid phase concentration evolution of picrocrocin, crocin I, and crocin II based on the real values of the equilibrium rate constant parameter, $K_{i,E}$, the extraction rate constant parameter, k^{eff}_i, and the initial concentration in solid phase, $q^{in}_i(x^{in}_{i,S}, \rho_S)$, in both batch and counter-current processes.
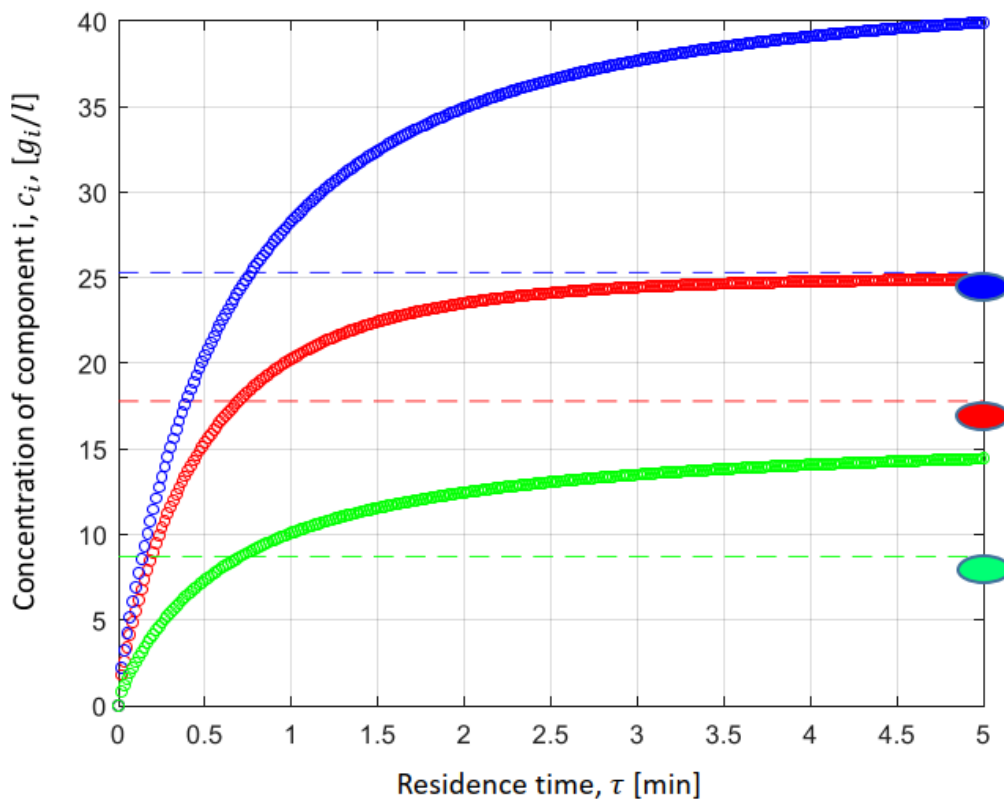
Figure 4.18: Estimated liquid phase concentration evolution of crocin I (blue curve), picrocrocin (red curve), and crocin II (green curve) in the continuous counter-current extraction operation for N-CSTR ($N = 20$) (Eq. 2.42) vs. batch process (Eq. 2.30). Blue, red and green elliptical points: estimated concentration of crocin I, picrocrocin, and crocin II in batch extraction process (by Eq. 2.30), respectively. Blue, red, and green dash lines are related to the equilibrium state of CI, PC, and CII in batch extraction process (by Eq. 2.32), respectively. Given Parameters: see Table 4.9

As it is clear, the superiority of the continuous counter-current process is the ability to exceed the equilibrium state of the batch extraction process and produce a higher extraction amount of the components (Figure 4.18).

Now, the results for the specific system considered for the extraction of picrocrcin,

crocin I and crcoin II from saffron powder in the composition solution 80% ethanol plus 20% water can be summarized. The equations A_1 (*Eq.* 2.43) and A_2 (*Eq.* 2.44) were used and they were validated in the independent work (Artimisinin project, Giang Truong Vu's thesis, 2023).

To compare the batch and continuous extraction methods, the estimated productivity and yield of picrocrocin, crocin I, and crocin II in the "**specific analysis**" were reviewed (method in Figure 4.18). The following table shows the estimated productivities and yields of picrocrocin, crocin I and crocin II for the closed batch vs. continuous counter-current extraction procedures at $\varepsilon = 0.7$, $\tau = 5\ min$ (star points on figures 4.17A2,B2,A3,B3) (specific analysis):

Table 4.11: Comparison of the estimated productivity (by Eq. 2.99 (for Ba) and Eq. 2.101 (for CC)) and recovery yield (by Eq. 2.104) of the closed batch (Ba) vs. counter-current (CC) extraction procedures for picrocrocin, crocin I and II. $V_{tot} = 1\ l$, $\dot{V}_S = 0.046\ l/min$ (Eq. 4.5), $\dot{V}_L = 0.155\ l/min$ (Eq. 4.6), $\varepsilon = 0.7$, $\tau{=}5\ min$

Component (i)	$Pr_i^{Ba}[g_i/min/l]$	$Y_i^{Ba}[\%]$	$Pr_i^{CC}[g_i/min/l]$	$Y_i^{CC}[\%]$
PC	2.76	71.05	3.90	99.50
CI	3.92	60.63	6.20	95.71
CII	1.35	55.60	2.25	92.02

It is worth noting that the volumetric flow rate of the liquid phase, $\dot{V}_L$, in counter-current mode was determined based on the phase ratio equation (Eq. 2.9):

$$\varepsilon = \frac{\dot{V}_L}{\dot{V}_L + \dot{V}_S} \tag{4.3}$$

$$\dot{V}_L = \frac{\dot{V}_S}{1 - \varepsilon} \tag{4.4}$$

Substituting Eq. 4.4 into Eq. 2.41 and then rearranging gives the volume flow rate of the solid phase , $\dot{V}_S$, in the counter-current process with assumed $V_{tot} = 1\ l$:

$$\dot{V}_S = \frac{V_{tot}}{\left(1 + \frac{1}{1-\varepsilon}\right) \times \tau} = \frac{1\ l}{\left(1 + \frac{1}{1-0.7}\right) \times 5\ min} = 0.046\ l/min \tag{4.5}$$

Therefore, the volume flow rate of the liquid phase was obtained as follows:

$$\dot{V}_L = \frac{0.046\ l/min}{1 - 0.7} = 0.155\ l/min \tag{4.6}$$

The results represent:

1) The estimated productivity of the CC process for the picrocrocin, crocin I and crocin II are roughly 30% , 37% and 40% higher, respectively, than in the Ba process.

It means, the superiority effect of the counter-current operation on the components with lower equilibrium rate constant (crocin II) is higher. It is worth mentioning that the estimated productivity of the batch process is based only on the extraction time without considering the dead time. Therefore, due to the dead time (preparation time for batch process), the real productivity of batch extraction process is lower than the values estimated in the table 4.11.

2) Recovery yield of the CC process for the PC, CI, and CII are roughly 28% ,35% and 36% higher than the Ba process, respectively.

3) Due to the larger amount of CI in the crude extract ($q_{CI}^{in} > q_{PC}^{in} > q_{CII}^{in}$) (see table 4.9), the productivity of CI is higher than PC and CII ($Pr_{CI} > Pr_{PC} > Pr_{CII}$).

4) Due to the larger equilibrium rate constant for PC ($K_{PC,E} > K_{CI,E} > K_{CII,E}$) (see table 4.9), the recovery yield of PC is higher than CI and CII ($Y_{PC} > Y_{CI} > Y_{CII}$).

5) It should be mentioned that in real extraction process there are some trapped solvent inside of the solid, which leads to the lower estimated productivity and recovery yield. Therefore, the wet solid phase should be squeezed at the end of the extraction time.

Last but not least, due to the high amount needed of saffron stigmas for the continuous counter-current extraction operation, the validation of the counter-current extraction process could not be done. It can be as an outlook project.

4.3   Solid-Liquid Chromatography

4.3.1   Total Porosity of the Column

As explained in the section 2.2.3.1, the determination of the total porosity ε_{tot} (Eq. 2.66) of the packing material requires the column dead time t_0, the volume of the empty column V_c, and the volume flow rate of the mobile phase $\dot{V}_L$. The dead time of the analytical column was experimentally estimated. Recording responses to pulse injections of a non-retained compound (uracil), a dead time $t_0^{exp.} = 1.5 \ min$ was measured at a flow rate of $\dot{V}_L = 1.2 \ ml/min$. However, after injecting the saffron crude extract onto the column, the retention time of the initial weakly retained undefined impurity was $t_0^{exp.} = 1.12 \ min$, which is even shorter than the retention time of uracil (as a non-retained compound). To obtain more realistic and reliable results, the dead time was considered based on the retention time of the initially detected undefined impurity in the saffron crude extract separation profile. The total volume of the empty column was $\dot{V}_c = 2.5 \ ml$ ($L_c = 150 \ mm$, $d_c = 4.6 \ mm$). Based on equation 2.66, the total porosity of the analytical column was estimated as follow:

$$\varepsilon_{tot} = \frac{t_0^{exp.} \times \dot{V}_L}{V_c} = \frac{1.12 \ min \times 1.2 \ ml/min}{2.5 \ ml} = 0.5376 \tag{4.7}$$

4.3.2 Estimation of Phase Equilibria

Isocratic elution profiles were recorded to investigate the influence of the volume fractions of the organic modifier, $\varepsilon_{L,mod}$, on the mean retention times of picrocrocin, crocin I and coricn II, and subsequently on the Henry constants of them, $K_{i,H}(\varepsilon_{L,mod})$. Following table 4.12 shows the influence of the volume fractions of the organic modifier (ethanol), $\varepsilon_{L,mod}$, on the mean retention times of the components:

Table 4.12: The influence of different volume fractions of ethanol ($\varepsilon_{L,mod}$) on the mean retention times (Figure 2.12) of picrocrocin (PC), crocin I (CI), and crocin II (CII) in isocratic elution profiles. (YMC-Triart Prep C18-S, 150×4.6 mm, 15 μm, 12 nm). t_0^{exp}=1.12 min, V_{inj}=5 μl, t_{inj}=0.00416 min, $\dot{V}_L$=1.2 ml/min

$Iso.^*$ ($\varepsilon_{L,mod}$)	$t_{R,PC}$ [min]	$t_{R,CI}$ [min]	$t_{R,CII}$ [min]
0.05	65.21	-	-
0.1	21.19	-	-
0.2	6	-	-
0.22	4.99	94.52	210
0.24	4.32	53.11	121.9
0.26	3.74	31.35	70.87
0.28	3.28	18.45	41.01
0.3	2.94	11.31	24.28
0.32	2.67	6.89	14.08
0.34	2.47	4.54	8.73
0.36	2.3	3.24	5.78
0.38	2.17	2.46	4.01
0.4	2.06	2.02	3.03
0.45	1.89	1.52	1.93
0.5	1.8	1.36	1.36

$Iso.^*$: Isocratic elution

The recorded retention times in table 4.12 were used to estimate Henry constants for each component by the Eq. 2.68:

$$\frac{dq_i(c_i)}{dc_i} = K_{i,H} = \left(\frac{t_{R,i}^{exp}}{t_0^{exp}} - 1 \right) \left(\frac{\varepsilon_{tot}}{1 - \varepsilon_{tot}} \right) \tag{4.8}$$

The Henry constant is the linear adsorption equilibrium parameter (in isothermal conditions and low concentrations). It can be used to develop and optimize a step-gradient elution with short cycle times, appropriate separation factors, and high productivities. Figure 4.19 shows the changes in Henry constants of picrocrocin, crocin I and crocin II by different constant volume fractions of modifier (ethanol) in reverse phase isocratic elutions.
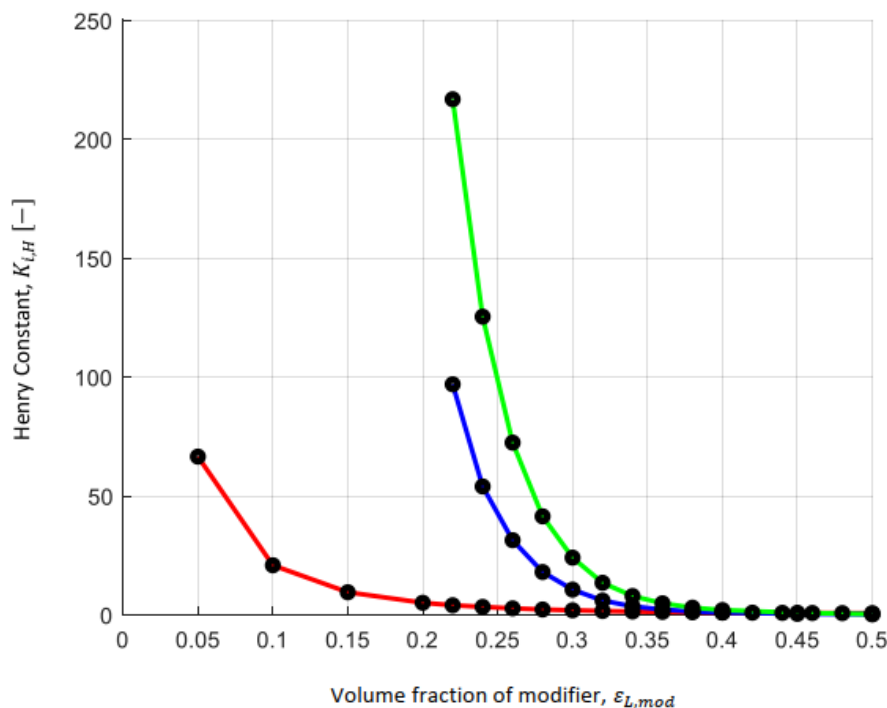
Figure 4.19: Henry constant vs. volume fraction of organic modifier (ethanol) in reverse phase isocratic elutions. Henry constants were estimated by the Eq. 4.8 and measured retention times. Picrocrocin (red line), crocin I (blue line) and crocin II (green line). t_0^{exp}=1.12 min, $\dot{V}_L$=1.2 ml/min, V_c=2.5 ml, ε_{tot}=0.5376

Inspecting the curves of the Henry constants led to an empirical expression that considers the effect of the volume fraction of the modifier:

$$K_{i,H}\left(\varepsilon_{L,mod}\right) = A_i e^{B_i \varepsilon_{L,mod}} + C_i e^{D_i \varepsilon_{L,mod}} \tag{4.9}$$

In the above function, A_i, B_i, C_i, and D_i are coefficients that can be adjusted to the experimental results:

Table 4.13: Empirical coefficients in the equilibrium exponential function

Component (i)	A_i	B_i	C_i	D_i
PC	243.8	-31.26	23.20	-8.13
CI	$2.84e^{17}$	-176.10	$3.66e^4$	-27.17
CII	$9.26e^4$	-27.53	0.017	5.979

It should be noted that the volume fraction of ethanol was in the range from 0.05 to 0.5 for picrocrocin and in the range from 0.22 to 0.5 for the crocin I and crocin II (Table 4.12). According to the empirical coefficients for the mentioned components, figure 4.20 illustrates the evolution of the chromatograms in the space-time domain for a column of length $z = L_c = 15$ cm for two different solvent compositions ($\varepsilon_{L,mod}$=0.22 and $\varepsilon_{L,mod}$=0.5) connected with Henry constants.
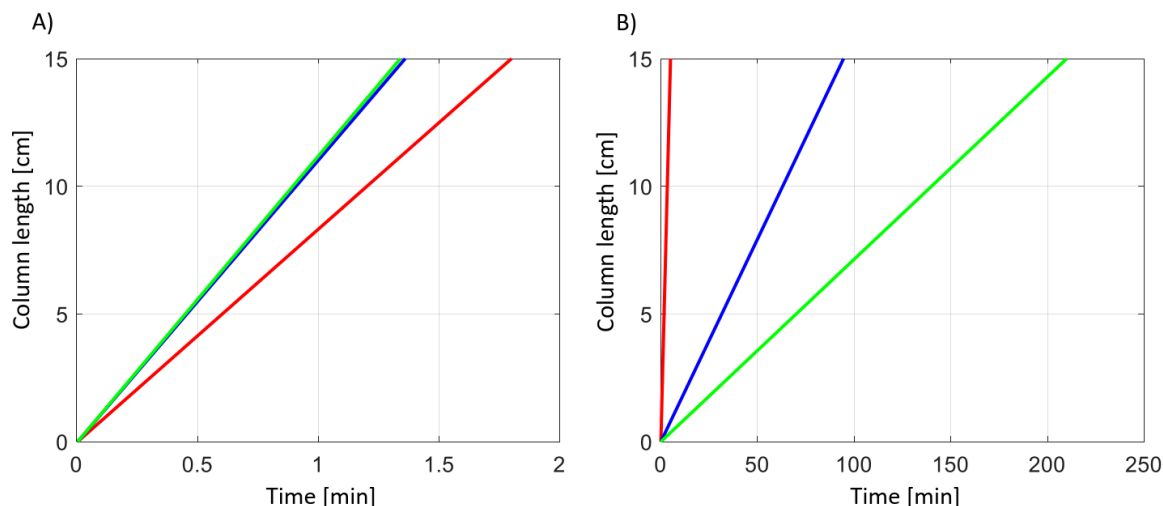
Figure 4.20: Effect of high and low volume fraction of organic modifier (ethanol) on retention times of picrocrocin (red line), crocin I (blue line) and crocin II (green line) in isocratic elutions. Figure A: $\varepsilon_{L,mod}$=0.5, $t_{R,PC}$=1.8 min, $t_{R,CI}$=1.36 min, $t_{R,CII}$=1.36 min. Figure B: $\varepsilon_{L,mod}$=0.22, $t_{R,PC}$=4.99 min, $t_{R,CI}$=94.52 min, $t_{R,CII}$=210 min

The slopes of the lines in Figure 4.20A and 4.20B represent the linear migration rates of picrocrocin, crocin I, and crocin II at high and low concentrations of the organic modifier (ethanol), respectively.

The exponential function (Eq 4.9) will be used in section 4.3.4 to predict the retention times of the components in each volume fraction of the modifier (by Eqs. 2.62, 2.63), and also to develop a three-step gradient elution minimizing cycle time and maximizing productivity.

4.3.3   Estimation of Kinetic Parameter

The number of theoretical plates is considered as the key kinetic parameter (see Eq. 2.73 and figure 2.12). The following figure 4.21 shows the bandwidths at the base of the peaks of picrocrocin, crocin I and crocin II in isocratic elutions in different volume fractions of the modifier ethanol:
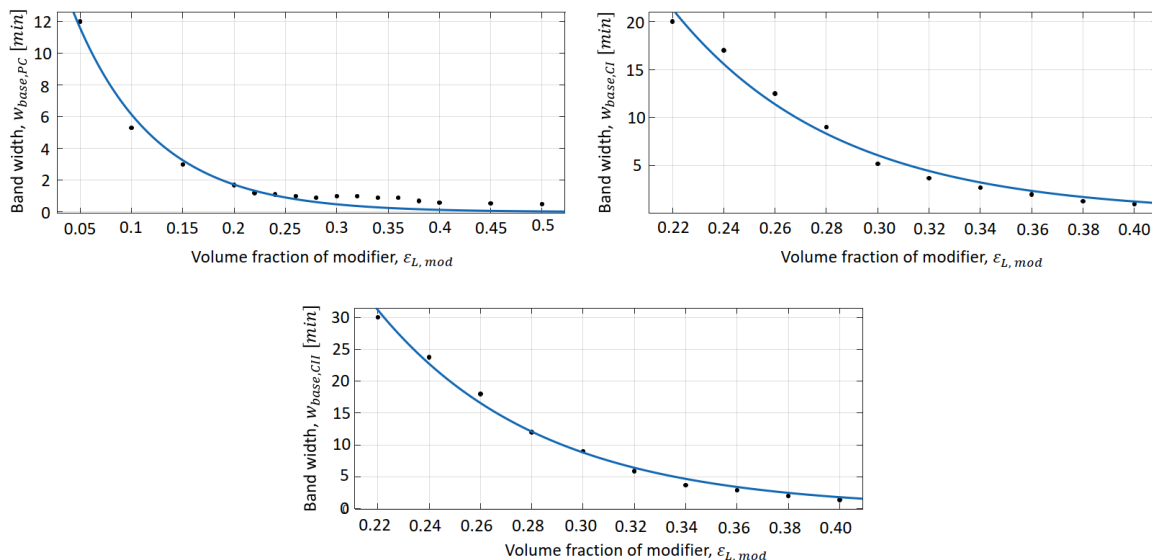
Figure 4.21: Effect of different volume fraction of ethanol (isocratic elution) on the bandwidth at the peak base of the picrocrocin, crocin I and crocin II

The study of the peak width of the above mentioned three components under isocratic elutions was used to parameterize an empirical expression depending on the volume fraction of the modifier to calculate the band width at the peak base of each component as a kinetic parameter:

$$w_{base,i}\left(\varepsilon_{L,mod}\right) = A_i e^{B_i \varepsilon_{L,mod}} \tag{4.10}$$

The empirical coefficients of the above function, and the range of the number of theoretical plats $(N(\varepsilon_{L,mod}))$ are:

Table 4.14: Empirical coefficients in the kinetic exponential function and the number of theoretical plates, in different $\varepsilon_{L,mod}$, for picrocrocin, crocin I and crocin II

Component (i)	A_i	B_i	$\varepsilon_{L,mod}$	$w_{base,i}$ $[min]$	$t_{R,i}$ $[min](table\ 4.12)$	$N(\varepsilon_{L,mod})(Eq.\ 2.73)$
PC	21.83	-12.68	[0.05:0.5]	[12:0.5]	[65.21:1.8]	[473:208]
CI	669.20	-15.67	[0.22:0.4]	[20:1]	[94.52:2.02]	[358:66]
CII	1002	-15.78	[0.22:0.4]	[30:1.4]	[210:3.03]	[784:75]

The peak width or number of theoretical plates is representative of column efficiency. The column efficiency is used to account the band broadening in the real separation profile and to avoid band overlapping between peaks or two injections. Based on the **assumption (I)**, the column efficiency was considered constant for isocratic and gradient elutions. However, for gradient elutions, there were some differences that were empirically adjusted.

4.3.4   Analytical Three-Step Gradient Elution

As mentioned in the subsection 3.3.2.2, a stepwise elution with three main steps is considered, which is relatively simple and easy to implement. In this step-gradient elution, picrocrocin, crocin I, crocin II, and final impurities are illustrated with red, blue, green, and purple colors, respectively.

The first step is to separate picrocrocin from the weakly retained undefined impurities. According to the results of isocratic elution with a volume fraction of 0.22 of ethanol, picrocrocin is separated from the initial undefined impurities and eluted from the column within five minutes (see Table 4.12). In this step, the weakly retained impurities are separated from picrocrocin and eluted in 2.5 minutes (see Figure 4.23). For an injection volume of 5 μl of the crude extract solution (5 g/l) with an injection time of 0.00416 min (Δt_{inj}) and dead time 1.12 min (t_0), the **ideal** first switching time $t_{sw,1}^{ideal}$ results from Eq. 2.84. Considering the column efficiency for picrocrocin by Eq. 4.10 ($2\sigma_{PC}$=0.6 min) and according to the assumption (I) (equality of column efficiency for isocratic and gradient elutions), the **real** first switching time, $t_{sw,1}^{real}$, was 4.58 min (Eq. 4.11):

$$t_{sw,1}^{real} = t_{sw,1}^{ideal} + 2\sigma_{PC} = 3.98 + 0.6 = 4.58 \tag{4.11}$$

Other target molecules, crocin I and crocin II, still remain in the column. To accelerate the migration rates of crocins I and II, the organic modifier content must be increased. To achieve sufficient separation between crocin I and II with acceptable elution time in the second gradient step, the volume fraction of organic modifier for the second step, $\varepsilon_{L,mod,2}$, was chosen to be 0.3. Indeed a higher volume fraction of the modifier in this step can lead to higher productivity but for low concentration injections. It means, a high volume fraction of modifier in step 2 results a small separation factor between crocin I and II, as well as low throughput and/or volume injection, generally leading to low productivity. Therefore, the gradient elution with $\varepsilon_{L,mod,2}$=0.3 was chosen, which had a reasonable separation factor, acceptable cycle time, **high throughput**, and acceptable component productivities.

According to the space and time intersections for crocin II at the ideal first switching time point (z^* and t^* in figure 4.22B, Eq. 2.92 and Eq. 2.93), the ideal second switching time point, $t_{sw,2}^{ideal}$, is easily determined by the Eq. 2.95. Considering the column efficiency for crocin II by Eq. 4.10 ($2\sigma_{CII}$=4.5 min) and according to the assumption (I), the real second switching time, $t_{sw,2}^{real}$, was 31.23 min (Eq. 4.12):

$$t_{sw,2}^{real} = t_{sw,2}^{ideal} + 2\sigma_{CII} = 26.73 + 4.5 = 31.23 \tag{4.12}$$

In the next step, the volume fraction of the organic modifier, $\varepsilon_{L,mod,3}$, was chosen to be

0.5, which is the largest value performed in isocratic elutions and suitable to wash out all remaining impurities. Due to the undetectable peaks and/or overlapping peaks of the terminal impurities in different volume fractions of the modifier in isocratic elutions, it was not possible to study their migration rate as an individual peak. Therefore, we could only estimate the Henry constant of the terminal impurities as a peak at a volume fraction of 0.5 of the modifier. Hence, the Henry constant of terminal impurities $K_{H,Imp.}$ estimated 3.5, which obtains by the Eq. 2.68. Thus, we assume that the terminal impurities are at the top of the column and do not move in the column during the first and second steps of the step-gradient elution. Therefore, the ideal third switching time would be the following:

$$t_{sw,3}^{ideal} = t_{sw,2}^{ideal} + t_{R,Imp.} - t_0 = t_{sw,2}^{ideal} + t_0 \left(1 + F K_{H,Imp.} \left(\varepsilon_{L,mod,3}\right)\right) - t_0 = 30.1 \quad (4.13)$$

Considering an **empirical** safety margin as column efficiency for the terminal impurities ($2\sigma_{Imp.}=3$ min), the real third switching time, $t_{sw,3}^{real}$, was 33.1 min (Eq. 4.14):

$$t_{sw,3}^{real} = t_{sw,3}^{ideal} + 2\sigma_{Imp.} = 30.1 + 3 = 33.1 \quad (4.14)$$

The last step is the equilibrium step, where the volume fraction of the modifier is reset to the first step ($\varepsilon_{L,mod,1}=0.22$). Under ideal conditions, the equilibrium time is equal to the dead time, ($t_{eq}^{ideal} = t_0 = 1.12$ min), which leads to the following ideal cycle time:

$$\Delta t_{cyc}^{ideal} = t_{sw,3}^{ideal} + t_{eq}^{ideal} = t_{sw,2}^{ideal} + t_0 \left(1 + F K_{H,Imp.} \left(\varepsilon_{L,mod,3}\right)\right) = 31.22 \quad (4.15)$$

However, due to the limited mass transfer rate and non-ideal fluid dynamics, the time required for the equilibrium step is longer than the dead time. To ensure that the peaks of two consecutive injections do not overlap, the time for the equilibrium step was set to almost 4.5-fold the dead time ($t_{eq}^{real} = 5$ min), which was determined empirically. Therefore, the actual total cycle time, Δt_{cyc}^{real}, was roughly 38 min:

$$\Delta t_{cyc}^{real} = t_{sw,3}^{real} + t_{eq}^{real} = 33.1 + 5 = 38.1 \quad (4.16)$$

The predicted three-step gradient trajectories of picrocrocin, crocin I, crocin II, and terminal impurities with ideal switching times $t_{sw,j}^{ideal}$ (ideal separation profile) illustrated in the following figure 4.22A.
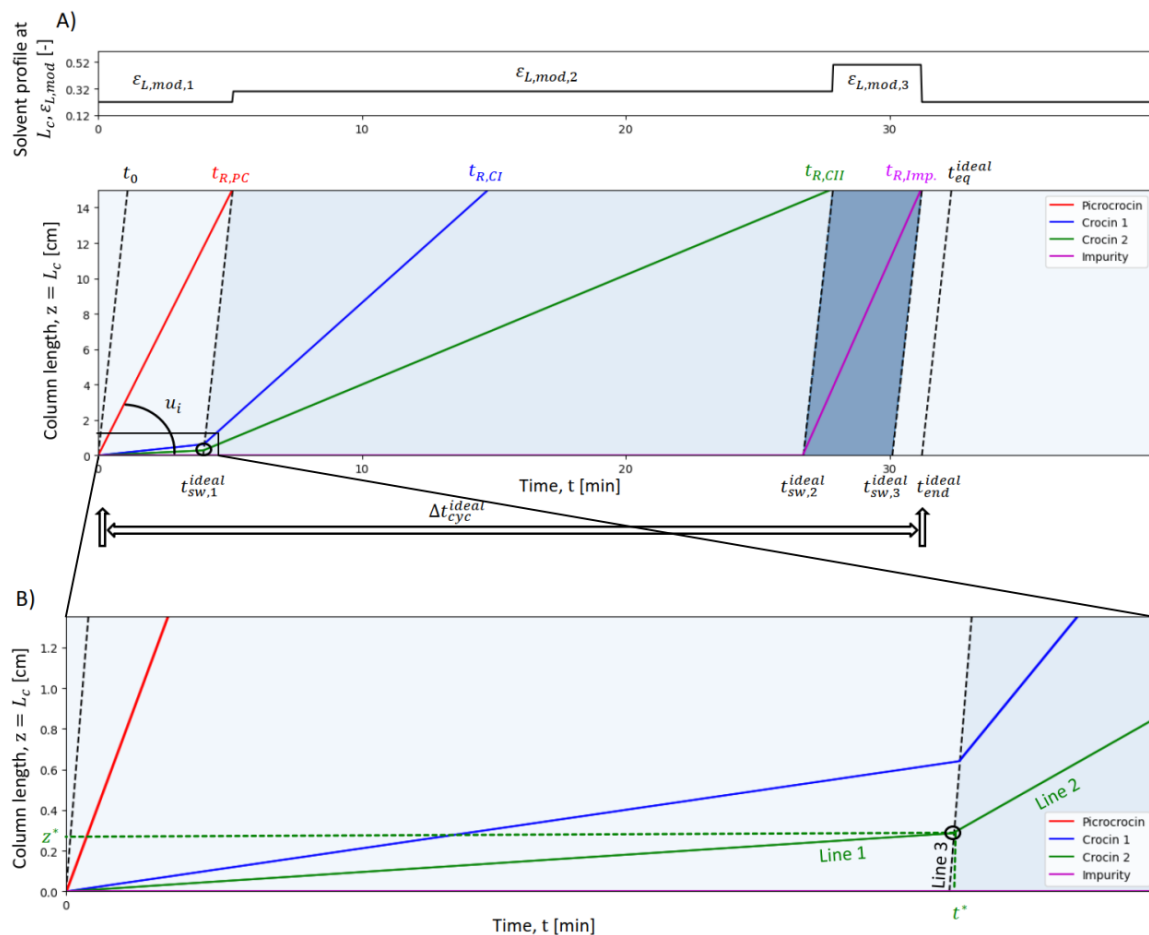
Figure 4.22: Graphical representation of the predicted three-step gradient elution (ideal separation profile). Picrocrocin (red line), crocin I (blue line), crocin II (green line), terminal impurities (purple line). $\varepsilon_{L,mod,1,2,3}$=0.22, 0.3, 0.5. $t_{R,PC,CI,CII,Imp.}$=5.09, 15.31, 28.1, 31.22 min. $t_{sw,1,2,3}^{ideal}$=3.98, 26.73, 30.1 min. Δt_{cyc}^{ideal}=31.22 min. Figure A: Diagram of the total trajectory. Figure B: Zoomed trajectory diagram around the first ideal switching time $t_{sw,1}^{ideal}$

The following table contains the estimated ideal and real switching times for the developed three-step gradient elution method:

Table 4.15: Developed three-step gradient elution along with ideal and real switching times, $\dot{V}_L$=1.2 ml/min

Step j $(j = 1, N)$	$\varepsilon_{L,mod,j}$	$t_{sw,j}^{ideal}$ [min]	$t_{sw,j}^{real}$ [min]
Step 1	0.22	3.98	4.58
Step 2	0.30	26.73	31.23
Step 3	0.50	30.10	33.10
Equilibrium	0.22	t_{end}^{ideal}=31.22	t_{end}^{real}=38.10

The following figure 4.20 illustrates the real separation profile of the saffron crude extract (in **analytical** column) using the developed three-step gradient elution method with real switching times $t_{sw,j}^{real}$:

Figure 4.23: Real separation profile of the saffron crude extract by the selected three-step gradient elution (Table 4.15) in **analytical scale**. Red, blue, green, and purple dash-lines: fractions of picrocrocin (PC), crocin I (CI), crocin II (CII), and terminal impurities, respectively. Three overlapping low concentration injections (c_{inj}^{crude}=1 g/l, V_{inj}=5 μl, Δt_{inj}=0.00416 min). Reverse phase chromatography (YMC-Triart Prep C18-S, 150×4.6 mm, 15 μm, 12 nm). $\dot{V}_L$=1.2 ml/min, t_0=1.12 min, $t_{R,PC}$=5.1 min, $t_{R,CI}$=16.2 min, $t_{R,CII}$=27.7 min, $t_{R,Imp.}$=35.4 min, $\Delta t_{cyc}^{exp.}$=40.1 min

Due to the different band broadening (column efficiency) in gradient elution compared to isocratic elution, the peak width of crocin II was narrower in gradient elution than in isocratic elution, resulting in complete elution of crocin II before the predicted real second switching time $t_{sw,2}^{real} = 31.23$ min, whereas this is not the case for picrocrocin in the first step due to isocratic elution in this step (see Figure 4.23). This difference in column efficiency and band broadening for crocin II in step-gradient elution is compensated by a broadened band when high concentrations (and/or large injection volumes) are injected.

On the other hand, to complete elution of the terminal impurities, the estimated real third switching time ($t_{sw,3}^{real}$) was empirically set 2 minutes longer. This is due to the higher affinity and retention of the terminal impurities in the step-gradient elution (see Figure 4.23). Therefore, the final cycle time was set 2 minutes longer than the estimated one ($\Delta t_{cyc}^{exp.}$=40.1 min).

Therefore, the three-step gradient elution test on the analytical C18 column was performed as shown in the figure 4.23. Three consecutive runs were performed on an analytical scale with good reproducibility (see Figure 4.23). Thus, the designed

three-step gradient elution, which was based on the assumption of a linear isotherm, was empirically validated (see predicted and empirical retention times of components in table 4.16).

Table 4.16: The predicted and experimental retention times of picrocrocin, crocin I, crocin II and final in the developed three-step gradient elution method. pred.: prediction, exp.: experimental, $\dot{V}_L$=1.2 ml/min

Component (i)	$t_{R,i}^{pred.}$ $[min]$	$t_{R,i}^{exp.}$ $[min]$
PC	5.09	5.10
CI	15.31	16.20
CII	28.10	27.70
Imp.	31.22	35.40

As can be seen, the difference between the predicted and experimental retention times for terminal impurities is nearly 4 minutes. Since it is not easy to obtain an accurate Henry constant for terminal impurities (a variety of impurities), this difference is between the predicted retention time and the experimentally determined retention time, and consequently between the estimated real third switching time and the experimentally determined third switching time.

Last but not least, since large volumes and high concentrations of feed are injected on a preparative column, the condition of volume and concentration overload must first be studied on an analytical column. When a large volume of feed solution was injected (see Figure 4.24), the elution bands of the target components were broadened and eluted slightly earlier (nearly 0.3 min for PC, 1 min for CI, and CII) than for low concentration injections, which means the isotherms in high concentration injections are nonlinear. To account for the nonlinearity, band broadening, and to ensure that the peaks would not overlap, the volume and concentration overload condition were optimized empirically (see Figure 4.24). The other parameters such as selectivity, retention factors, and resolutions [111] are listed in the Appendix tables A.3 and A.4.
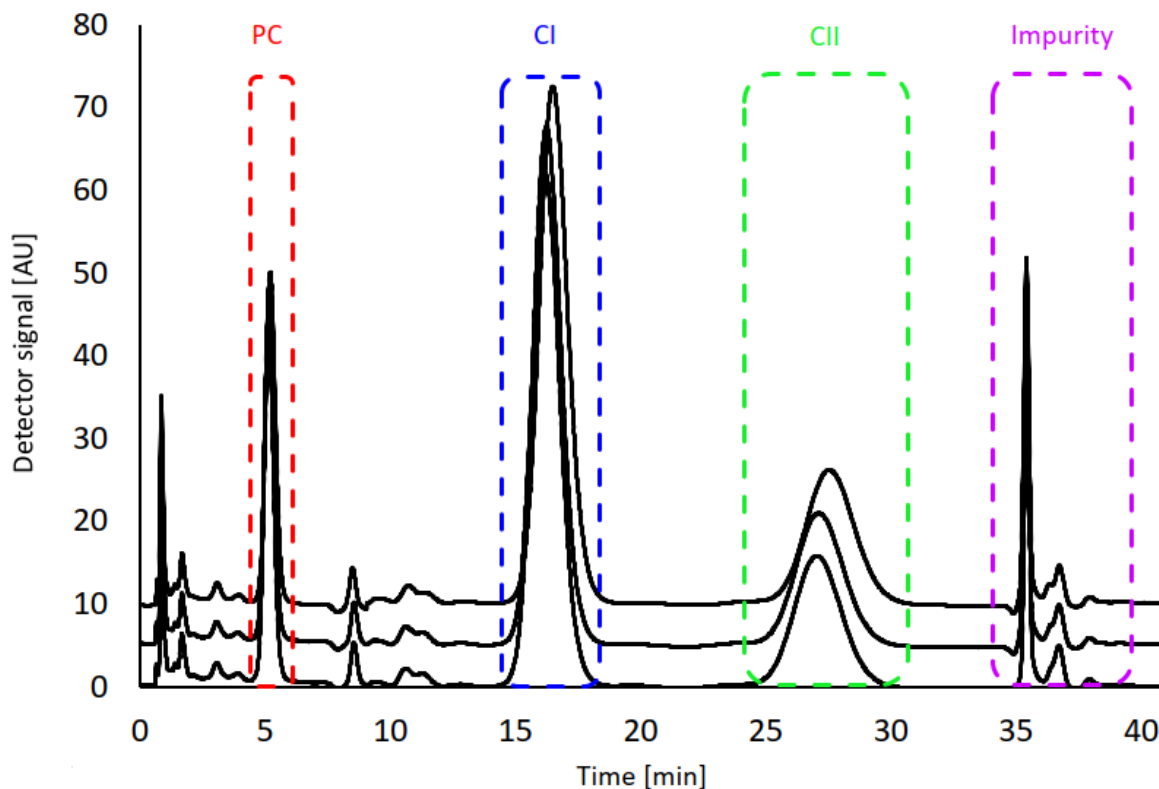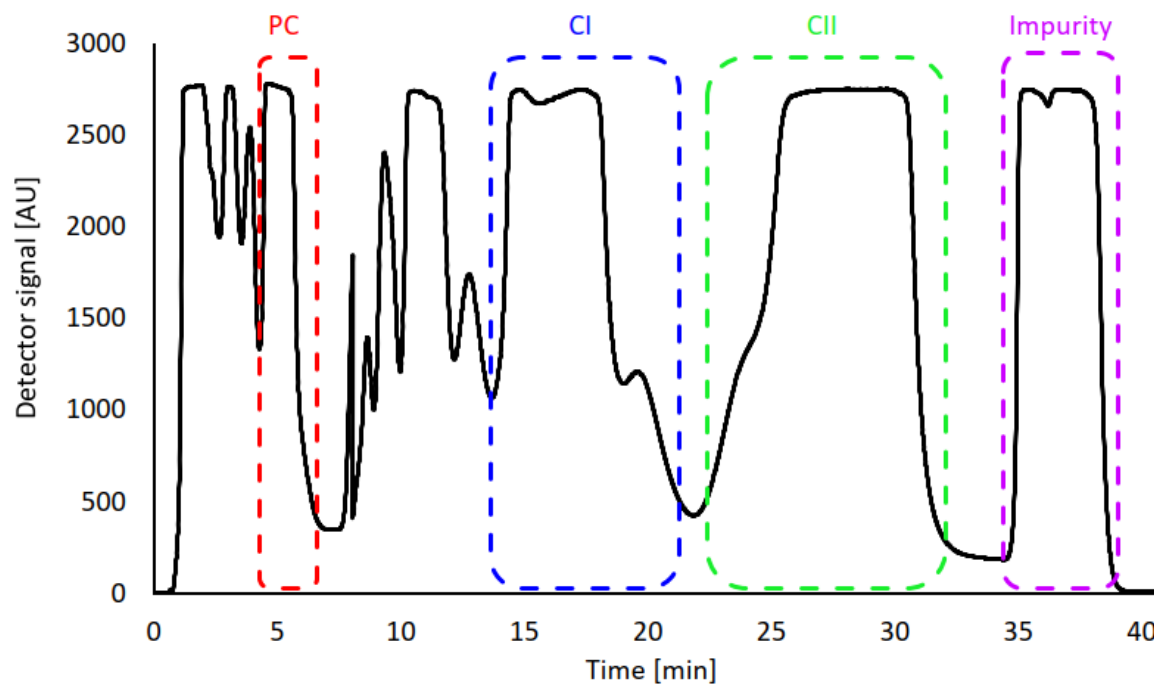
Figure 4.24: Real separation profile of saffron crude extract by the developed three-step gradient elution on the **analytical column**. Red, blue, green, and purple dash-lines: fractions of picrocrocin (PC), crocin I (CI), crocin II (CII), and terminal impurities, respectively. Overloaded injection (c_{inj}^{crude}=75 g/l, V_{inj}=0.167 ml, t_{inj}=0.15 min). $\dot{V}_L$=1.2 ml/min, t_0^{exp}=1.12 min, $t_{R,PC}$=4.8 min, $t_{R,CI}$=15.2 min, $t_{R,CII}$=26.2 min, $t_{R,Imp.}$=35.4 min, Δt_{cyc}^{real}=40.1 min

Since we chose step gradient conditions with relatively large resolutions, up to 12.5 mg of the feed mixture (saffron dry crude extract) can be separated with 2.5 ml column volume. The expected throughput is 7.5 $g/h/l$ (mass of feed mixture/time for separation/volume of column).

4.3.5   Preparative Column Efficiency

The performance of the packed preparative column can be assessed by a test chromatogram. As a first test, 10 mg of uracil was dissolved in 2 ml of 0.22 volume fraction of ethanol in aqueous solution, and injected as t_0 substance. An isocratic elution was performed using 0.22 volume fraction of the organic modifier ethanol at a flow rate appropriate for the column diameter (35 ml/min):
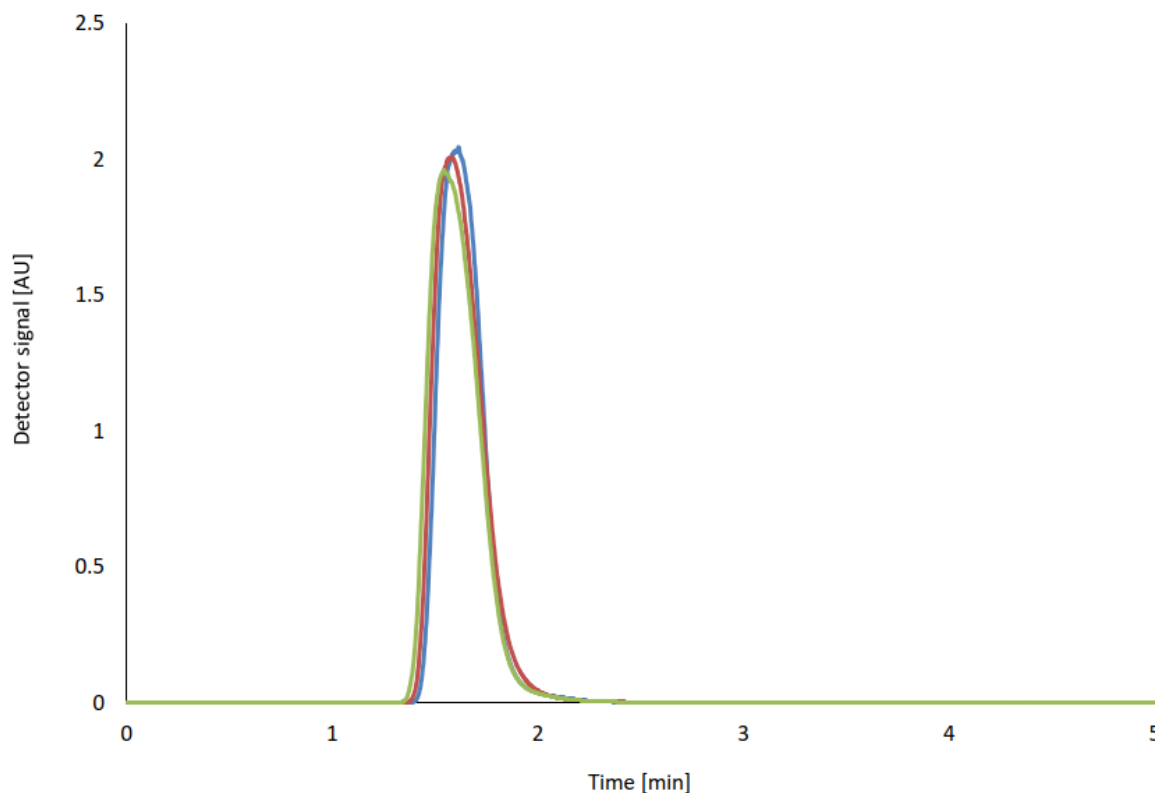
Figure 4.25: Pulse injection of uracil as non-retained substance on the packed preparative column (YMC-Triart Prep. C18, L_c=148.1 mm, d_c=25 mm, 15 μm, 12 nm). $\dot{V}_L$=35 ml/min (Eq. 2.80), t_0^{exp}=1.5 min, λ=254 nm

Three injections of uracil were repeatable, and the peak shapes were nearly Gaussian. In the second assay, 100 mg of saffron crude extract powder was dissolved in 2 ml ethanol/water solution (22%EtOH,78%water) and injected onto the preparative column. The HPLC separation method was the developed three-step gradient elution (see Table 4.15) at a flow rate of 35 ml/min (Eq. 2.80) corresponding to the column diameter:
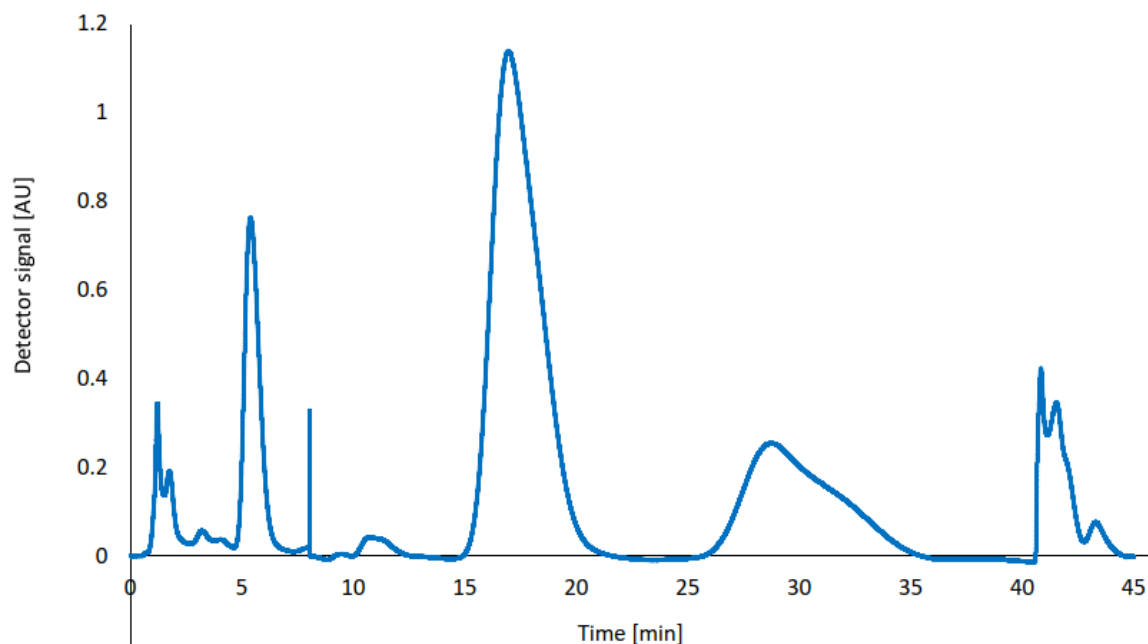
Figure 4.26: Separation profile of the saffron crude extract on the packed preparative column. $\dot{V}_L$=35 ml/min (Eq. 2.80)

Retention times, bandwidth, and number of theoretical plates for picrocrocin, crocin I, and crocin II on the preparative packed column are shown in Table 4.17:

Table 4.17: Retention time, band width, and number of theoretical plates for picrocrocin, crocin I, and crocin II on the packed preparative column, $\dot{V}_L$=35 ml/min, λ=254 nm between 0 and 8 min, λ=440 nm between 8 and 45 min

Component (i)	$t_{R,i}$ $[min]$	w_{base} $[min]$	$\bar{N}_i$ $(Eq.$ 2.73$)$
PC	5.43	2.35	86
CI	17.06	6.021	129
CII	28.8	9.57	145

Separation profile, column efficiency (number of theoretical plates, $\bar{N}_i$) and peak shape show good acceptable quality of the packed preparative column. The separation behavior is quite similar to the separation profile in the analytical chromatogram (see Figure 4.23), and it is repeatable. The retention times and band broadening of the components are slightly longer and broader than for the analytical column, especially for the more retained components, i.e. crocin II and the terminal impurities (crocin $III - V$ and safranal), which means more affinity and retention of them on to the packing of the preparative column that led to a bit longer cycle time (45min). However, this is completely acceptable. Therefore, the packed preparative column was qualified for the preparative chromatography based purification.

4.3.6   Preparative Three-Step Gradient Elution Based Purification

To scale-up a chromatographic separation process, a large-volume column is used to increase the production rate. The equation 2.80 was used for scaling-up the analytical conditions to the preparative scale.

$$\left(\frac{L_c d_c^{large}}{L_c d_c^{small}}\right)^2 = \frac{\dot{V}_L^{large}}{\dot{V}_L^{small}} = \frac{V_{inj}^{large}}{V_{inj}^{small}} \qquad (4.17)$$

With approximately the same column length, the volumetric flow rate, $\dot{V}_L$, and the injection volume, V_{inj}, for the preparative scale (L_c=148.1 mm, d_c=25 mm) are as shown in Table 4.18.

Table 4.18: Scaling of parameters from analytical to preparative chromatography (using Eq. 4.17). Developed three-step gradient elution method. Reverse phase chromatography (YMC-Triart Prep C18-S 150×4.6 mm (analytical column) and 148.1×25 mm (preparative column), 15 μm, 12 nm), c_{inj}^{crude} = 75 g/l, ID: Inner diameter

Scale	ID [mm]	$\dot{V}_L$ [ml/min]	V_{inj} [ml]	m_{inj}^{crude} [mg]
Analytical	4.6	1.2	0.167	12.52
Preparative	25	35	5	375

It should be mention that the term "crude" connect to the extraction section. In principle it comes from crude extract, which was discussed in the extraction section. Performing the developed three-step gradient elution (see Table 4.15), with the scaled up injection volume and volumetric flow rate (see Table 4.18), on the packed preparative column gave the following separation profile of the saffron crude extract:
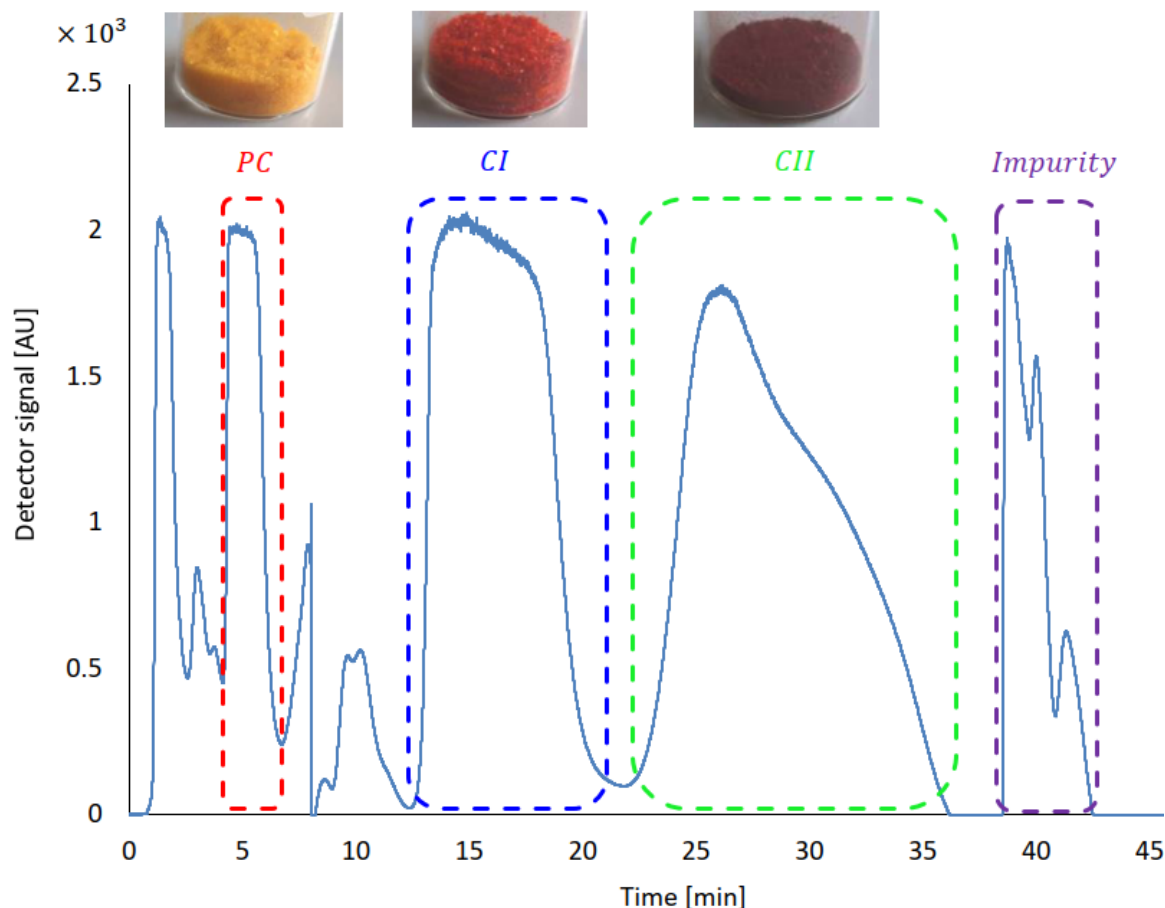
Figure 4.27: Preparative separation of saffron crude extract by the developed three-step gradient elution ($\varepsilon_{L,mod,j} = 0.22, 0.30, 0.50$) (see Table 4.15). YMC-Triart Prep C18 (L_c=148.1 mm, d_c=25 mm, 15 μm, 12 nm). $\dot{V}_L$=35 ml/min, t_{inj}=0.15 min, t_0=1.12 min, $t_{R,PC}$=4.7 min, $t_{R,CI}$=14.8 min, $t_{R,CII}$=25.5 min, $t_{R,Imp.}$=38.5 min, $\Delta t_{cyc}^{exp.}$= 45 min

As explained earlier, due to the effects of components on each other in the high concentration and large volume of the injection solution, nonlinear chromatography occurs on a preparative scale. Based on the assumption (II), we assumed that there is no nonlinearity in the overloaded injections. However, in reality, we found a shift in retention times (earlier elution), increasing band broadening, and different shapes of band profiles. The retention times of PC, CI, and CII were 0.4, 1.4, and 2.2 min shorter, respectively, for nonlinear chromatography (see Figure 4.27) than for linear chromatography (see Figure 4.23). The effect of nonlinearity on picrocrocin is smaller than for crocin I and crocin II. The reason for this difference is the sugar-like structure of picrocrocin as a monoterpene glycoside. The adsorption isotherms of some sugars are approximately linear in all concentration ranges [111, 119]. Therefore, the second and third switching times were empirically modulated slightly due to earlier elution, greater band broadening, and slightly different retention of terminal impurities on the large column. Therefore, the total cycle time at the preparative scale is 5 min longer than at the analytical scale. It is worth noting that the maximum absorbance wavelengths of picrocrocin and crocins are 254 nm and 440 nm, respec-

tively. Therefore, the selected wavelength of the detector is 254 *nm* between zero and eight minutes, after which the wavelength is switched to 440 *nm*. At the end, the fractions of the picrocrocin, crocin *I* and crocin *II* were collected manually. The collected fractions were concentrated to less than 100 *ml* using an industrial rotary evaporator (BUCHI, Switzerland) and then converted into pure fine powders using a freeze dryer (ZiRBUS technology GmbH, VaCo2, max temp -50℃, Germany) (see Figure 4.28). At the end, picrocrocin powder (with 98.34% purity) had light yellow color, crocin *I* powder (with 98.3% purity) had red color and crocin *II* powder (with 96.64% purity) had deep red color.
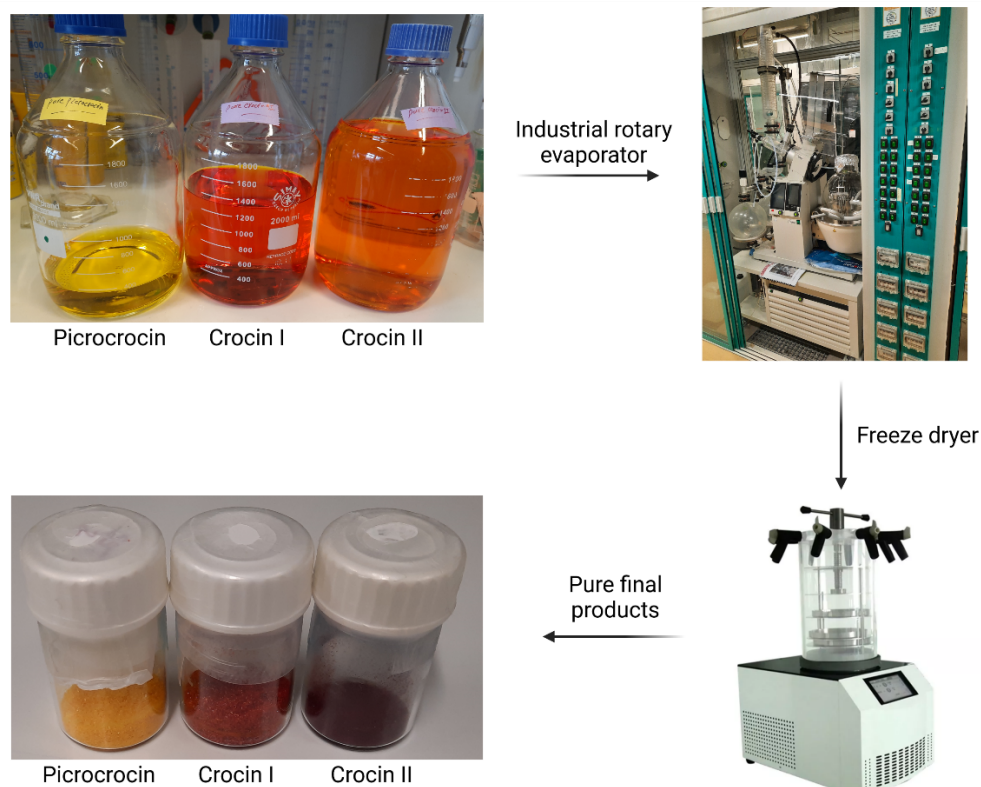
Figure 4.28: Schematic representation of the drying process of the collected fractions picrocrocin, crocin *I*, and crocin *II* from the preparative HPLC

4.3.7 Performance Evaluation of the Chromatography Process

4.3.7.1 Preparative Three-Step Gradient Elution

The developed three-step gradient elution was used to improve throughput and shorten cycle time to maximize productivity with acceptable product purity and recovery yield of target components. This elution method was scaled up to the preparative scale (by Eq. 4.17) and implemented on the large column with dimensions L_c=148.1 *mm*, d_c=25 *mm*, resulting in the following productivity (Eq. 2.99), percentage yield (Eq. 2.103), and purity (Eq. 2.98) of the collected fractions of picrocrocin,

crocin I, and crocin II:

Table 4.19: Productivity, percentage yield, and purity evaluation of the collected fractions of picrocrocin, crocin I, and crocin II on a preparative scale (Prep). c_{inj}^{crude}=75 g/l, V_{inj}=5 ml, m_{inj}^{crude}=0.375 g, $\Delta t_{cyc}^{exp.}$=45 min, $m_{Ads.}$=42.7 g, $V_c = 0.073\ l$. coll.: collected

Component (i)	$c_{i,inj}$ [g/l]	$m_{i,inj}$ [g]	$m_{i,coll}$ [g]	$Pr_i^{Prep.}$ [$g_i/day/g_{Ads}$]	$Pr_i^{Prep.}$ [$g_i/min/l$]	$Y_i^{Prep.}$ [%]	$Pu_i^{Prep.}$ [%]
PC	11.25	0.05625	0.05371	0.040	0.016	95.5	98.34
CI	18.75	0.09375	0.09187	0.069	0.028	98	98.30
CII	7.05	0.03525	0.03313	0.025	0.010	94	96.64

It should be mentioned that due to the larger amount of crocin I in the crude extract (feed), it has higher productivity than picrocrocin and crocin II, and for same reason the productivity of picrocrocin is larger than crocin II ($Pr_{CI}^{Prep.} > Pr_{PC}^{Prep.} > Pr_{CII}^{Prep.}$).

4.4 Comparison of the Extraction and Chromatography Processes

The following table provides a summary of the achieved purity, productivity, and yield of picrocricn, crocin I and crocin II for the extraction and chromatography processes studied experimentally:

Table 4.20: Summary of performance evaluations in continuous counter-current extraction and chromatography (three-step gradient) processes

Process	Component (i)	$Pu_i^{Process}$ [%]	$Pr_i^{Process}$ [$g_i/min/l$]	$Y_i^{Process}$ [%]
	PC	14.9	3.90	99.5
Extraction (Extr.)	CI	23.9	6.20	95.71
	CII	8.3	2.25	92.02
	PC	98.34	0.016	95.5
Chromatography (Chrom.)	CI	98.30	0.028	98
	CII	96.64	0.010	94

The results achieved contribute to provide productivities of the two processes (see Table 4.20) studied alone. It also allows to evaluate options to connect them. The process specific productivity is:

$$Pr_i^{Process} = \frac{\dot{m}_i^{Process}}{V^{Process}} \quad (4.18)$$

Direct coupling of the extraction (Extr.) and chromatography (Chrom.) processes requires:

$$\dot{m}_i^{Extr.} = \dot{m}_i^{Chrom.} \quad (4.19)$$

Therefore, an "Expansion Ratio (ER)" of the chromatographic column volume compared to the continuous counter-current extraction column volume ($V^{Chrom.}/V^{Extr.}$) can be estimated as follows:

$$ER_i = \frac{V^{Chrom.}}{V^{Extr.}} = \frac{Pr_i^{Extr.}}{Pr_i^{Chrom.}} \tag{4.20}$$

Using the productivities of table 4.20, the expansion ratios, ER_i, for picrocrocin, crocin I, and crocin II will be roughly 244, 222, and 225, respectively. Hence, to make a continuous connection between the extraction and chromatography processes, the chromatographic column volume should be more than 200 times bigger than the volume of the continuous counter-current extraction apparatus.

At the end, depending on requested productivity of picrocrocin, crocin I, and crocin II (defined certain job from the harvest), and considering the obtained productivity determines the necessary size of the counter-current machine. Then, utilizing the expansion ratio, ER_i, and the estimated volume of the large counter-current apparatus, the volume of the preparative chromatography column can be determined.

Matching the two productivities in continuous counter-current and chromatography would mean to match the scales. We can have a faster process (extraction) and a slower process (chromatography). The first requires a smaller equipment and the second a bigger equipment.

Chapter 5

Conclusions and Outlook

In this study, the provision and productivity of extracting from saffron and further purifing of picrocroin, crocin I and crocin II were investigated during extraction and chromatographic based purification processes.

Well-established knowledge regarding extraction processes, in general, is used to generate estimates of extraction productivities for the case considered and to compare different process options. Here, in this study, we reported results of improving the access to the three main and effective ingredients of saffron, namely picrocrocin (PC), crocin I (CI), and crocin II (CII) by performing single-stage batch extraction, then multiple sequential batches extraction steps. These experiments provided a basis for estimating the essential phase equilibrium of the components and evaluating their extraction kinetics. Based on this quantitative description of the fundamental aspects of the extraction process namely thermodynamics and kinetics constants, it was possible to quantify more advanced and productive extraction processes such as a continuously operated counter-current process that is suggested and modeled herein.

The results show that the productivity of the target components is higher in the continuous counter-current extraction than in the batch extraction methods. This is due to the potential of overcoming thermodynamic limitations due to CC operation. This is due to the throughput and time of the process, which is continuously improved in the counter-current method, resulting in higher productivity. The estimated productivity of picrocrocin, crocin I, and crocin II in the counter-current (CC) method were 3.9, 6.2, 2.25 $g_i/min/l$, respectively. Different productivity of the components is due to the different feed composition. The estimated productivity in CC process for picrocrocin, crocin I and crocin II were respectively 30%, 37%, and 40% higher than the estimated ones in the batch extraction method. This different percents in CC process is due to the different thermodynamic values of components ($K_{PC,E} > K_{CI,E} > K_{CII,E}$), which leads to the higher potential of overcoming thermodynamic limitations of CC process on the component with smaller thermodynamic value (crocin II) (see Figure 4.18).

The estimated recovery yield of picrocrocin, crocin I and crocin II in CC process were 99.50%, 95.71% and 92.02%, respectively. This is due to the higher thermodynamic value of picrocrocin than crocin I and crocin II ($K_{PC,E} > K_{CI,E} > K_{CII,E}$), which leads to the higher recovery yield of picrocrocin than crocin I and crocin II ($Y_{PC} > Y_{CI} > Y_{CII}$). The recovery yield of picrocrocin, crocin I and crocin II in the CC process were respectively 28%, 35%, and 36% higher than that in the batch extraction process. This is again due to the different thermodynamic values of components ($K_{PC,E} > K_{CI,E} > K_{CII,E}$), which leads to the higher potential of overcoming thermodynamic limitations of CC process on the component with smaller thermodynamic value (crocin II) (see Figure 4.18).

In the solid-liquid chromatography separation method, isocratic and gradient elutions were used for the separation and purification of the picrocrocin, crocin I, and crocin II from saffron crude extract. For systematic method development, the retention behavior of the components and their peak widths in different volumetric fractions of modifier (ethanol), $\varepsilon_{L,mod}$, were studied by isocratic elutions on a C18 column. In other words, the isocratic elutions were intended to investigate the influence of the different volume fractions of the organic modifier, $\varepsilon_{L,mod}$, on the Henry constants of picrococin, crocin I and II, $K_{i,H}(\varepsilon_{L,mod})$. The Henry constant is known as an isothermal linear equilibrium parameter used to develop and optimize the three-step gradient elution with shorten cycle time, appropriate separation factors, and high productivity. The validated developed three-step gradient elution was scaled up to the preparative HPLC to increase the production rate of the components. The productivity of the both analytical and preparative HPLC columns for the picrocrocin, crocin I and crocin II were 0.016, 0.028, and 0.010 $g_i/min/l$, respectively, which showed more higher production rate of preparative column than the analytical one. The recovery yield of the collected fractions of picrocrocin, crocin I, and crocin II from the preparative HPLC column were 95.5%, 98%, and 94%, respectively. The purity of the collected fractions of picrocrocin, crocin I and crocin II were 98.34%, 98.30%, and 96.64%, respectively.

Therefore, There is a tools for both scaling up things for that same volume there is a higher productivity of performing the extraction to get it out, then later to purify it by chromatography. Finally, as an **outlook**:

1) The experimental validation of the continuous counter-current extraction process. It should be performed as the next study.

2) Investigation of the nonlinearity of the extraction and preparative chromatography processes, and the corresponding models.

3) The continuous chromatographic techniques, such as SMB, can be used for the continuous purification with higher productivity.

Bibliography

[1] F. Mosca, G. I. Hidalgo, J. Villasante, and M. P. Almajano, "Continuous or batch solid-liquid extraction of antioxidant compounds from seeds of sterculia apetala plant and kinetic release study," *Molecules*, vol. 23, no. 7, p. 1759, 2018.

[2] S. Z. Bathaie, A. Farajzade, and R. Hoshyar, "A review of the chemistry and uses of crocins and crocetin, the carotenoid natural dyes in saffron, with particular emphasis on applications as colorants including their use as biological stains," *Biotechnic & Histochemistry*, vol. 89, no. 6, pp. 401–411, 2014.

[3] S. Guan, Q. Pu, Y. Liu, H. Wu, W. Yu, Z. Pi, S. Liu, F. Song, J. Li, and D.-A. Guo, "Scale-up preparation of crocins i and ii from gardenia jasminoides by a two-step chromatographic approach and their inhibitory activity against atp citrate lyase," *Molecules*, vol. 26, no. 11, p. 3137, 2021.

[4] M. Pashirzad, M. Shafiee, A. Avan, M. Ryzhikov, H. Fiuji, A. Bahreyni, M. Khazaei, S. Soleimanpour, and S. M. Hassanian, "Therapeutic potency of crocin in the treatment of inflammatory diseases: Current status and perspective," *Journal of Cellular Physiology*, vol. 234, no. 9, pp. 14601–14611, 2019.

[5] M. Ghiasian, F. Khamisabadi, N. Kheiripour, M. Karami, R. Haddadi, A. Ghaleiha, B. Taghvaei, S. S. Oliaie, M. Salehi, P. Samadi, *et al.*, "Effects of crocin in reducing dna damage, inflammation, and oxidative stress in multiple sclerosis patients: A double-blind, randomized, and placebo-controlled trial," *Journal of Biochemical and Molecular Toxicology*, vol. 33, no. 12, e22410, 2019.

[6] Y. Xie, Q. He, H. Chen, Z. Lin, Y. Xu, and C. Yang, "Crocin ameliorates chronic obstructive pulmonary disease-induced depression via pi3k/akt mediated suppression of inflammation," *European journal of pharmacology*, vol. 862, p. 172640, 2019.

[7] A. Talaei, M. H. Moghadam, S. A. S. Tabassi, and S. A. Mohajeri, "Crocin, the main active saffron constituent, as an adjunctive treatment in major depressive disorder: A randomized, double-blind, placebo-controlled, pilot clinical trial," *Journal of affective disorders*, vol. 174, pp. 51–56, 2015.

[8] M. A. Yorgun, "Effects of crocin on diabetic maculopathy: A placebo-controlled randomized clinical trial.," *American Journal of Ophthalmology*, vol. 204, pp. 141–142, 2019.

[9] A. Colapietro, A. Mancini, A. M. D'Alessandro, and C. Festuccia, "Crocetin and crocin from saffron in cancer chemotherapy and chemoprevention," *Anti-Cancer Agents in Medicinal Chemistry (Formerly Current Medicinal Chemistry-Anti-Cancer Agents)*, vol. 19, no. 1, pp. 38–47, 2019.

[10] X. Pu, C. He, Y. Yang, W. Wang, K. Hu, Z. Xu, and J. Song, "In vivo production of five crocins in the engineered escherichia coli," *ACS Synthetic Biology*, vol. 9, no. 5, pp. 1160–1168, 2020.

[11] N. S. Koulakiotis, E. Pittenauer, M. Halabalaki, A. Tsarbopoulos, and G. Allmaier, "Comparison of different tandem mass spectrometric techniques (ESI-IT, ESI-and IP-MALDI-QRTOF and vMALDI-TOF/RTOF) for the analysis of crocins and picrocrocin from the stigmas of Crocus sativus L.," *Rapid Communications in Mass Spectrometry*, vol. 26, no. 6, pp. 670–678, 2012.

[12] B. Montalvo-Hernández, M. Rito-Palomares, and J. Benavides, "Recovery of crocins from saffron stigmas (crocus sativus) in aqueous two-phase systems," *Journal of Chromatography A*, vol. 1236, pp. 7–15, 2012.

[13] R. Kumar, V. Singh, K. Devi, M. Sharma, M. Singh, and P. S. Ahuja, "State of art of saffron (crocus sativus l.) agronomy: A comprehensive review," *Food Reviews International*, vol. 25, no. 1, pp. 44–85, 2008.

[14] M. Lautenschläger, M. Lechtenberg, J. Sendker, and A. Hensel, "Effective isolation protocol for secondary metabolites from saffron: Semi-preparative scale preparation of crocin-1 and trans-crocetin," *Fitoterapia*, vol. 92, pp. 290–295, 2014.

[15] F. Hadizadeh, S. Mohajeri, and M. Seifi, "Extraction and purification of crocin from saffron stigmas employing a simple and efficient crystallization method," *Pakistan Journal of Biological Sciences*, vol. 13, no. 14, pp. 691–698, 2010.

[16] H. Caballero-Ortega, R. Pereda-Miranda, and F. I. Abdullaev, "Hplc quantification of major active components from 11 different saffron (crocus sativus l.) sources," *Food Chemistry*, vol. 100, no. 3, pp. 1126–1131, 2007.

[17] A. Bolhasani, S. Bathaie, I. Yavari, A. Moosavi-Movahedi, and M. Ghaffari, "Separation and purification of some components," *Asian Journal of Chemistry*, vol. 17, no. 2, pp. 725–729, 2005.

[18] S. Raghavan, J. Hansen, S. Sonkar, S. Kumar, M. Panchapagesa, E. H. Hansen, K. R. Hansen, and K. Kumar, *Methods and materials for recombinant production of saffron compounds*, US Patent App. 14/237,542, Sep. 2014.

[19] P. Lozano, M. Castellar, M. Simancas, and J. Iborra, "A quantitative high-performance liquid chromatographic method to analyse commercial saffron (crocus sativus l.) products.," *Journal of Chromatography A*, vol. 830, no. 2, pp. 477–483, 1999.

[20] M. Carmona, A. Zalacain, J. E. Pardo, E. López, A. Alvarruiz, and G. L. Alonso, "Influence of different drying and aging conditions on saffron constituents," *Journal of Agricultural and Food Chemistry*, vol. 53, no. 10, pp. 3974–3979, 2005.

[21] S. A. Ordoudi and M. Z. Tsimidou, "Saffron quality: Effect of agricultural practices, processing and storage," in *Production Practices and Quality Assessment of Food Crops Volume 1*, Springer, 2004, pp. 209–260.

[22] M. Lage and C. L. Cantrell, "Quantification of saffron (crocus sativus l.) metabolites crocins, picrocrocin and safranal for quality determination of the spice grown under different environmental moroccan conditions," *Scientia horticulturae*, vol. 121, no. 3, pp. 366–373, 2009.

[23] A. M. Sánchez, M. Carmona, C. P. del Campo, and G. L. Alonso, "Solid-phase extraction for picrocrocin determination in the quality control of saffron spice (crocus sativus l.)," *Food Chemistry*, vol. 116, no. 3, pp. 792–798, 2009.

[24] C. P. Del Campo, M. Carmona, L. Maggi, C. D. Kanakis, E. G. Anastasaki, P. A. Tarantilis, M. G. Polissiou, and G. L. Alonso, "Effects of mild temperature conditions during dehydration procedures on saffron quality parameters," *Journal of the Science of Food and Agriculture*, vol. 90, no. 4, pp. 719–725, 2010.

[25] C. P. Del Campo, M. Carmona, L. Maggi, C. D. Kanakis, E. G. Anastasaki, P. A. Tarantilis, M. G. Polissiou, and G. L. Alonso, "Picrocrocin content and quality categories in different (345) worldwide samples of saffron (crocus sativus l.)," *Journal of agricultural and food chemistry*, vol. 58, no. 2, pp. 1305–1312, 2010.

[26] Y. Tong, X. Zhu, Y. Yan, R. Liu, F. Gong, L. Zhang, J. Hu, L. Fang, R. Wang, and P. Wang, "The influence of different drying methods on constituents and antioxidant activity of saffron from china," *International journal of analytical chemistry*, vol. 2015, 2015.

[27] M. Zougagh, A. Rıéos, and M. Valcárcel, "Determination of total safranal by in situ acid hydrolysis in supercritical fluid media: Application to the quality control of commercial saffron," *Analytica chimica acta*, vol. 578, no. 2, pp. 117–121, 2006.

[28] M. Negbi, *Saffron: Crocus sativus L.* CRC press, 1999.

[29] H. Lopez-Corcoles, A. Brasa-Ramos, F. Montero-Garcia, M. Romero-Valverde, and F. Montero-Riquelme, "Phenological growth stages of saffron plant (crocus sativus l.) according to the bbch scale," *Spanish Journal of Agricultural Research*, vol. 13, no. 3, e09SC01–e09SC01, 2015.

[30] S. Sampathu, S. Shivashankar, Y. Lewis, and A. Wood, "Saffron (crocus sativus linn.)—cultivation, processing, chemistry and standardization," *Critical Reviews in Food Science & Nutrition*, vol. 20, no. 2, pp. 123–157, 1984.

[31] M. A. Behdani, M. J. Al-Ahmadi, and H.-R. Fallahi, "Biomass partitioning during the life cycle of saffron (crocus sativus l.) using regression models," *Journal of Crop Science and Biotechnology*, vol. 19, pp. 71–76, 2016.

[32] A. M. Husaini, A. N. Kamili, M. Wani, J. Teixeira da Silva, and G. Bhat, "Sustainable saffron (crocus sativus kashmirianus) production: Technological and policy interventions for kashmir," *Functional Plant Science and Biotechnology*, vol. 4, no. 2, pp. 116–127, 2010.

[33] M. Behnia, A. Estilai, and B. Ehdaie, "Application of fertilizers for increased saffron yield," *Journal of Agronomy and Crop Science*, vol. 182, no. 1, pp. 9–15, 1999.

[34] K. Erden and A. Özel, "Influence of delayed harvest on yield and some quality parameters of saffron (crocus sativus l.)," *J. Agric. Biol. Sci*, vol. 11, pp. 313–316, 2016.

[35] B. L. Raina, S. G. Agarwal, A. K. Bhatia, and G. S. Gaur, "Changes in pigments and volatiles of saffron (crocus sativusl) during processing and storage," *Journal of the Science of Food and Agriculture*, vol. 71, no. 1, pp. 27–32, 1996.

[36] B. Acar, H. Sadikoglu, and M. Ozkaymak, "Freeze drying of saffron (crocus sativus l.)," *Drying Technology*, vol. 29, no. 14, pp. 1622–1627, 2011.

[37] L. Cossignani, E. Urbani, M. S. Simonetti, A. Maurizi, C. Chiesi, and F. Blasi, "Characterisation of secondary metabolites in saffron from central italy (cascia, umbria)," *Food Chemistry*, vol. 143, pp. 446–451, 2014.

[38] V. Maghsoodi, A. Kazemi, and E. Akhondi, "Effect of different drying methods on saffron (crocus sativus l) quality," 2012.

[39] M. Sarfarazi, S. M. Jafari, and G. Rajabzadeh, "Extraction optimization of saffron nutraceuticals through response surface methodology," *Food analytical methods*, vol. 8, pp. 2273–2285, 2015.

[40] P. Winterhalter and M. Straubinger, "Saffron—renewed interest in an ancient spice," *Food Reviews International*, vol. 16, no. 1, pp. 39–59, 2000.

[41] F. Bouvier, C. Suire, J. Mutterer, and B. Camara, "Oxidative remodeling of chromoplast carotenoids: Identification of the carotenoid dioxygenase csccd and cszcd genes involved in crocus secondary metabolite biogenesis," *The Plant Cell*, vol. 15, no. 1, pp. 47–62, 2003.

[42] T. Radjabian, M. H. Namin, H. Ebrahimzadeh, B. Ghareyazie, S. Gharavi, N. Tafreshi, *et al.*, "In vitro expression of apocarotenoid genes in crocussativus l.," *African Journal of Biotechnology*, no. 8, 2009.

[43] H. Pfander and H. Schurtenberger, "Biosynthesis of c20-carotenoids in crocus sativus," *Phytochemistry*, vol. 21, no. 5, pp. 1039–1042, 1982.

[44] B. Camara, P. Hugueney, F. Bouvier, M. Kuntz, and R. Monéger, "Biochemistry and molecular biology of chromoplast development," *International review of cytology*, vol. 163, pp. 175–247, 1995.

[45] S. S. Kadian and M. Garg, "Pharmacological effects of carotenoids: A review," *International Journal of Pharmaceutical Sciences and Research*, vol. 3, no. 1, p. 42, 2012.

[46] M. Nagatoshi, K. Terasaka, M. Owaki, M. Sota, T. Inukai, A. Nagatsu, and H. Mizukami, "Ugt75l6 and ugt94e5 mediate sequential glucosylation of crocetin to crocin in gardenia jasminoides," *FEBS letters*, vol. 586, no. 7, pp. 1055–1061, 2012.

[47] N. Li, G. Lin, Y.-W. Kwan, and Z.-D. Min, "Simultaneous quantification of five major biologically active ingredients of saffron by high-performance liquid chromatography," *Journal of Chromatography A*, vol. 849, no. 2, pp. 349–355, 1999.

[48] M. Schmidt, G. Betti, and A. Hensel, "Saffron in phytotherapy: Pharmacology and clinical uses.," *Wiener Medizinische Wochenschrift (1946)*, vol. 157, no. 13-14, pp. 315–319, 2007.

[49] M. Lechtenberg, D. Schepmann, M. Niehues, N. Hellenbrand, B. Wünsch, and A. Hensel, "Quality and functionality of saffron: Quality control, species assortment and affinity of extract and isolated saffron compounds to nmda and $\sigma 1$ (sigma-1) receptors," *Planta Medica*, vol. 74, no. 07, pp. 764–772, 2008.

[50] W. Si, L. Xiong, H. Zhou, H. Wu, Z. Liu, G. Liu, Y. Liu, A. Shen, and X. Liang, "Comprehensive characterization of ingredients in crocus sativus l. from different origins based on the combination of targeted and nontargeted strategies," *Food Chemistry*, vol. 397, p. 133 777, 2022.

[51] J. O. L. IBORRA, M. R. CASTELLAR, M. A. CÁNOVAS, and A. R. MANJÓN, "Tlc preparative purification of picrocrocin, htcc and crocin from saffron," *Journal of Food Science*, vol. 57, no. 3, pp. 714–716, 1992.

[52] G. L. ALONSO, M. R. SALINAS, J. GARIJO, and M. A. SÁNCHEZ-FERNÁNDEZ, "Composition of crocins and picrocrocin from spanish saffron (crocus sativus l.)," *Journal of Food Quality*, vol. 24, no. 3, pp. 219–233, 2001.

[53] A. M. Sánchez, M. Carmona, A. Zalacain, J. M. Carot, J. M. Jabaloyes, and G. L. Alonso, "Rapid determination of crocetin esters and picrocrocin from saffron spice (crocus sativus l.) using uv–visible spectrophotometry for quality control," *Journal of Agricultural and Food Chemistry*, vol. 56, no. 9, pp. 3167–3175, 2008.

[54] P. Lozano, D. Delgado, D. Gomez, M. Rubio, and J. Iborra, "A non-destructive method to determine the safranal content of saffron (crocus sativus l.) by supercritical carbon dioxide extraction combined with high-performance liquid chromatography and gas chromatography," *Journal of Biochemical and Biophysical Methods*, vol. 43, no. 1-3, pp. 367–378, 2000.

[55] M. Castellar, H. Montijano, A. Manjón, and J. Iborra, "Preparative high-performance liquid chromatographic purification of saffron secondary metabolites," *Journal of Chromatography A*, vol. 648, no. 1, pp. 187–190, 1993.

[56] S. Z. Bathaie and S. Z. Mousavi, "New applications and mechanisms of action of saffron and its important ingredients," *Critical reviews in food science and nutrition*, vol. 50, no. 8, pp. 761–786, 2010.

[57] M. Scotter, "Overview of eu regulations and safety assessment for food colours," in *Colour additives for foods and beverages*, Elsevier, 2015, pp. 61–74.

[58] S. Z. Mousavi and S. Z. Bathaie, "Historical uses of saffron: Identifying potential new avenues for modern research," *Avicenna Journal of Phytomedicine*, vol. 1, no. 2, pp. 57–66, 2011.

[59] S. Akhondzadeh, H. Fallah-Pour, K. Afkham, A.-H. Jamshidi, and F. Khalighi-Cigaroudi, "Comparison of crocus sativus l. and imipramine in the treatment of mild to moderate depression: A pilot double-blind randomized trial [isrctn45683816]," *BMC complementary and alternative medicine*, vol. 4, pp. 1–5, 2004.

[60] M. Moshiri, M. Vahabzadeh, and H. Hosseinzadeh, "Clinical applications of saffron (crocus sativus) and its constituents: A review," *Drug research*, vol. 65, no. 06, pp. 287–295, 2015.

[61] M. Butnariu, C. Quispe, J. Herrera-Bravo, J. Sharifi-Rad, L. Singh, N. M. Aborehab, A. Bouyahya, A. Venditti, S. Sen, K. Acharya, *et al.*, "The pharmacological activities of crocus sativus l.: A review based on the mechanisms and therapeutic opportunities of its phytoconstituents," *Oxidative medicine and cellular longevity*, vol. 2022, 2022.

[62] A. Assimopoulou, Z. Sinakos, and V. Papageorgiou, "Radical scavenging activity of crocus sativus l. extract and its bioactive constituents," *Phytotherapy Research: An International Journal Devoted to Pharmacological and Toxicological Evaluation of Natural Product Derivatives*, vol. 19, no. 11, pp. 997–1000, 2005.

[63] Y. Chen, H. Zhang, X. Tian, C. Zhao, L. Cai, Y. Liu, L. Jia, H.-X. Yin, and C. Chen, "Antioxidant potential of crocins and ethanol extracts of gardenia jasminoides ellis and crocus sativus l.: A relationship investigation between antioxidant activity and crocin contents," *Food Chemistry*, vol. 109, no. 3, pp. 484–492, 2008.

[64] S. A. Ordoudi, C. D. Befani, N. Nenadis, G. G. Koliakos, and M. Z. Tsimidou, "Further examination of antiradical properties of crocus sativus stigmas extract rich in crocins," *Journal of agricultural and food chemistry*, vol. 57, no. 8, pp. 3080–3086, 2009.

[65] M. A. Papandreou, M. Tsachaki, S. Efthimiopoulos, P. Cordopatis, F. N. Lamari, and M. Margarity, "Memory enhancing effects of saffron in aged mice are correlated with antioxidant protection," *Behavioural brain research*, vol. 219, no. 2, pp. 197–204, 2011.

[66] S. Verma and A. Bordia, "Antioxidant property of saffron in man.," *Indian journal of medical sciences*, vol. 52, no. 5, pp. 205–207, 1998.

[67] Y. Wang, T. Han, Y. Zhu, C.-J. Zheng, Q.-L. Ming, K. Rahman, and L.-P. Qin, "Antidepressant properties of bioactive fractions from the extract of crocus sativus l.," *Journal of natural medicines*, vol. 64, pp. 24–30, 2010.

[68] S. Akhondzadeh, N. Tahmacebi-Pour, A.-A. Noorbala, H. Amini, H. Fallah-Pour, A.-H. Jamshidi, and M. Khani, "Crocus sativus l. in the treatment of mild to moderate depression: A double-blind, randomized and placebo-controlled trial," *Phytotherapy Research: An International Journal Devoted to Pharmacological and Toxicological Evaluation of Natural Product Derivatives*, vol. 19, no. 2, pp. 148–151, 2005.

[69] H. Hosseinzadeh, G. Karimi, and M. Niapoor, "Antidepressant effects of crocus sativus stigma extracts and its constituents, crocin and safranal, in mice," *Journal of Medicinal Plants*, vol. 3, no. 11, pp. 48–58, 2004.

[70] S. Patel, M. Sarwat, and T. H. Khan, "Mechanism behind the anti-tumour potential of saffron (crocus sativus l.): The molecular perspective," *Critical Reviews in Oncology/Hematology*, vol. 115, pp. 27–35, 2017.

[71] F. I. Abdullaev, "Cancer chemopreventive and tumoricidal properties of saffron (crocus sativus l.)," *Experimental biology and medicine*, vol. 227, no. 1, pp. 20–25, 2002.

[72] H. Greenlee, "Natural products for cancer prevention," in *Seminars in oncology nursing*, Elsevier, vol. 28, 2012, pp. 29–44.

[73] O. Oguntibeju, E. Truter, and A. Esterhuyse, "The role of fruit and vegetable consumption in human health and disease prevention," *Diabetes Mellitus-Insights and Perspectives*, vol. 3, no. 2, pp. 172–180, 2013.

[74] A. Bolhassani, A. Khavari, and S. Z. Bathaie, "Saffron and natural carotenoids: Biochemical activities and anti-tumor effects," *Biochimica et Biophysica Acta (Bba)-reviews on cancer*, vol. 1845, no. 1, pp. 20–30, 2014.

[75] E. S. Paykel, "Depression: Major problem for public health," *Epidemiology and Psychiatric Sciences*, vol. 15, no. 1, pp. 4–10, 2006.

[76] B. Amin, A. Nakhsaz, and H. Hosseinzadeh, "Evaluation of the antidepressant-like effects of acute and sub-acute administration of crocin and crocetin in mice," *Avicenna journal of phytomedicine*, vol. 5, no. 5, p. 458, 2015.

[77] A. Asai, T. Nakano, M. Takahashi, and A. Nagao, "Orally administered crocetin and crocins are absorbed into blood plasma as crocetin and its glucuronide conjugates in mice," *Journal of agricultural and food chemistry*, vol. 53, no. 18, pp. 7302–7306, 2005.

[78] M. Ivanović, M. Islamčević Razboršek, and M. Kolar, "Innovative extraction techniques using deep eutectic solvents and analytical methods for the isolation and characterization of natural bioactive compounds from plant material," *Plants*, vol. 9, no. 11, p. 1428, 2020.

[79] M. Liakopoulou-Kyriakides and D. Kyriakidis, "Croscus sativus-biological active constitutents," *Studies in natural products chemistry*, vol. 26, pp. 293–312, 2002.

[80] A. Amanpour, A. S. Sonmezdag, H. Kelebek, and S. Selli, "Gc–ms–olfactometric characterization of the most aroma-active components in a representative aromatic extract from iranian saffron (crocus sativus l.)," *Food chemistry*, vol. 182, pp. 251–256, 2015.

[81] E. Masi, C. Taiti, D. Heimler, P. Vignolini, A. Romani, and S. Mancuso, "Ptr-tof-ms and hplc analysis in the characterization of saffron (crocus sativus l.) from italy and iran," *Food chemistry*, vol. 192, pp. 75–81, 2016.

[82] V. Sujata, G. Ravishankar, and L. Venkataraman, "Methods for the analysis of the saffron metabolites crocin, crocetins, picrocrocin and safranal for the determination of the quality of the spice using thin-layer chromatography, high-performance liquid chromatography and gas chromatography," *Journal of Chromatography A*, vol. 624, no. 1-2, pp. 497–502, 1992.

[83] H. Himeno and K. Sano, "Synthesis of crocin, picrocrocin and safranal by saffron stigma-like structures proliferated in vitro," *Agricultural and Biological Chemistry*, vol. 51, no. 9, pp. 2395–2400, 1987.

[84] D. Basker, "Saffron chemistry," in *Saffron*, CRC Press, 1999, pp. 54–60.

[85] S. Visvanath, G. Ravishankar, and L. Venkataraman, "Induction of crocin, crocetin, picrocrocin, and safranal synthesis in callus cultures of saffron: Crocus sativus l," *Biotechnology and applied biochemistry (USA)*, 1990.

[86] P. Corti, E. Mazzei, S. Ferri, G. G. Franchi, and E. Dreassi, "High performance thin layer chromatographic quantitative analysis of picrocrocin and crocetin, active principles of saffron (crocus sativusl.-iridaceae): A new method," *Phytochemical Analysis*, vol. 7, no. 4, pp. 201–203, 1996.

[87] M. Kabiri, H. Rezadoost, and A. Ghassempour, "A comparative quality study of saffron constituents through hplc and hptlc methods followed by isolation of crocins and picrocrocin," *LWT*, vol. 84, pp. 1–9, 2017.

[88] S. A. Pathan, S. Alam, G. K. Jain, S. M. Zaidi, S. Akhter, D. Vohora, R. K. Khar, and F. J. Ahmad, "Quantitative analysis of safranal in saffron extract and nanoparticle formulation by a validated high-performance thin-layer chromatographic method," *Phytochemical Analysis: An International Journal of Plant Chemical and Biochemical Techniques*, vol. 21, no. 3, pp. 219–223, 2010.

[89] M. Jalali-Heravi, H. Parastar, and H. Ebrahimi-Najafabadi, "Characterization of volatile components of iranian saffron using factorial-based response surface modeling of ultrasonic extraction combined with gas chromatography–mass spectrometry analysis," *Journal of Chromatography A*, vol. 1216, no. 33, pp. 6088–6097, 2009.

[90] M. Jalali-Heravi, H. Parastar, and H. Ebrahimi-Najafabadi, "Self-modeling curve resolution techniques applied to comparative analysis of volatile components of iranian saffron from different regions," *Analytica Chimica Acta*, vol. 662, no. 2, pp. 143–154, 2010.

[91] M. D'Auria, G. Mauriello, and G. L. Rana, "Volatile organic compounds from saffron," *Flavour and Fragrance Journal*, vol. 19, no. 1, pp. 17–23, 2004.

[92] A. Loskutov, C. Beninger, G. Hosfield, and K. Sink, "Development of an improved procedure for extraction and quantitation of safranal in stigmas of crocus sativus l. using high performance liquid chromatography," *Food Chemistry*, vol. 69, no. 1, pp. 87–95, 2000.

[93] E. Karimi, E. Oskoueian, R. Hendra, and H. Z. Jaafar, "Evaluation of crocus sativus l. stigma phenolic and flavonoid compounds and its antioxidant activity," *Molecules*, vol. 15, no. 9, pp. 6244–6256, 2010.

[94] M. Valle Garcıéa-Rodrıéguez, J. Serrano-Diaz, P. A. Tarantilis, H. Lopez-Corcoles, M. Carmona, and G. L. Alonso, "Determination of saffron quality by high-performance liquid chromatography," *Journal of Agricultural and Food Chemistry*, vol. 62, no. 32, pp. 8068–8074, 2014.

[95] K. Lech, J. Witowska-Jarosz, and M. Jarosz, "Saffron yellow: Characterization of carotenoids by high performance liquid chromatography with electrospray mass spectrometric detection," *Journal of mass spectrometry*, vol. 44, no. 12, pp. 1661–1667, 2009.

[96] A. Tamborrino, A. Taticchi, R. Romaniello, C. Perone, S. Esposto, A. Leone, and M. Servili, "Assessment of the olive oil extraction plant layout implementing a high-power ultrasound machine," *Ultrasonics Sonochemistry*, vol. 73, p. 105 505, 2021.

[97] D. W. Green and M. Z. Southard, *Perry's chemical engineers' handbook*. McGraw-Hill Education, 2019.

[98] L. Maggi, M. Carmona, A. Zalacain, C. D. Kanakis, E. Anastasaki, P. A. Tarantilis, M. G. Polissiou, and G. L. Alonso, "Changes in saffron volatile profile according to its storage time," *Food Research International*, vol. 43, no. 5, pp. 1329–1334, 2010.

[99] S. A. Mohajeri, H. Hosseinzadeh, F. Keyhanfar, and J. Aghamohammadian, "Extraction of crocin from saffron (crocus sativus) using molecularly imprinted polymer solid-phase extraction," *Journal of separation science*, vol. 33, no. 15, pp. 2302–2309, 2010.

[100] H. Nerome, M. Ito, S. Machmudah, H. Kanda, M. Goto, *et al.*, "Extraction of phytochemicals from saffron by supercritical carbon dioxide with water and methanol as entrainer," *The Journal of Supercritical Fluids*, vol. 107, pp. 377–383, 2016.

[101] M. G. Goleroudbary and S. Ghoreishi, "Response surface optimization of safranal and crocin extraction from crocus sativus l. via supercritical fluid technology," *The Journal of Supercritical Fluids*, vol. 108, pp. 136–144, 2016.

[102] G. Aliakbarzadeh, H. Sereshti, and H. Parastar, "Pattern recognition analysis of chromatographic fingerprints of crocus sativus l. secondary metabolites towards source identification and quality control," *Analytical and Bioanalytical Chemistry*, vol. 408, pp. 3295–3307, 2016.

[103] J. Rubert, O. Lacina, M. Zachariasova, and J. Hajslova, "Saffron authentication based on liquid chromatography high resolution tandem mass spectrometry and multivariate data analysis," *Food Chemistry*, vol. 204, pp. 201–209, 2016.

[104] C. Da Porto and A. Natolino, "Extraction kinetic modelling of total polyphenols and total anthocyanins from saffron floral bio-residues: Comparison of extraction methods," *Food Chemistry*, vol. 258, pp. 137–143, 2018.

[105] A. Kyriakoudi, A. Chrysanthou, F. Mantzouridou, and M. Z. Tsimidou, "Revisiting extraction of bioactive apocarotenoids from crocus sativus l. dry stigmas (saffron)," *Analytica chimica acta*, vol. 755, pp. 77–85, 2012.

[106] H. Sereshti, R. Heidari, and S. Samadi, "Determination of volatile components of saffron by optimised ultrasound-assisted extraction in tandem with dispersive liquid–liquid microextraction followed by gas chromatography–mass spectrometry," *Food chemistry*, vol. 143, pp. 499–505, 2014.

[107] L. Ferrara, D. Naviglio, and M. Gallo, "Extraction of bioactive compounds of saffron (crocus sativus l.) by ultrasound assisted extraction (uae) and by rapid solid-liquid dynamic extraction (rslde)," *European Scientific Journal*, vol. 10, no. 3, 2014.

[108] P. A. Tarantilis and M. G. Polissiou, "Isolation and identification of the aroma components from saffron (crocus sativus)," *Journal of Agricultural and Food Chemistry*, vol. 45, no. 2, pp. 459–462, 1997.

[109] C. D. Kanakis, D. J. Daferera, P. A. Tarantilis, and M. G. Polissiou, "Qualitative determination of volatile compounds and quantitative evaluation of safranal and 4-hydroxy-2, 6, 6-trimethyl-1-cyclohexene-1-carboxaldehyde (htcc) in greek saffron," *Journal of agricultural and food chemistry*, vol. 52, no. 14, pp. 4515–4521, 2004.

[110] H. Schmidt-Traub, M. Schulte, A. Seidel-Morgenstern, and H. Schmidt-Traub, *Preparative chromatography*. Wiley Online Library, 2012.

[111] A. Seidel-Morgenstern, "Preparative chromatography,"

[112] J. Prado and M. Rostagno, *Natural product extraction: principles and applications*. Royal Society of Chemistry, 2022.

[113] Y.-X. Song, A. Furtose, D. Fuoco, Y. Boumghar, and G. S. Patience, "Meta-analysis and review of cannabinoids extraction and purification techniques," *The Canadian Journal of Chemical Engineering*,

[114] A. Seidel-Morgenstern, "Experimental determination of single solute and competitive adsorption isotherms," *Journal of Chromatography A*, vol. 1037, no. 1-2, pp. 255–272, 2004.

[115] J. D. Seader, E. J. Henley, and D. K. Roper, *Separation process principles: With applications using process simulators*. John Wiley & Sons, 2016.

[116] H. M. Irving, H. Freiser, and T. S. West, *Compendium of analytical nomenclature: definitive rules 1977*. Elsevier, 2017.

[117] I. Molnar and C. Horváth, "Reverse-phase chromatography of polar biological substances: Separation of catechol compounds by high-performance liquid chromatography.," *Clinical chemistry*, vol. 22, no. 9, pp. 1497–1502, 1976.

[118] K. Hostettmann, M. Hostettmann, A. Marston, *et al.*, "Preparative chromatography techniques," *Applications in Natural Product Isolation*, 1986.

[119] G. Guiochon, A. Felinger, and D. G. Shirazi, *Fundamentals of preparative and nonlinear chromatography*. Elsevier, 2006.

[120] S. Sircar and J. Hufton, "Why does the linear driving force model for adsorption kinetics work?" *Adsorption*, vol. 6, pp. 137–147, 2000.

[121] C. Fanali, P. Haddad, C. Poole, M.-L. Riekkola, *et al.*, "Liquid chromatography: Fundamentals and instrumentation," in *Liquid Chromatography: Fundamentals and Instrumentation: Second Edition*, vol. 1, Elsevier, 2017, pp. 1–784.

[122] G. Goring, "A modified kremser equation for stagewise countercurrent processes," *Separation Science*, vol. 5, no. 2, pp. 113–120, 1970.

[123] B. D. Smith and W. Brinkley, "General short-cut equation for equilibrium stage processes," *AIChE Journal*, vol. 6, no. 3, pp. 446–450, 1960.

[124] J. W. Gibbs, "On the equilibrium of heterogeneous substances," 1879.

[125] C. Wibowo and K. M. Ng, "Conceptual design of crystallization processes," in *Conceptual Design of Crystallization Processes*, De Gruyter, 2020.

[126] W. Beckmann, *Crystallization: Basic concepts and industrial applications*. John Wiley & Sons, 2013.

[127] H.-K. Rhee and N. Amundson, "Equilibrium theory of the parametric pump," *Industrial & Engineering Chemistry Fundamentals*, vol. 9, no. 2, pp. 303–304, 1970.

[128] K. Row and J. Lee, "Determination of retention factors of phospholipids in gradient hplc," *Chromatographia*, vol. 51, pp. 61–64, 2000.

[129] J. W. Lee and K. H. Row, "Determination of retention factors of aromatic compounds by gradient-elution reverse-phase high performance liquid chromatography," *Korean Journal of Chemical Engineering*, vol. 19, pp. 978–985, 2002.

[130] S. Qamar, N. Rehman, G. Carta, and A. Seidel-Morgenstern, "Analysis of gradient elution chromatography using the transport model," *Chemical Engineering Science*, vol. 225, p. 115 809, 2020.

[131] P. Jandera and J. Churacek, *Gradient elution in column liquid chromatography: theory and practice*. Elsevier, 1985.

[132] B. L. Murphy and R. D. Morrison, "Introduction to environmental forensics," 2014.

[133] H. H. Billiet, *Gradient elution in column liquid chromatography:(journal of chromatography library, vol. 31), p. jandera and j. churáček, elsevier, 1985. us* $79.00/Dfl.245.00(xix + 510 pages)ISBN0 - 444 - 42124 - 6$, 1985.

[134] J. M. Woodley, "Advances in enzyme technology—uk contributions," *History of Modern Biotechnology II*, pp. 93–108, 2000.

[135] L. R. Snyder and J. W. Dolan, *High-performance gradient elution: the practical application of the linear-solvent-strength model.* John Wiley & Sons, 2007.

[136] L. R. Snyder, J. J. Kirkland, and J. W. Dolan, *Introduction to modern liquid chromatography.* John Wiley & Sons, 2011.

[137] C. F. Poole, *The essence of chromatography.* Elsevier, 2003.

[138] K. Robards and D. Ryan, *Principles and practice of modern chromatographic methods.* Academic Press, 2021.

Appendix A

Appendix

A.1 Additional Tables for Both Separation Techniques

The following tables A.1 and A.2 are about the expressions of the objective function equation for picrocrocin and crocin II, respectivelly. The obtained data from the two set of experiments N^{Ba} and N^{SBa} led to the estimation of the thermodynamic parameter ($K_{i,E}$) by the Weighted Least Squares equation (WLS) (subsection 4.2.2). The tables A.3 and A.4 are related to the further parameters of the developed three-step gradient elution in the chromatography process (Table 4.15 and Figure 4.23 in subsection 4.3.4).

Table A.1: Expressions of the objective function equation for picrocrocin. A,B,...,H = Different variants of weight term. n: Class of weight term specific to each category of experiments. Ba : extraction procedure with one batch, SBa : extraction procedure with several successive batches

Process	No. (j)	$c_{i,j}^{exp.}$	A	B	C	D	E	F	G	H	Class (n)
	-	-	A	B	C	D	E	F	G	H	-
	1	1.4896	1	1	0	1	1	1	1	1	I
	2	2.9489									
Ba	3	4.3467									
	4	5.7550									
	N^{Ba}=5	7.2193	↓	↓							
	$N^{Ba}+1$=6	6.0153	0	1	↓	↓	↓	↓	↓	↓	↓
	7	1.3930				0.9	0.9	0.9	0.9	0.8	II
	8	9.9411				↓	↓	↓	↓	↓	↓
	9	0.2755				0.7	0.6	0.5	0.4	0.4	III
	10	3.5459									
SBa	11	12.7271				↓	↓	↓	↓	↓	↓
	12	0.0655				0.4	0.3	0.2	0.1	0.1	IV
	13	1.1397									
	14	7.1550				↓	↓	↓	↓	↓	↓
	$N=N^{Ba}+N^{SBa}$=15	15.32	↓	↓	↓	↓	↓	↓	↓	↓	↓

Table A.2: Expressions of the objective function equation for crocin II. A,B,...,H = Different variants of weight term. n: Class of weight term specific to each category of experiments. Ba : extraction procedure with one batch, SBa : extraction procedure with several successive batches

Process	No. (j)	$c_{i,j}^{exp.}$	A	B	C	D	E	F	G	H	Class (n)
	-	-	A	B	C	D	E	F	G	H	-
	1	0.0453	1	1	0	1	1	1	1	1	I
	2	0.2040									
	3	0.4365									
Ba	4	0.7275									
	5	1.5747									
	6	2.3431									
	7	3.1016									
	$N^{Ba}{=}8$	3.7961	↓	↓							
	$N^{Ba}+1{=}9$	3.8542	0	1	↓	↓	↓	↓	↓	↓	↓
	10	1.2847				0.9	0.9	0.9	0.9	0.8	II
	11	6.3433				↓	↓	↓	↓	↓	↓
	12	0.3589				0.7	0.6	0.5	0.4	0.4	III
	13	2.5695				↓	↓	↓	↓	↓	↓
SBa	14	5.8616									
	15	0.1293				0.4	0.3	0.2	0.1	0.1	IV
	16	1.043									
	17	3.21									
	$N = N^{Ba} + N^{SBa}{=}18$	4.97	↓	↓	↓	↓	↓	↓	↓	↓	↓

Table A.3: Other parameters of the developed three-step gradient elution (Table 4.15 and Figure 4.23). $t_{inj}{=}0.00416\ min$, $t_0^{exp.}= 1.12\ min$, $\dot{V}_L{=}1.2\ ml/min$

Component i	$t_{R,i}$ [min]	k_i (Eq. A.1)	$w_{1/2,i}$ [min]	σ_i (Eq. A.2)	N_i (Eq. 2.72)	$HETP$ [mm] (Eq. 2.74)
PC	5.1	3.55	0.7062	0.30	289	0.52
CI	16.2	13.46	2	0.85	363	0.41
CII	27.7	23.73	2.64	1.125	606	0.24

Retention factor:

$$k_i = \frac{t_{R,i} - t_0}{t_0} \tag{A.1}$$

Central moment:

$$\sigma_i = \frac{w_{1/2,i}}{\sqrt{5.54}} \tag{A.2}$$

Table A.4: Selectivity (Eq. A.3), central moment (Eq. A.4) and resolution (Eq. A.5) of picrocrocin (1), crocin I (2) and crocin II (3) for the developed three-step gradient elution (Figure 4.23)

α_{12}	α_{13}	α_{23}	σ_{21}	σ_{31}	σ_{32}	R_{21}	R_{31}	R_{32}
3.79	6.68	1.76	0.57	0.71	0.98	4.86	7.95	2.93

Selectivity:

$$\alpha = \alpha_{12} = \frac{k_2}{k_1} \tag{A.3}$$

Central moment:

$$\sigma_{21} = \frac{\sigma_1 + \sigma_2}{2} \tag{A.4}$$

Resolution:

$$R_{21} = \frac{t_{R,2} - t_{R,1}}{4\sigma_{21}} \tag{A.5}$$

A.2 Additional Figures for Both Separation Techniques

Figure A.1 illustrates the effect of different volume flow rate of mobile phase, in the solid-liquid chromatography, on the Height of the theoretical plates, $HETP$, of crocin II, which is used to select the volume flow rate with highest number of theoretical plates (subsections 2.2.3.3. and 3.3.2.1). Figures A.2, A.3, and A.4 show respectively the mass analysis of the picrocrocin, crocin I and rocin II of the saffron crude extract using the online LC-MS-QTOF technique. Figures A.5, A.6, and A.7 show the experimentally concentration-time curves of picrocrocin, crocin I and crocin II, respectively, in different dosages. $D_S = [10:50]$ g/l (Eq. 2.12), $\varepsilon_{est.} = [0.97 : 0.87]$ (Eq. 2.9). Figures A.8 and A.9 represents the theoretically and experimentally liquid phase concentrations of picrocrocin and crocin I in each stage of the sequential batches extraction process (Figure 3.5), which evaluate the calulated liquid phase concentration by Eq. 2.30 in comparison with the empirical liquid phase concentrations of component i. Figures A.10 and A.11 represent the overlapping the theoretical and experimetal concentration-time curves for picrocrocin and crocin II to estimate their extraction kinetic rate constant, k_i^{eff}, (subsection 4.2.3). At the end, figures A.12 and A.13 represent the two-loop effects of the phase ratio, ε, and the residence time, τ, on the real (dimensioned) concentration, productivity and recovery yield of crocin I and crocin II in both batch (Ba) (Eq. 2.30) and counter-current (CC) (Eq. 2.42) processes with real numbers.
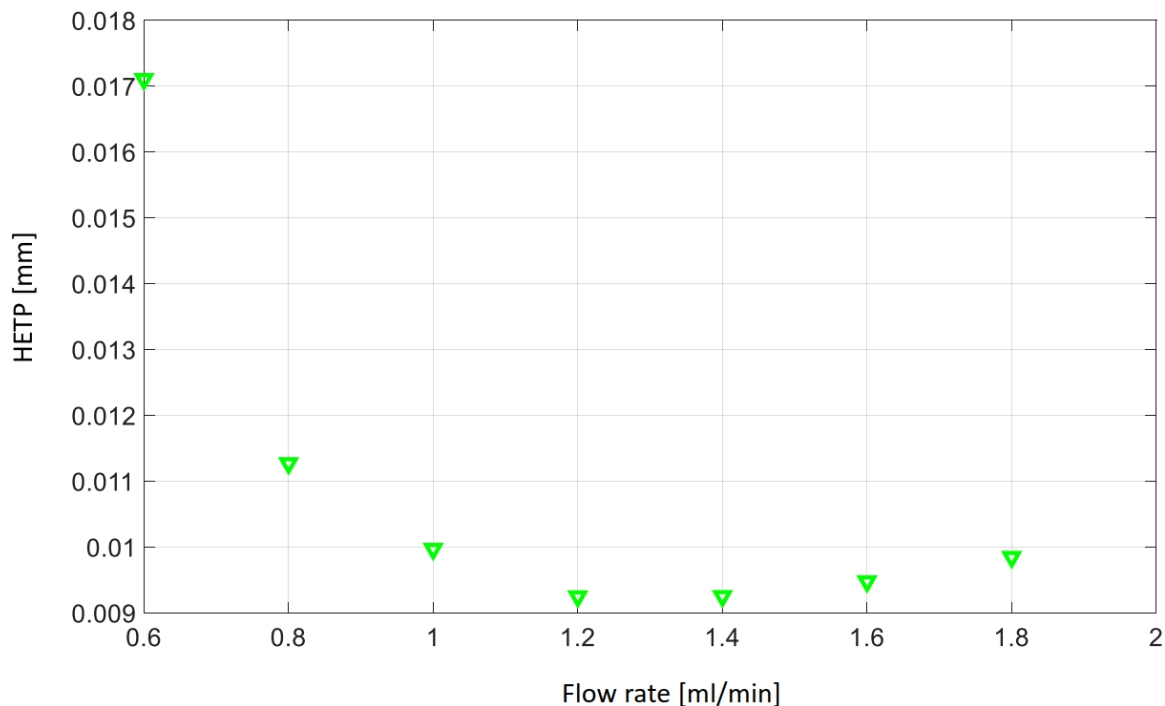
Figure A.1: Height of the theoretical plates, $HETP$, of crocin II (green triangles) in different flow rates
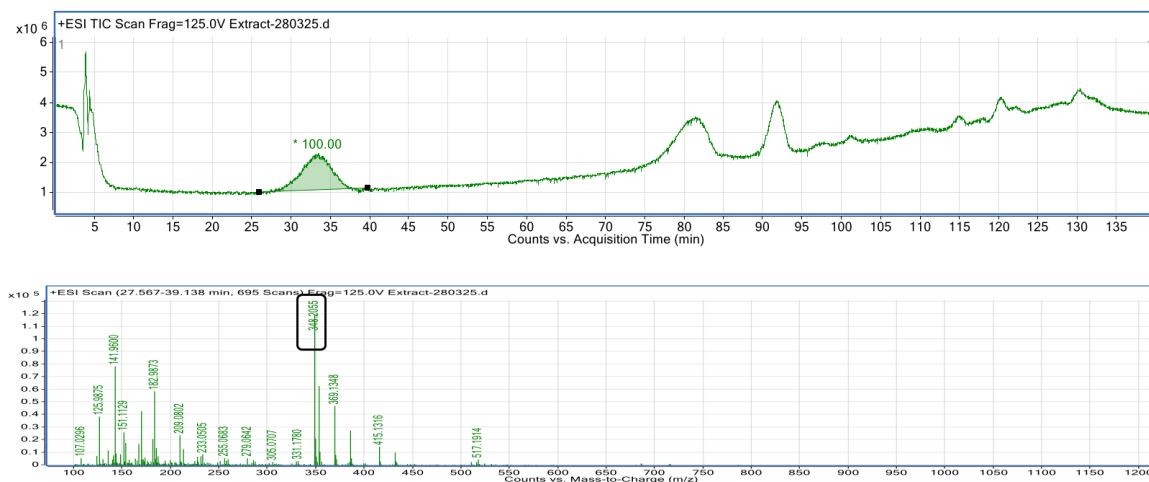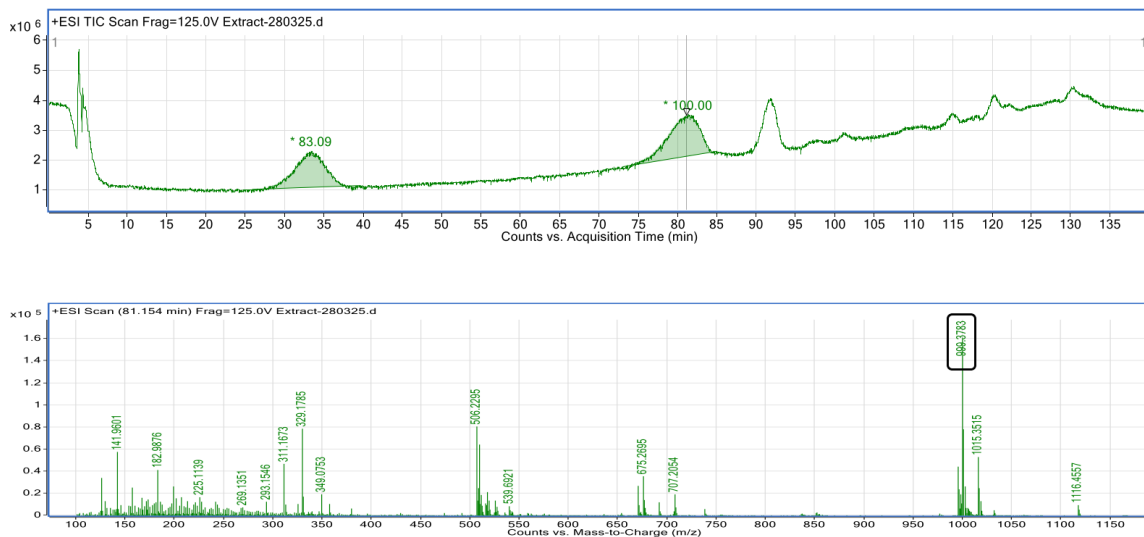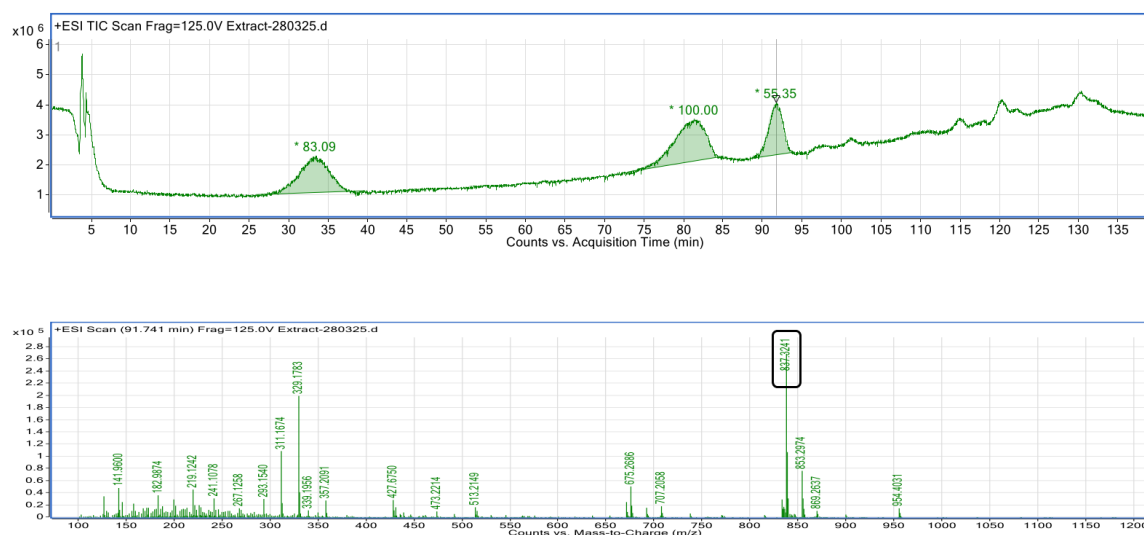

Figure A.2: Mass analysis of the picrocrocin of the saffron crude extract using the online LC-MS-QTOF technique (Q-TOF-LC-MS 6530, Agilent Technology, CA, US). Separation method: see caption of figure 4.2. Top figure: +ESI TIC Scan of the saffron crude extract. Down figure: +ESI TIC Scan in 27.567-39.138 min, which shows ammonium-adduct mass of picrocroicn $[M + NH_4]^+$=348.2 m/z. $\dot{V}_L = 0.4\ ml/min$

Figure A.3: Mass analysis of the crocin I of the saffron crude extract using the online LC-MS-QTOF technique (Q-TOF-LC-MS 6530, Agilent Technology, CA, US). Separation method: see caption of figure 4.2. Top figure: +ESI TIC Scan of the saffron crude extract. Down figure: +ESI TIC Scan at 81.15 min, which shows sodium-adduct mass of crocin I $[M + Na]^+$=999.37 m/z. $\dot{V}_L = 0.4\ ml/min$
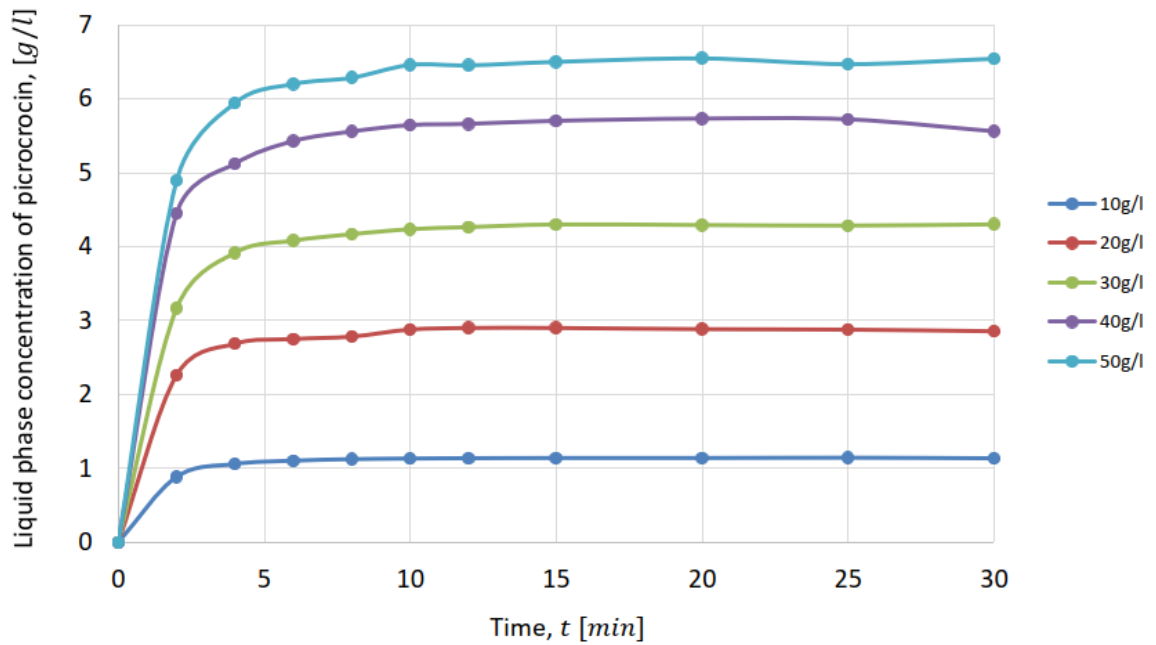

Figure A.4: Mass analysis of the crocin II of the saffron crude extract using the online LC-MS-QTOF technique (Q-TOF-LC-MS 6530, Agilent Technology, CA, US). Separation method: see caption of figure 4.2. Top figure: +ESI TIC Scan of the saffron crude extract. Down figure: +ESI TIC Scan at 91.74 min, which shows sodium-adduct mss of crocin II $[M + Na]^+$=837.32 m/z. $\dot{V}_L = 0.4\ ml/min$

Figure A.5: Concentration-time curves of picrocrocin in different dosages. $D_S = [10:50]$ g/l (Eq. 2.12), $\varepsilon_{est.} = [0.97 : 0.87]$ (Eq. 2.9). It should be mentioned that the epsilons were estimated regarding to the internal liquid phase (amount of trapped liquid in solid phase)
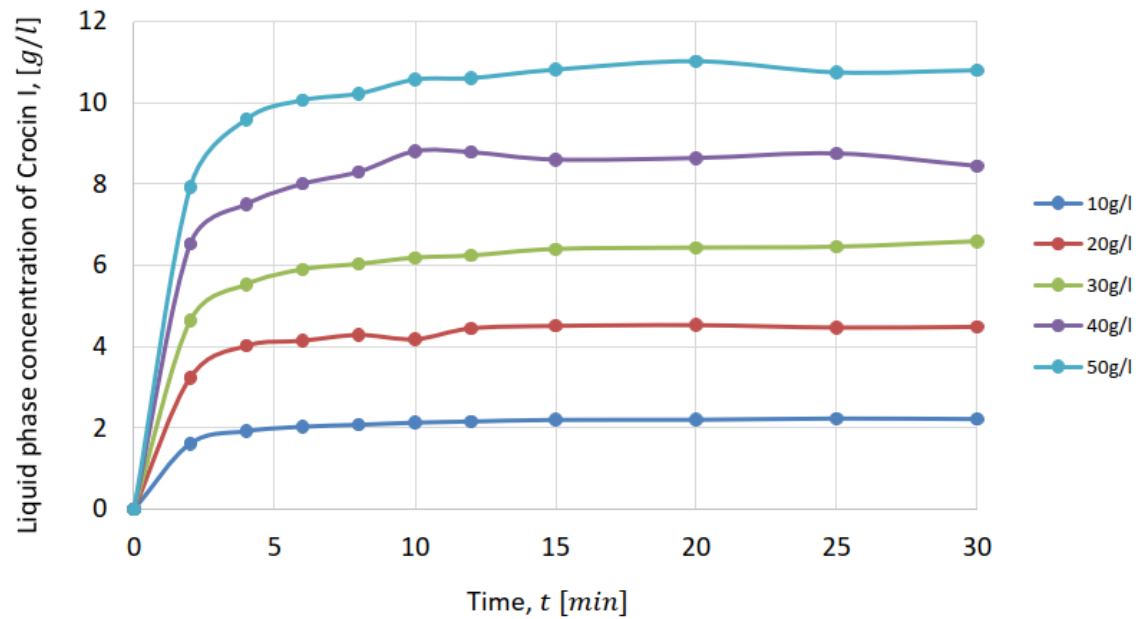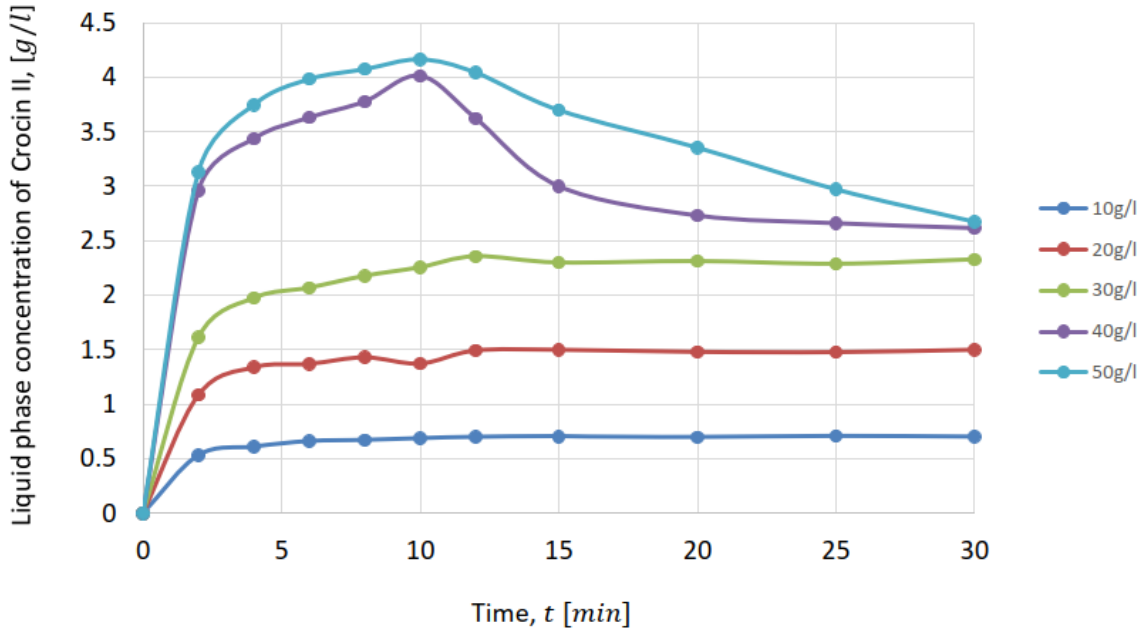

Figure A.6: Concentration-time curves of crocin I in different dosages. $D_S = [10:50]$ - g/l (Eq. 2.12), $\varepsilon_{est.} = [0.97 : 0.87]$ (Eq. 2.9). It should be mentioned that the epsilons were estimated regarding to the internal liquid phase (amount of trapped liquid in solid phase)

Figure A.7: Concentration-time curves of crocin II in different dosages. $D_S = [10{:}50]$ g/l (Eq. 2.12), $\varepsilon_{est.} = [0.97 : 0.87]$ (Eq. 2.9). It should be mentioned that the epsilons were estimated regarding to the internal liquid phase (amount of trapped liquid in solid phase)

Figure A.8: Theoretically and experimentally liquid phase concentration of **picro-crocin** (PC) in each stage of the sequential batches extraction process (Figure 3.5). $x^0_{i,S} = 0.15$ g_i/g_S (Eq. 2.4, Table 4.3), $\varepsilon_{est.} = 0.87$ (Eq. 2.9), $D_S = 50$ g/l (Eq. 2.12), $K_{i,E} = 1.052$ (Table 4.6)

1st Row	$c_{CII,1}^{The.} = 3.86\ [g/l]$ $c_{CII,1}^{exp.} = 3.85\ [g/l]$ (Extractor 1)		
2nd Row	$c_{CII,2}^{The.} = 1.42\ [g/l]$ $c_{CII,2}^{exp.} = 1.28\ [g/l]$ (Extractor 2)	$c_{CII,3}^{The.} = 5.87\ [g/l]$ $c_{CII,3}^{exp.} = 6.34\ [g/l]$ (Extractor 3)	
3rd Row	$c_{CII,4}^{The.} = 0.58\ [g/l]$ $c_{CII,4}^{exp.} = 0.35\ [g/l]$ (Extractor 4)	$c_{CII,5}^{The.} = 3.26\ [g/l]$ $c_{CII,5}^{exp.} = 2.56\ [g/l]$ (Extractor 5)	$c_{CII,6}^{The.} = 6.10\ [g/l]$ $c_{CII,6}^{exp.} = 5.86\ [g/l]$ (Extractor 6)

4th Row	$c_{CII,7}^{The.} = 0.095\ [g/l]$ $c_{CII,7}^{exp.} = 0.13\ [g/l]$ (Extractor 7)	$c_{CII,8}^{The.} = 0.99\ [g/l]$ $c_{CII,8}^{exp.} = 1.04\ [g/l]$ (Extractor 8)	$c_{CII,9}^{The.} = 3.14\ [g/l]$ $c_{CII,9}^{exp.} = 3.21\ [g/l]$ (Extractor 9)	$c_{CII,10}^{The.} = 5.78\ [g/l]$ $c_{CII,10}^{exp.} = 4.97\ [g/l]$ (Extractor 10)

Figure A.9: Theoretically and experimentally liquid phase concentration of **crocin II** (CII) in each stage of the sequential batches extraction process (Figure 3.5). $x_{i,S}^0 = 0.094\ g_i/g_S$ (Eq. 2.4, Table 4.3), $\varepsilon_{est.} = 0.87$ (Eq. 2.9), $D_S = 50\ g/l$ (Eq. 2.12), $K_{i,E} = 0.536$ (Table 4.6)
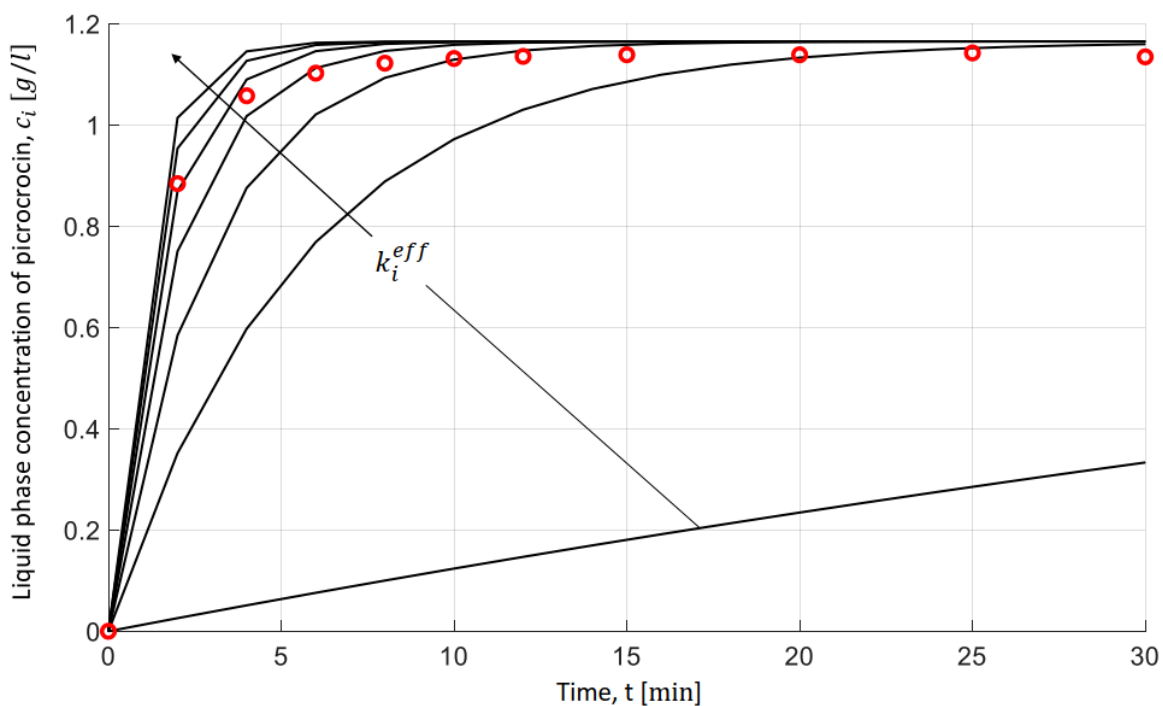

Figure A.10: Overlapping the experimental concentration-time curve of picrocrocin (red circles from Figure 4.4) with the theoretical concentration-time curves calculated by the Eq. 2.30 (black curves). Enrichment of the liquid phase. The arrow shows the changes of the kinetic parameter from low to high values. $K_{i,E}=1.052$, $x_{i,S}^0 = 0.15\ g_{i,S}^0/g_S^0$, $D_S=10\ g/l$
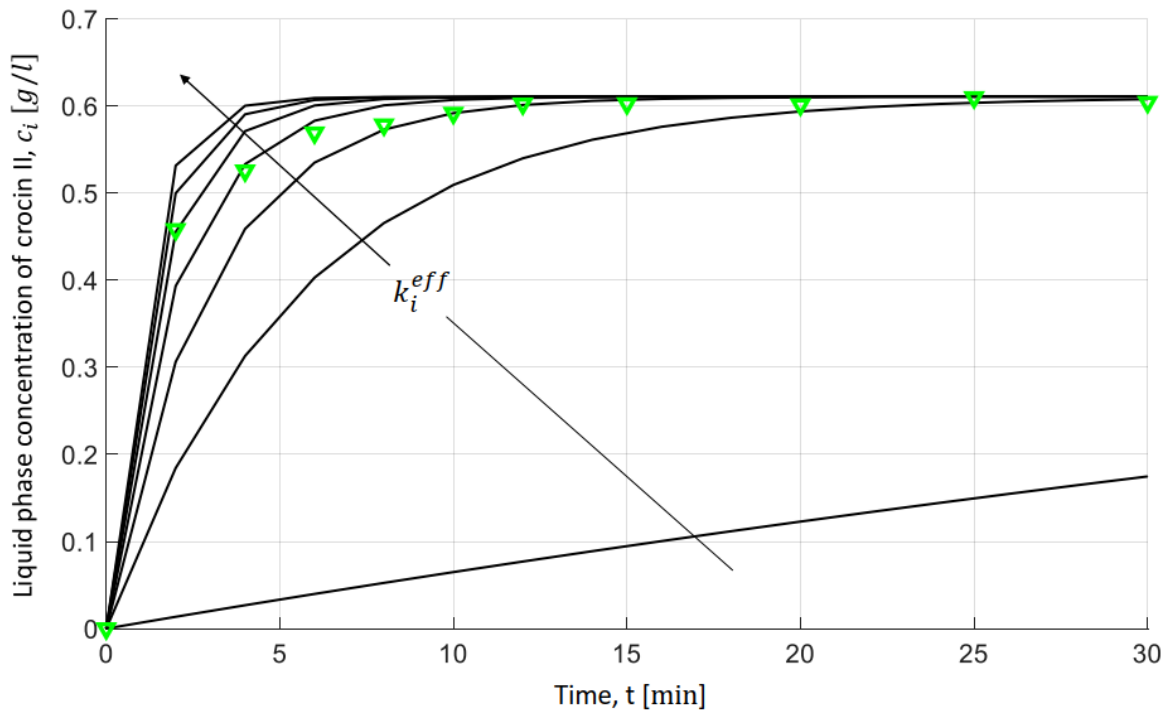
Figure A.11: Overlapping the experimental concentration-time curve of crocin II (green triangles from Figure 4.4) with the theoretical concentration-time curves calculated by the Eq. 2.30 (black curves). Enrichment of the liquid phase. The arrow shows the changes of the kinetic parameter from low to high values. $K_{i,E}$=0.536, $x_{i,S}^0$= 0.094 $g_{i,S}^0/g_S^0$, D_S=10 g/l
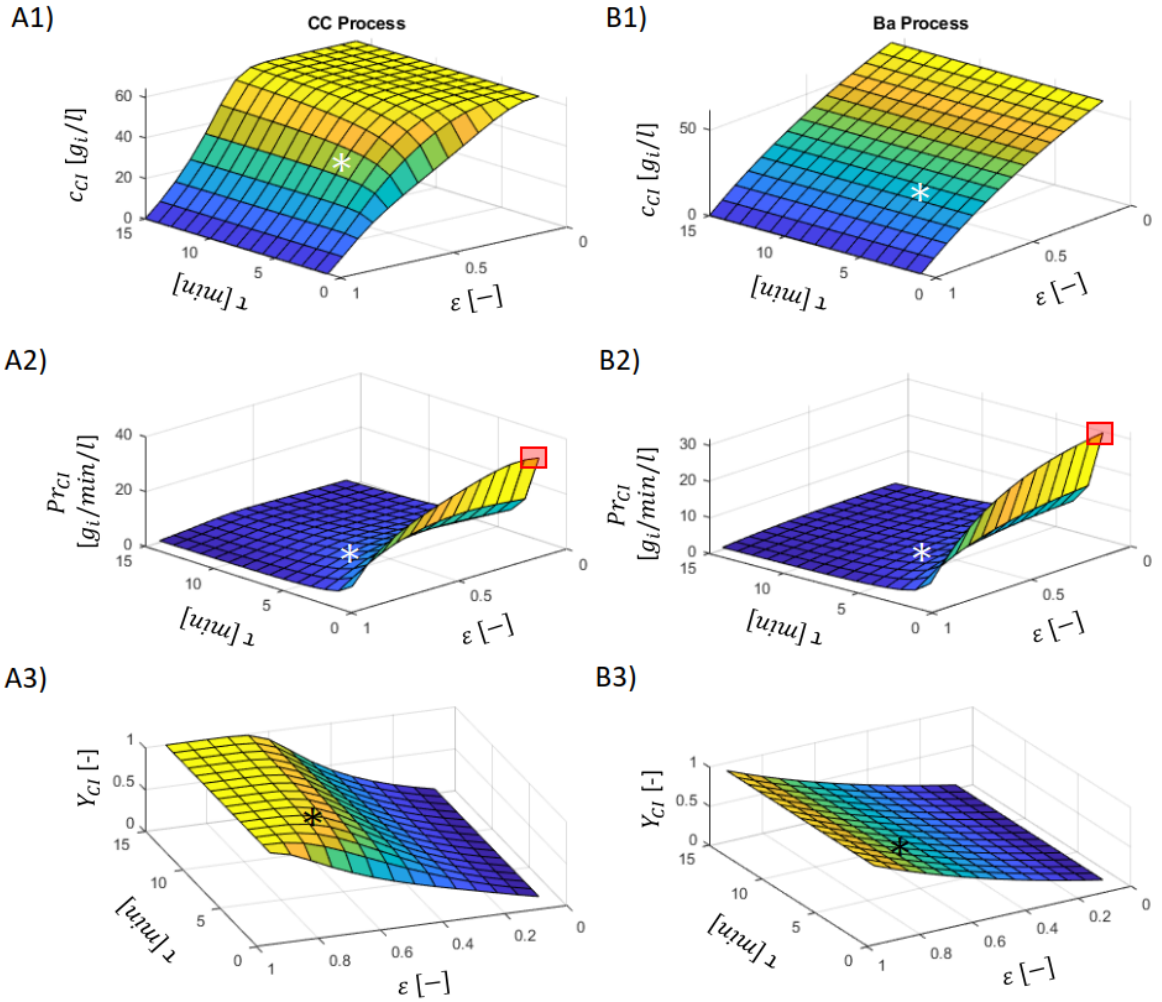
Figure A.12: The two-loop effects of ε and τ on the real (dimensioned) concentration, productivity and recovery yield of crocin I in both batch (Ba) (Eq. 2.30) and counter-current (CC) (Eq. 2.42) processes. $k_{CI}^{eff} = 0.50$ [1/min], $K_{CI,E} = 0.66$, $q_{CI}^{in} = 97.33$ [g_{CI}/l], $N = 20$, ε in [0:1], τ in [0.001:15]. Star points: Concentration, productivity and recovery yield in $\varepsilon = 0.7$ and $\tau = 5$ [min] (specific analysis). Given parameters: Table 4.9
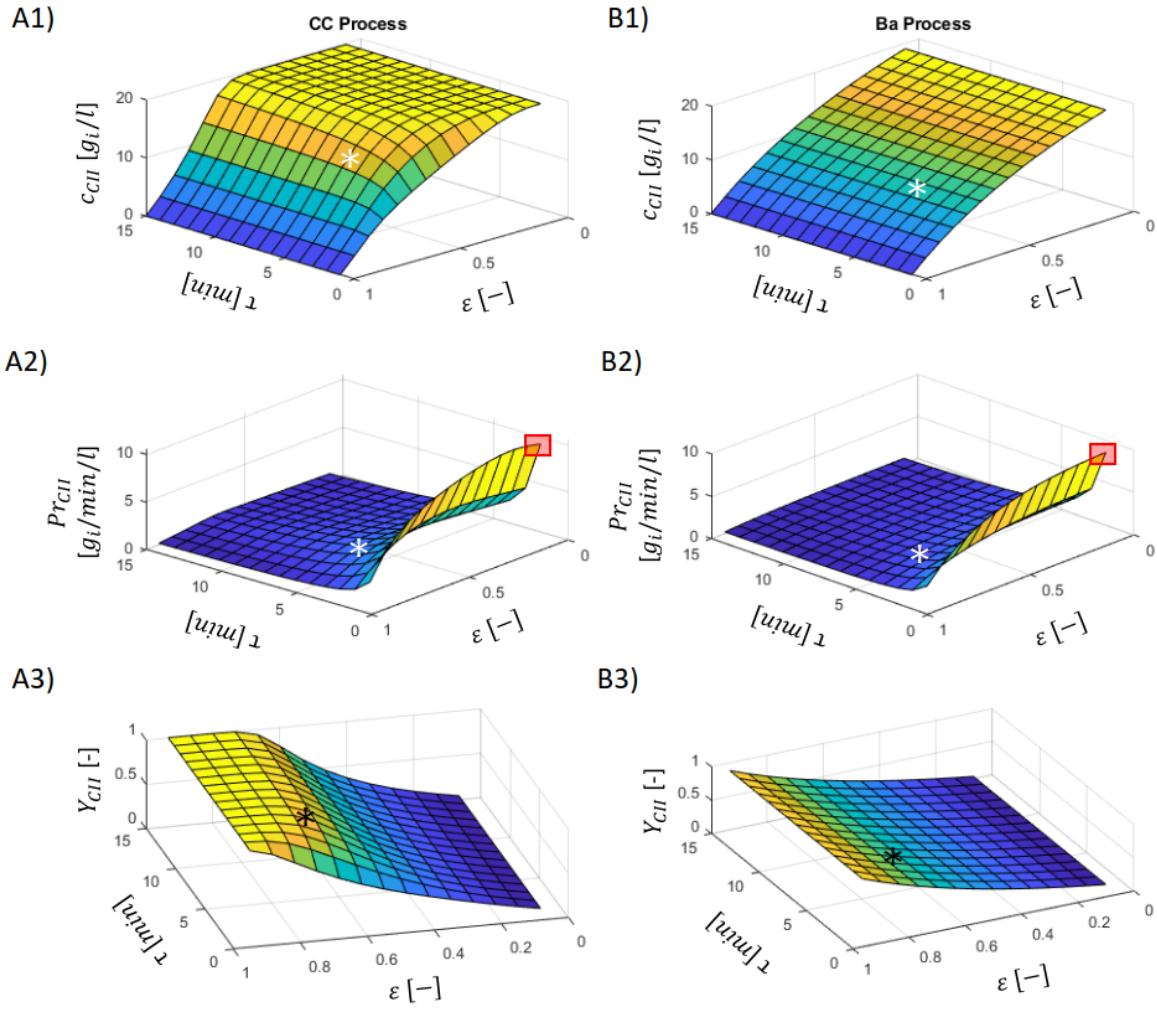
Figure A.13: The two-loop effects of ε and τ on the real (dimensioned) concentration, productivity and recovery yield of crocin II in both batch (Ba) (Eq. 2.30) and counter-current (CC) (Eq. 2.42) processes. $k_{CII}^{eff} = 0.49$ $[1/min]$, $K_{CII,E} = 0.536$, $q_{CII}^{in} = 36.6$ $[g_{CII}/l]$, $N = 20$, ε in $[0{:}1]$, τ in $[0.001{:}15]$. Star points: Concentration, productivity and recovery yield in $\varepsilon = 0.7$ and $\tau = 5$ $[min]$ (specific analysis). Given parameters= Table 4.9